Addis Ababa University

College of Technology and Built Environment

School of Civil and Environmental Engineering

Assessment of Material Characteristics, Mechanical Performance, Durability, and Shrinkage of Bamboo Fiber Reinforced Concrete for Sustainable Construction

By

Muluken Awulachew Asres

Advisor: Professor Girma Zerayohannes

Co-Advisors: - Dr. Ing. Adil Zekaria

Dr. Denamo Addissie

A Ph.D. Dissertation submitted to the School of Graduate Studies of Addis Ababa University in partial fulfillment of the requirements for the Degree of Doctor of Philosophy (Ph.D.) in Civil Engineering, Structural Engineering Stream

May, 2026

Addis Ababa University
College of Technology and Built Environment
School of Civil and Environmental Engineering

Doctoral Dissertation Approval Sheet

The undersigned have examined the dissertation entitled "**Assessment of Material Characteristics, Mechanical Performance, Durability, and Shrinkage of Bamboo Fiber Reinforced Concrete for Sustainable Construction**" presented by **Muluken Awulachew Asres**, a candidate for the degree of **Doctor of Philosophy in Civil Engineering, Structural Engineering Stream,** and hereby certify that it is worthy of acceptance.

Submitted by

	Signature	Date
Muluken Awulachew Asres Candidate (Ph.D.)	Signature	07 May 2026 Date

Approved by the board of examiners:

	Signature	Date
Prof. Girma Zerayohannes Advisor	Signature	28 May 2026 Date
Dr. Ing. Adil Zekaria Co-Advisor	Signature	28 May 2026 Date
Dr. Denamo Addisie Co-Advisor	Signature	28 May 2026 Date
Dr. Bahiru Bewket External Examiner	Signature	18 May 2026 Date
Dr. Abreham Gebre Internal Examiner	Signature	May 19, 2026 Date
Dr. Yenesew Mengiste Chairman	Signature	03 JUN, 2026 Date
Dr. Yenesew Mengiste SCEE Head	Signature	03 JUN, 2026 Date

Office of the Vice Executive Dean for Academic Affairs

Declaration

I, Muluken Awulachew Asres, certify that the dissertation "**Assessment of Material Characteristics, Mechanical Performance, Durability, and Shrinkage of Bamboo Fiber Reinforced Concrete for Sustainable Construction**" is an accurate reflection of the work I have done since enrolling in the Ph.D. program at Addis Ababa University, College of Technology and Built Environment, School of Civil and Environmental Engineering. It has not previously been a part of the dissertation submitted to this or any other institution for a degree, diploma, or other qualifications. I acknowledge that this dissertation was conducted under the supervision of Prof. Dr. Ing Girma Zerayohannes, Dr. Ing Adil Zekaria, and Dr. Denamo Adissie.

From this study, the following manuscripts were developed. Their status is presented in the following table.

No	Title	Type	Journal	Publisher	Status
1	Experimental study of Yushania alpina bamboo fiber	Article	Material research express	IOP Publishing	Published
2	Bamboo fiber impact on the long-term mechanical properties of concrete	Article	Journal of Natural Fibers	Taylor and Francis	Published
3	Long-term Durability Study of Bamboo Fiber Reinforced Concrete	Article	ASM Science Journal	Akademi Sains Malaysia	Under review
4	Tensile Properties of Yushania alpina bamboo fiber	Book of abstracts	Conference	Ethiopian Institute of Architecture, Building Construction, and City Development (EiABC) and Bauhaus University-Weimar	Published

Muluken Awulachew Asres

Date ______________________

Signature __________________

Acknowledgments

I begin by expressing my deepest gratitude for the continuous blessings and guidance of God, which have been a constant source of strength throughout this research journey.

I am profoundly indebted to my esteemed supervisors, Prof. Girma Zerayohannes, Dr. Ing. Adil Zekaria, and Dr. Denamo Addisie, for their exceptional mentorship, unwavering support, and invaluable expertise. Their insightful guidance and constructive feedback have been instrumental in shaping this dissertation. I am truly grateful for their dedication and the significant time they invested in my academic growth.

I would like to present my sincere acknowledgment to Dr. Esayas G/Yohannes and Dr. Abreham Gebre for their valuable comments, suggestions, and encouragement extended to me for the fruitful accomplishment of the study.

I extend my sincere appreciation to the College of Technology and Built Environment for the financial support, which provided the essential resources and infrastructure necessary to conduct this research effectively.

My sincere thanks also go to Ato Fikeru Bedada, Ato Demessew Melaku, Ato Biniam Fentaw, Wr. Wubet Gebreyes, and Wr. Embet Gebre Mariyam for their kind facilitation of the materials laboratory, ensuring a smooth and efficient research process. I am also grateful to Ato Asnake Teshom for his assistance in facilitating access to the sanitary laboratory.

Furthermore, I would like to thank Ato Yohannes Asres, Ato Yacob Meskele, and Ato Kebreab Mengesha for their assistance with the often-laborious process of bamboo fiber extraction. Their support was essential in obtaining the necessary materials for this research.

I owe Ato Feysel Abdela for his help in the preparation of the solution of chemicals used for the durability study.

I am also grateful to Aser Construction PLC for generously providing the coarse aggregate used in this study. Their contribution of materials was vital to the experimental phase of this research.

Finally, I extend my sincere thanks to Ato Getachew Teshome and Ato Abdiwak Bekele for their practical help in the preparation of the setup required to record humidity and temperature data. Their assistance in this technical aspect should be greatly appreciated.

I am deeply indebted to my wife, Dr. Lemlem Tamrat, my son, Zemariyam Muluken, and my daughter, Betselot Muluken, for their understanding, patience, and unconditional love. To my mother, Wr. Yirgedie Birhan, and my father, Ato Awulachew Asres, I am aware of how much you supported me, not only through your prayers, but also by visiting my experiments. I would like to thank my brother, Dr. Hailegeorgis Awulachew, for his ongoing support and encouragement.

Last but not least, I want to express my heartfelt gratitude to my friends for their unwavering moral support, the strength and motivation I needed to persevere and complete this program.

Abstract

Concrete is the dominant structural material used worldwide in most infrastructures. While it has commendable engineering properties, including compressive strength and the ability to attain the various shapes desired, concrete is known to be relatively weak in resisting tensile forces and brittle. Finite resources and synthetic fibers were exploited to address the weakness of concrete. These fibers are found to be unfavorable for the environment and questionable from a sustainability perspective. Therefore, researchers aimed to utilize the vast bamboo plantation wealth as a fiber source. However, research on the engineering properties of bamboo fiber in concrete is limited. Moreover, those studies were conducted for a very short duration, a maximum of 90 days. Conversely, the existence of thousands of bamboo species and their variability necessitates further investigations into the fibers of the other species and how they affect the range of concrete properties.

Therefore, this research is designed and carried out in two phases. The first phase assesses the impact of extraction methods on the bamboo species, Yushania alpina. The second phase investigates the impact of incorporating these fibers on various concrete properties, including slump, compressive strength, split tensile strength, flexural strength, brittleness, cracking, performance in adverse environments, volume of voids, absorption capacity, and time-dependent behavior, specifically drying shrinkage of concrete. The impacts of mechanical, chemical, and combined extraction techniques on the absorption, chemical composition, morphology, thermal properties, and tensile strengths of the bamboo fiber were examined. On the other hand, the mechanical and durability properties were examined for 365 days, while the shrinkage was examined for 197 days. For this purpose, concrete specimens containing bamboo fiber in amounts of 0%, 0.25%, 0.5%, 0.75%, and 1.0% by volume of concrete were prepared. The results of the investigations of bamboo fiber revealed that chemically extracted fibers showed the highest tensile strength, the removal of attachments on the surface of the fibers, the reduction of lignin content, reduced water absorption capacity, reduced diameter, increased surface roughness, and improved thermal properties. The composite of bamboo fiber and concrete showed results that are correlated with the dose of bamboo fiber. Accordingly, concrete with a bamboo fiber content of 0.5% or higher exhibited less performance in compressive, split tensile, and flexural strength, as well as durability. The study revealed that when the bamboo fiber dose in the concrete is 0.25%, it has comparable compressive strength and durability properties to plain concrete. The highest split tensile strength, the highest flexural strength, the lowest drying shrinkage, and reduced crack width were attained in specimens containing 0.25% bamboo fiber. The existing shrinkage prediction models were not satisfactorily able to trace the drying shrinkage development. Therefore, a new model is formulated and proposed for the use of bamboo fiber-reinforced concrete. Finally, bamboo fiber with a low dose can be utilized in construction.

Keywords: Sustainability, bamboo fiber, mechanical properties, brittleness, cracking, durability, shrinkage, relationships, prediction equation

Contents

List of Tables

List of Figures

1 Introduction

Sustainability was defined by the World Commission on Environment and Development (WCED) as meeting the needs of the present without compromising the ability of future generations to meet their own needs (Development, 1987). There is a native American saying that Chief Seattle's speech, made in 1854, was “We do not inherit the earth from our ancestors. We borrow it from our children”(Kitissou, 2004).

Hence, on a planet with finite natural resources and an ever-growing demand for infrastructure, structural engineers of the future must consider the environmental, economic, and social sustainability. Therefore, the trend of the future is for sustainable construction. Sustainable engineering design decreases material consumption, enhances the quality of life for people, delivers better economic performance, and conserves natural resources for future generations(J.A. Ochsendorf, 2005a).

Extensive concrete utilization in various infrastructures is unquestionable. To mention, it has been utilized in buildings, bridges, roads, hydraulic structures, railways, airports, harbours, tunnels, and canals. The reasons for the application of concrete in such a wide range of structures are the dependable compressive strength, fire resistance, low permeability, capacity to serve for a long time, and ability to give desired shapes(Hashemifard et al., 2012)(Neville, 2002).

While it has these good qualities, concrete is known to be relatively weak towards tensile forces and has low ductility. These poor qualities of concrete result in poor performance of structures for seismic load and cracks that arise due to shrinkage(Wu et al., 2019). For this reason, steel reinforcement bars are laid inside the formwork, and then concrete is poured to get the designed structural forms. The poor tensile property of concrete is augmented by embedding the steel reinforcement bar; however, there are concrete cracks that occur through which they serve as a pathway for water, air, and various chemicals that can deteriorate the physical and mechanical properties of concrete(Pease, 2010).

Fibers are the other options being exploited to enhance the tensile and ductility characteristics of concrete (Q. Zhao et al., 2016). Adding steel and synthetic fibers to concrete is in practice and can enhance its mechanical characteristics. The effect of the incorporation of these fibers mitigates the cracking of concrete initiated during the early age. Managing the cracking of concrete at the early age of concrete is very important to ensure the longevity of structures. On the other hand, the time-dependent concrete properties, creep and shrinkage, are also other perspectives where the added fibers play a positive role(Tošić et al., 2020; Q. Zhao et al., 2016). However, concerns have been raised about steel and synthetic fibers from sustainability and environmental perspectives. The current utilization of steel fibers in concrete is dependent on finite resources(Koichi Minami and Masakazu Terai, 1999).

There are various symptoms that verifying relying on finite construction materials will impact the sustainability of the provided infrastructure in the coming period. The impact is not limited by the challenge faced in providing the required infrastructure; extensive explorations of finite construction materials will have an immense effect on the planet and thus on people's lives(Beiser, 2019).

Environmental pollution is attributed to the release of CO_2 to the atmosphere from the industries for the production of steel fibers and the non-biodegradability of synthetic fibers. Depletion of natural resources is also another major concern for human beings to achieve the basic needs, specifically housing. Depletion of natural finite resources is alarming when considering the continuous population growth and the needs associated with it. The sum of these triggers is to study and propose a reasonable alternative construction material. Therefore, researchers are trying to find out new alternative construction techniques that can replace partially or fully the current construction materials. Moreover, recycling used materials is also a core attractive area to ensure sustainability in construction.

The existing fiber-reinforced concrete construction utilizes extensively fibers obtained from steel, which are manufactured from finite resources at a faster rate than nature can replenish, have an environmental effect on the change of landscape, use high energy, and have more significant carbon emissions. Synthetic fibers and glass fibers are also hired as optional sources of fiber. However, these also do not escape from creating a risk to the environment as they are not degradable within a short period and their production processes negatively affect the atmosphere (J.A. Ochsendorf, 2005a), (Koichi Minami and Masakazu Terai, 1999), (Naik, 2008), (Nabi Saheb & Jog, 1999), (Behera et al., 2018).

Hence, towards sustainability, the investigation of bio-fiber as a reinforcing element in concrete to improve its tensile strength, ductility, and reduce crack mouth opening will be of great technological improvement to the construction engineering, and an enormous contribution to our planet. To this extent, the fibrous concrete composite has been identified as being insufficiently studied in the aspect of its behavior under sustained load over a long time, either under one-dimensional compressive load, Uniaxial tensile (direct tensile) load, or flexural (bending) load. In order to adopt these recyclable, renewable, green materials and sustainable high-performance concrete as innovative engineering construction products, their optimum performance under long-term loading must be understood (Jamaludin et al., 2019). Therefore, Bamboo, as one material to achieve sustainable construction, is drawing many researchers' attention due to its wide plantation, good mechanical characteristics, and reasonably short harvest time. Concrete reinforced with fiber extracted from Bamboo, which is Bamboo Fiber Reinforced Concrete (BFRC), is one line of bio-fiber reinforced concrete.

Possible plants that are under investigation for utilizing the fiber obtained from them are Sisal, Jute, Kenaf, and Bamboo, which are among the list to mention. However, their fiber yield is less compared to bamboo, which has the highest fiber yield (kg/hectare) that reaches up to 3120kg/hectare (Trujillo et al., 2012). Moreover, bamboo fiber showed acceptable engineering properties for utilization.

Ethiopia has more than 1 million ha of land covered by two indigenous species called African Alpine Highland Bamboo (Yushania alpina) and a Monotypic Genus of Lowland Bamboo (Oxytenanthera abyssinica) (Hailu & Gitima, 2023). This coverage is 67% of the total African bamboo plantation area. The examination of the impact of fiber extracted from these species and the effect of incorporation of these fibers on concrete is interesting because of the difficulty in making a conclusion on the limited research output thus far(S.K. Paudel, 2008).

Therefore, this study focused on the characteristics of Yushania alpina bamboo fiber and the impact of its inclusion in concrete on the durability, mechanical, and shrinkage properties of concrete.

1.1 Statement of the problem

Population number increment is closely allied to various aspects such as economic development, resource consumption, environmental protection, and social welfare, with complex and far-reaching connections within these factors(Fei Pang, Guo Miao, Yingxu Li, 2024). The provision of infrastructure for the continuously increasing population is becoming a challenge, especially if the economic model is linear. The current linear model of "take-make and dispose" is contributing to environmental degradation and resource depletion(Jacinta Dsilva, Saniya Zarmukhambetova, 2023). Moreover, the natural imbalance is a threat to the existence of human beings due to pollution emanating from industries. One of those huge industries is those used for the production of materials utilized in the construction industry(J.A. Ochsendorf, 2005a).

The construction sector industry has a considerable global impact, utilizing around 40 % of raw materials and is accountable for 39 % of total CO_2 emissions, of which at least 11 % comes from manufacturing building materials and products(Council, 2019). This exerts a substantial pressure on the environment. One of the materials used in the construction process is fiber. Concrete is known for its poor qualities towards tensile forces and is exposed to the impacts of shrinkage and creep. To complement these drawbacks of the concrete, steel and other man-made fibers are used in its production. The extensive use of these materials poses a threat to the planet Earth, either from exhaustion of finite resources or the release of carbon dioxide during their manufacturing. Moreover, longer years of requirement for degradation of these materials is the other important issue.

The other economic model that is considered good for the resource consumption of the ever growing population and threats to the environment from carbon emission and degradation is the circular economy(Jacinta Dsilva, Saniya Zarmukhambetova, 2023). Therefore, engineering design needs to address sustainability by the reduction of material consumption, improving the quality of life, and achievement of economic performance through the preservation of natural resources for future generations(J.A. Ochsendorf, 2005b).

Utilization of bio-fibers draws interest to address those environmental and sustainable threats. For this reason, jute, sisal, kenaf, and enset fibers are entering into the production of various engineering branches like automotive, aviation, maritime, construction, and Packaging(Sapuan et al., 2022). However, using only those plants for fiber has demonstrated a deficiency of supply, which could lead to the use of the relevant natural resources, ensuring sustainability doubtful. Due to difficulties obtaining free land, efforts to expand the cultivation of those plants to increase the production of plant fiber have stalled. Even the creation of new farmlands by clearing the existing land cover will have an irreversible impact on the natural habitat (Rawatan & Buluh, 2018).

Hence, bamboo is found as an excellent sustainable source of fiber, achieving a circular economy. This emanates from its capacity to rapidly self-generate, mature quickly, its plantation spread globally, and has many growing potential areas(King, 2019).

Accordingly, scholars examined the implications of the utilization of bamboo in different corners of the globe. Studies show that the use of Bamboo as reinforcement in structures like beams shows appreciable strength increment over the plain ones, as a result of which bamboo can substitute steel satisfactorily (Ghavami, 2005). Bamboo fiber shows good improvement in qualities like concrete compressive, tensile, and flexural strength, and better crack management (Bindu et al., 2016). The Bamboo fibers can be used as innovative fibers in SCC (self-compacting concrete) to enhance the strength of concrete and improve the ductility of concrete, and its post-cracking load-carrying capacity (Kavitha & Felix Kala, 2016). Targeting C-25 concrete, a study has been conducted for different percentages of bamboo fiber addition, and the performance of the concrete showed improvement(Reta, 2017). Such promising outcomes of the research are encouraging to further work on the use of bamboo in concrete construction, specifically in fiber concrete.

Therefore, the proper use of bamboo fibers will contribute to balancing the ecosystem instead of the use of plastic or metallic fibers in concrete construction, which are products of industries (Terai & Minami, 2012). Moreover, the process of production of Bamboo fiber can be seen as one area for creating huge job opportunities that are important for social stability (Gupta & Kumar, 2008).

Ethiopia is endowed with bamboo plantations and has conducive conditions for expansion of it, and its applications in Ethiopia are for the production of household utilities, floor mats, fencing, and traditional house construction. In addition, bamboo is being utilized as a source of energy for food cooking. The scope of its utilization in comparison with the potential of the country is minimal. On the other hand, it is a valuable task to explore the rooms to investigate different forms of bamboo in concrete so that its contribution can be taken one step forward. In line with this interest, the impact of bamboo fiber application in concrete is found to be important to research.

Hence, partial substitution or full substitution of the usual industrial construction materials will have a significant meaning on sustainable construction. In this regard, bamboo is passing through different studies to exploit its advantage of positive role in sustainable construction. Those studies conducted are on species that are not found in Ethiopia, hence, they will not be directly used to exploit their findings. It has been noted that there are many kinds of bamboo species on earth whose physical as well as mechanical properties greatly vary. Generalization is not valid based on the findings of studies conducted on some bamboo species. This implies conducting a study on each species is appropriate(S.K. Paudel, 2008) (Al., 2008). Therefore, researching to know the effect of fibers extracted from bamboo species found in Ethiopia on concrete behavior is worthwhile.

Finally, the following are found as gaps that have not been given much attention by researchers.

1. Effects of extraction method on the properties of indigenous highland bamboo fiber
2. Impact of indigenous highland bamboo fiber incorporation on the mechanical performance of concrete
3. Durability properties of concrete reinforced with indigenous highland bamboo fiber
4. Shrinkage properties of concrete reinforced with indigenous highland bamboo fiber

1.2 Research questions

The following are the questions that this research aimed to address.

1. What are the impacts mechanical, chemical and combined extraction methods on the tensile strength, chemical composition, morphology, and thermal stability of Yushania alpina bamboo fiber?
2. To what extent does the addition of varying volume of fractions of bamboo fiber influence the fresh, mechanical, brittleness and crack characteristics concrete compared with Normal Plain Concrete (NPC)?
3. What are the impacts of bamboo fiber incorporation on the durability properties of concrete over 365-day period?
4. How does the addition of bamboo fiber affect the drying shrinkage properties of concrete hybrid, and can a better mathematical model be developed to predict this time-dependent behaviour where existing models fail?

1.3 Objectives of the study

This study addressed the mechanical, durability, and time-dependent characteristics of Bamboo Fiber Reinforced Concrete (BFRC). The study was conducted on one of the two indigenous species, namely Yushania alpine (Arundinaria Alpina), commonly known as Highland Bamboo, when used as fiber in concrete production.

The following are the specific objectives of this study.

1. The characteristics of bamboo fiber extracted by various methods
2. To examine the mechanical properties of Bamboo Fiber Reinforced Concrete (BFRC) made from varying volume fractions of Yushania alpine bamboo fiber and make a comparison with Normal Plain Concrete (NPC)
3. To assess the durability of concrete reinforced with varying percentages of Bamboo fiber (BFRC)
4. To examine the shrinkage characteristics of Bamboo Fiber Concrete Composite (BFRC) and develop a shrinkage prediction equation

1.4 Scope

The experiment was conducted on Bamboo Fiber Reinforced Concrete made from the indigenous Bamboo species. It is true that concrete by itself is a composite material; however, to emphasize the aim of this research, the composite will contain bamboo fiber and be named Bamboo Fiber Reinforced Concrete. The research will center on the assessment of the impact of various extraction techniques on bamboo fiber, followed by examination of the performance of Bamboo Fiber Concrete Composite from mechanical, durability, and shrinkage perspectives.

The scope of this research encompasses a comprehensive evaluation of bamboo fiber reinforced concrete (BFRC), beginning with an analysis of the physical, tensile and chemical characteristics of bamboo fibers extracted through various methods. Prior to the mix design process, a rigorous laboratory investigation of the sand and coarse aggregates will be conducted to ensure material quality. The study focuses on the specific mix proportioning of BFRC using a matrix composed exclusively of Ordinary Portland Cement (OPC), particularly excluding the use of any chemical admixtures.

The core assessment involves a detailed examination of the mechanical behavior of BFRC, established through a direct comparison with Normal Portland Concrete (NPC). Furthermore, the research evaluates the long-term performance of the composite by investigating the impact of bamboo fiber on the durability of the concrete. Finally, the study examines how the incorporation of these natural fibers influences the shrinkage behavior; which is time dependent characteristics, of the concrete matrix.

1.5 Significance of the study

This research aims to explore and unveil the fundamental behaviors of fibers extracted from indigenous highland bamboo using various techniques, providing a comprehensive understanding of their potential as a reinforcing agent. Specifically, the study will investigate the mechanical characteristics and durability properties of concrete reinforced with these fibers, while simultaneously explaining the complex relationships between various mechanical characteristics. Furthermore, the investigation will address time-dependent characteristics, with a particular focus on the shrinkage behavior of the bamboo fiber-concrete hybrid. Ultimately, the findings of this study are intended to enrich the existing knowledge base of bio-fiber reinforced concrete, provide critical data for future building code development, and serve as a catalyst for subsequent research in sustainable engineering materials.

1.6 Outline of the dissertation

Nine chapters are included in this dissertation, and each chapter provides information and findings related to the research objectives. An outline of this thesis is shown below:

Chapter 1 presents a general introduction, questions, objectives, scope, and significance of the study.

Chapter 2 is concerned with the critical review of the relevant and related literature. This began by reviewing literature from the general to that related to the objectives of the study. A brief explanation about the bamboo plant is also incorporated here.

Chapter 3 provides the materials and methods used for the study.

Chapter 4 is dedicated to the result and discussions. The sub topics of this chapter address the followings.

- The characterization of bamboo fiber extracted from Yushania alpina using mechanical, chemical, and combined methods. The impacts of the extraction methods on the properties of bamboo fiber are presented by conducting FTIR, SEM, and TGA.

- The evaluation of the impact of the addition of bamboo fiber on compressive, split tensile, and flexural strengths of concrete. The impacts of the bamboo fiber on brittleness and cracking of concrete are prescribed in this part. Furthermore, the relationships among the mechanical properties and the trend of strength development are elaborated and presented.

- The effects of bamboo fiber in the durability properties of concrete. This will be addressed by conducting an experiment. The experiments are alkaline attack, acid attack, volume of voids, and absorption examinations of concrete reinforced with bamboo fiber.

- Presents bamboo fiber impact in the concrete shrinkage property. The existing prediction equations or models are to be evaluated in the concrete reinforced with bamboo fiber. Then, the proposed prediction model will be provided in this chapter.

- Show the impact of bamboo fiber in concrete pavement design, length computation, and ground floor slab design

Chapter 5 presents conclusions of this dissertation and recommendations for further research on bamboo fiber and bamboo fiber reinforced concrete.

2 Literature Review

2.1 General

Various industries have been utilizing steel, carbon, graphite, and glass fibers to reinforce polymer composites. These polymer matrix composites have been extensively examined for their high performance. Their end-of-life disposal mode is unknown because of their non-recyclable and non-degradable nature. Because of climate change and the environment concerns, researchers are interested in using natural fibers in place of synthetic fibers. Natural fibers are classified as animal fibers containing protein, such as silk, wool, hair, etc., and plant fibers – bamboo, sisal, hemp, flax, etc. get attention for environmental concerns(Subash. S, Stanly Jones Retnam. B, 2017).

However, exploitation of fiber-reinforced concrete in building structures have been rather limited. This has been mainly due to minimum experimental research on the characteristics of structural elements and, consequently, the deficiency of design guide lines in building standards and codes. It was not until the 2008 edition that fiber-reinforced concrete was documented as a structural material in the ACI Code(James K. Wight, 2012). However, the utilization of fibers in construction is an old technique and basically founded on waste products collected after harvesting crops(Rota Font et al., 2024). In concrete construction, to obtain fiber from a sustainable and renewable source is a timely research area, which includes fiber obtained from bamboo(Koichi Minami and Masakazu Terai, 1999).

This literature review for the present study is done broadly in the direction of concrete reinforced with bamboo fiber for sustainability.

This comprehensive literature review, which is being conducted in relation to the current study, is primarily concentrated on the characteristics of concrete that incorporates bamboo fiber as a reinforcement material, with the predominant aim of enhancing sustainability and environmental viability in construction practices. Towards this aim, some insightful findings of the literature survey are included on other fibers that are plant based. The literature review navigates through the basic fiber concept, existing fiber applications, plant fibers, bamboo plant, bamboo fiber, how to get bamboo fiber, and various properties of concrete containing bamboo fiber.

2.2 Fibers

Fibers are short, discrete materials commonly randomly distributed throughout a matrix, which can be mortar, concrete, or asphalt. The purpose of applying fibers in these matrices is to enhance the engineering properties and create a structure that better responds to internal actions (C. Gong et al., 2023; Mohajerani et al., 2019; Mukhopadhyay & Khatana, 2015; Wahyudi & Mudiyono, 2024).

The use of fibers for strengthening is not a new concept. The notion of fibers in a brittle mix was originally reported by Egyptians, who utilized animal hair and straw as reinforcement for bricks and walls in their homes (Kavitha & Felix Kala, 2016)(Phong et al., 2012). The fibers in different forms, such as natural fibers, etc., were mainly used to enhance the load-carrying capacity of elements. Their use dates back to the Roman period (300 BC–476 AD), wherein the earliest concrete was found to contain fibers. Straw-reinforced mud bricks were found at a number of historic and old sites in the Middle East, dating back to approximately 10,000 years ago. The indigenous populations in the USA were using sun-dried adobe bricks, which were believed to be prepared by mixing sand, clay, and straw(H. Singh, 2022).

Since ancient times, fibers have been used to strengthen materials that are not durable. A pueblo house constructed around 1540, thought to be the oldest house in the USA, is constructed of sun-baked adobe reinforced with straw(Association, 2022). Teff straw is one of the oldest natural fibers that has been used for mud plastering and mud-brick baking as a reinforcement fiber since ancient times in Ethiopia(Tadesse, 2019).

Fibers exist in different forms, and because of this, there are various categories of them. Fibers are obtained from various sources that can be broadly categorized into synthetic or man-made and natural, where each of these is further dissected as shown in Figure 2.1 and Figure 2.2(Ghori et al., 2018; Lv et al., 2022; Preethikaharshini et al., 2022).

Natural fiber encompasses a wide range of materials that are derived from many sources, including plants, animals, and geological phenomena(Suwinarti et al., 2023). Fibers obtained from various chemicals, or regenerated from plant fibers, are categorized as man-made or synthetic fibers(Stegmaier et al., 2005)(R. A. Khan, 2023).

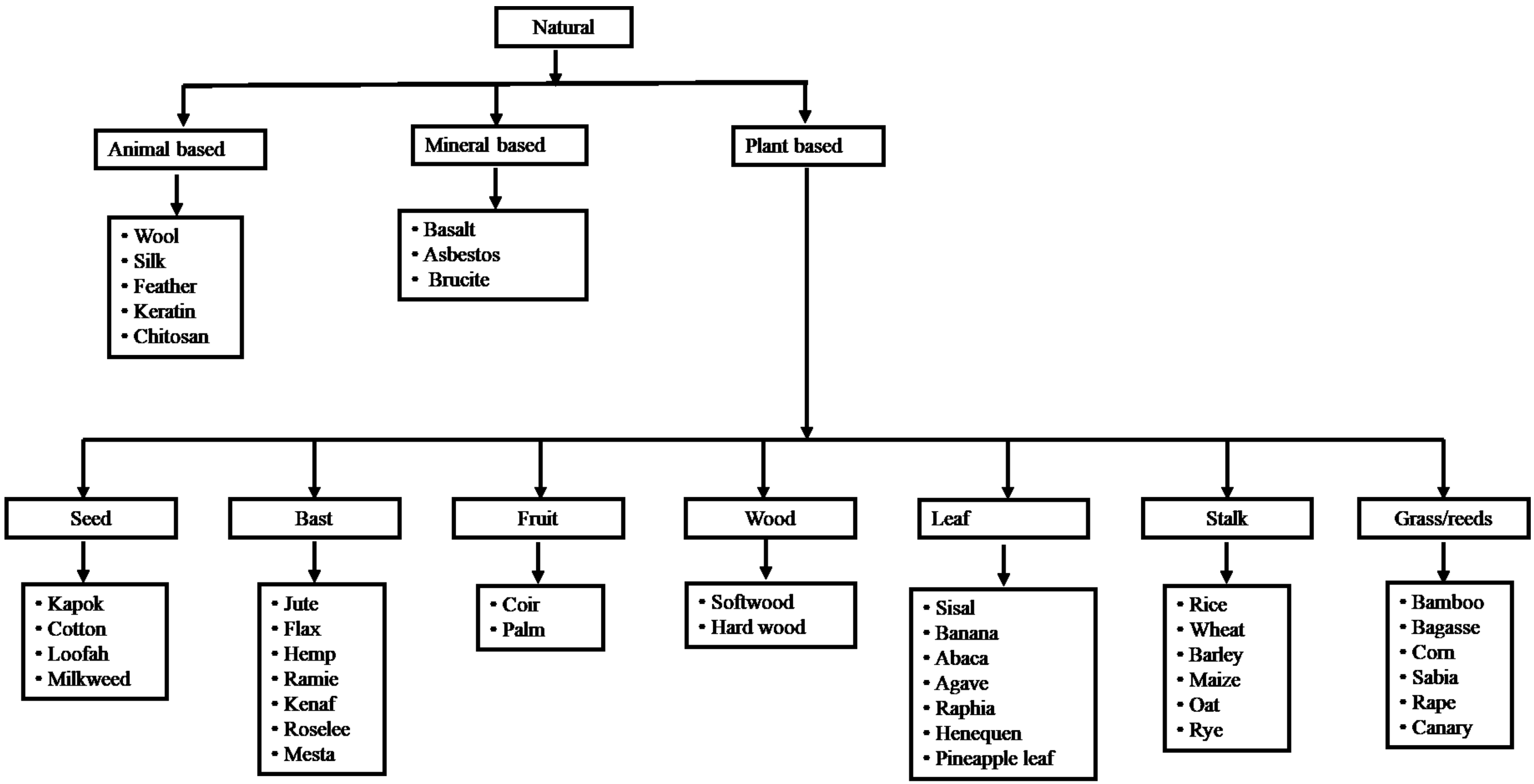

Figure 2.1. Classification of natural fibers

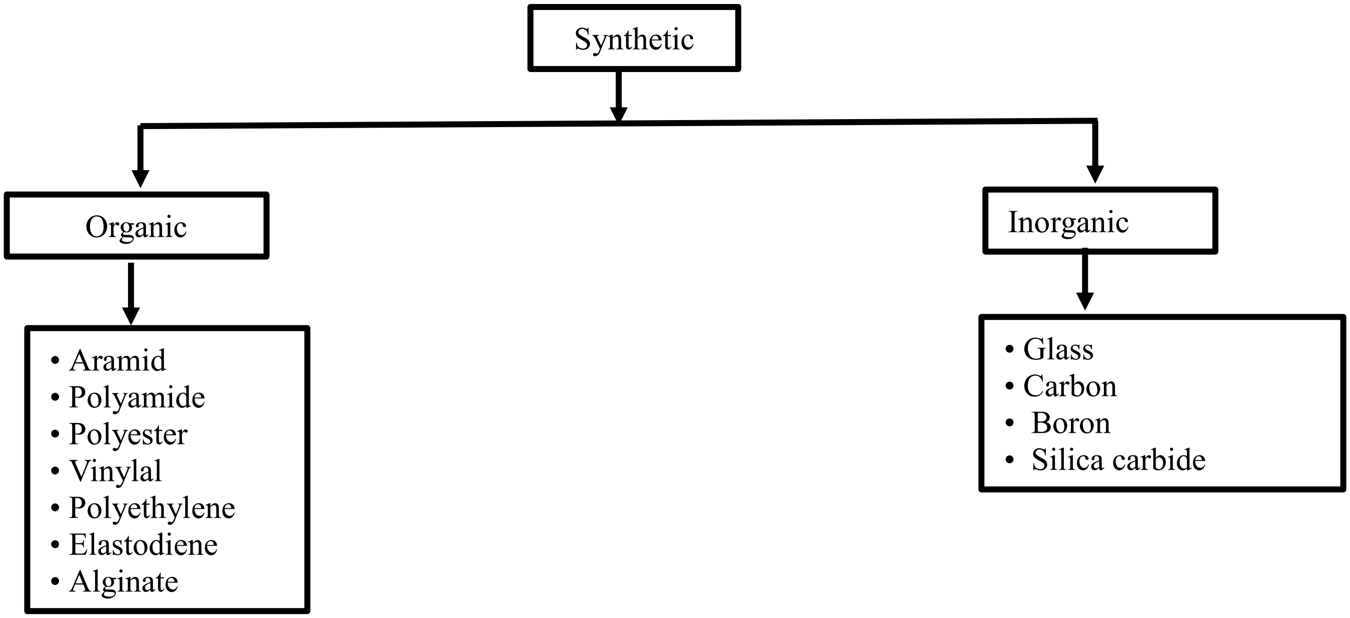

Figure 2.2. Classification of synthetic fibers

2.2.1 Fibers Utilizations

Fibers are added to concrete to complement its brittleness and tensile weakness. Short discontinuous fibers are mixed uniformly and dispersed throughout the concrete to arrest cracks that appear on the concrete due to shrinkage and loads(Er. H. Mehra, 2004).

Table 2.1. Application of fibers

Fiber	Applicability
Steel	Precast panels, sewer pipe, concrete roof, industrial floors, tunnel components, bridge panels, shell structures, pavement, foundation, and precast concrete slab
Glass	Bridge decks, pressure vessels, and tunnel linings
Polypropylene	Piles, walkways, floor slabs, slabs on grade, shotcrete, underwater pipes
Asbestos	Pipes, fireproofing materials, sewer pipes, and roofs
Carbon	Boat hulls, scaffold boards. Membrane structures
Nylon	Floor slabs, slabs on grade, shotcrete

Thus far, steel fibers, glass fibers, asbestos, carbon fibers, and polyethylene fibers have been exploited in concrete in various parts of infrastructures as presented in Table 2.1(Mohajerani et al., 2019)(V. S. Parameswaran, T. S. Krishnamoorthy & Balasubramanian, 2013)(Abbasi Dezfouli, 2019). The limitations of man-made fibers due to their non-degradability involve disposal, recycling, and impact on the environment, leading to pollution of the surrounding environment. Some of them are produced from finite sources, which means they are nonrenewable(Senthilkumar et al., 2018)(Gao et al., 2022).

2.3 Plant fibers

These are thin threads obtained from plants, generally composed of cellulose, hemicellulose, and lignin(Jones et al., 2010). The plentiful obtainability and accessibility of plant fibers are the primary reasons for a renewed interest in sustainable technologies. When considering composite materials, their importance spans environmental friendliness, lightweight design, and encouraging engineering characteristics(Ramesh et al., 2017).

The behaviours of plant fibers are governed by:

- the proportions of cellulose, hemicellulose, and lignin (Suwinarti et al., 2023)
- harvest time (Liu et al., 2015)
- extraction technique(Diouf & Gning, 2024)
- aspect ratio (Senthilkumar et al., 2018)(Xun Gao, Deju Zhu, Shutong Fan, Md Zillur Rahman, Shuaicheng Guo, 2022)(Sayed et al., 2023).
- treatment method(Muthuselvan Balasubramanian, R. Saravanan, 2024)

Table 2.2. Mechanical properties of some plant fibers (Osorio et al., 2011)

Fiber	Density (g/cm^3)	Diameter(μm)	Elongation at failure (%)	Tensile strength (MPa)	E-Modulus (GPa)
Bagasse	-	490	-	70	-
Coir	1.2	-	30	175	4-6
Cotton	1.5-1.6	20	7.0-8.0	287-597	5-13
Curaua	1.38	66	3.9	913	30
Flax	1.5	50-100	2.7-3.2	345-1035	50-70
Hemp	1.10	120	1.6	389-900	35
Henequen	-	180	3.7-5.9	430-570	10-16
Jute	1.3	260	1.5-1.8	393-773	26
Kenaf	1.31	106	1.8	427-519	23-27
Pineapple	1.32	-	2.4	608-700	25-29
Ramie	1.5	34	3.6-3.8	400-938	24-32
Sisal	1.5	50-80	2.0-2.5	337-413	8-10
Bamboo	0.88-1.1	100-200	-	391-713	18-55

Fibers obtained from various plants were examined, and various important parameters that have practical implications are presented in Table 2.2.

Due to the acceptable engineering properties, plant fibers are getting applications in various lines. Long bamboo fibers to be used as reinforcement in structural composites was obtained by the mechanical extraction procedure. A single-fiber tensile examination at four various span lengths for fibers of the bamboo species Guadua angustifolia was conducted. Strength values of 800 MPa and Young's modulus of 43 GPa were attained. Composites of unidirectional bamboo fiber/epoxy (BFC) were produced with untreated and alkali-treated fibers to assess the effectiveness of the new reinforcing material. Flexural experiments were conducted on composites with two fiber orientations (longitudinal and transverse).

Table 2.3. Application of plant fibers

Fiber type	Applicable area	References
Sisal	building materials, aerospace, sport industry, consumer items, automobile parts, geotextile, slope stabilization	(F. Khan et al., 2024)(De Castro Ho et al., 2024)(Sanjay et al., 2016)(Shah et al., 2016)
Flax	building materials, consumer items, automobile parts, aerospace, and the sports industry	(De Castro Ho et al., 2024)(Sanjay et al., 2016)(Shah et al., 2016)
Hemp	building materials, consumer items, automobile parts, aerospace, and the sports industry,	(De Castro Ho et al., 2024)(Sanjay et al., 2016)(Shah et al., 2016)
bamboo	building materials, consumer items, automobile parts	(Phong et al., 2012)(C. Chen et al., 2022)
Jute	medical, consumer items, building materials, automobile parts, geotextiles, slope stabilization	(F. Khan et al., 2024)(Radhakrishnan, 2014)
Kenaf	Building materials, erosion control, geotextile, aerospace, and the sports industry,	(F. Khan et al., 2024)(Shah et al., 2016)

The longitudinal flexural strength is higher when untreated fibers are used, while the treatment is advantageous in the longitudinal flexural stiffness of the composite. At lower alkali concentrations, the transverse strength shows an increase, but the transverse three-point bending strength of untreated bamboo in epoxy is already quite high at around 33 MPa. The results demonstrate that these bamboo fibers present a natural and renewable option to reinforce composites in many applications where these days glass fiber and traditional natural fibers are used (Osorio et al., 2011). Table 2.3 summarizes some of the plant fiber utilizations.

Natural Fiber-reinforced composites are used for strengthening of old or ancient masonry, which is important to conserve man-made heritage structures, specifically old buildings constructed using masonry technology(Miur, 2013). Ensuring the longevity of structures is another way of addressing sustainability. That means they have a role in reducing waste and the rate of depletion of natural resources to replace existing aged structures.

Plant fibers are considered important engineering materials, despite having hydrophilic properties. For these reasons, scholars conducted intensive research to address these shortcomings of plant fibers. According to Issam E. et (Karthik et al., 2024), the drawback of plant fibers in relation to moisture can be improved through surface modifications like chemical treatments to enhance fiber-matrix compatibility. Due to the employment of various treatment methods, the mechanical properties, durability, and bond with the matrix showed improvement(Muhammad Nasir Amin et al., 2022)(Z. H. Zhu et al., 2020)(Matykiewicz, D., Barczewski, M., Mysiukiewicz, O., & Skórczewska, 2019)(Hill, C.A.S. and Abdul Khalil, 2000).

2.4 Bamboo plant

Bamboo belongs to a grass family among the seven groups of plant fibers, namely – grass, stalk, wood, fruit, seed, bast, and leaf (Jawaid & Abdul Khalil, 2011) (Subash. S, Stanly Jones Retnam. B, 2017). The subfamily Bambusoideae of the grass family Poaceae is where the bamboo plant belongs. Bamboo is a natural lignocellulosic composite comprising cellulose fibers embedded within a matrix of lignin and hemicellulose(Gupta, Anu and Kumar, 2008). On the planet Earth, bamboo encompasses 1225–1662 species in approximately 75–105 genera(Emamverdian et al., 2020)(Canavan et al., 2017). The global bamboo area coverage is more than 36 million ha(Kassahun & Dawuro, 2014). Bamboo, a perennial plant, is basically divided into two major parts: the underground part of the stem is called rhizomes, and the upper portion, i.e., stem, is called culms(Z. Ahmad et al., 2021).

In contrast to other plants, it initially grows in full diameter from the ground and continues rising up to maximum height without branching until 3–4 months old, and at this point, leaves and branches appear from nodes. The main parts of a bamboo stem are Cavity, diaphragm, node, branch, internode, and wall. Rhizomes, roots, culms, branches, leaves, and flowers are the primary components of a bamboo plant. The main parts of a bamboo stem are shown in Figure 2.3.

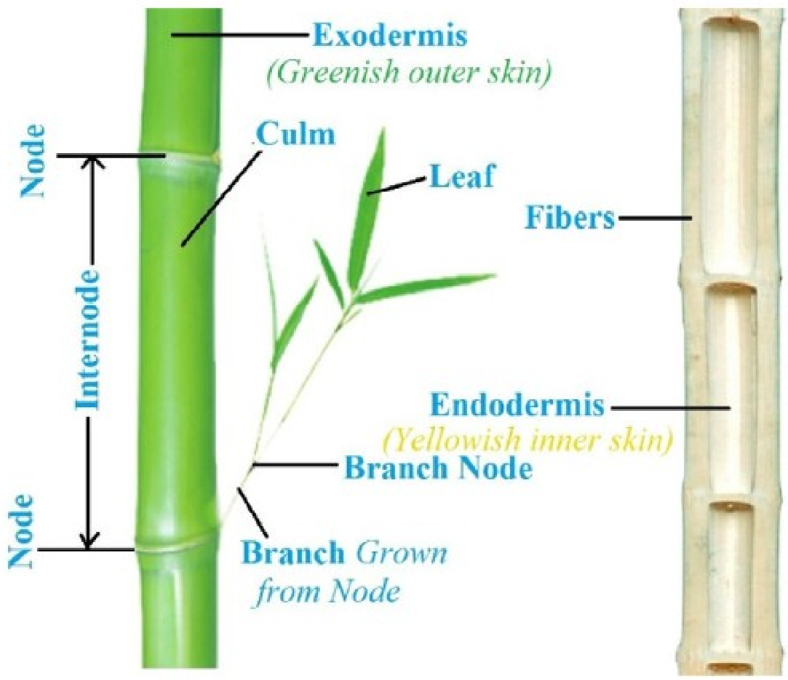

Figure 2.3. Different parts of bamboo steam (Rocky & Thompson, 2018)

An internode or culm is the hollow cylindrical portion between two nodes. Exodermis is the outer part of the bamboo stem that comprised of the green portion with dense vascular bundles. Endodermis is the inner part of the stem which comprised of the yellow portion with rare vascular bundles. The main cellulosic part is found between the exodermis and endodermis (Rocky & Thompson, 2018).

The culm is generally composed of about 50% parenchyma cells, 40 % fibers, and 10 % vascular bundles (Vessels, sieve tubes with companion cells). Slender form, long, and often forked at the ends characterized the fibers. They exist around the vascular bundles as sheaths and as isolated strands. Forty percent of the mass of the culm is a fiber. The vascular bundle contains the two metaxylem vessels, fibers, and the metaphloem of sieve tubes with companion cells. The primary chemical ingredients of the culm tissue are cellulose (73.83%), hemicellulose (12.49%), and lignin (10.16%). The density of bamboo differs from about 0.4 to 0.9 g/cm^3, depending on the anatomical structure, such as the quantity and distribution of fibers around the vascular bundles. Accordingly, density increases along the culm from the bottom to the top and from the inner layer to the outer part (Ramprasad et al., 2018).

Bamboo is widely found in Asia, Africa, and Latin America, though its geographic range is primarily determined by climatic conditions. It is widely spread in the tropical and subtropical zones between approximately 46°N and 47°S latitude(Troya Mera & Xu, 2014). The global bamboo plant distribution is shown in Figure 2.4. Most developing countries are located within the natural habitat of bamboo, one of the strongest naturally growing materials. It is not unreasonable to consider its impact on the local building and construction industry. Therefore, it is meaningful to find advantage from bamboo's fast growth, its unrivaled capability to store CO2, its encouraging mechanical strength and renewability, and activate all these features in a new innovative material technology that delivers a lighter, stronger, and inexpensive material alternative to steel that corrosion does not have an impact on(Dirk, 2014). Bamboo can be used as an alternative in regions where steel is scarce(I. K. Khan, 2014).

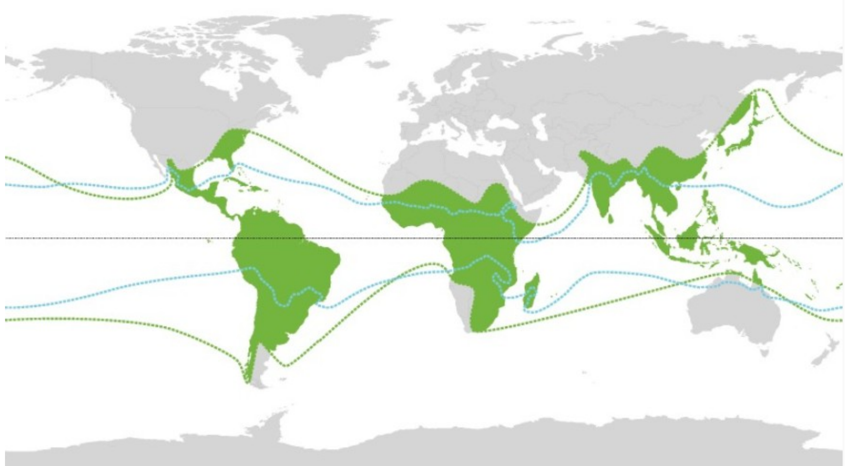

Figure 2.4. Global bamboo natural bamboo habitat (Hebel et al., 2015)

A total of 115 species are widely distributed among 48 countries in the African region. In Africa, a total of 115 species are found widely distributed among 48 countries. This covers wide areas that span from the western coast of Senegal to the eastern part of Mauritius, and it stretches from Morocco in the north to South Africa in the south(Bahru, 2021).

Ethiopia has a vast bamboo resource base that puts it among the countries in the world endowed with it. The country has 1.47 million ha of bamboo coverage, which is 7% of the global share and 67% of the African share. There are basically two bamboo species which are indigenous, namely Oldeania alpina (Yushania Alpina) and Oxytenanthera abyssinica, that are commonly known as highland and lowland bamboo, respectively(Mekonnen et al., 2014)(Sebrala, 2021). The land coverage or distribution of these species is shown in Figure 2.5.

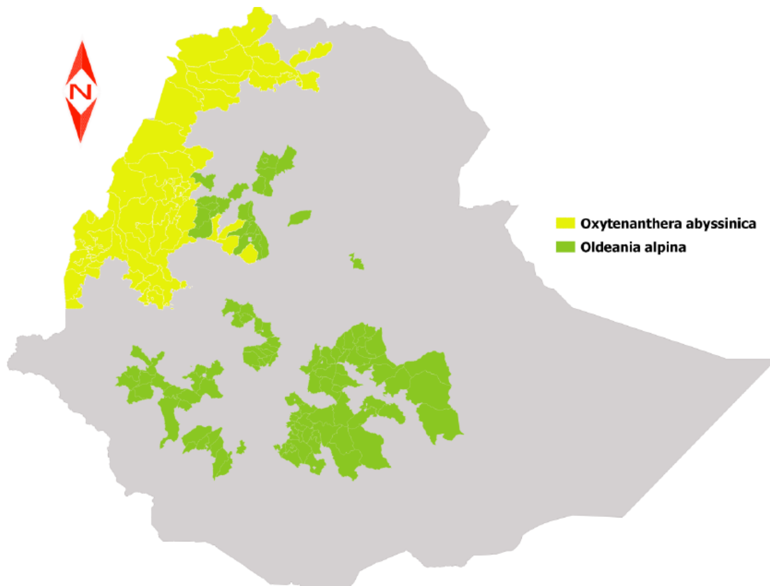

Figure 2.5. Indigenous bamboo distribution in Ethiopia (Sebrala, 2021)

These two indigenous bamboo species are categorized in Category I, which is among the 44 globally identified as a priority list of bamboo species(Thang et al., 2022). In addition to the native species, Ethiopia has introduced twenty-three different bamboo species from seven genera, brought from Asia and South America, since 2007, for their various economic advantages. The adopted species were grown successfully (Mulatu et al., 2016a; Tesfay & Negusse, 2024).

Bamboo is unique because it can address the three human basic needs: food, shelter, and clothing (W. Liese, J. Welling, 2015),(L. Wang, 2010),(Gupta & Kumar, 2008). Good mechanical characteristics, possibility of harvest within four years, ability to grow by itself after cutting, higher fiber yield, less biomass waste, and contribution to the reduction of unemployment are attributes that make the attractive values to select use of extracted fiber from Bamboo(Reta, 2017)(Trujillo et al., 2012) Bamboo has very good mechanical properties in comparison with its weight due to longitudinally aligned fibers (Banik, 2015). In Asia, Bamboo is known as the poor man's timber/poor man's gold/ green gold because growing, harvesting, and processing are essential subsistence activities (Gupta, Anu and Kumar, 2008).

Bamboo, starting from vegetation up to utilization, plays a significant role in avoiding air pollution, and even after the end of providing service, it degrades easily (Bentur & Mindess, 2020). Bamboo is a candidate species with a high potential for carbon sequestration and fixation (Zhuang et al., 2015)(Chaudhary et al., 2024). Moreover, bamboo plants have tremendous potential to avert environmental pollution by absorbing nitrogen from the air and assist in keeping or reviving forest coverage in a short time because a forest tree takes nearly 60 years on average to be replaced after cutting; while the bamboo plants may take very short years (S. Ahmad et al., 2014) (Rocky & Thompson, 2018).

The amount of fiber that can be obtained from a plant is the other parameter when considering the supply of fiber. According to Trujillo (Trujillo et al., 2012), bamboo has the highest fiber yield compared with other plants and shows acceptable engineering properties. Studies show that per equal unit of load-bearing capacity, bamboo requires the least energy for its production, which is followed by timber, reinforced concrete, and steel(Liese, 1985).

Bamboo helps to conserve biodiversity, manage soil and water, provide biomass, and assist the rural economy. Bamboo can play a key role in many of the Sustainable Development Goals (SDGs), but although the goals are interrelated, the relevance of bamboo is not the same for all. Moreover, as bamboo does not grow universally on our planet, the relevance of bamboo for each SDG differs from nation to nation(H. Zhao et al., 2022)(HansFriederich, 2021). Seven of the 17 Sustainable Development Goals identified by the United Nations that bamboo can contribute to are marked in Figure 2.6. Countries considered bamboo as one means to reduce the unemployment rate by planning and implementing strategies(Gupta, Anu and Kumar, 2008).

In another document, Goal 2 and Goal 3 are considered that bamboo has roles. Bamboo is well-suited to several of the UN Sustainable Development Goals (SDGs), as it plays important roles in biodiversity, land restoration, and livelihood enhancement. Specifically Goal 1: No Poverty, Goal 2: Zero Hunger, Goal 3: Good health and Well-being, Goal 6: Clean Water and Sanitation, Goal 7: Affordable and Clean Energy, Goal 8: Decent Work and Economic Growth, Goal 11: Sustainable Cities and Communities, Goal 12: Responsible Consumption and Production, Goal 13: Climate Action and Goal 15: Life on Land are areas of SDGS where bamboo has potential to contribute (Group, 2024).

Figure 2.6. Identified bamboo contribution for SDGs (H. Zhao et al., 2022)

2.5 Bamboo fiber

Bamboo fiber can be viewed as a composite, as it consists of cellulose microfibrils in an amorphous matrix of lignin and hemicellulose(Shah et al., 2016). Majorly, the chemical components of bamboo fiber are cellulose, hemicellulose, and lignin in proportions of 38.91-73.53%, 12.49-30.63%, and 18.57-26%, respectively(Geremew et al., 2024; JI, 2018; Tolessa et al., 2017)(Kudva et al., 2024). The bamboo fiber orientation is parallel to the longitudinal direction of the culm.

Parenchyma cells and the sclerenchyma cells are constituents of tissues that build up the internal structure of bamboo. These parenchyma cells consist of vascular bundles. These vascular bundles play a major part in the strength. The number of vascular bundles present in it determines the strength of the fibers. The higher the vascular bundles higher the strength of fibers(Mahesh & Kavitha, 2016).

The density of bamboo fiber varies due to the species type, age, method of extraction, and the treatment method employed(Kudva et al., 2024)(Awotwe-Mensah et al., 2024). Treatment or extraction methods conducted under an alkaline environment showed an increase in the density of bamboo fiber(Kudva et al., 2024). The range of density of bamboo fiber is between 0.451 and 1.26g/cc(Kudva et al., 2024)(Rusch, 2019).

The tensile strength of the bamboo fiber is comparatively greater among the plant fibers(Gao et al., 2022). Studies show that bamboo fiber has tensile strength as high as 800 MPa(Osorio et al., 2018).

Bamboo fiber can be used as a feasible substitute for glass and polymer fiber (Nabi Saheb & Jog, 1999), (Behera et al., 2018) as well as a green and sustainable or environmentally friendly fiber reinforcement (Mechanics, 2019)(Trujillo et al., 2012). Bamboo fibers have been useful in many industries, ranging from pulp, paper, textile, and part of automotive through to construction(Phong et al., 2012). Furthermore, the exploitation of bamboo fiber in building materials reduces the carbon footprint(Y. Hu et al., 2025).

2.6 Bamboo fiber extraction

Bamboo is composed of cellulose fibers embedded in a lignin matrix(Chaowana et al., 2015). Fibers obtained from the inner culm wall have the best properties. On the other hand, the location of the fiber over the culm length does not have a substantial influence on the mechanical properties(Osorio et al., 2011).

There are methods to extract fiber from bamboo culms. These are mostly mechanical, chemical, and a combination of mechanical and chemical extraction. However, there are studies that have shown additional methods, known as the biological extraction method and a combination of mechanical, biological, and chemical methods(Rocky & Thompson, 2018; Subash. S, Stanly Jones Retnam. B, 2017).

2.6.1 Mechanical extraction method

Under this method, there are different extraction techniques like steam explosion or heat steaming, crushing, grinding, rolling in a mill, and retting. The mechanical extraction method is good because it has less environmental impact.

Bamboo fibers were obtained or extracted using the mechanical method as shown in Figure 2.7, and different percentages of fiber content in concrete were studied to get the optimum value(Kavitha & Kala, 2016).

Raw Bamboo | Striped Bamboo | Striped Bamboo under roller | Bamboo fiber

Figure 2.7. Mechanical production of Bamboo fiber (Kavitha & Kala, 2016)

2.6.1.1 Steam explosion technique

To effectively separate the fibrous and non-fibrous parts of the culms, the prepared bamboo strips are to be placed in a steam explosion chamber(Rocky & Thompson, 2018). In the steam explosion process, the cell walls of the fibers are cracked. In addition the bamboo fibers become soft, enabling their extraction(Zakikhani et al., 2014b). In this technique, 2 MPa pressure and 210ºC temperatures for 5 minutes applied on the bamboo chips. The lignin is separated from the cell wall of the fiber (Shao et al., 2009).

2.6.1.2 Crushing

In this method a roller crusher is used to cut the raw bamboo into small pieces. Then, by a pin-roller the small pieces were extracted into coarse fiber. In order to remove their fat, the coarse fibers were boiled at 90 °C for 10 hours ahead of putting them in a dehydrator. Then, they were dried in the rotary dryer(Phong et al., 2012).

2.6.1.3 Grinding

Culms of bamboo without nodes were sliced into strips and immersed in water for 24 h. Then, a knife was used to cut the drenched strips into smaller pieces. The wider strips were fed through an extruder, and small bamboo chips were found by cutting the longer strips. Next, short bamboo fibers were obtained by grinding bamboo chips with a high-speed blender. This step was maintained for 30 min. Various sieves with various apertures were used to separate the fibers by size. At the end, the extracted fibers were dried in an oven for 72 h at 105 °C (Zakikhani et al., 2014b).

2.6.1.3 Rolling in a mill

Fiber extraction was done using a rolling mill in a different approach. One approach of extraction was to soak small pieces of bamboo that are obtained from the culm, pass them through a rolling mill. The other approach was that those pieces were passed through a rolling mill without soaking. Another approach was passing through the roller was done after sliced bamboos were steamed and soaked (Subash. S, Stanly Jones Retnam. B, 2017).

2.6.1.4 Retting

For three days, stripped obtained from peeled bamboo culms were soaked in water and then beaten, scraped with a sharp-edged tool, and finally combed. Others avoid scrap and comb instead; raw bamboo was simply cut into several longitudinal parts that were put in water at room temperature for two months. Anaerobic and aerobic retting methods are proven techniques for separating the bundles from the culm(Zakikhani et al., 2014b).

2.6.2 Chemical extraction method

Caustic chemicals, such as sodium hydroxide (NaOH), sodium triphosphate ($Na_5P_3O_{10}$), sodium sulfate (Na_2SO_4), sodium carbonate (Na_2CO_3), sodium hydrogen phosphate (Na_2HPO_4), sodium silicate (Na_2SiO_3), and sodium citrate ($C_6H_5Na_3O_7$) are conventional chemicals used for extracting fibers in this method(Fu et al., 2012).

The chemical extraction techniques, such as chemical retting and alkali or acid retting, are used to remove or reduce the lignin content from the fibers(Subash. S, Stanly Jones Retnam. B, 2017).

2.6.2.1 Chemical Retting

On one study bamboo culm was sliced into 2cm strips and the strips were roasted at 150°C for 30 minutes. The strips were then soaked in water for 24 hours at 60°C and dried in open air prior to eliminate further impurities. Further, the fiber bundles were cooked with 2% sodium silicate, 2% sodium sulphate, 2% sodium polyphosphate, and 0.5% NaOH (w/v) solutions at 100°C for 60 minutes at 1:20 bamboo to liquor ratio. The fibers were then washed with hot water and treated with 0.04% xylanase and 0.5% diethylene triamine pentacetic acid at 70°C with pH 6.5 for 60 minutes. Another one, the fibers obtained were again cooked at 100°C for 60 minutes with the same procedure, but with 0.7% NaOH. The fibers were then put in a polyethylene bag and bleached with 0.5% sodium silicate, 4% H_2O_2, and 0.2% sodium hydroxide for 50 minutes. The liquor ratio was kept at 20, and the pH was maintained at 10.5. Lastly, the fibers are treated with 0.5% sulphuric acid for 10 minutes, and after emulsification for 5 days, refined bamboo fibers were obtained (Subash. S, Stanly Jones Retnam. B, 2017).

In another study, bamboo culm was cut in the longitudinal direction with a slicer into thin strips. The fibers separated manually were soaked in Zn $(NO_3)_2$ solution with 1%, 2%, and 3% concentrations at a 1:20 material to liquor ratio. These fibers were put at 40°C for 116 hours in neutral pH and kept in a BOD incubator, and then they were boiled in water for 1 hour (V. Kaur et al., 2013).

2.6.2.2 Alkali or Acid retting

In the alkali retting method, strips of bamboo were cooked with 1.5N NaOH solution in a stainless-steel container at 70°C for 5 hours. Next, the strips of bamboo that were alkali-treated were pressed using a press machine, and by using a steel nail, fibers were separated. Finally, these extracted fibers were washed by water, and the extracted fibers were dried in an oven(Ichihara, 2004). In another study, bamboo strips in the size of chips were immersed in NaOH with 4% mass per volume for 2 hours. To obtain the fiber in pulp form, this process was repeated several times at a certain pressure (Kumar et al., 2010). In another exploration, small bamboo strips were immersed in 1N sodium hydroxide solution for 72 hours to facilitate the extraction of fibers(Deshpande et al., 1999).

2.6.3 Biological extraction method

Biological extraction methods are commonly applied to cellulose fibers in two different ways,

(1) exposure to suitable enzymes or

(2) microbial culture.

The enzymatic techniques are usually exploited to bamboo for fiber extraction. Among these enzymes are hemicellulose, cellulose, pectinase, xylanase, and lignin-oxidizing enzymes such as manganese peroxidases (MnP), lignin peroxidases (LiP), and laccases. This technique is not considered suitable for bamboo textile fiber extraction, due to it being an extremely slow and lengthy procedure; currently, the method is not economically feasible(Rocky & Thompson, 2018).

2.6.4 Combined extraction method

It is usually the use of both mechanical and chemical extraction methods, which is known as the combined extraction method.

There are two methods, such as compression molding and roller mill technique, which are usually used next to the chemical treatment. In this process, firstly, the bamboo strips are treated with alkali in both procedures. Then, the treated bamboo strips based on the compression molding method were pressurized between two plates with a 10-ton load. Starting bed thickness and time are two parameters that affect the quality of the fibers. In the second method, the alkali-treated strips were rolled by force between two rollers (Zakikhani et al., 2014a).

2.7 Impact of extraction methods on bamboo fiber

The extraction technique is one of the phenomena that determines the characteristics of bamboo fiber. The influences of the mechanical, chemical, and combined mechanical and chemical extraction methods on the mechanical and physical characteristics of bamboo fibers are given in Table 2.4.

Table 2.4. Bamboo fiber properties across different extraction methods (Zakikhani et al., 2014b)

Fiber	Extraction procedure	Young's modulus (GPa)	Tensile strength (MPa)	Fiber length (mm)	Density (gm/cm^3)	Fiber diameter (µm)
Bamboo	Mechanical					
	Steam explosion	17	516	-	-	-
	Steam explosion	36±13	441±220	-	-	15-210
	Steam explosion	28	383	-	-	-
	Steam explosion	35.9	441	-	-	0.8-125
	Steam explosion	35.45	615-865	-	-	-
	Steam explosion	25.7±140	308±185	-	-	195±150
	Rolling mill	-	270	220-270	-	100-600
	Grinding	18-30	450-800	-	1.4	-
	Retting	35.91	503	-	0.91	-
	Crushing	38.2±16	420±170	-	-	262±160
	Chemical					
	Chemical	19.67	341	-	0.89	-
	Chemical	18	450	10	1.3	270
	Chemical	22	329	-	-	-
	Alkaline	30	419	-	-	-
	Alkaline	26.1±14.5	395±155	-	-	230±180
	Combined mechanical and chemical					
	Chemical + Compression	-	645 Max:1000	>10	0.8-0.9	50-400 HC:150-250
	Chemical + Rolling mill	-	370 Max:480	120-170	-	HC:50-100

2.8 Fiber-reinforced concrete

According to E. N. Antoine 2018 (Naaman, 2018), fiber reinforced concrete (FRC) is defined as concrete with suitable discontinuous fibers added to it for the purpose of achieving a desired level of performance in a particular property (or properties). Fiber reinforced concrete is one of the categories of composite materials, as shown in Figure 2.8, produced by adding continuous (aligned) and discontinuous (short) fibers into the base matrix(Kaw, 2005)(Alene, 2013).

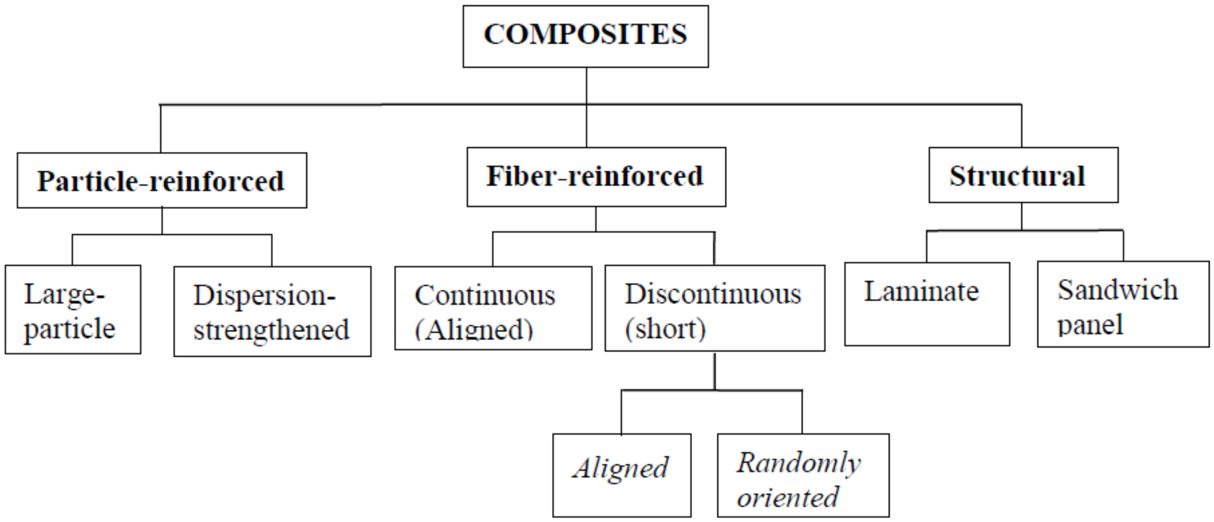

Figure 2.8. Composite materials classification

The fibers used can be steel, glass, synthetic, or natural. Traditional applications of fiber reinforced concrete include slabs on ground, tunnel liners, and architectural elements. The purpose of fibers in these elements have been primarily to use as a replacement of minimum reinforcement for cracking control and, to a lesser degree, replacement of minimum shear and/or flexural reinforcement. The amount of fibers added to the concrete depends on the type of fiber and target performance, but practical considerations limit the quantity of fiber in structural elements to approximately 1.5 percent by volume(James K. Wight, 2012). They can also be used in composite metal deck, pavement, embankments, shotcrete in mining, septic tanks, vaults, and manufactured concrete products like landscape products and shingles(Association, 2022).

2.9 Bamboo fiber reinforced concrete

A composite material produced from mixing of concrete and bamboo fibers of various lengths, diameters, and specified dosages is bamboo fiber reinforced concrete. The potential of bamboo fiber in concrete was examined through conducting experiments. The purpose of adding bamboo fiber into concrete is to complement the characteristics of concrete that are weak. These are the tensile strength, ductility, and cracking.

2.9.1 Characteristics of fresh bamboo fiber reinforced concrete

The fresh concrete properties refer to behaviours exhibited by concrete from the moment it is mixed until it hardens(Suryakanta, 2015). The fresh concrete properties have an impact on the application of the produced mix. Furthermore, they serve as very good indicators of the properties of concrete in its hardened state (Bheel et al., 2021).

Workability, segregation, and bleeding are the important fresh properties of concrete. There are various techniques to evaluate the fresh properties of concrete. Slump, compaction, flow, and penetration tests are some of the methods to check the quality of the concrete mix at the fresh state(Dinku, 2002)(Charles Camp, 2024).

As per J. Ahmad (J. Ahmad et al., 2023a), bamboo fiber reduced the workability of concrete, like other types of fibers such as steel. Studies have witnessed that the addition of bamboo in concrete reduced the workability and bleeding of concrete(J. Ahmad et al., 2023a)(Ede et al., 2020a). Taking into consideration workability, 1% fiber is considered the optimum value, which will give higher splitting tensile strength, compressive strength, and flexural strength (Kavitha & Kala, 2016).

2.9.2 Characteristics of hardened bamboo fiber reinforced concrete

2.9.2.1 Compressive strength

Materials' or structures' ability to bear uniaxial compressive force is the compressive strength. The value of the uniaxial compressive stress achieved when the material is in a state of collapse is the ultimate compressive stress(Siddique & Mehta, 2014). The compressive strength of concrete is determined by applying a load on standard cube or cylinder samples using a compressive testing machine until failure. The applied load changed to stress by taking the ratio of the applied load to the contact area between the machine and the samples.

The compressive strength value is the most utilized parameter to assure the quality of the concrete casted in construction sites. Moreover, it is one of the inputs in commercial software to conduct the design and analysis of various concrete structures. Therefore, the compressive strength is a very important parameter in the investigation of characteristics of concrete produced when mixing the usual ingredients with various materials. It is also an easy method to carry out and enables us to forecast other properties like split tensile, flexural, and modulus of elasticity.

Water to cement ratio, cement type, supplementary materials, aggregate, curing condition (moisture and temperature), age of concrete, and rate of loading are the factors that control the compressive strength(James K. Wight, 2012)(M. A. Salih et al., 2020).

The impact of the incorporation of bamboo fiber on the compressive strength of concrete was investigated on some of the species, and the findings of those studies are summarized and depicted in Table 2.5.

The conducted compressive strength studies end up with mixed results. Some indicated that they found an increment, and others a decrement. This is attributed to the variations of the species that imply variations of mechanical properties of the fiber, experiment design, and the interaction between the fiber and paste(Peng et al., 2024)(Zhong & Zhang, 2020)(Import, 2023)(Anokye et al., 2016).

Table 2.5. Compressive strength of concrete summary

Species type	Location	Duration	Bamboo dose	Dimension	Remark	Ref.
Not mentioned	Japan	56 days	1%, 2%, 3%	aspect ratio 50	Decreased	(Terai, 1999)
Phyllostachys Pubescens	China	28 days	0.13kg/m^3, 0.26kg/m^3, 0.39kg/m^3	15 mm x 20 mm, length 10, 20, 30mm	Increased	(X. Zhang et al., 2012)
Yushania Alpina	Gurage Zone, Ethiopia	28 days	0%, 0.1%, 0.2%, 0.3% be weight of concrete	Aspect ratio 30-100	Increased	(Reta, 2017)
Not mentioned	Nigeria	28 days	0.25%, 0.5%, 0.75%, 1.0% by weight cement	50mm length	Increased	(Ede et al., 2020a)
Not mentioned	China	28 days	0.5%, 1.0%, 2.0% by volume of concrete	aspect ratio 15-45	Decreased	(C. Zhang et al., 2013)
Bambusa Vulgaris	Malaysia	28 days	0.5%, 1.0%, 1.25% by weight of concrete	aspect ratio 40	Increased	(Osmi et al., 2024)
Not mentioned	India	28 days	0.5%, 0.75%, 1.0%, 1.25% by weight	aspect ratio 40	Increased	(Kavitha, 2018)
Not mentioned	Indonesia	28 days	1.0%, 1.5%, 2.0%, 2.5% by weight	2-3cm length	Increased	(Wulan et al., 2024)
Not mentioned	China	28 days	0.5%, 1.0%, 1.5% by volume	1cm, 2cm, 3cm length 0.18-0.25mm diameter	Increased	(Peng et al., 2024)
Not mentioned	India	28 days	1.0%, 1.5%	5X3X24mm	Increased	(Tejashwini & R, 2024)

2.9.2.2 Splitting tensile strength

The capacity of concrete to resist tensile loads is usually referred to as the tensile strength of concrete. The compressive strength of concrete depends on the tensile strength on the meso-scale(Talaat et al., 2021). Hence, the tensile strength of concrete has impacted the load-bearing behaviour of concrete structures; this is specifically true in unreinforced concrete structures. Moreover, when the stresses induced due to thermal and shrinkage effects reached the limit of the tensile strength of concrete, cracking happened. This is especially paramount phenomenon during the early ages of concrete. The composition of concrete, moisture, temperature, curing conditions, and age influence the tensile strength(Reinhardt, 2013).

The tensile strength of concrete determination is done by conducting an indirect method called split tensile strength. The test is carried out by applying a load on a standard cylinder along the longitudinal axis, where the line that connects the top contact point and the bottom contact point should pass through the center of the cylinder as shown in Figure 2.9(James K. Wight, 2012). Due to the applied load stress developed along the diameter of the specimen. This is localized compressive stress at the top and bottom and nearly uniform tensile stress across the rest part of the diameter as shown in Figure 2.9. The split tensile strengths of concrete reinforced with bamboo fiber showed an increment as shown in Table 2.6.

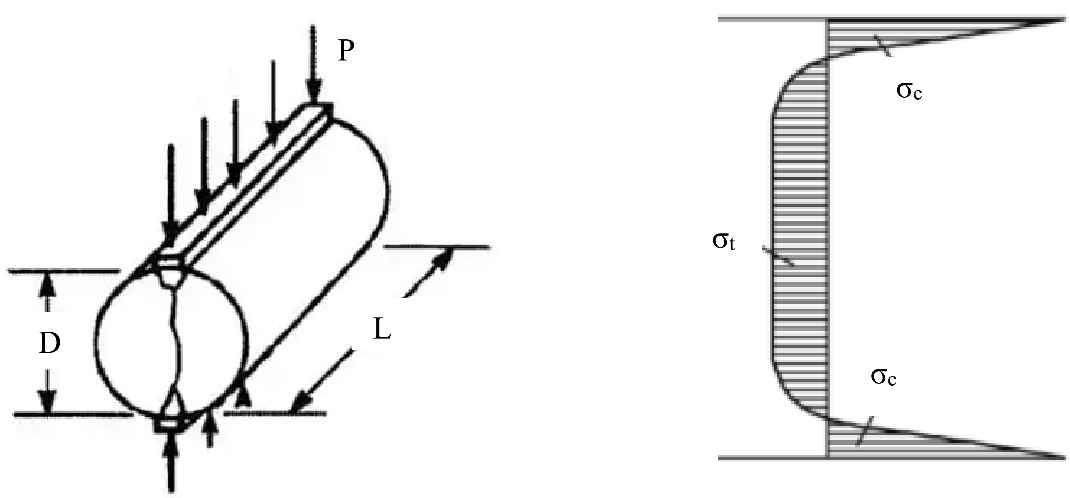

Figure 2.9. Splitting tensile applied load and stress distribution

2.9.2.3 Flexural strength

The other method for knowing the tensile strength is the flexural test. The flexural test is conducted by center point loading or two-point loading. The flexural tensile strength is also identified as the modulus of rupture. When the bending force acts downward on a simply supported beam at the ends, the fibers below the neutral axis experience tensile stress, and the extreme end fibers are exposed to the maximum tensile stress(Dinku, 2002). The modulus of rupture is the value of the maximum tensile stress at the extreme fiber. The flexural test assesses the ability of an unreinforced concrete beam or slab to withstand failure in bending(Taher et al., 2024). It is the most valuable parameter used in the design of road pavement structure(Hussain et al., 2020). The flexural tensile strengths of concrete reinforced with bamboo fiber showed an increment as shown in Table 2.6.

The addition of bamboo fiber into concrete improved both the split and flexural strength of the concrete. However, the experiment conducted by M. Terai and K. Minami (Koichi Minami and Masakazu Terai, 1999) showed a decrease in flexural strength of concrete due to the presence of the bamboo fiber in the concrete. The study revealed that the poor bonding between the fiber and the concrete contributed to this reduction.

Table 2.6. Splitting and flexural tensile strength of concrete summary

Species name	Location	Duration	Bamboo dose	Dimension of fiber	Observation		Ref.
					Split tensile	Flexural	
Not mentioned	Japan	56 days	1%, 2%, 3%	aspect ratio 50	Increased	decreased	(Terai, 1999)
Phyllostachys Pubescens	China	28 days	$0.13 kg/m^3$, $0.26 kg/m^3$, $0.39 kg/m^3$	cross section 15 mm x 20 mm, length 10mm, 20mm, 30mm	Increased	Not done	(X. Zhang et al., 2012)
Yushania Alpina	Gurage Zone, Ethiopia	28 days	0%,0.1%,0.2%, 0.3% by weight concrete	aspect ratio 30-100	Increased	Increased	(Reta, 2017)
Not mentioned	Nigeria	28 days	0.25%, 0.5%, 0.75%, 1.0% by weight cement	50mm length	Increased	Not done	(Ede et al., 2020a)
Not mentioned	China	28 days	0.5%, 1.0%, 2.0% by volume of concrete	aspect ratio 15-45	Increased	Increased	(C. Zhang et al., 2013)
Bambusa Vulgaris	Malaysia	28 days	0.5%, 1.0%, 1.25% by weight of concrete	aspect ratio 40	Increased	Not done	(Osmi et al., 2024)
Not mentioned	India	28 days	0.5%, 0.75%, 1.0%, 1.25% by weight	aspect ratio 40	Increased	Increased	(Kavitha, 2018)

Not mentioned	India	28 days	1.0%, 1.5%	5 x3 x24mm	Increased	Increased	(Tejashwini & R, 2024)
Not mentioned	China	28 days	0.5%, 1.0%, 1.5% by volume	1cm, 2cm, 3cm length 0.18-0.25mm diameter	Increased	Increased	(Peng et al., 2024)

2.9.3 Bamboo fiber reinforced concrete durability properties

Over the expected service life of concrete structures, they are expected to continue in good performance in rendering their functions by maintaining the appropriate strength and serviceability. The concrete through this service life must be able to withstand the deterioration due to the surrounding environment. Concrete that can exist and serve within a deteriorating environment is said to be durable(Neville, 2002). Durability property has a great contribution to the sustainability concept. Because the use of more durable materials implies a longer lifespan of structures through the reduction of the frequency of consumption of materials, which is directly related to the reduction of wastes and gases that have an impact on sustainability(Rauf et al., 2024; Zamathula et al., 2024). The long-term performance of concrete is influenced not solely by the mechanical properties that it develops over time but also significantly affected by the various environmental conditions to which it is subjected throughout its service life(Youssari et al., 2023).

It follows that concrete must be able to resist the processes of deterioration to which it can be expected to be exposed. It is necessary that every concrete structure should continue to perform its intended functions, that is, maintain its required strength and serviceability, during the specified or traditionally expected service life. Such concrete is said to be durable. It is important to notice that durability does not mean an unlimited life, nor does it mean resisting any action on concrete. Moreover, it is these days realized, although it was not so in the past, that, in many circumstances, routine maintenance of concrete is essential(Neville, 2002).

Durability of concrete mainly depends on the ease with which fluids, both liquids and gases, can enter into, and move through, the concrete; this is usually mentioned as the permeability of concrete; strictly speaking, the flow through a porous medium is referred as permeability(Neville, 2002). This is dependent on the material type and their proportion in the making of concrete, which has a direct influence on the response of concrete to an adverse environment. Moreover, the age of concrete exposed to the adverse environment affects the durability of concrete.

During the early age of concrete, the concrete is more of on fluid state where unhydrated cement has a higher proportion and the volume of solids is less(Seyam & Nemes, 2023). By this time chemicals can easily trace through the fluid and get the opportunity to access the unhydrated part to have chemical reaction. Therefore, early age exposure of concrete to an adverse environment critically affects the durability of concrete.

To examine the durability properties of concrete absorption, permeability, volume of voids, sorptivity, mercury intrusion porosimetry, acid attack, alkaline attack, chloride penetration, freezing and thawing, abrasion, and erosion tests to be employed on specimen sizes prepared based on standards. Despite the encouraging findings on mechanical qualities of bamboo fiber reinforced concrete, there have been very few even better to say none experimental explorations on the durability qualities(Chen, X., & Zhu, 2024).

D. M. Ali et al (Diana Mohamed Ali, Siew Choo Chin, Chao Bao, 2024) conducted a durability study on concrete containing bamboo and basalt fibers. It was a study conducted on hybrid fiber-reinforced concrete. The details information, like species type and years of the bamboo from which the fiber is extracted not mentioned in the study. The durability study was conducted for 90 days, and the experiment types were water absorption, acid attack, and water permeability. The experimental study showed that specimens of concrete reinforced with hybrid bamboo and basalt fiber reduction of 28.6% in water permeability and 3.9% in mass loss compared with the unreinforced control specimens.

S. Kavitha and D G Ashwini (Sajjala Kavitha and Ashwini D G, 2022) examined durability properties of bamboo fiber reinforced self-compacting concrete with ground granulated blast-furnace slag and alccofine. The bamboo fiber obtained from the undescribed species dose was 1.0%, and the experiment was conducted by putting specimens in a 5% solution of sulfuric acid and sodium sulphate. The evaluation was done by observing mass loss and compressive strength after 90 days. The investigation showed that concrete containing bamboo fiber showed similar levels of degradation of compressive strength, while causing less weight loss than the normal self-compacting concrete.

An investigation of the chloride-ion permeability of C30 concrete by adding fibers obtained from factory waste but unknown bamboo species with different treatments (untreated, treated with calcium hydroxide solution, and treated with sodium hydroxide solution) and different dosages was conducted by Yong L. et. al(Luo et al., 2024). The bamboo fiber length of 4cm at dosages of 2.01, 4.02, 6.03, 8.04, and 10.05 kg/m^3 was used for the preparation of the samples used for the subsequent experiment. Compared to untreated bamboo fibers, treated bamboo fibers improve the resistance to chloride-ion permeability in concrete, with an enhancement rate between 14 % and 17 %.

The impact of bamboo fiber on water absorption was investigated by adding bamboo sticks obtained from an unknown species. The bamboo fibers were added at 20%, 30%, and 40% by weight to modify epoxy resin. The information about the adhesion between the particles and the matrix in the interface region can provided by water absorption test. The experiment unveiled that the addition of bamboo results in increased water absorption capacity(Banga et al., 2015).

2.9.4 Bamboo fiber reinforced concrete shrinkage properties

2.9.4.1 Concrete shrinkage

The phenomenon of shrinkage in concrete can be broadly defined as the gradual and time-dependent decrement of either the overall volume or the linear dimensions of the hardened concrete material(James K. Wight, 2012) (Maghfouri et al., 2020). It happened predominantly attributed by the complex processes of moisture loss that happen within the concrete matrix over time. The moisture loss is broadly seen as an internal and external process. In case of internal, the moisture in the matrix is consumed for the hydration process, while the external is the moisture lost to the environment due to temperature and wind effects(Neville, 2002).

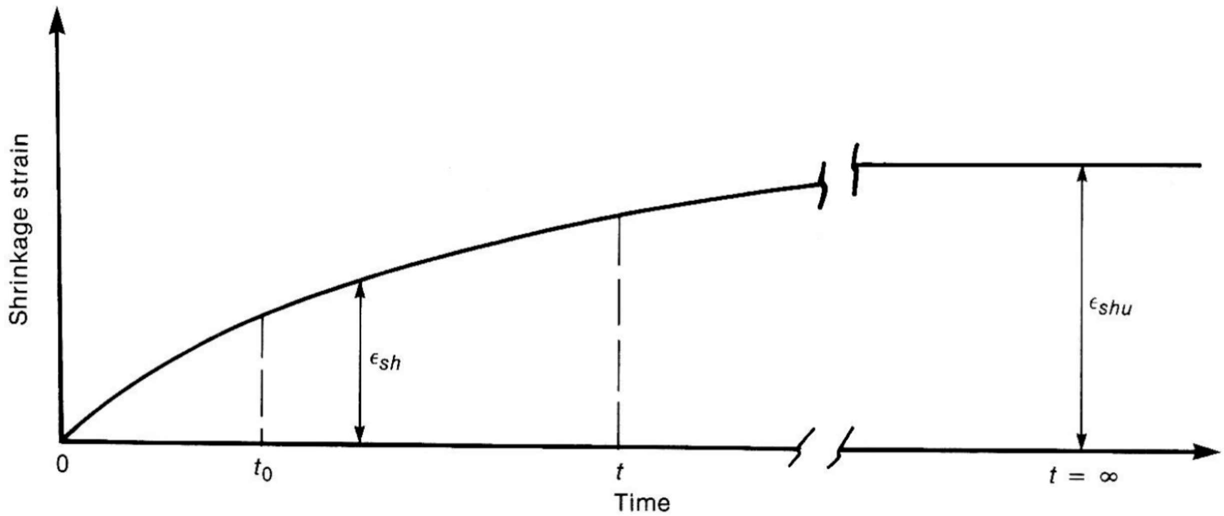

Figure 2.10. Shrinkage of an unloaded specimen(James K. Wight, 2012)

Volume change of concrete is an unavoidable phenomenon that happens from the very beginning of its formation and continues throughout the concrete's life, as shown in Figure 2.10. As a result, concrete structures are susceptible to self-stress or shrinkage cracking, which can cause serious structural defects as well as reduce the serviceability, durability, and aesthetics of the concrete structure(Saliba et al., 2011).

The structural capacity or performance of concrete composites can also be mainly governed by time-dependent deformation of structural elements. This deformation arises as a result of sustained load, generally referred to as creep, or moisture loss due to unrestrained shrinkage. Shrinkage is the result of moisture lost due to either through the hydration process or migration to the surrounding atmosphere(Gribniak et al., 2010).

2.9.4.2 Types of shrinkages

Concrete experiences plastic, chemical, autogenous, drying, and carbonation shrinkage following its placement (Gribniak et al., 2010). These shrinkages happened at various ages of the concrete. Some of them may act simultaneously, and others happen only at an early age of concrete. Early age shrinkage results in concrete cracks, which will have an effect on the durability of concrete structures. The migration of moisture through these cracks will corrode the embedded reinforcement bars, and also, the freezing and thawing effect will further increase crack openings. Fibers are found to be important in managing those early cracks, which in effect long duration of concrete structures could be met (Sekar, 2019).

2.9.4.2.1 Plastic Shrinkage

Concrete in its semi-fluid or plastic state undergoes shrinkage. This is identified as plastic shrinkage. It is the phenomenon observed at the very early age of concrete following its placement. After placement of concrete, moisture from the exposed surface migrates through evaporation. This will draw water from the underlayers of the top surface, known as bleed water. When the rate of surface evaporation is higher than the bleed water, plastic shrinkage is initiated. During the casting of concrete, materials like aggregate and paste migrate towards the bottom. On the other hand, the paste material with free water takes the top part. Evaporation of this water triggers shrinkage, and this shrinkage is named as plastic shrinkage(Matalkah et al., 2019).

2.9.4.2.2 Chemical shrinkage

The total volume of the concrete making ingredients after mixing shows a reduction in volume when compared to their total volume ahead of mixing. This reduction happens due to the hydration process. This type of reduction in volume is called chemical shrinkage. It is well identified as the driving force of self-desiccation, autogenous shrinkage (AGS), and drying shrinkage (Ghanem et al., 2024).

2.9.4.2.3 Autogenous shrinkage

It is an early-age phenomenon that occurs soon after mixing due to self-desiccation. The phenomenon of autogenous shrinkage in ordinary concrete is not significant when the water-to-binder ratio (w/b) is larger than 0.45(Shengwen Tang, Desheng Huang, 2021), which has an impact in the case of high-strength concrete where the water-to-cement ratio is purposely lower. In the hydration process, the water in the concrete is utilized. If there is no water for the process, an increment of capillary pressure happens while the decrement of internal relative humidity. Therefore, this capillary pressure induces tensile stresses that result in volume reduction.

Autogenous shrinkage is the concrete property that happens before the exposure of concrete to the atmosphere, as shown in Figure 2.11, and the effect of this shrinkage cannot be neglected in the case of high-strength concrete.

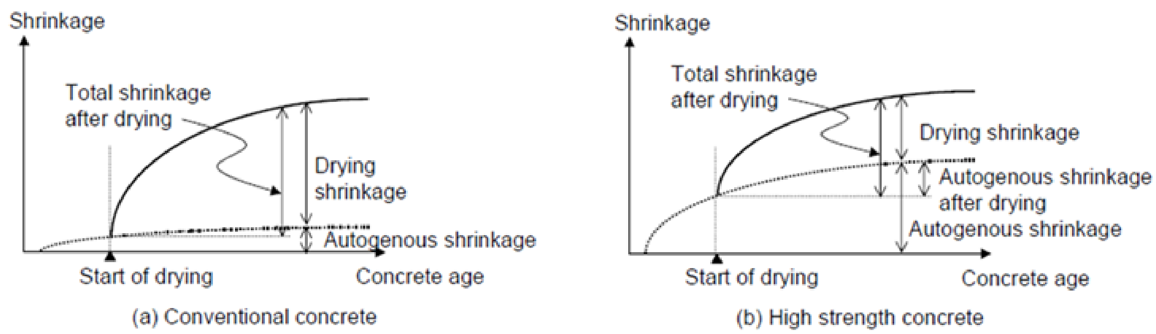

Figure 2.11. Shrinkage in conventional and high-strength concrete(Sakata & Shimomura, 2004).

According to C. Clarke (Clarke, 2009), the shrinkage that resulted from water within pores is consumed within the hydration of the concrete mix. This means the shrinkage behaviour does not have a correlation with the dimensional change due to moisture loss to the atmosphere. In the case of a normal water-to-cement ratio, the effect of autogenous shrinkage is very small, in contrast to high-strength concrete with a low water-to-cement ratio. The consequences of autogenous shrinkage are significant when the water-to-cement ratio is no higher than 0.33. As per ACI (ACI Committee 209, 2008), autogenous shrinkage will have a major component when the water-to-cement ratio is low. Water-to-cement ratio (w/c) less than 0.4 and compressive strength greater than 60MPa is stated as the demarcation line of concrete to have significant autogenous shrinkage.

2.9.4.2.4 Drying shrinkage (Free shrinkage)

Concrete through time performs to balance between the internal humidity with the lower surrounding environmental humidity. Hence, there will be diffusion of water into the environment. This will result in a volumetric change in the hardened concrete.

The volume decrement of concrete due to the exclusion of moisture from the surface towards the surrounding environment is identified as drying shrinkage. It happens throughout the life of the concrete structure. In the capillaries, tensile stress develops due to the migration of water to the atmosphere, which pulls the concrete particles together. These particles' closeness means a reduction in volume. A shrinkage strain of 400-1000με can be observed due to this kind of shrinkage(Folliard et al., 2003). Within 4 to 12 hours of concrete casting, the autogenous shrinkage effect starts, while the drying shrinkage effect starts when the sample is devoid of curing(Thomas et al., 2015).

Drying shrinkage occurs when water in capillary pores is lost to the environment. This will happen when concrete is exposed to an environment that has less than 100% relative humidity and will continue to occur until the relative humidity external humidity conditions equilibrate with the inside concrete humidity conditions. Unsealed specimens were prepared to determine the change in dimension due to the hydration process. Then the drying shrinkage strain of the concrete was found by subtracting the strain of a sealed specimen from that of an unsealed specimen (Sakata K., 2001).

Within the first 24 hours, early-stage shrinkage deformation occurs on the way the concrete is setting and starts hardening. Moreover, the deformation starting from 24 hours onwards is classified as long-term shrinkage deformation(Holt, 2001).

2.9.4.2.5 Carbonation shrinkage

Carbonation shrinkage is the other type of volume reduction caused by the chemical reaction between the carbon dioxide, CO_2, from the atmosphere, with concrete. The carbon dioxide from the air reacts with calcium hydroxide, Ca $(OH)_2$, of concrete, giving calcium carbonate, which results in pore structure reduction in concrete. The carbonation process is a chemical process that transforms from the less dense carbon hydroxide to the denser calcium carbonate. This results in a decrease of volume, and this decrement in volume is carbonation shrinkage(Cepcianska et al., 2021).

2.9.5 Factors governing the shrinkage of concrete

There are various factors that affect the shrinkage characteristics of concrete. Summarizing those factors can be broadly classified into two categories, based on research findings(Pulecio-Díaz et al., 2024)(P. T. and X. Wang, 2014).

These are

Intrinsic factors: The factors associated with the ingredients of concrete, the geometry, and the size of the sample could be seen under this. Ingredients of concrete should be seen as a broad term that covers the materials beyond the usual ones (aggregate, cement, sand, and water) in the umbrella. These are admixtures, fibers, and any partial replacements to the basic concrete-making materials.

Extrinsic factors: Determinant factors that are not within the specimen, but rather influential from outside, could be seen in this part. These can also be identified as environmental factors. Temperature, humidity, wind, and curing method have an impactful effect on the shrinkage characteristics of concrete. The response of concrete to these extrinsic factors is influenced by the materials used in its making.

2.9.6 Studies on the shrinkage of various forms of bamboo and concrete hybrids

Some insightful research has been conducted on the impact of bamboo on the shrinkage characteristics of concrete.

Che Rosely et al., 2024 (Che Rosely, N. A. N., Wan Jusoh, W. A., Osman, M. H., Syed Zin, S. M. F., Adnan, S. H., Roslan, M. N., Md Desaa, M. S., & Othman, 2024) conducted a study to address the impact of partial replacement of cement with bamboo biochar powder on the drying shrinkage of mortar. The source of the biochar powder was Gignatocholoa abociliata. The cement replacement was at 5%, 10%, 15%, and 20%; then a comparison was conducted with 0%, which was the control. The study was conducted for the indoor and outdoor exposure for a duration of 150 days. The study revealed significant drying shrinkage reduction at 5% cement replacement.

Yeh et al., 2024 (Yeh et al., 2024) addressed the impact of untreated and sodium hydroxide-treated bamboo fiber of size between 6 and 16 mesh on the drying shrinkage of cementitious composites for a 28-day duration through the experiment. The study discovered that specimens containing treated bamboo fiber showed a significant reduction in drying shrinkage.

Bamboo fiber obtained after processing waste bamboo and vacuum heat-treated was employed in the making of cementitious composite, and then the experiments comprising drying shrinkage were conducted(Yeh & Yang, 2023). However, the experiment addressed the impact of various bamboo fibers treated with various temperature values under specified humidity values. Untreated bamboo fiber was not included for comparison in the study. As per this study, specimens containing bamboo fiber treated with a higher temperature value showed a reduction in the drying shrinkage at an early age. On the other hand, the investigation showed specimens made of heat-treated bamboo fiber and put in a higher humidity value had a lower dry shrinkage magnitude.

Andreola et al., 2024 (Andreola et al., 2024) conducted research in Brazil on the use of bamboo particles in the making of concrete. The study addressed the impact of the bamboo particles on the drying shrinkage of concrete for 90 days. The study provided that the drying shrinkage at the end of the study was in the range of 2500 and 5000με.

2.10 Concrete shrinkage prediction models

Over the past years, numerous shrinkage prediction models have been extensively documented in the literature. These models can be roughly categorized into two groups: empirical models, such as the fib Model Code for Concrete Structures 2010, and mechanism-based theoretical models, for example, the thermodynamic model proposed by Powers (Ye & N, 2016). Empirical models are mostly formulated through statistical regression analysis of field-collected or experimentally measured data(Ye & N, 2016).

Prediction equation of drying shrinkage could also approach taking into consideration concrete as a result of a two-phase composite model, as aggregate and matrix. This approach requires the determination of the modulus of elasticity of the matrix, fine and coarse aggregates(Eguchi & Teranishi, 2005). In order to determine the prediction equation for stating the drying shrinkage of concrete with higher accuracy, the authors' earlier prediction equation based on a two-phase composite model is changed to base on three-phase model, and is extended to the form considering of the effects of member size and shape, and relative humidity of the environment. Here, cement paste, fine aggregate, and coarse aggregate are the elements of the three-phase model (Teranishi, 2010).

On the other hand, the shrinkage of concrete prediction models of code equations are empirical and developed based on the statistical study on experimental data(Freidriks & Thesis, 2015)(Khairallah., 2019). According to ACI209R-92, the prediction equation of shrinkage is related to the concrete curing mechanism (ACI Committee 209, 1998).

There are various developed concrete shrinkage predictions by institutions and researchers. The prediction equations developed by the American Concrete Institute (ACI Committee 209, 1998), Eurocode drying shrinkage model (Standard, 2004) , Bazant and Baweja B3 (ACI Committee 209, 1998), the Sakata shrinkage prediction model (Sakata, 1996), and GL2000 (Gardner and Lockman) (ACI Committee 209, 1998) were employed for drying shrinkage prediction.

I. ACI 209R-94 Model

This is an empirical model formulated through statistical analysis of experimental data. The formulation is a product of a hyperbolic function with various correction factors. Those correction factors are

γ_{tc} = curing time coefficient

γ_{RH} =relative humidity coefficient

γ_{vs} = volume-surface ratio factor

γ_{s} = slump factor

γ_{φ} = fine aggregate to the total aggregate ratio

γ_{c} = cement content factor

γ_{a} = air content factor

The hyperbolic function is

$\varepsilon_{(t,tc)} = \frac{t-t_c}{f+(t-t_c)} * \varepsilon_{\varpi}$ -- 2.1

The ultimate shrinkage (S_{ϖ}) is

$\varepsilon_{\varpi} = 780 * 10^{-6} * \gamma_{tc} * \gamma_{RH} * \gamma_{vs} * \gamma_{s} * \gamma_{\varphi} * \gamma_{c} * \gamma_{a}$ ---2.2

f is the parameter to consider the volume-to-surface ratio computed by

f = $26 * e^{[1.42*10^{-2}(\frac{V}{S})]}$ ---2.3

Where V is the volume and S is the surface area

Those correction factors are devised to take care of the mix proportions, curing conditions, environmental humidity, and member geometry.

II. Eurocode drying shrinkage model

The concrete shrinkage (ε_{cs}) in the European standard is given by the addition of the drying shrinkage (ε_{cd}) and autogenous shrinkage (ε_{ca}) as shown in Equation 2.4.

$\varepsilon_{cs} = \varepsilon_{cd} + \varepsilon_{ca}$ --2.4

Where:

ε_{cs} = total shrinkage strain

ε_{cd} = drying shrinkage strain

ε_{ca} = autogenous shrinkage

The drying shrinkage development through time is estimated by

$\varepsilon_{cd}(t) = \beta_{ds}(t, t_s) * k_h * \varepsilon_{cd,0}$ --2.5

Where:

k_h= the coefficient dependent on the notional size h_0

$\varepsilon_{cd,0}$ = the basic drying shrinkage strain computed by the following equation

$\varepsilon_{cd,0} = 0.85 * \left[(220 + 110 * \alpha_{ds1}) * exp\left(-\alpha_{ds2} * \frac{f_{cm}}{f_{cmo}}\right)\right] * 10^{-6} * \beta_{RH}$ ---------------------2.6

Where:

β_{RH}= factor to consider the relative humidity and computed as follows

$\beta_{RH} = 1.55 * [1 - \left(\frac{RH}{RH_0}\right)^3]$ ---2.7

RH= relative humidity

RH_0= 100%

f_{cm}= the mean compressive strength (MPa)

f_{cmo}= 10Mpa

α_{ds1} and α_{ds2} = coefficients governed by the cement type

$\beta_{ds}(t, t_s)$= the factor to consider the time and cross-sectional area calculated by

$\beta_{ds}(t, t_s) = \frac{(t-t_s)}{(t-t_s)+0.04*\sqrt{h_0}^3}$ ---2.8

t = age of concrete under consideration, days

t_s= age of concrete when the curing ends

h_0= notional cross-section size of the specimens in mm

$= \frac{2*A_c}{u}$ --2.9

A_c= cross-sectional area of concrete

u = perimeter of the cross-sectional area exposed to drying

The autogenous shrinkage strain estimated by

$\varepsilon_{ca}(t)$=$\beta_{as}(t) * \varepsilon_{ca(\infty)}$ ---2.10

$\varepsilon_{ca(\infty)}$= $2.5 * (f_{ck} - 10) * 10^{-6}$ --2.11

and

$\beta_{as}(t)$=$1 - \exp(-0.2t^{0.5})$ ---2.12

where t is given in days

f_{ck}= characteristics compressive strength of concrete

This model considers relative humidity, the cement type, time, and cross-sectional impact in the shrinkage strain.

III. Bazant and Baweja (B3) Model

This model is applicable to concrete specimens produced using OPC (Ordinary Portland Cement) and is the result of the culmination of work that started in the 1970s. The model was calibrated by a computerized data bank comprising data obtained in various laboratories. The model is formulated as

$\varepsilon_{sc}(t, t_c) = -\varepsilon_{sh\infty} * k_h * S(t - t_0)$ ---2.13

Where

$\varepsilon_{sh\infty}$= the ultimate shrinkage strain computed by

$\varepsilon_{sh\infty} = -\alpha_1 * \alpha_2 * [1.9 * 10^{-2} * w^{2.1} * fc^{-0.28} + 270] * \left(\frac{607}{4+0.85*607}\right)^{\frac{1}{2}} * \left(\frac{4+0.85*(t_0+\tau_{sh})}{t_0+\tau_{sh}}\right)^{\frac{1}{2}}$ -2.14

α_1 = factor dependent on cement type

The values are 1.0, 0.85, and 1.1 for type I cement, type II cement, and type III cement, respectively.

α_2= factor to consider the curing method

The values are 0.75 for steam-curing, 1.2 for sealed or normal curing in air with initial protection against drying, and 1.0 for curing in water or at 100% relative humidity.

w is the water content in kg/m3

fc is compressive strength at the 28^{th} day age of concrete

to is the

k_h= humidity dependent factor

k_h= $1 - h^3$ for h $\leq$ 0.98

$= -0.2$ for h $= 1$ (swelling in water)

= linear interpolation for $0.98 \leq h \leq 1$

$S(t - t_0)$ = the equation that relates the time and size as presented below

$s(t - t_0) = \tanh(\frac{(t-t_0)}{\tau_{sh}})^{\frac{1}{2}}$ ---2.15

t = age of the concrete

t_0 = age when the curing ends

τ_{sh} = the factor that takes into consideration size and computed using

$\tau_{sh} = 0.085 * t_0{}^{-0.08} * f_{cm28}{}^{-0.25} * \left[2 * k_s * \left(\frac{V}{S}\right)\right]^2$ ---2.16

k_s = cross-section shape factor

It is 1, 1.15, 1.25, 1.30, and 1.55 for an infinite slab, an infinite cylinder, an infinite square prism, a sphere, and a cube respectively.

Cement type, humidity, compressive strength, curing duration, volume, shape, water content, age, and mode of curing are considered in this model.

IV. Sakata shrinkage prediction model

This model has been formulated using a statistical method conducted on many experimental data(Sakata & Shimomura, 2004)(Sakata, 1996). The model expression is

$\varepsilon_{sh}(t, t_0) = \frac{\varepsilon_{sh\infty}*(t-t_0)}{\beta+(t-t_0)}$ ---2.17

$\varepsilon_{sh\infty} = \frac{\alpha*(1-h)*W}{(1+\eta*t_0)*(1+150*exp\left\{\frac{-500}{f_{c(28)}}\right\})}$ ---2.18

Where

ε_{sh}= The final shrinkage strain value

$\varepsilon_{sh\infty}$= The ultimate shrinkage strains

t = Age of concrete

t_0 = age concrete curing ends or drying begins

α = factor to consider the cement type

h = relative humidity

W = water content (kg/m^3)

$f_{c(28)}$ = 28th days compressive strength (MPa)

The model takes into consideration the cement type, duration of curing, relative humidity, water content, compressive strength, and age of concrete in the shrinkage prediction process.

V. GL2000 prediction model

The GL2000 model is developed empirically based on experimental data. It considers the concrete strength, humidity, size of the concrete specimen, shape of the concrete specimen, and age. The equation is stated as follows.

$$\varepsilon_{sh}(t, t_c) = \varepsilon_{shu} * \beta(h) * \left[\frac{t-t_c}{(t-t_c)+0.12*(V/S)^2}\right]^{\frac{1}{2}} \text{ ----------2.19}$$

Where

ε_{shu} = is the ultimate shrinkage computed by

$$\varepsilon_{shu} = 900 * k * \left(\frac{30}{f_{cm28}}\right)^{\frac{1}{2}} * 10^{-6} \text{ ----------2.20}$$

f_{cm28} = the mean compressive strength of concrete

$\beta(h)$= the correction factor for humidity calculated by

$$\beta(h) = (1 - 1.18 * h^4) \text{ ----------2.21}$$

V = volume

S = surface

h = humidity

t_c= age of concrete begins dry

t = age of concrete

The shrinkage properties or characteristics were sufficiently predicted from equations derived based on 100-day shrinkage data(Branson & Schumann, 1970). Based on experimental data conducted between 7 and 28 days, a one-year shrinkage value was predicted with acceptable or tolerable error(Brooks & Neville, 1978).

Equations were developed to predict time-dependent behaviour of reinforced concrete, taking the reinforcement ratio as one additional parameter in already developed, well-known equations. In the study, prediction equations of CEB-FIB 90, ACI 209, GL 2000, and JTG D 62-2004 were used to examine which one is best closer to the experimental data for 0.0%, 0.5%, 1.0%, 2% and 3.9% ratios of longitudinal reinforcement bars within concrete beam for a period of 200days. ACI 209 was found to show better prediction, and then the equation is re-evaluated, and a modified prediction equation is developed based on the calibration result obtained from the experiment(Sun et al., 2019).

An experimental study was conducted to study autogenous and drying shrinkage of fiber-reinforced lightweight-aggregate concrete for a period of 270 days. The test parameters of the study were the volume of fraction of steel fiber, water-to-binder ratio, two kinds of coarse lightweight aggregate, fine lightweight aggregate, and manufactured sand. The autogenous shrinkage study was conducted on sealed specimens, while this was not the case for drying shrinkage. The result showed the effect of those parameters on the development of the two shrinkage behaviors. Moreover, an equation was developed taking into account the volume fraction of steel fiber as one variable in the case of drying shrinkage. The test result showed that the increment of values of both autogenous and drying shrinkage beyond 200 days is less than 3% (S. Zhao et al., 2016).

Drying shrinkage and mechanical properties of alkali-activated mortar (AAM), using waste glass powder, were studied for a period of 56 days. The specimen's preparation and testing procedure were designed based on the Chinese code. Prismatic samples with 40mm x 40mm x 160mm in dimension were prepared, and the samples were put in standard curing conditions for 48 hours before relocating them into a drying shrinkage box whose temperature is at 20+/-2 ºC, and humidity 60+/-5%. The factors that influence the drying shrinkage behaviour through time also similarly affect the characteristics of the compressive strength. As a result, the study further showed the relation between compressive strength and drying shrinkage. In the field, measurement of drying shrinkage is not as such easy as the compressive strength. Artificial neural network used to describe the prediction equation using age and compressive strength as variables used in the prediction equation(J. Gong & Qu, 2020). Here, the study also considered the variation of the amount or percentage of application of glass powder-based additives.

The artificial neural network (ANN) was used to develop the model used for predicting drying shrinkage based on the large database of experimental outputs issued from literature (RILEM Data Bank)(Bal & Buyle-bodin, 2013). When the graph is prepared with respect to time, the shape of the shrinkage profile resembles a growth curve, as shown in Figure 2.12. Different curve equations are proposed, and the best fit is selected based on a statistical procedure to get values of the constants (Branson & Schumann, 1970)(Gaylard, 2011)(S. X. Hu et al., 2019).

Different possible equations to fit the experimental data of shrinkage have been developed. The constants there are determined through the recommended non-linear regression analysis to predict the constants within those equations (Sakata K., 2001)(Branson & Schumann, 1970)(Gaylard, 2011).

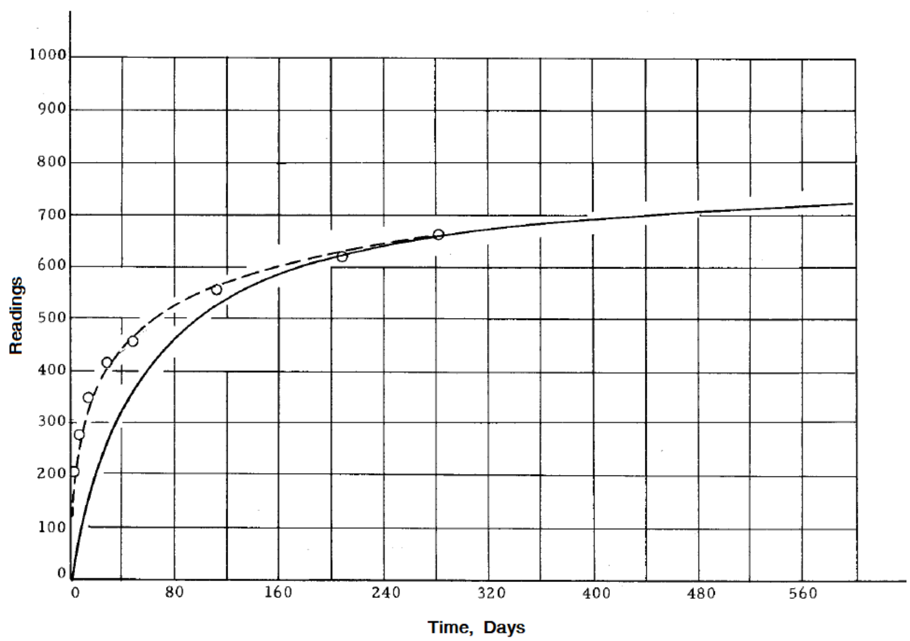

Figure 2.12. Shape of growth curve (Branson & Schumann, 1970)

3 Materials and Methods

3.1 Materials and methods of examination of bamboo fiber

This section presents the origin of the materials and the methodologies employed to systematically explore the impacts of a variety of extraction processes on the characteristics of the fiber.

3.1.1 Materials

The materials used to examine the effect of mechanical, chemical, and a combination of the two extraction methods are listed subsequently.

3.1.1.1 Bamboo

The bamboos that were employed for this particular study were methodically obtained from Ethiopia, with a specific focus on Hagereselam town, which is located within the geographical boundaries of the Sidama regional state, at an altitude of approximately 2600 meters above the mean sea level. The age of the bamboo selected for the experiment was three years old. The age determination was made possible through a personal expertise in this and experience of the local planters, combined with a strict adherence to the established guidelines that have been expressed by prior researchers in the field(Mekonnen et al., 2014)(Kavitha & Kala, 2016)(Mulatu et al., 2016b)(Dessalegn et al., 2021).

3.1.1.2 Sodium hydroxide

The chemical compound utilized for the purposes of both the chemical extraction as well as the combined mechanical and chemical methods for fiber extraction was sodium hydroxide, which was contained within a 1kg container. The sodium hydroxide was provided as a tiny, pellet-like shape. Solution of sodium Hydroxide (NaOH) is a commonly used chemical to dissolve the hydroxyl (OH) groups and generate rearranged fiber structures. In addition to this, the chemical solution reduced fiber components such as hemicelluloses, lignin, waxes, and oils, which enhance the surface roughness of the fiber(J. Ahmad et al., 2023b).

3.1.2 Methodology for the assessment of bamboo fiber

3.1.2.1 Bamboo fiber extraction methods

In order to get the fibers from the bamboo culm, mechanical, chemical, and combined methods were used as discussed in the subsequent paragraphs.

The comprehensive process of bamboo preparation that is integral to the extraction procedure is visually represented in Figure 3.1, which serves as an important reference for understanding the methodology employed in this study. Attention paid to detail in both the sourcing and preparation of the bamboo is critical to ensuring the integrity and reliability of the research outcomes. Ultimately, this experimental work sets the stage for a deeper exploration into the properties and potential applications of bamboo fibers derived from this specific ecological context.

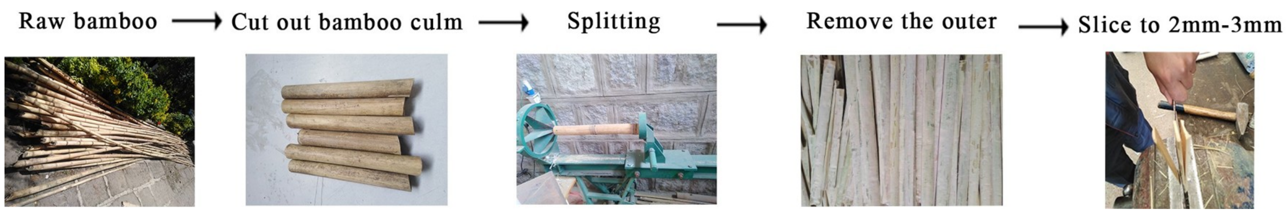

Figure 3.1. Bamboo preparation for fiber extraction

Once the bamboo is sliced to 2mm to 3mm thick, the extraction process is continued to get the fibers from five approaches.

Five distinct types of extraction methods were employed for the sliced bamboo of size 2mm to 3mm to obtain the fibers used for subsequent examination. Those approaches are summarized and presented as follows.

- The first method, which is classified as a mechanical approach, involved soaking the sliced bamboo in clear water for five days. Then the fibers were extracted by beating and combing each sliced, soaked bamboo. After that, the fibers were exposed to direct sunlight for drying for three days. The sun drying stage was followed by oven drying for three hours at 60°C.

- The second approach employed was the combined method. In this specific approach, the fibers obtained from the first method were taken. However, those fibers were taken at the stage before exposing them to direct sunlight. The fibers were soaked in a 4% NaOH solution for 12 hours. Next, the fibers were taken out of the container where they were exposed to direct sunlight for three days. The sundried fibers were further dried in an oven at 60 °C for three hours.
- The other techniques used for extracting fibers were the third, fourth, and fifth. Those methods were applied to the bamboo slices. For this purpose, solutions of sodium

hydroxide (NaOH) were prepared at concentrations of 3%, 6%, and 9%, which were used in the third, fourth, and fifth methods, respectively. The bamboo slices were immersed and watched there for three days. The bamboo slices were washed in continuously flowing water to remove the remnants of sodium hydroxide. After this, the slices were beaten and combed to get the fibers. The extracted fibers were then taken to direct sunlight for three days, followed by oven drying at 60°C for a three-hour duration.

To make sure the sodium hydroxide was significantly removed, the fibers obtained from the chemical and combination methods were washed for an hour with constantly flowing water and then analyzed using a PH meter.

3.1.2.2 Chemical analysis

The complicated chemical compositions intrinsic in the dried bamboo fibers were methodically established through the process of reducing these fibers into tiny fragments, thereby facilitating a complete analysis. For the determination of the cellulose, hemicellulose, and lignin content present within the fibers, the gravimetric method as outlined and proposed by Ayeni et al. (Ayeni et al., 2015) was cautiously employed to ensure the examination of these basic components.

3.1.2.3 Absorption and moisture content

The moisture content was assessed utilizing a sample weighing approximately 1 gram, which was sun-dried for a duration of three days. Subsequently, the samples derived from each extraction method were subjected to a drying process in a 60°C oven for a period of 5 hours prior to weighing. After this initial weighing, the samples were returned and put into the oven for an additional hour at 60°C to confirm the stability of the weight. This procedure was repeated until the difference between two successive oven-dried weights was negligible. On the other hand, the absorption capacity was calculated by comparing the weight of the oven-dried fiber to the weight of the fiber following a 24-hour immersion. The percentage of moisture capacity is expressed as the ratio of the difference between the oven-dried weight and the sun-dried weight to the oven-dried weight. Conversely, the absorption capacity is defined as the ratio of the difference between the weight after immersion and the oven-dried weight to the oven-dried weight (Buson et al., 2018)(Ovat et al., 2015).

3.1.2.4 Tensile testing

The tensile testing was done using a TEXTECHNO STATIMAT ME+ machine with a load cell of 100N and a loading rate of 1mm per minute (Osorio et al., 2011)(ASTM, 2015). The gauge length was fixed to 25mm as per ASTM C 1557. The cross-sectional area is calculated once the density is obtained(Biswas et al., 2013)(Defoirdt et al., 2010). Hence, equation 3.1, formulated by the relationship among mass, density, and length, is used to know the fiber's cross-sectional area to be used to obtain the tensile strength.

$$A_b = \frac{m}{\rho * l} \quad \text{--} 3.1$$

Where

A_b bamboo fiber area

ρ density of the bamboo fiber

l length of the bamboo fiber loaded to the machine

m mass of the bamboo fiber corresponding to the length measured

For this purpose, a ruler and balance were used for the determination of the length and mass of each fiber, respectively. A density measurement apparatus was used to determine the density. All these measurements and experiments were carried out at room temperature within the laboratory.

The magnitude of the density of C3 (fibers extracted using the chemical method of 3% NaOH) is 1 g/cc, C6 (fibers extracted using the chemical method of 6% NaOH) is 1 g/cc, C9 (fibers extracted using the chemical method of 9% NaOH) is 1 g/cc, M (mechanically extracted fiber) is 0.8 g/cc, and MC (fibers extracted using the combined method) is 0.9 g/cc. The reasons for the increment in density of fiber extracted using chemical techniques are the internal structure rearrangement of the fiber, the reduction of materials with less density, and the effect on pores due to the alkaline solution effect (A. E. Bekele et al., 2022)(Loganathan et al., 2020)(Umashankaran & Gopalakrishnan, 2020).

The influences of mechanical, combined, and chemical (with three distinct solutions of NaOH extraction) methods were examined on 15 fibers picked from each technique. Therefore, a tensile test was performed on 75 fiber specimens. The tensile strength of each tested fiber was calculated using equation 3.2.

$$\sigma_b = \frac{T}{A_b} \text{ -- } 3.2$$

Where

σ_b tensile stress in the bamboo fiber

T recorded applied tensile force on the bamboo fiber

A_b area of the bamboo fiber computed by Equation 3.1

The tensile stress data has to be verified for confidence that the outliers are omitted in the subsequent data analysis. To identify and then reduce outliers the IQR (interquartile range) criterion was employed. After the data is put in descending order, the five parameters will be taken. These are the lowest values (Dl), the median of the whole data (M), the median of the lower half data below the median (Q1), the median of the upper half data above the median (Q2), and the highest value (Du). The data within Q1-1.5*IQR to Q2+1.5*IQR are used for the data analysis, where IQR = Q2-Q1(Zhou et al., 2021)(Seltman, 2018).

3.1.2.5 Fourier Transform Infrared

Fourier transform infrared (FTIR) spectroscopy depends on the absorbance or transmittance of infrared light. When a sample is exposed to IR radiation, some of the radiation is transmitted by the sample, and some is absorbed. The subsequent spectrum characterizes the molecular absorption or transmission, creating a unique molecular pattern in the sample. It helps in detecting key chemical components of the fiber and offers information on fiber quality and chemical changes due to the extraction process or treatments. Therefore, the FTIR spectra of bamboo fibers extracted through the employed methods were obtained from a thermo-scientific IS50 ABX spectrometer of German origin within the range of 4000–400 cm^{-1}, with a resolution of 16 cm^{-1} and 32 scans. The FTIR employed was attenuated total reflectance (ATR), which does not require complex sample preparation.

3.1.2.6 Thermal analysis
A thermogravimetric analyzer (Model HCT-1) with temperatures ranging from 25 °C to 800 °C at a rate of 20 °C per minute in an air atmosphere was used to examine the thermal stability of the extracted bamboo fibers.

3.1.2.7 Scanning Electron Microscope
A Scanning Electron Microscope (SEM) is an instrument that uses electrons for image formation to examine the structure, surface morphology, and composition of materials. It is possible to view factors such as size, surface roughness, and the presence of contaminants or flaws through high-resolution imaging. In this experiment, a scanning electron microscope (SEM) was utilized to know about the morphology of the bamboo fibers gained through various extraction techniques. A Joel scanning electron microscope, model JCM 6000 PLUS at X1000, was used to study fiber surface morphologies. Before examination, the fiber specimens were sputter-coated with a thin layer of gold in a vacuum chamber. The sputter-coating conductive material results in better image formation because this approach avoids the accumulation of electrons on the surface of the fiber.

3.1.2.8 Analysis of variance for bamboo fiber assessment
An analysis of variance (ANOVA) was conducted to conclude if the methods of extraction employed had caused substantial tensile strength variation among the bamboo fibers. Tukey's standardized test was also performed at a 95% probability level to detect which method of extraction was significant.

3.2 Materials and methods of examination of bamboo fiber concrete hybrid
3.2.1 Materials
3.2.1.1 Fine aggregate
River sand brought from the local supplier was used for the experiment.

Table 3.1. Fine aggregate properties

Description	Result	Remark as per ASTM C33
Fineness modulus	2.84	2.3 – 3.1
Silt Content (%)	2.1	≤5.0
Specific gravity	2.457	2.4-2.9
Bulk Density (g/cc)	1.534	
Absorption (%)	2.965	0-4%

The moisture content, the fineness modulus, absorption, and the specific gravity were examined as per ASTM C 566, ASTM C136, and ASTM C 128, respectively. The characteristics of the sand obtained are shown in Table 3.1. In addition, the conducted grain size distribution proved that the sand meets the requirements set in Art. 6.1 of ASTM C33 (ASTM, 2003b) as shown in Figure 3.2.

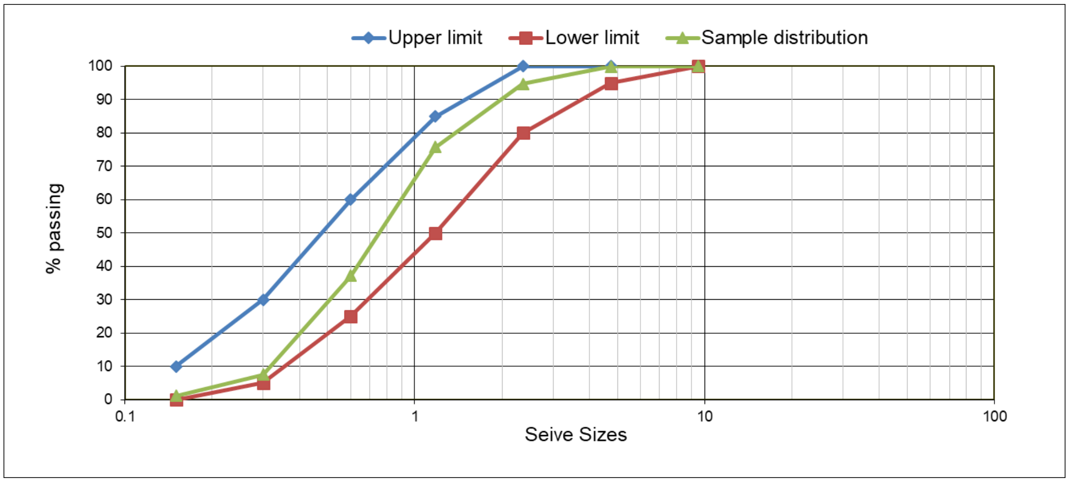

Figure 3.2. Grain size distribution of fine aggregate

3.2.1.2 Coarse aggregate

The investigation employed crushed basaltic rock from the Aser concrete batching factory in Addis Ababa, Ethiopia. The grain size distribution was carried out as per ASTM C 33(ASTM, 2003b) and ASTM C136 (ASTM, 2001a), and the results were within the limits displayed in Figure 3.3.

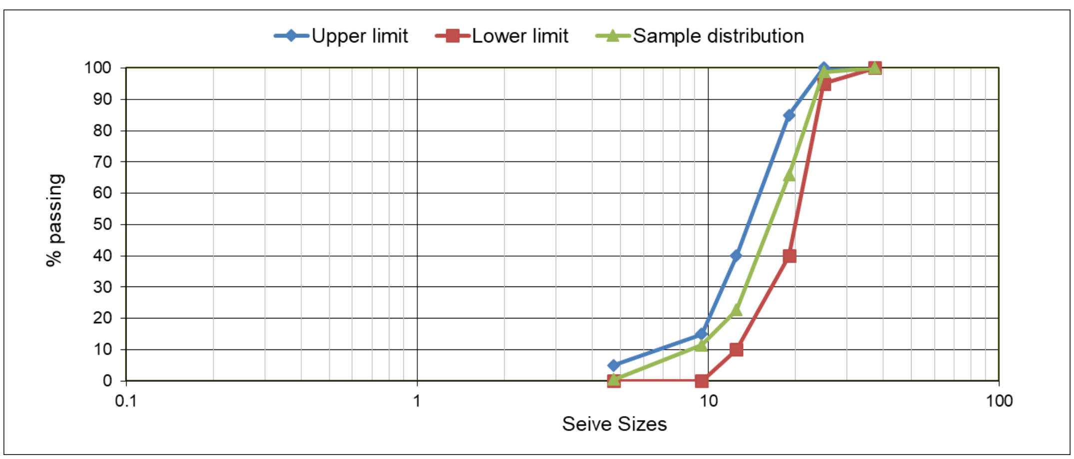

Figure 3.3. Grain size distribution of coarse aggregate

The bulk density and specific gravity of the coarse aggregate are 1.608 g/cc and 2.659 g/cc, respectively. Water absorption in the aggregate sample was determined to be 1.426%. All of these values are determined to fall within the range of ASTM C33(ASTM, 2003b).

3.2.1.3 Cement

Ordinary Portland cement (OPC), which is manufactured by Derba Cement Factory purchased from the Addis Ababa market. The cement has a grade of 42.5 type N CEM I conforming to Ethiopian Standards CES:28(Agency, 2013).

3.2.1.4 Water

The quality and amount of water have a significant impact on the quality of the produced concrete. The quantity of water added to the specimens was determined based on the water-to-cement ratio prescribed by the British Department of the Environment (DOE) method (D C Teychenné, R E Franklin, 1997) and adjusted through trial mixes.

The water used in concrete production must be of potable (drinkable) quality. Therefore, tap water available from the laboratory supply was utilized to prepare the specimens.

3.2.1.5 Bamboo fiber

The bamboo fiber used was extracted from the Yushania alpina, commonly known as highland bamboo. The fibers were extracted through the chemical method by retting in 6% NaOH solution and then combing. The long fibers were cut into pieces with a size distribution shown in Table 3.2. Higher than 50 aspect ratios showed greater modulus of elasticity, which is important in the making of composites(Osorio et al., 2018).

Table 3.2. Bamboo fiber properties

Description	Value
Aspect ratio	70.95±18.34
Diameter (μm)	400±86.58
Length (mm)	27.23±4.41
Tensile strength (N/mm^2)	392.1±95.97
Shape	straight
Density (g/cc)	1.0

3.2.2 Methods

3.2.2.1 Mix design

Mix design of concrete is an approach to determine the proportions of concrete-making ingredients to achieve the desired performance. The mix design process commenced after determining the properties of the ingredients. A characteristic strength of 25MPa with a target strength of 38 MPa was designed with 732 kg/m^3 sand, 1098kg/m^3 coarse aggregate, 350 kg/m^3 cement, and water 202 kg/m^3 according to the design of normal concrete mixes published by the British Department of the Environment (DOE)(D C Teychenné, R E Franklin, 1997).

Table 3.3, presented below, summarizes the weight of ingredients required to produce 1 m^3 of concrete (Koichi Minami and Masakazu Terai, 1999). The bamboo fiber addition was made based on the percentage of the volume of concrete at 0%, 0.25%, 0.5%, 0.75%, and 1.0%.

Table 3.3. Ingredients quantity for 1m^3 of concrete

Code	Bamboo fiber (%)	Cement (Kg)	Coarse aggregate (kg)	Sand(kg)	Water (kg)	Bamboo fiber (kg)
S0	0.00	350	1098	732	202	0.00
S25	0.25	350	1094.5	729.5	202	2.50
S50	0.50	350	1090.5	727	202	5.00
S75	0.75	350	1086.5	724.5	202	7.50
S100	1.00	350	1083	722	202	10.00

3.2.2.2 Specimen preparation

Mixing of the ingredients (cement, sand, coarse aggregate, and bamboo fiber) was carried out using a Linosella mixer with a capacity of 300 liters. After conducting a trial, the following procedures were implemented in this study.

1. Cement, sand, a quarter of the aggregate, and one-third of the fiber were added by dispersing while the mixer was rotating.

2. A quarter of the coarse aggregate was added, followed by the addition of one-third of the fiber by spreading while the mixer was rotating. Water, which was a quarter of the total amount, was added.

3. While the mixer was rotating, a quarter of the coarse aggregate and a quarter of the total amount of water were added.
4. The remaining coarse aggregate was added, followed by the addition of one-third of the fiber by carefully distributing it into the mix while the mixer was rotating. Water, which was a quarter of the total amount, was added.
5. The remaining water was added, and the mixer was rotating for five minutes before discharging.

This procedure avoids the balling effect of fiber and helps to achieve better fiber distribution. Figure 3.4 shows how the fiber distribution looks during the dry mix and at the end of the mix.

a) During dry mix b) End of mixing

Figure 3.4. Bamboo fiber distribution during different phases of mixing

After the completion of mixing, the concrete was poured on a plastic sheet put over the ground floor as shown in Figure 3.4 (b).

Then, molds used for the specimen's preparation were filled by taking from the poured concrete. The molds used for evaluation of properties of concrete were 150mm cubes for compressive strength, a cylinder with a diameter of 100mm and 200 height for split tensile strength, a prism with 100mm by 100mm by 500mm dimensions for flexural strength, 75mm steel cubes for volume of voids and absorption examination, and 75mm by 75mm by 285mm steel prism molds for shrinkage examination.

3.2.2.3 Slump and density

The concrete slump was measured using an inverted slump cone as shown in Figure 3.5, adhering to the procedures stipulated in ASTM C143(ASTM, 2003a).

Figure 3.5. Slump test measurement

The density of the samples was measured after measuring and recording their weight before conducting the compression test. Then the ratio of the weight to the volume of the cube yields the required density as documented in the literature (Ismail & AL-Hashmi, 2008) (Althoey et al., 2022).

3.2.2.4 Compressive strength

The compressive strength test was conducted on the standard cube size of a 150mm specimen at a loading rate of 0.28 MPa/s as per ASTM C39 (ASTM, 2001b). The compressive strengths were calculated as equation 3.3.

$$f_c = \frac{p}{l^2} \qquad \text{------------------------------------} 3.3$$

Where

f_c = ultimate compressive strength, in MPa

p = ultimate compressive axial load exerted on the cube, in N

l = one side length of the cube, in mm

The samples were taken from the mold 24 hours after casting and stored in a water bath until the test day. The specimens were loaded using Controls compression testing equipment with a capacity of 3000 kN, as indicated in Figure 3.6. Three replica specimens were created for each type of exam. The loading rate on the compression machine was maintained constant, and the specimens were loaded until failure. The ultimate load applied to the specimen during failure was recorded.

Figure 3.6. Compressive strength machine

3.2.2.5 Splitting tensile strength

Three 100mm diameter and 200mm height cylinder specimens for each type of specimen category were prepared. The specimens were in their mold for 24 hours before being demolded and taken to a water bath, where they were to be kept until their date test. When their age reached for testing, the specimens were put in a control testing machine as shown in Figure 3.7, at a constant loading rate of 0.017MPa/s as per ASTM C496 (ASTM, 1996).

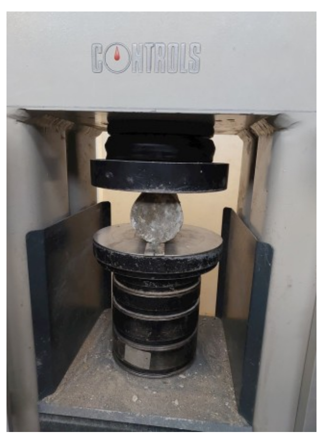

Figure 3.7. Sample in split tensile testing

The splitting tensile strength was computed using equation 3.4

$$F_f = \frac{2*P}{\pi*D*L} \quad \text{---} 3.4$$

Where

F_f = split tensile strength, in MPa

P = Maximum applied load, in N

D = Diameter of cylinder, in mm

L = Length of the cylinder, in mm

3.2.2.6 Flexural strength

The specimens were kept in their mold for 24 hours. Then they were cured in a water bath until their age matured for examination. Three replicas per category were prepared. The flexural strength of the samples was conducted using Controls equipment (Refer to Figure 3.8) at the age stated with a specimen size of 100mmX100mmX500mm at a loading of 0.015MPa/s as per ASTM C78 (ASTM, 2002).

Figure 3.8. Set up for flexural strength

The flexural strength was computed using equation 3.5

$$f_f = \frac{p*L}{b*h^2} \quad \text{--3.5}$$

Where

f_f = flexural strength, in MPa

p = maximum applied load, in N

h = depth of the prism, in mm

b = width of the prism, in mm

L = Center to center between supports, in mm

3.2.2.7 Brittle examination

In design of structures for seismicity ductility of the material used has impact. This property can be traced by taking the brittleness. Therefore, the ratio of the split tensile strength to the compressive strength was used to examine the impact of the bamboo fiber on the brittleness property of concrete(Golewski, 2023; S. Zhang et al., 2021).

3.2.2.8 Image analysis

Image analysis was used to determine the mean crack width that appears at the end of the flexural test. For this purpose, the ImageJ software was used. After the flexural test, acetone ($(CH_3)_2CO$) was sprayed over the surface of the sample for detailed visual detection of the crack appearance. Then, the pictures of specimens from each category were taken for the subsequent crack width analysis using ImageJ software (Mahfuzur Rahman et al., 2019). The specimen and caliper ruler were photographed together using a high-resolution mobile phone to get a picture as shown in Figure 3.9 (a).

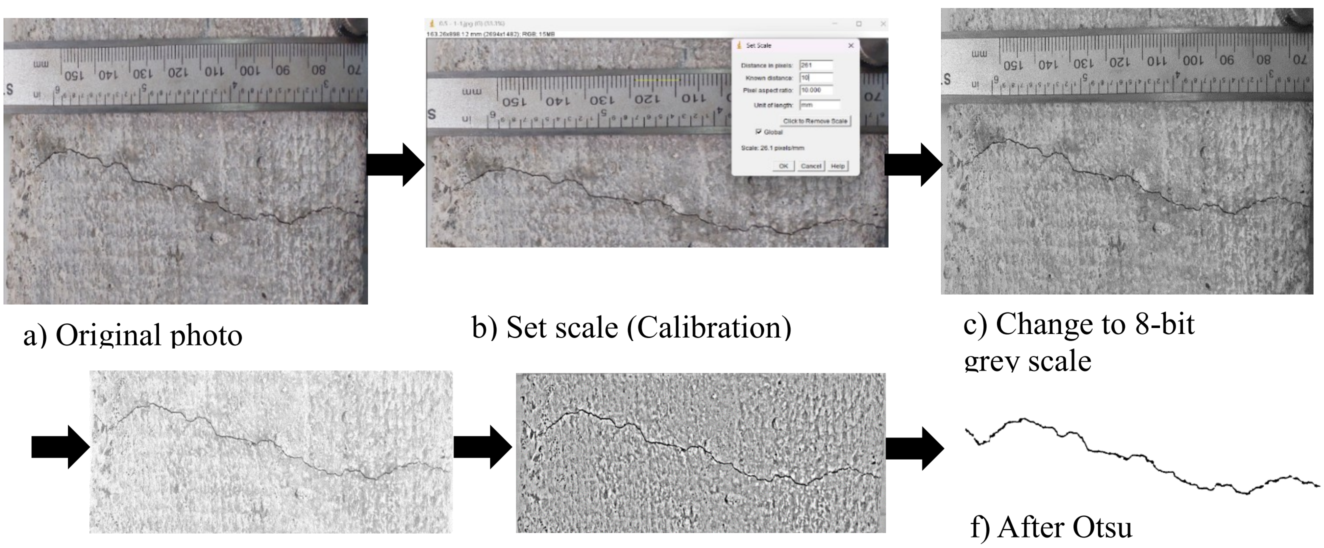

a) Original photo b) Set scale (Calibration) c) Change to 8-bit grey scale

d) Subtract background e) Bandpass filter applied f) After Otsu thresholding and cleaning

Figure 3.9. Crack width measurement procedure

After the specimen's picture with the caliper ruler was imported into the ImageJ image analysis software, calibrating the picture was conducted. After this, the image was changed to a gray level by selecting 8-bit. Bandpass filter was applied to enhance the cracks' edges, followed by Otsu thresholding and cleaning to well define the cracks. Then the crack widths were measured at 20 locations with a spacing of 5cm along the crack. The average crack width and standard deviations were computed based on twenty data points. The crack width measurement process is summarized and presented in Figure 3.9.

3.2.2.9 Acid attack

The acid attack was conducted by soaking the specimens of cube size 150mm in a 5% solution of sulphuric acid(Tayeh et al., 2021)(Arasilan gkumaran.v, 2017). After casting, the specimens were kept in a water bath for 28 days and air-dried for 15 days in the laboratory atmosphere. After recording the masses of samples, they were taken into polyethylene drums containing a 5% solution of sulphuric acid. The specimens were in the solution of sulphuric acid for 365 days. Figure 3.10 presents the ages corresponding to each testing type.

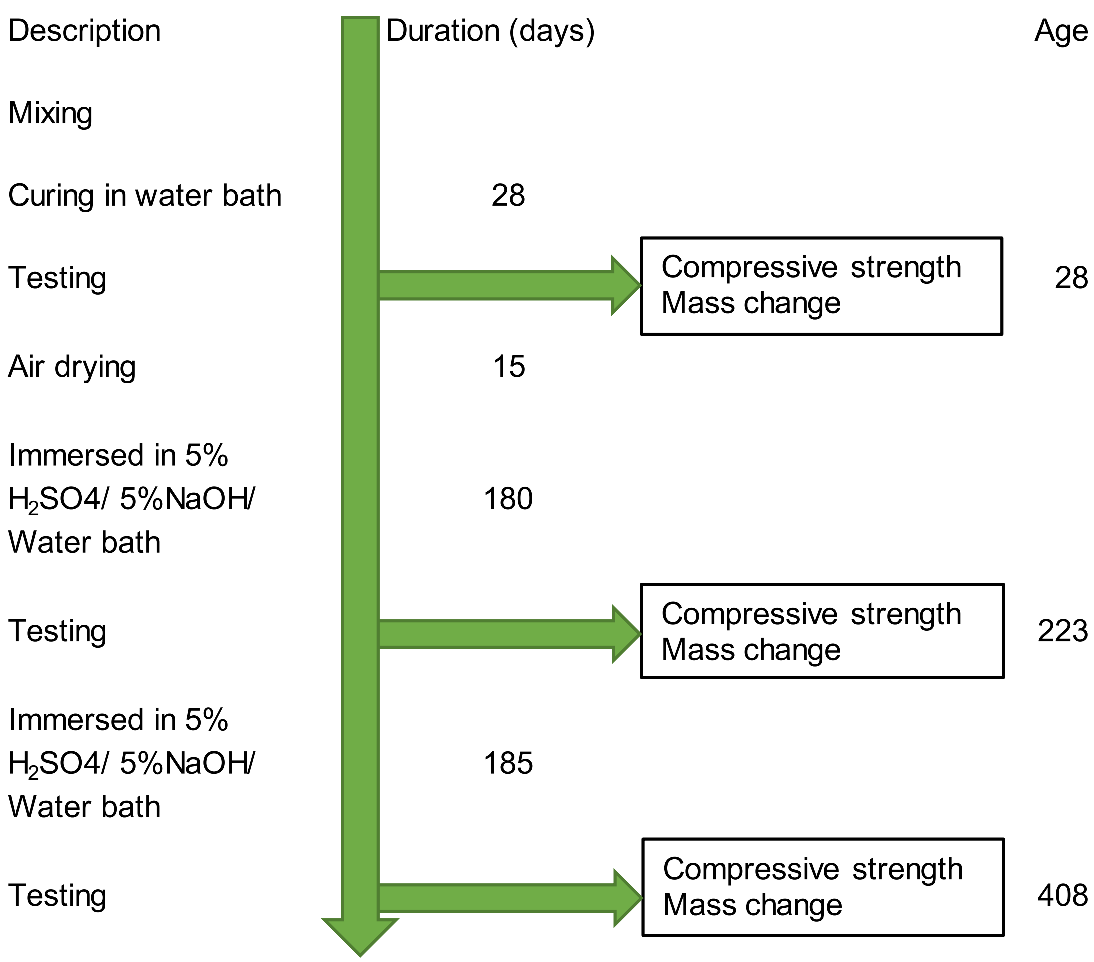

Figure 3.10. Tests and corresponding age

3.2.2.10 Alkaline attack

The alkaline attack was conducted by immersing the specimens of cube size 150mm within a 5% solution of sodium hydroxide(Tayeh et al., 2021)(Arasilan gkumaran.v, 2017). After casting, the specimens were kept in the water bath for 28 days, followed by air drying for 15 days within the laboratory atmosphere. After recording the masses of each sample, they were taken into polyethylene drums that had a 5% solution of sodium hydroxide. The specimens were in the solution of sodium hydroxide for 365 days. Figure 3.9 presents the ages corresponding to each testing type.

3.2.2.11 Solution concentration determination

The concentration of both sodium hydroxide and sulfuric acid was made 5%. This was done to create similar setups with other numerous studies(Tayeh et al., 2021)(Arasilan gkumaran.v, 2017). Such kind of concentrations are reasonable to conduct the examinations reasonably. If the concentration is very low, the solution effect will be very slow, and the test procedure will take a long time. If it is very high, deterioration may happen very quickly and, hence, will hinder a detailed examination, because the deterioration of concrete is a function of the concentration of solutions according to the earlier studies(Beddoe & Dorner, 2005). The PHs of the two categories were monitored using a PH meter shown in Figure 3.11 to ensure the acidity or alkalinity of the environment throughout the study period.

Figure 3.11. PH meter

3.2.2.12 Sample placement

In order to identify each sample after the duration of exposure, the specimen's placement position was marked on the container prepared for this purpose, as shown in Figure 3.12.

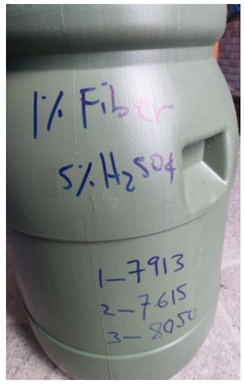

Figure 3.12. Specimens positioned in an acidic solution

3.2.2.13 Control specimen

Control specimens of 150mm cube size were cast and cured for 28 days in a water bath. Then, they were air-dried for 15 days in a laboratory atmosphere. Subsequently, they were put in the water bath for the same period of duration, similar to those put in the acidic and alkaline environment. Figure 3.9 presents the ages corresponding to each testing type.

3.2.2.14 Examination of the adverse environmental effects

The effect of the adverse environmental conditions (acid attack and alkaline attack) was evaluated by conducting compressive strength tests on a standard cube size of 150mm specimen at a loading rate of 0.28 MPa/s as per ASTM C39 (ASTM, 2001b). The compressive strengths were calculated from the ratio of the applied load to the surface area of one side of the cube. The compressive testing machine, called Control, with a capacity of 3000 KN, was used for the experiment. The specimens retrieved from acidic, alkaline, and normal environments were tested to determine their compressive strength at the prescribed ages. Then, the recorded compressive strengths were inserted into equation 3.6 to determine the variations developed in the specimens due to the acidic or alkaline environment.

$$\Delta\sigma_c(\%) = \frac{(\sigma_o - \sigma_f)*100}{\sigma_o} \text{ -- 3.6}$$

Where

$\Delta\sigma_c(\%)$ = Percentage of compressive strength change

σ_o = the compressive strength of specimens recorded before immersion in the solution (acidic or alkaline) or the compressive strength of specimens retrieved from the water bath. This is the compressive strength value at the 28th day.

σ_f = the compressive strength of specimens after immersion in the solution (acidic, or alkaline, or water bath) for the prescribed periods

The other mechanism to assess the acid and alkaline effect on the specimens was through mass loss due to such an effect. For this purpose, the mass of every specimen was measured and recorded before putting them in the prepared sodium hydroxide or sulphuric acid solution. Then, when their age reached for the compressive strength test, their mass was recorded again before being crushed by the compressive testing machine, as shown in Figure 3.13.

(a) Specimens marked with their mass ahead of pouring the solution (The numbers are the masses of the specimens)

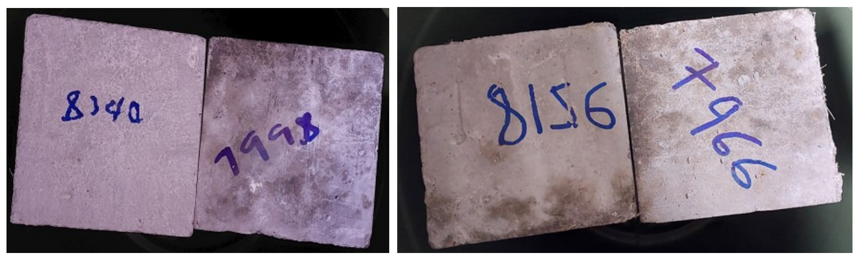

(b) Specimens picked and ready for mass measurement and compressive strength test (recovered from 5% NaOH solution)

(c) Specimens picked and ready for mass measurement and compressive strength test (recovered from 5% H_2SO_4 solution)

Figure 3.13. Samples appearance through the test procedure

After obtaining these masses, equation 3.7 was used to calculate mass changes that happened due to the immersion of the specimens in the solutions of sodium hydroxide or sulphuric acid.

$$\Delta m(\%) = \frac{(m_o - m_f) * 100}{m_o} \quad \text{------------------------------} 3.7$$

Where

$\Delta m(\%)$= mass change in percentage

m_o = masses of specimens recorded before immersion in the solution (acidic or alkaline) or the masses of specimens retrieved from the water bath

m_f = recorded masses of the specimens after immersion in the solution (acidic or alkaline, or water bath) for the prescribed periods

3.2.2.15 Volume of voids and absorption

As per ASTM C 642-97 (ASTM, 1997), samples with a 75mm cube size were prepared and used to conduct the volume of permeable voids and absorption capacity tests at the ages of 180 days and 365 days, which were counted from the 28-day curing age.

3.2.2.16 Assessment of volume of voids and absorption

The masses of specimens were recorded after oven-drying (Figure 3.14a), saturated after immersion (Figure 3.14b), and boiling (Figure 3.14c) as specified in ASTM C 642-97(ASTM, 1997).

(a) Oven drying samples (b) immersion in water (c) boiling in a bath

Figure 3.14. Volume of voids and absorption examination

Water absorption and the total volume of voids of the concrete were computed from saturated, suspended, and oven-dry masses of the specimens. The tests were conducted after 180 and 365 days. Specimens were put in an oven at 110 ° C for 24 hours and then cooled. The mass was recorded and then put for an additional 24 hours at a temperature of 110 ° C in an oven. When the difference between the two masses was found to be less than 0.5%, the second mass was taken as the oven-dried mass (M_D) of the samples. Then, the samples were immersed in water at room temperature for 48 hours. After this, their mass was recorded and put back for another 24 hours and weighed again. Ahead of taking them to balance, moisture on the surfaces of each sample was removed using a towel. When the difference among these masses was below 0.5%, the second mass was taken as a saturated one (M_S). Then, samples were put in a bath and boiled for 5 hours to get the boiled mass (M_B). Finally, the specimens' submerged weight was recorded as M_{su}. The absorption capacity (A_C) and total volume of voids (V_{vo}) are computed using equations 3.8 and 3.9.

$$A_C = \frac{M_S - M_D}{M_D} \quad \text{------------------------------------3.8}$$

$$V_{vo} = \frac{M_B - M_D}{M_B - M_{Su}} \quad \text{------------------------------------3.9}$$

The impact of the bamboo fiber dose on the total volume of voids was examined by calculating the variation with respect to the control specimen from Equation 3.10.

$$V_{bf/c} = \frac{V_{bf} - V_c}{V_c} * 100 \quad \text{------------------------------------3.10}$$

Where

$V_{bf/c}$ = the relative variation of volume of voids between the control and bamboo fiber reinforced samples in percentage

V_{bf}= the volume of voids of concrete at the specific bamboo fiber dose

V_c= is the volume of voids of the control specimen

3.2.2.17 Drying shrinkage examination

Molds shown in Figure 3.15 for the production of samples were fabricated as per ASTM C490. The molds were prepared with internal dimensions to get a 75mm square cross-section and a 285mm long prism. To measure the specimens in length compactor end gage studs were produced. All these were manufactured at the workshop of the School of Mechanical and Industrial Engineering, College of Technology and Built Environment, Addis Ababa University.

Figure 3.15. Fabricated mold

A control chamber was constructed with a temperature and humidity controller (Figure 3.16). The control chamber was placed in one dedicated room for this study. Rooms for such control need to be away from disturbances. The chamber has a display board to monitor the humidity and temperature inside it and a glass window to provide visual access, as shown in Figure 3.18 (a). The chamber has a fan to keep humidity uniform within the chamber, Figure 3.18 (c). An ultrasonic humidifier was used for the intended humid air supply, putting it in a barrel of water, Figure 3.18 (c). Holes were provided at the back of the chamber for the exhaust, Figure 3.18 (b). Bulbs were installed to be used as a source of heat, Figure 3.18 (c).

Arduino setup was designed to install an SD memory card so that temperature and humidity readings could be recorded every 10-minute interval throughout the duration of the study, Figure 3.18 (d). In order to avoid any disturbance during the supply of water, a tube was inserted at the back of the chamber, Figure 3.18 (b).

To ensure a smooth touch between the surface of the samples and the steel bars, a hard-plastic cover was wrapped around the steel bars, Figure 3.18 (c). This allowed the samples to move freely, avoiding any restraining effects during shrinkage. An additional digital humid meter was placed inside the control chamber to confirm the readings of the controller. Figure 3.18 shows the samples in the control chamber, thermometer, and related setups.

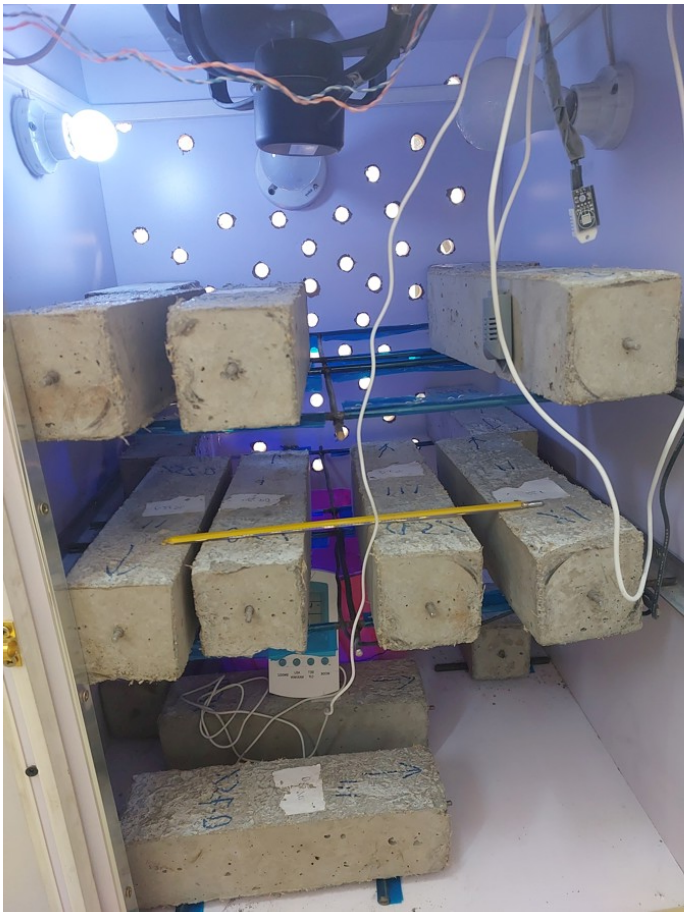

Figure 3.16 Specimens in the humidity chamber

The length compactor with an analog dial gauge of accuracy 0.002mm was used for the length measurement. To ensure the avoidance of any disturbances, the table on which the length compactor was placed was marked. Moreover, the place where the length compactor was put was marked. Daily visual inspection was conducted to ensure that the stability of the setups is not affected. Figure 3.17 presents the marks of the legs of the table on the ground floor and the bottom plate of the compactor on top of the table.

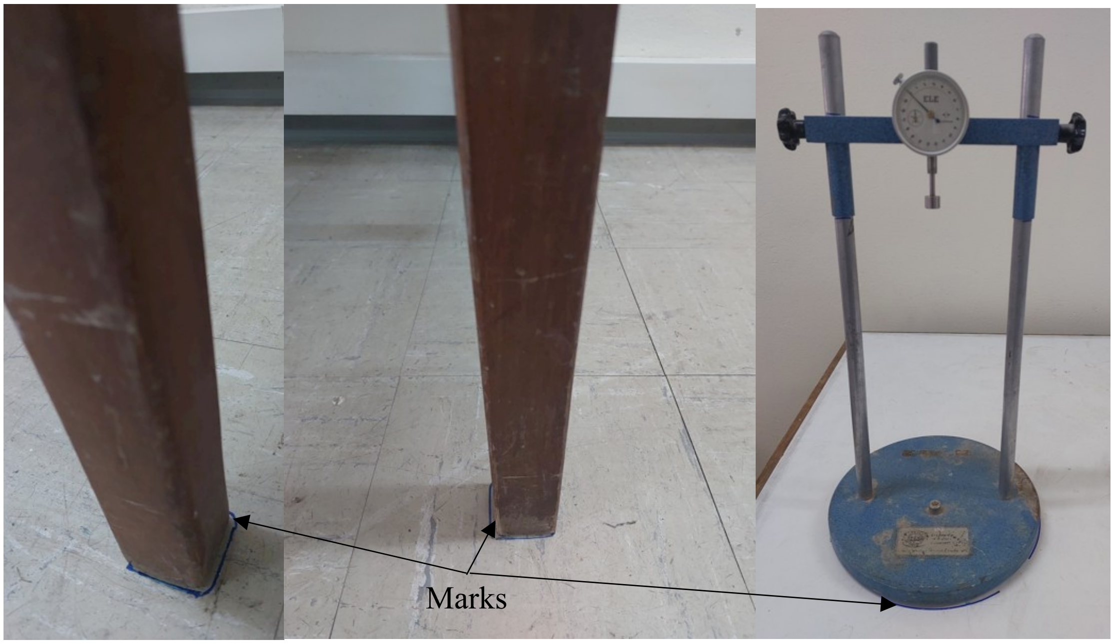

Figure 3.17. Table legs and base of compactor marked

75mm X 75mm X 285mm concrete prism-shaped specimens with 0%, 0.25%, 0.5%, 0.75%, and 1.0% bamboo fiber doses were prepared. As per ASTM C157, three replicas were cast for each bamboo fiber dose level.

All specimens remain in their mold for 24 hours. Then the samples were demolded carefully, and their measurements were taken using a length compactor. Immediately after the measurement, the specimens were placed back into the humidity chamber. The temperature and humidity levels of the chamber were 22±3^{o}C and 60±5%, respectively(H. Zhang et al., 2020).

(a)Front of the chamber

(b) Rear view of the chamber

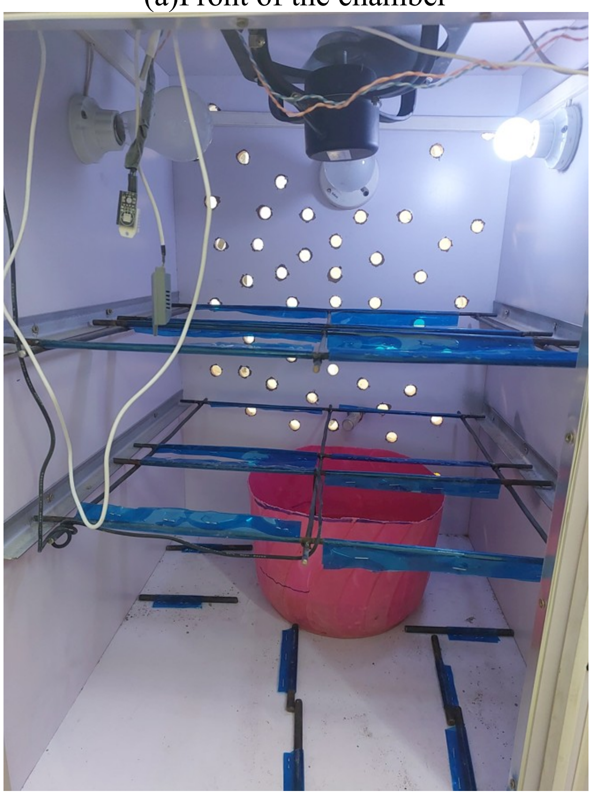

(c)Internal view of the chamber

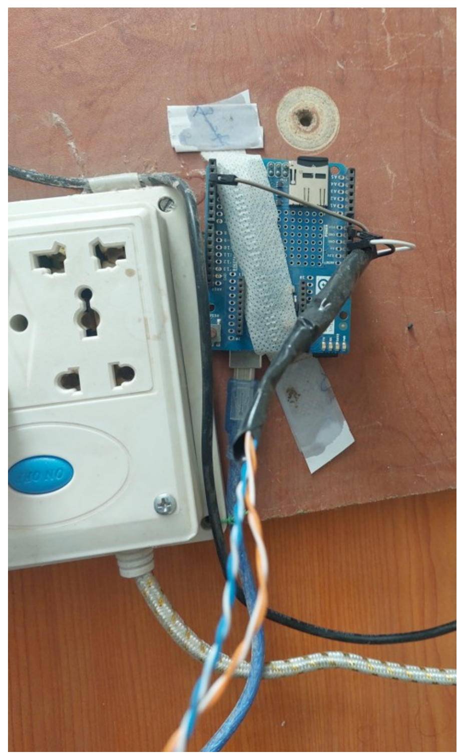

(d) Data recorder with SD card

Figure 3.18. Control chamber

To capture shrinkage behavior within the early hours, measurements were taken at two-hour intervals for the first six hours. Recording of readings proceeds daily for the first ten days, weekly for a month, and monthly until the end of the study(Folliard et al., 2003). The duration of the study was conducted for 198 days. Meyers (Meyers et al., 1970) stated that shrinkage characteristics can be adequately predicted from equations derived based on 100-day shrinkage data. Studies showed that drying shrinkage can reach a steady state around the age of 200 days(P. Chen et al., 2018).

The early hours of readings are important to get an insight into the shrinkage happening within the first day after demolding. The daily readings conducted in the first ten days are helpful in capturing the shrinkage phenomenon happening substantially due to volumetric changes, due to the migration of moisture towards the atmosphere, and depletion of the moisture in the concrete for the chemical reaction that leads towards strength gaining. The weekly recording for a monthly duration is to trace the tendency of shrinkage, while the rate tends to slow down. Such practices were exercised by various researchers. After the duration has elapsed so far, the rate of shrinkage tends to decline. Therefore, a single reading per month is enough until the end date of the experiment.

Throughout all the measurements, the position of the prisms was kept similar; that is, facing upward and facing towards the reader were on the same side, as shown in Figure 3.19. This helped to ensure consistency in measurement.

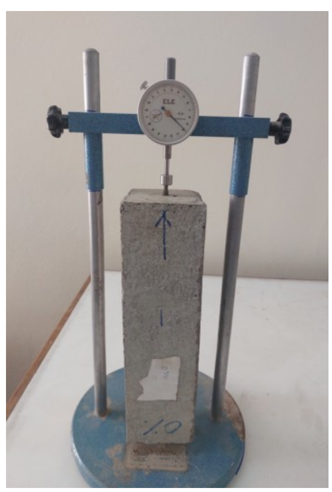

Figure 3.19. samples in the length compactor

The shrinkage strain of the samples was calculated by applying Equation 3.11(Židanavičius et al., 2023).

$$\varepsilon_{cs}(t, t_0) = \frac{\Delta l(t_0) - l_{cs}(t)}{L_0} \quad \text{--- 3.11}$$

Where

$\varepsilon_{cs}(t, t_0)$ = the total shrinkage strains of the specimen as time t

$\Delta l(t_0)$ = the initial length reading of the specimen

$l_{cs}(t)$ = length reading of the specimen at time t

L_0 = is the gauge length

3.2.2.18 Regression analysis

Regression analysis was conducted to select the best-fitting function for the set of data obtained in this study(A. Abubakar et al., 2022; J. Abubakar et al., 2025). For this purpose, RStudio version R-4.2.3 was employed; then the relations among the mechanical properties (compressive strength versus split tensile strength, compressive strength versus flexural strength, and flexural strength versus split tensile strength) were examined. Linear, power, and exponential functions were employed, and the best-fitting function was selected by comparing the R^2 value.

On the other hand, the capacity of the Excel spreadsheets was employed for the evaluation of the drying prediction equations and to propose a new drying shrinkage prediction equation for bamboo reinforced concrete. Before the development of the prediction equation, RStudio was used to split the data, with 80% of the collected data used to train or develop the prediction model and the remaining 20% of the data for testing the proposed model.

The method of nonlinear least squares is used for the regression analysis for the determination of the parameters in the prediction model. Accordingly, minimization of the sum of the squares of residuals was the way taken to formulate the best model, and the curve fit the data (Rafi & Nasir, 2016)(Montgomery, D. C. and Runger, 2003).

3.2.2.19 Statistical analysis of bamboo fiber reinforced concrete

A statistical analysis, known as analysis of variance (ANOVA), was conducted to assess whether the incorporation of bamboo fiber into concrete significantly influenced its various properties. Tukey test and T-score was employed to further investigate the most impact full bamboo fiber amount or dosage.

3.2.2.20 Trend examination

The impact of bamboo fiber on the strength gain of concrete throughout the study period is the other important concept. Therefore, the trends of various properties of the concrete and bamboo fiber hybrids were examined using an Excel spreadsheet.

3.2.3 Samples preparation

3.2.3.1 Samples for the study of mechanical properties of bamboo fiber reinforced concrete

Table 3.4. Types and number of specimens per test

No	Sample type	Test type	Number of samples per test type	Ages
1	S0	Density	21	7, 14, 28, 56, 90, 180, and 365 days
		Compressive strength		7, 14, 28, 56, 90, 180, and 365 days
		Split tensile strength		7, 14, 28, 56, 90, 180, and 365 days
		Flexural strength		7, 14, 28, 56, 90, 180, and 365 days
2	S25	Density	21	7, 14, 28, 56, 90, 180, and 365 days
		Compressive strength		7, 14, 28, 56, 90, 180, and 365 days
		Split tensile strength		7, 14, 28, 56, 90, 180, and 365 days
		Flexural strength		7, 14, 28, 56, 90, 180, and 365 days
3	S50	Density	21	7, 14, 28, 56, 90, 180, and 365 days
		Compressive strength		7, 14, 28, 56, 90, 180, and 365 days
		Split tensile strength		7, 14, 28, 56, 90, 180, and 365 days
		Flexural strength		7, 14, 28, 56, 90, 180, and 365 days
4	S75	Density	21	7, 14, 28, 56, 90, 180, and 365 days
		Compressive strength		7, 14, 28, 56, 90, 180, and 365 days
		Split tensile strength		7, 14, 28, 56, 90, 180, and 365 days
		Flexural strength		7, 14, 28, 56, 90, 180, and 365 days
5	S100	Density	21	7, 14, 28, 56, 90, 180, and 365 days
		Compressive strength		7, 14, 28, 56, 90, 180, and 365 days
		Split tensile strength		7, 14, 28, 56, 90, 180, and 365 days
		Flexural strength		7, 14, 28, 56, 90, 180, and 365 days

The total number of samples for the study was 105 per test type. The distribution and the ages at which examination of density, compressive, split tensile, and flexural strengths were conducted are presented in Table 3.4.

3.2.3.2 Samples for the study of durability properties of bamboo fiber reinforced concrete

The experiment type and amount of sample per bamboo dosage at respective ages of concrete are presented in Tables 3.5 and 3.6.

Table 3.5. Specimen number for acid and alkaline attack tests

Medium	Age (days)	Number of specimens per bamboo fiber dose				
		0%	0.25%	0.5%	0.75%	1.0%
Water bath	223	3	3	3	3	3
	408	3	3	3	3	3
Acidic	223	3	3	3	3	3
	408	3	3	3	3	3
Alkaline	223	3	3	3	3	3
	408	3	3	3	3	3
Control	28	3	3	3	3	3

Table 3.6. Specimen number for volume of voids and absorption examination

Age (days)	Test type	Number of specimens per bamboo fiber dose				
		0%	0.25%	0.5%	0.75%	1.0%
180	Volume of voids and absorption	3	3	3	3	3
365	Volume of voids and absorption	3	3	3	3	3

3.2.3.3 Samples for the study of shrinkage properties of bamboo fiber reinforced concrete

The number of samples corresponding to the type of test and the age when the test was conducted to evaluate the impact of bamboo fiber on the drying shrinkage of concrete are listed in Table 3.7

Table 3.7. Specimens of shrinkage

No	Sample type	Test type	Number of samples per test (75mm X 75mm X 285mm)	Ages (days)
1	Concrete + 0% bamboo fiber	Unrestrained drying shrinkage measurement	3	1,2,3,4,5,6,7,8,9,10,19,26,33,40,70,101,131,162,197
2	Concrete + 0.25% bamboo fiber	Unrestrained drying shrinkage measurement	3	1,2,3,4,5,6,7,8,9,10,19,26,33,40,70,101,131,162,197
3	Concrete + 0.50% bamboo fiber	Unrestrained drying shrinkage measurement	3	1,2,3,4,5,6,7,8,9,10,19,26,33,40,70,101,131,162,197
4	Concrete + 0.75% bamboo fiber	Unrestrained drying shrinkage measurement	3	1,2,3,4,5,6,7,8,9,10,19,26,33,40,70,101,131,162,197
5	Concrete + 1.0% bamboo fiber	Unrestrained drying shrinkage measurement	3	1,2,3,4,5,6,7,8,9,10,19,26,33,40,70,101,131,162,197

4 Results and Discussions

4.1 Yushania alpina bamboo fiber examination

4.1.1 Introduction

The characteristics of bamboo fiber are affected by the type of species, location, and method of extraction. Mechanical, chemical, and a combination of mechanical and chemical methods are identified for the extraction of fiber from bamboo culms. These extraction methods have their own merits and demerits, and there are no definite demarcations when comparing their advantages. The impacts of these extraction methods range from the quality of fiber that can be obtained to their expenses(Subash. S, Stanly Jones Retnam. B, 2017) (Phong et al., 2012)(F. Wang & Shao, 2020).

Different studies revealed diverse outcomes on the tensile strength of fiber extracted from bamboo. Shah et al.'s (Shah et al., 2016) assessment showed that the steam explosion method was the optimum way to extract fiber from bamboo. Phong et al.(Phong et al., 2012) obtained bamboo fiber with the maximum tensile strength when the mechanical method was used for the extraction. On the other hand, the research results of Rawatan et al. (Rawatan & Buluh, 2018) presented that bamboo fiber had a tensile strength increase due to the alkaline treatment. Among the numerous bamboo fiber treatments, the alkaline treatment is the most basic and effective at improving the mechanical interlocking or bonding between the matrix and the fiber (Hashim et al., 2017). This is accomplished by roughening the smooth external surface and decreasing the fiber diameter, hence the aspect ratio increases. Sodium hydroxide removes hemicelluloses, wax, lignin, oils, and other impurities attached to the outer surface of the plant fibers and undertakes a reaction with the hydroxyl group. Due to this, the water absorption capacity of the fiber is also reduced. However, the alkaline solution used for the treatment has to be limited within some percentage of concentration so that the fiber will not be degraded, and that will decrease the tensile strength (Behera et al., 2018)(Shah et al., 2016)(Hashim et al., 2017)(Ede et al., 2020b)(N. Kaur et al., 2017).

The impact of an alkaline environment on the chemical composition of biofibers, which include hemicellulose, lignin, cellulose, and impurities, is an important consideration in the investigation of natural fibers. Jing et al. (Jing et al., 2023) presented the alterations of physical, chemical, and mechanical qualities of palm fibers when they were exposed to the alkaline medium. Moreover, the study proved that the characteristics of the fibers differ due to the interactions that happen in the alkaline environment.

Therefore, this study was designed to investigate the impacts of the employment of mechanical, chemical, and combined extraction techniques on the fiber obtained from Yushania alpina bamboo species.

4.1.2 Results and Discussions

4.1.2.1 Impact of the extraction methods on the chemical compositions of bamboo fibers

This study presented that the chemical compositions of bamboo fibers extracted by mechanical, chemical, and combined techniques have different proportions (Table 4.1). The percentage of cellulose showed an increase in the case of fibers extracted chemically because of the decrease in lignin and hemicellulose. Therefore, the extraction method is the cause of the varied chemical composition of bamboo fiber. Chemical compositions of natural fibers were affected by factors such as fiber sources, locality in which it grows, extraction process, and maturity(Safwan et al., 2018).

Table 4.1. Bamboo fibers main chemical constituents

Extraction method	Code	Cellulose (%)	Hemicellulose (%)	Lignin (%)
Mechanical (Physical)	M	39.40	28.13	25.91
Combined (Mechanical + Chemical)	MC	42.44	29.46	20.85
Chemical (3% NaOH)	C3	51.45	20.43	20.40
Chemical (6% NaOH)	C6	59.31	12.31	20.75
Chemical (9% NaOH)	C9	60.03	13.39	19.2

The chemical composition assessment showed that fibers exposed to an alkaline medium during their extraction process had less lignin and hemicellulose content. Likewise, Martijanti et al. (Martijanti et al., 2020) carried out a chemical composition assessment on the fibers of the Gigantochloa apus and Bambusa tuldoides bamboo species. Due to the use of a NaOH solution for fiber extraction, cellulose showed an increase, while hemicellulose and lignin showed a reduction. The amounts of hemicellulose, cellulose, and lignin of those species were in the range of 16.21%–19.15%, 46.91%–55.68%, and 16.93%–21.30%, respectively.

There is an association between the mechanical properties of bamboo fiber and the fiber's chemical composition. According to B. Singh and Y. Dessalegn (B. Singh & Dessalegn, 2021) and S.Y. Zhang et al (S. Y. Zhang et al., 2013), there was an increase in the tensile strength of bamboo fiber because of the observed decrease in the lignin content in the fiber.

4.1.2.2 Impact of the extraction methods on the tensile strength of bamboo fibers

The recorded readings of the tensile force exerted on the bamboo fiber, their mass, and length are included in the annex. Table 4.2 presents the mean tensile strengths of the samples in each category of extraction methods. The values in the parentheses represent the standard deviation. Such deviations were common characteristics observed in fibers extracted from plant sources(Phong et al., 2012) (Alves Fidelis et al., 2013). Unlike industrial products, this variability arises from the non-uniformity of fibers caused by the extraction process and the intrinsic variation within the plant.

Table 4.2. Tensile properties of bamboo fiber obtained by different extraction methods

Extraction method	Code	Mean Diameter, μm	Mean Tensile strength, MPa
Mechanical (Physical)	M	385.29 (± 14.63)	205.46 (± 129.06)
Combined (Mechanical + Chemical)	MC	349.36 (± 21.37)	234.71 (± 112.47)
Chemical (3% NaOH)	C3	262.73 (± 15.49)	385.78 (± 163.45)
Chemical (6% NaOH)	C6	231.60 (± 9.94)	392.10 (± 95.97)
Chemical (9% NaOH)	C9	236.87 (± 13.68)	387.73 (± 163.81)

The tensile strengths of bamboo fibers extracted chemically were greater than those obtained by other methods. 205.5 MPa was the mean tensile strength value of bamboo fiber extracted using the mechanical technique (M), and there was a slight enhancement when the combined technique (MC) is used for the extraction.

The tensile strength of fibers obtained by retting in a 6% NaOH solution increased by 90.84% when compared to mechanical or physical techniques. In comparison to the mechanical method, retting in the 9% NaOH solution improves the tensile strength of the bamboo fiber by 88.72%. The tensile strength of the bamboo fiber extracted by retting in the 3% NaOH solution improved by 87.77% in comparison with the result achieved from the mechanical extraction method.

The tensile strength of the bamboo fibers extracted by the combination of mechanical and chemical methods is more by 14.23% than that of the mechanical technique. However, the combined method produced fibers with reduced tensile strength compared to the chemical method.

In comparison to the physical or mechanical method, the diameter of bamboo fibers extracted by retting in 3% NaOH, 6% NaOH, and 9% NaOH was reduced by 31.81%, 39.89%, and 38.52%, respectively. This finding aligns with the recommendation that using a higher alkaline concentration during the extraction can reduce the diameter of the fiber. This is because the alkaline medium during the extraction process washed away waxes and other impurities attached to the fibers. On the other hand, the tensile strength of the bamboo fibers was found in the range typical of high-performance natural fibers(Alves Fidelis et al., 2013).

The ANOVA analysis revealed a statistically significant ($p < 0.05$) increase in the tensile strength of bamboo fiber when the chemical method of extraction was employed. Tukey's standardized test showed that there are statistically insignificant variations among the tensile strengths of the fibers extracted using the chemical method. Nevertheless, this test showed that the use of a 6% NaOH solution for extracting bamboo fiber has a significant impact on the tensile strength in comparison with the mechanical method.

4.1.2.3 Moisture content and extraction method impact on the bamboo fibers absorption

The moisture content of extracted fibers by the employed method is shown in Table 4.3. Moreover, the effect of the extraction methods on the bamboo fibers' absorption capacity is shown in the same table.

Table 4.3. Absorption capacity and moisture content

Code	Extraction method	Absorption (%)	Moisture Content (%)
M	Mechanical	60.30	6.62
C3	Chemical (3% NaOH)	59.03	6.86
C6	Chemical (6% NaOH)	57.09	6.56
C9	Chemical (9% NaOH)	57.83	6.33
MC	Combined	59.15	6.57

As presented in Table 4.3, the absorption capacity is on the decrement side when retting in a solution of NaOH is used to obtain the fibers. This is because of the decrease of impurities and other hydrophilic constituents in the fiber when immersed in an alkaline environment during the extraction procedure (Yimer & Gebre, 2023)(Raghunathan, V., Ayyappan, V., Dhilip, J. D. J., Sundarrajan, D., Rangappa, S. M., & Siengchin, 2023).

The experiment verified that the diameter of the bamboo fibers found by the chemical technique was decreased, as shown in Table 4.2. The decrease in diameter of the fibers implies an increase in the surface area. According to Leonard Y.(Mwaikambo, 2009), Fiber bundles with smaller diameters have reduced porosity, which can be one reason for reduced absorption capacity. The other significant parameter to study when applying it to the concrete is its absorption capacity, because this will have an impact on the final composite product. The fibers extracted using the chemical extraction technique showed a lower absorption capacity. The values found in this experimental assessment are comparable with previous study findings (Espitia et al., 2018).

4.1.2.4 Impact of extraction method on the functional groups of bamboo fibers

Figure 4.1 shows FTIR spectra of bamboo fibers obtained using the employed methods.

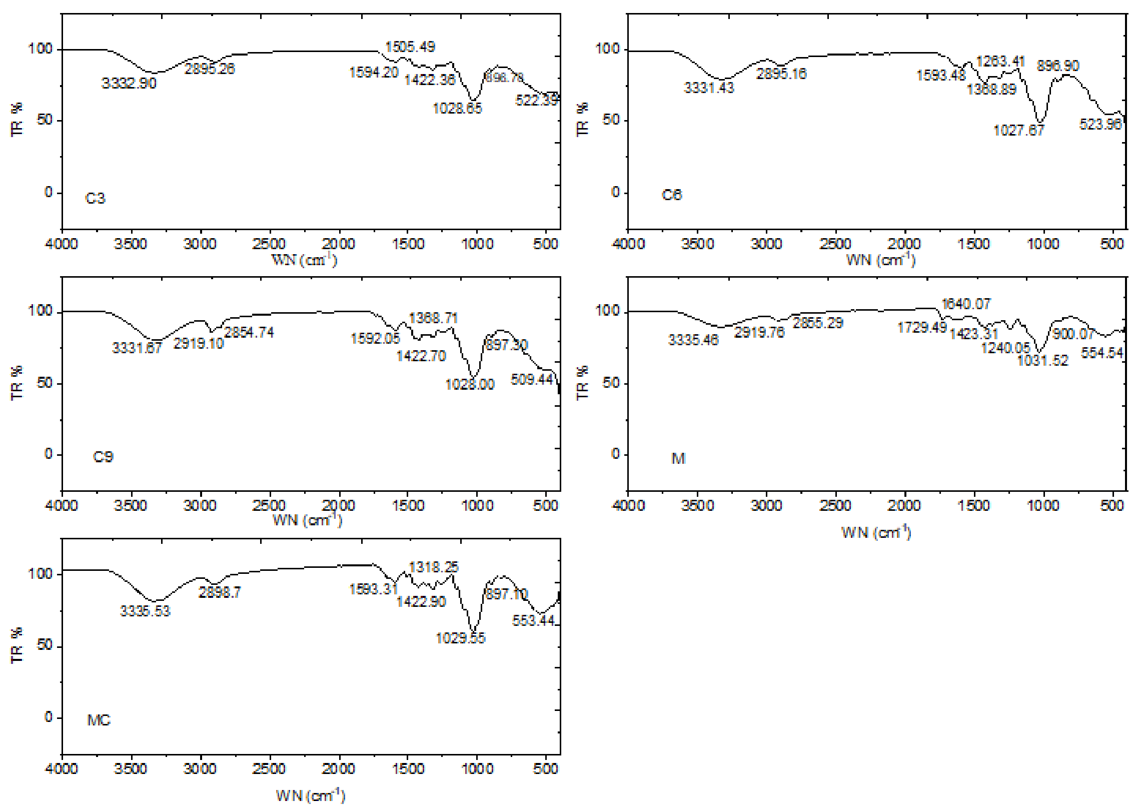

Figure 4.1. FTIR (Fourier transform infrared) spectroscopy analysis of bamboo fibers

In FTIR analysis, the reduction, disappearance, and appearance of peak values at various wave numbers are used to trace changes among the specimens collected. Accordingly, the conducted FTIR experiment shows that fibers extracted from Yushania alpina species have free hydroxyl alcohol, which is an O-H stretching bond functional group whose peak value fell in the range of 3300 cm^{-1} to 4000 cm^{-1}, similar to other species. However, unlike other species, the examined specimens did not reveal additional peaks within the range (Khusairy et al., 2016), as presented in Table 4.4.

The other peak value was detected at 1729.49 cm^{-1} on fiber extracted by mechanical method or retting in pure water, and this peak vanishes on fibers obtained by using other extraction methods. The vanishing of peaks at this value is due to the NaOH solution used for their extraction. The nonappearance of a peak at this value is attributed to the elimination of hemicellulose, which is the carbonyl group(Dody et al., 2008). The other range, where the peak is observed, is within 1640 cm^{-1} to 1680 cm^{-1}, which is C=C alkenes, the lignin indicator range. In this research, there is a peak at 1640.07 cm^{-1} in the case of fiber extracted by employing the mechanical method, which demonstrates a decrease in fibers extracted using the combined technique and the chemical method(H. Chen et al., 2017). This designates the decrease of lignin due to the fiber exposed to the NaOH solution during the extraction process. The decrease of lignin contributes to an increase in the tensile strength, as proposed by scholars (Pramudi et al., 2021). Generally, due to the absence of new functional groups, there was a similarity among the FTIR spectra of all the specimens (K. Zhang et al., 2018).

Table 4.4. Characterization and spectral analysis of bamboo fiber

Bond-Functional Group (Khusairy et al., 2016) (Bayu et al., 2019)	Yushania alpina bamboo fiber					Treated bamboo (Bambusa shrep) (cm^{-1}) (Khusairy et al., 2016)
	M (cm^{-1})	MC (cm^{-1})	C3 (cm^{-1})	C6 (cm^{-1})	C9 (cm^{-1})	
O-H stretching, Free Hydroxyl-Alcohol, Water, Phenols						3837.06, 3722.61, 3597.24
O-H stretching, H-bonded-Alcohol, Water, Phenols	3335.46	3335.53	3332.90	3331.43	3331.67	3336.85
C-H Stretching (CH; CH_2; CH_3) Carboxylic Acids	2919.76, 2855.29	2898.75	2895.26	2895.16	2919.10, 2854.74	2912.51
C=O Stretching, Carbonyl	1729.49					
C=C Stretching-Alkenes (lignin)	1640.07	1593.31, 1506.62	1594.20, 1505.49	1593.48	1592.05	1685.79
C-H bending – Alkanes (Cellulose; hemicellulose; lignin)	1423.31, 1372.89, 1320.73, 1240.05	1452.56, 1422.90, 1366.84, 1318.25, 1264.04	1422.35, 1365.53, 1319.89, 1261.31	1422.20, 1368.89, 1319.18, 1263.41	1422.70, 1368.71, 1318.52, 1262.2	1402.25
C-O Stretching -Alcohol (Cellulose; hemicellulose; lignin)	1156.28 1031.52	1029.55	1155.2, 1028.65	1156.32, 1027.67	1155.55, 1028.00	1026.13
C-H "oop"-Aromatic (lignin)	900.07	897.1	896.78	896.9	897.30	

4.1.2.5 Thermal Analysis of bamboo fiber extracted by various methods

The thermal degradation properties of the bamboo fibers were studied using TGA and are shown in Figure 4.2. The thermal degradation phase comprises hemicellulose degradation, moisture loss, lignin degradation, and cellulose degradation.

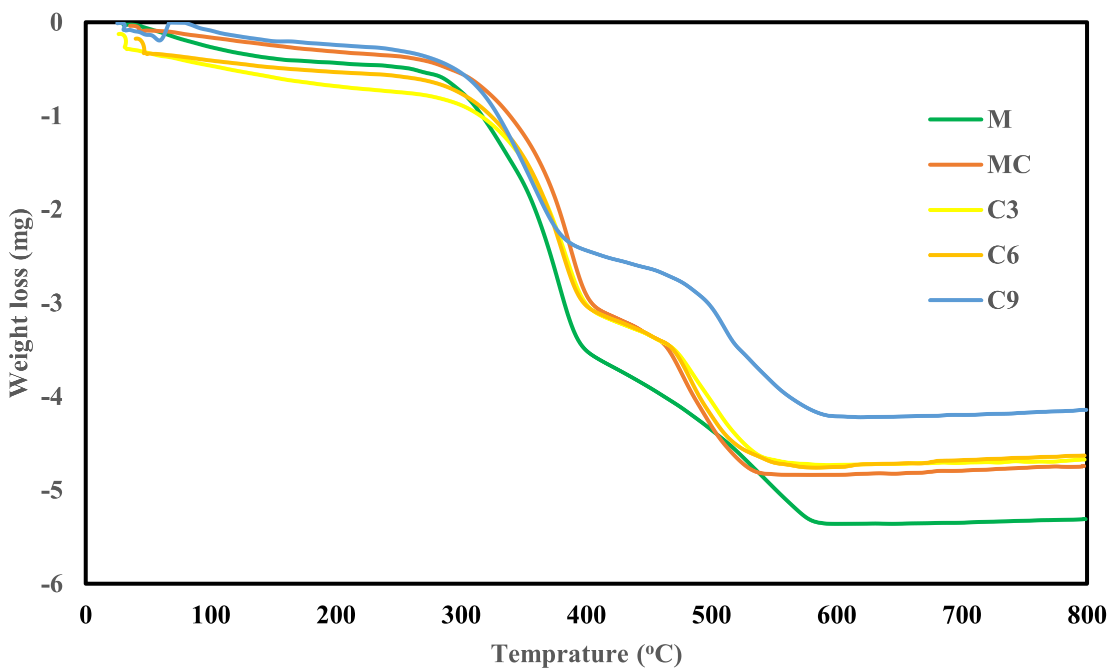

Figure 4.2. TGA graph of bamboo fibers

The initial phase of weight loss was found within the range from 25 °C up to 180 °C, related to the evaporation of water in the fibers. Then the degradation of cellulosic chemicals followed; this occurred from 200°C to 550°C. The degradation of hemicellulose is completed around 400 °C. Lignin degradation began at a temperature less than 200 °C and extended to a wide range up to the end temperature, which contributed to the acceleration of the reaction of cellulose and hemicellulose (Udhayakumar et al., 2023)(Fang et al., 2023). The third degradation, which is cellulose, was completed around 500°C. The end phase of degradation was lignin.

As presented in the graph, there was a move towards the right when the bamboo fibers were soaked in the solution of sodium hydroxide associated with the extraction method. Because of this, the bamboo fibers obtained by using the combined and chemical methods showed better thermal characteristics than those mechanically extracted (Fang et al., 2023). Generally, better thermal was observed on fibers threated with alkaline solution due to decreased hemicellulose and other waxy substances attached on the fiber(Nwankwo et al., 2025).

4.1.2.6 Impact of the extraction method on the morphology of bamboo fibers

The internal structure or morphology of the bamboo fibers was inspected using the scanning electron microscope (SEM), and the obtained image is presented below in Figure 4.3.

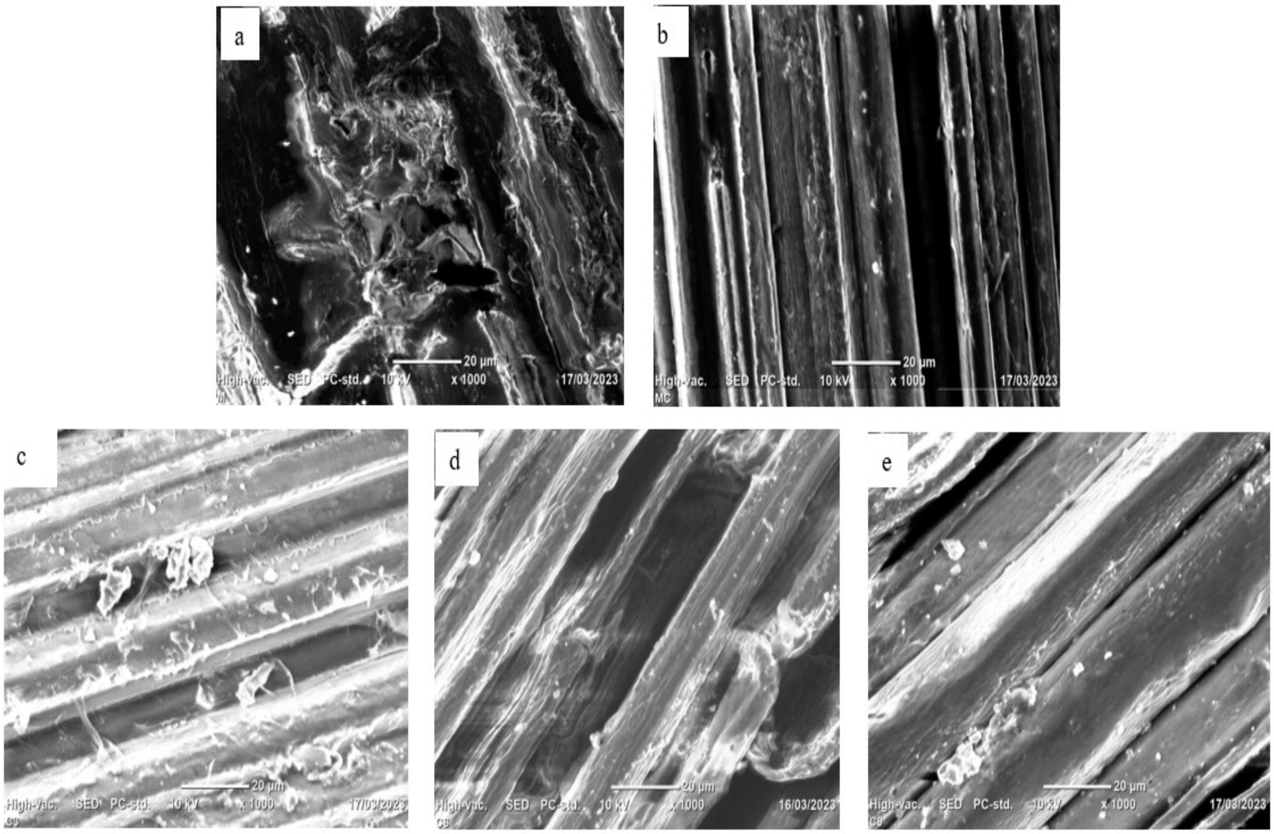

Figure 4.3 SEM images at X1000 (a) Mechanical, (b) Combined, (c) 3% NaOH, (d) 6% NaOH, (e) 9% NaOH

As per Figure 4(a), the fiber extracted by means of the physical or mechanical technique has an accumulation of soft tissue, which is due to wax and impurity attachments (Bayu et al., 2019). On the other hand, fibers found by passing through the combined method of extraction have impurities attached to the surface of the fiber, as shown in Figure 4(b). As per Figure 4(c), residuals of impurities are detected on the bamboo fiber obtained by using the chemical method of extraction when retting in a solution of 3% NaOH concentration is used. Fibers extracted by the chemical method with retting in 6% NaOH concentrations showed a nearly rough and clean surface, as revealed in Figure 4(d). Figure 4(e) demonstrates fibers extracted by the chemical method with retting in a 9% concentrated solution of NaOH. These fibers were found to show a rough surface, and holes appeared, which aligns with previous research findings (X. Zhang et al., 2015)(Rao et al., 2018)(A. A. Salih et al., 2020)(B. Singh & Dessalegn, 2021). The surfaces of the fibers found using the chemical extraction method became clean. Elimination of impurities and the presence of some roughness on bamboo fibers extracted by employing the chemical technique is good for utilization in composites. This is because there will be better adhesion of the fibers within the matrix (K. Zhang et al., 2018).

4.1.3 Summaries

This comprehensive study methodically addressed the multirange effects that the extraction techniques exert on the diverse properties inherited in the fiber that is derived from the species Yushania alpina, which is found in Ethiopia, particularly within the Sidama regional state, around Hager Selam town.

From this study, the following findings are drawn.

- The diameter of the fibers obtained through the chemical technique was less than that extracted through the mechanical method.
- The chemical method of extraction gave tensile strength enhancement of more than 90% than that of the mechanical technique. In ascending order, the mechanical method, the combined method, and the chemical method gave the tensile strength of bamboo fiber.
- The FTIR study demonstrated that there was no new functional group created because of the chemical NaOH used for the fiber extraction. On the other hand, impurities, waxes, and lignin are removed. The removal of these substances improves the bond in the utilization of composites. The decrease of lignin in fibers extracted by applying chemical procedures contributed to an improvement of their tensile strength.
- The mass loss observed in the case of mechanically extracted fibers was higher than that of the other procedures at the specified range of temperatures, and the graph was pulled to the left direction. This indicates that chemical and combined methods of bamboo fiber extraction showed better thermal properties.
- The chemical extraction procedure by itself can be taken as one way to obtain treated bamboo fiber to get better characteristics, which is significant for its subsequent application in a composite. The absorption capacity was in the range of the other species investigated, and the outcome is encouraging for utilization in composites.

- Bamboo fibers extracted using the chemical technique of extraction showed decreased lignin and hemicellulose and increased cellulose in their composition.
- The bamboo fiber morphology was found to be rougher as the concentration of NaOH used increased for its extraction. However, excess concentration has an impact on the fiber. When using a NaOH concentration of 9% for the extraction of the fibers, their surface became rougher, and holes appeared.
- The tensile strength of this bamboo fiber was found in the high-performance natural fiber range.

The chemical technique employed for the extraction resulted in bamboo fibers exhibiting higher mean tensile strength, better thermal properties, and improved morphology. This has encouraging implications for its application in composites. Therefore, bamboo fiber will play a significant role in realizing sustainable construction. Furthermore, this is very beneficial for nations targeting to exploit their bamboo resources for composite construction by decreasing their dependence on fibers that are imported and environmentally unfriendly.

4.2 Bamboo fiber reinforced concrete (BFRC) mechanical properties examination

4.2.1 Introduction

The characteristics of concrete are governed by its constituents. In order to improve the poor tensile and ductility behaviors of concrete, various forms of fiber addition have been practiced. Due to sustainability issues, there is an interest in looking for and researching alternative fibers from plant sources, including bamboo. Accordingly, there are research endeavors on the utilization of bamboo fiber for improving the weaknesses of concrete. Those previously conducted researches were on very limited species of bamboo among the thousands. Moreover, it is known that the behaviors of the fibers are highly variable with the species, localities, and method of extraction. Therefore, in this topic, the impacts of the bamboo fiber obtained from the species called Yushania alpina on the slump, mechanical properties, and cracking of concrete are dealt with. Moreover, the trend of strength development and the relationships between compressive versus split tensile, compressive versus flexural, and flexural versus split tensile strengths are addressed. The functions that represent well the relationships between these mechanical properties are also included.

4.2.2 Results and discussion

4.2.2.1 Impact of bamboo fiber on the concrete slump

In this study, the workability of the concrete produced by incorporating bamboo fiber was examined through a slump cone. The ease of fresh concrete for transportation and its placement is expressed as workability. This is an important parameter for determining where the concrete is to be used. Highly workable concrete is required in areas where there is congestion of reinforcement bars, while low workable concrete has applications in pavements and large sections (Ismail & AL-Hashmi, 2008). Concrete with 0% bamboo fiber has shown the highest workability; however, this is in the range of medium workability as presented in Figure 4.4. The next workable concrete was achieved when the bamboo fiber was at 0.25% and 0.5%. These three specimen types satisfied the requirement of a slump range from 25mm to 75mm to be used for pavement, slabs, and mass concrete(Day et al., 2002). The rest are low workable ranges. The workability reduction was attributed to the presence of bamboo fibers that absorb a portion of the water that was free for lubrication and paste formation. Moreover, the fibers have an impact on hindrance the flow of concrete due to the creation of interwoven among them(Okeola et al., 2018a)(Tolêdo Filho et al., 1999).

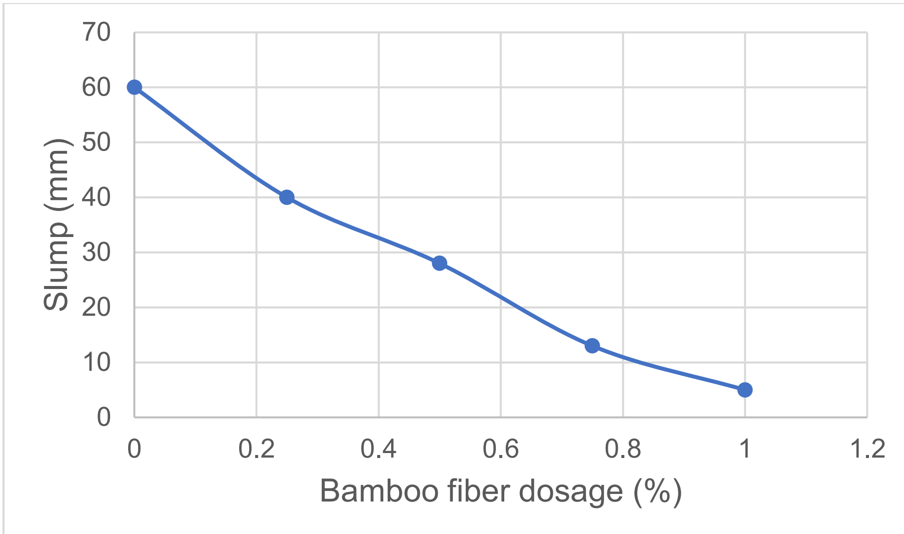

Figure 4.4. Slump versus bamboo fiber dose

4.2.2.2 Impact of bamboo fiber on the concrete density

The density value from an average of three replicas is given in Table 4.5. In the case of normal-weight concrete, the bulk density range is between 2.2g/cc and 2.6g/cc (Neville, 2002). Therefore, all the samples satisfied the normal weight concrete criteria. As the fiber dosage added to the concrete increased, the density of the final hardened concrete decreased. This was attributed to the bamboo fiber taking the place of other denser constituent materials, namely sand, aggregate, or cement (Okeola et al., 2018a).

Table 4.5. Densities of samples

Sample ID	Density (g/cc)						
	7^{th} days	14^{th} days	28^{th} days	56^{th} days	90^{th} days	180^{th} days	365^{th} days
S0	2.432	2.433	2.434	2.445	2.451	2.454	2.454
S25	2.406	2.404	2.408	2.419	2.438	2.441	2.443
S50	2.388	2.389	2.393	2.396	2.398	2.405	2.408
S75	2.375	2.376	2.381	2.388	2.392	2.393	2.398
S100	2.345	2.345	2.355	2.359	2.376	2.379	2.379

4.2.2.3 Impact of bamboo fiber on the compressive strength of concrete

The compressive strength test result at the specified ages is presented after computing the mean of the triplicates as shown in Table 4.6.

Table 4.6. Compressive strength on the specified days of sample age

Bamboo fiber dose (%)	Compressive strength (MPa)						
	7	14	28	56	90	180	365
0%	20.647	21.650	37.897	43.067	43.230	49.000	50.317
0.25%	21.870	22.863	38.390	42.473	43.620	48.943	49.923
0.50%	20.253	21.070	34.887	40.883	42.063	45.780	47.223
0.75%	17.080	21.060	30.513	37.230	37.797	40.930	41.530
1.00%	15.460	19.020	28.580	32.407	34.950	35.487	37.387

As shown in Figure 4.5, the compressive strength has decreased as the fiber dosage increased to 1.0%. The compressive strength between concrete without bamboo fiber and with 0.25% bamboo fiber showed comparable values. As the dosage of the fiber increased, the respective compressive strengths attained reduced. Especially, concrete samples with 0.75% and 1.0% bamboo fiber dosage showed the least compressive strength. S100 gave a lesser compressive strength value than the target value set in the mix design (Okeola et al., 2018b). The reduction of the compressive strength is due to layered fibers in the cement matrix and entrapped air, which has an affect the adhesion and effective bridging effect among aggregates (Kurpińska et al., 2022) (Abbas et al., 2022).

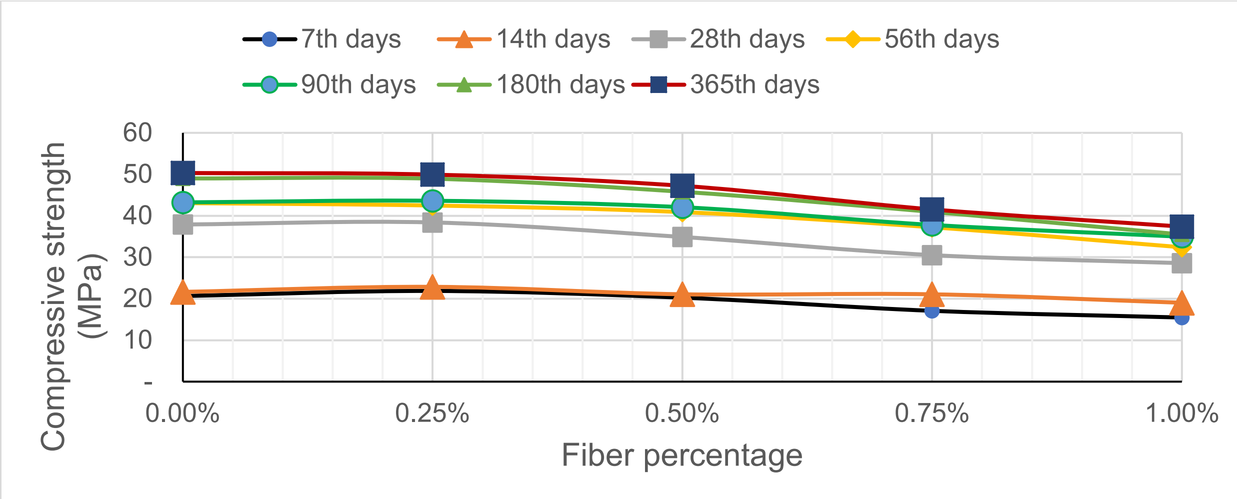

Figure 4.5 Compressive strength versus bamboo fiber dose

The strength development with age is presented in Figure 4.6. The rate of strength gain was high up to the 28th age of concrete, then the increment rate declined up to age 56. After 180 days, the rate of strength increments is very minimal. This could be observed from the slope along the graph.

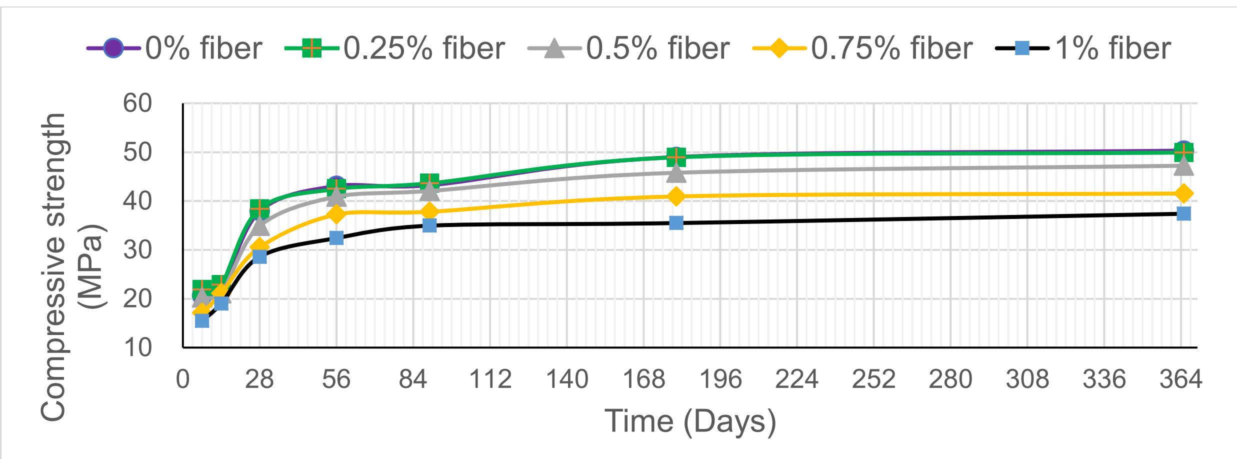

Figure 4.6. Compressive strength versus time

A comprehensive one-way analysis of variance (ANOVA) test was methodically done at a significance level of 0.05, which subsequently revealed that the variation in the percentage content of bamboo fiber exerts a considerable influence on the compressive strength of concrete when measured at various intervals, specifically at the 7-day (F = 39.375, F crit = 3.478), at the 14-day (F = 25.955, F crit = 3.478), at the 28-day (F = 32.633, F crit = 3.478), at the 56-day (F = 42.188, F crit = 3.478), at the 90-day (F = 46.941, F crit = 3.478), at the 180-day (F = 36.445, F crit = 3.478), and finally at the 365-day (F = 34.715, F crit = 3.478).

4.2.2.4 Impact of bamboo fiber on the splitting tensile strength of concrete

The split tensile strength test result at the specified ages is presented after computing the mean of the triplicates, as shown in Table 4.7.

Table 4.7. Splitting tensile strength on the specified days of sample age

Bamboo fiber dose (%)	Split tensile strength (MPa)						
	7	14	28	56	90	180	365
0%	1.298	1.575	1.679	1.699	1.741	1.911	2.163
0.25%	1.550	1.888	2.044	2.104	2.124	2.206	2.469
0.50%	1.361	1.528	1.783	1.891	1.967	2.038	2.289
0.75%	1.291	1.363	1.629	1.879	1.895	1.983	2.194
1.00%	1.160	1.389	1.533	1.584	1.633	1.964	2.048

The splitting tensile strength properties of the concrete samples with 0%, 0.25%, 0.5%, 0.75%, and 1.0% dosages of bamboo fiber are exhibited in Figures 4.7 and 4.8.

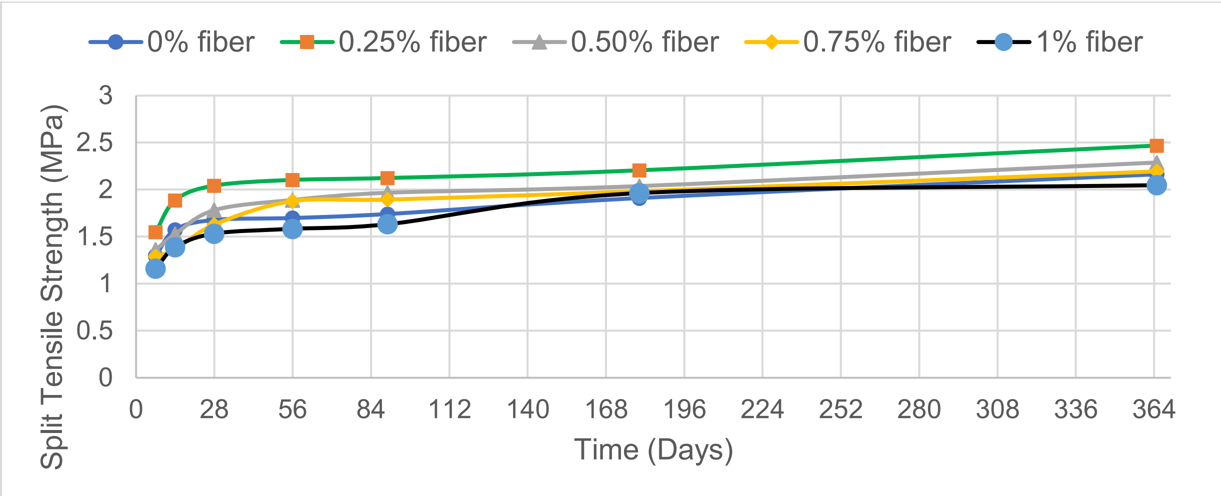

Figure 4.7. Splitting tensile strength versus age of concrete

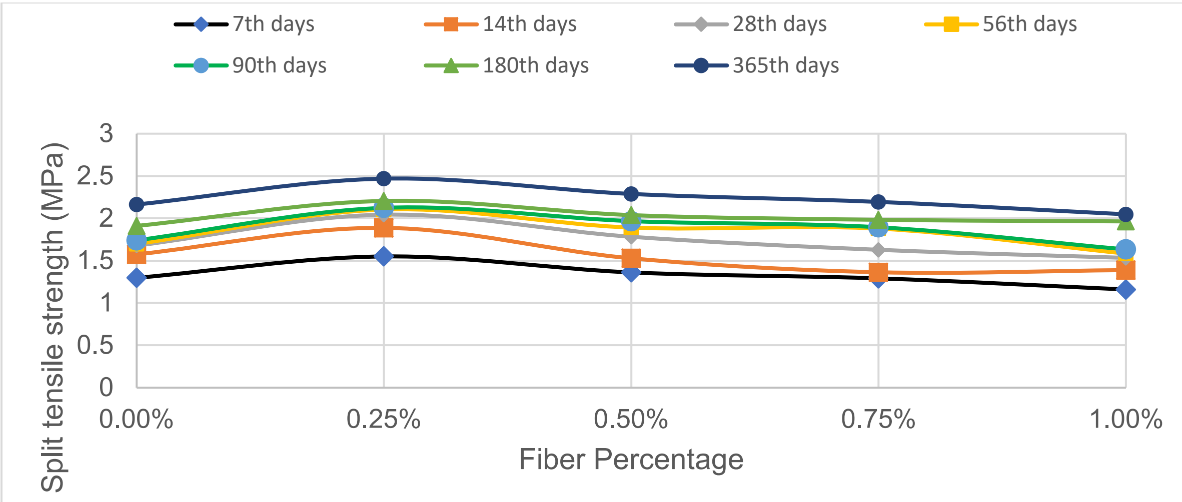

Figure 4.8. Splitting tensile strength versus dosage of bamboo fiber

From the experiment, the splitting tensile strength increment rate is higher up to the 28th day of the concrete age; after this, the rate of increment declines. However, there is little improvement in the case of the value of the split tensile strength. The addition of bamboo fiber improved the split tensile strength value by up to 21.74% in the case of samples that have 0.25% bamboo fiber. The values of split tensile strength of S25 and S50 on the 7th day were found to be higher than S0. T-score showed addition of 0.25% bamboo fiber has significant impact on the increment on the splitting tensile strength performance of concrete. Improvement in split tensile strength is helpful in resisting cracking at the early age of concrete as well as during the service period of structures (Safiuddin et al., 2018) (Ningrum et al., 2024). Split tensile strength is a critical mechanical property of concrete reflecting its ability to withstand tensile forces. It is an important parameter for evaluating concrete performance, particularly in earthquake-prone areas where tensile forces can lead to catastrophic failures (Madhavi et al., 2017). The increment of split tensile strength of concrete due to the presence of bamboo fiber has a positive impact on such failures. On the other hand, with a further dosage increment to 1.0% bamboo fiber, the value of split tensile strength showed a decline. This may be due to several interrelated factors associated with the increased presence of fibers within the concrete matrix that originates from less cohesion and ends up with reduced bonding and strength(Antwi-afari et al., 2024)(Agboola, B. D., Onabote, E. J., Nwauju, C. D., Braimoh, S. O., Ejigboye, P. O., Ajamu, S. O., & Gana, 2024).

A one-way analysis of variance (ANOVA) examination was performed at a significance threshold of 0.05, which subsequently indicated that the variability in the percentage composition of bamboo fiber in the concrete significantly impacts the split tensile strength of concrete when assessed at various ages of concrete, specifically at the 7th day (F = 11.859, F crit = 3.478), at the 14th day (F = 6.99, F crit = 3.478), at the 28th day (F = 24.523, F crit = 3.478), at the 56th day (F = 11.648, F crit = 3.478), at the 90th day (F = 31.12, F crit = 3.478), at the 180th day (F = 7.227, F crit = 3.478), and at the 365th day interval (F = 7.942, F crit = 3.478).

4.2.2.5 Impact of bamboo fiber on the flexural strength of concrete

The flexural strength test result at the specified ages is presented after computing the mean of the triplicates, as shown in Table 4.8.

Table 4.8. Flexural strength on the specified days of sample age

Bamboo fiber dose (%)	Flexural Strength (MPa)						
	7	14	28	56	90	180	365
0%	2.930	3.253	3.600	3.677	3.710	3.810	4.007
0.25%	3.227	3.570	4.037	4.127	4.213	4.233	4.563
0.50%	3.210	3.227	3.450	3.493	3.610	3.793	4.113
0.75%	2.313	3.027	3.160	3.197	3.587	3.630	4.017
1.00%	2.277	2.967	3.060	3.107	3.167	3.420	4.057

The values of Table 4.8 are used to get the graphs presented in Figures 4.9 and 4.10. The flexural strength of concrete with 0.25% bamboo fiber dosage has attained the highest value, which is 13.57% higher than plain concrete at the 28th day of the concrete age. The flexural strength of S25 achieved within 7 days was comparable to the flexural strength of S0 attained at 28th days. This is very important to avoid early age cracking that arises associated with shrinkages (Kulkarni et al., 2023). T-score showed that 0.25% bamboo fiber addition has significant impact on the improvement of the flexural performance of concrete. Higher flexural strength is beneficial in pavement construction(Gholami et al., 2024). In other cases, samples with 1% bamboo fiber showed the lowest performance, which is a reduction of flexural strength up to 22.3%. For each sample, the flexural strength gain was at an increment rate for days up to the 28th, while after this, the increment was not at the same rate. From the experiment, the rate of increment in flexural strength is minimal after the 14th day of concrete in comparison with the rate attained by the compressive strength.

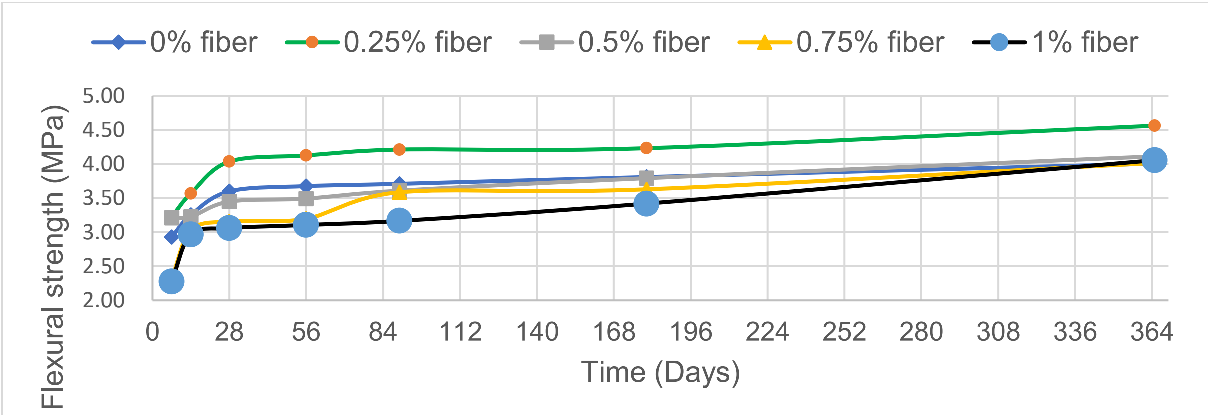

Figure 4.9. Flexural strength with time

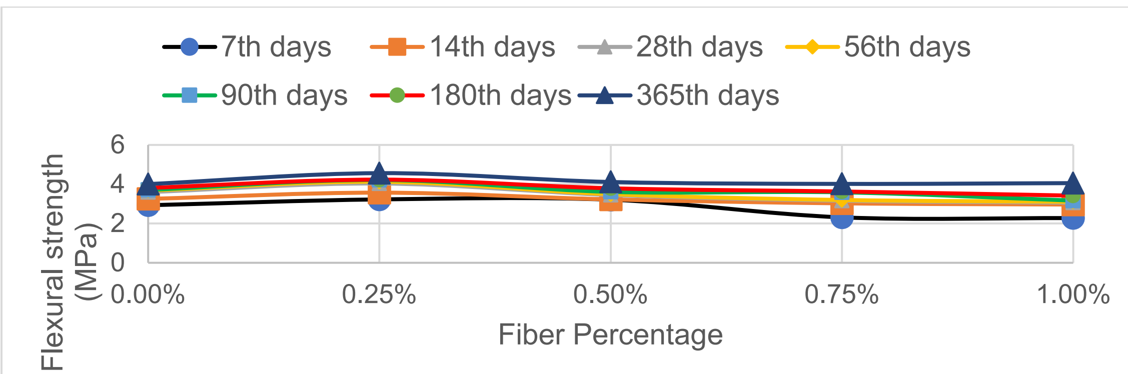

Figure 4.10. Flexural strength with fiber dosage

A one-way analysis of variance (ANOVA) was conducted with a significance level set at 0.05, which revealed that the variation in the percentage of bamboo fiber incorporated into the concrete exerts a significant influence on the flexural strength of the concrete when evaluated at different ages, specifically on the 7th day (F = 17.924, F crit = 3.478), on the 14th day (F = 4.178, F crit = 3.478), on the 28th day (F = 13.84, F crit = 3.478), on the 56th day (F = 20.983, F crit = 3.478), on the 90th day (F = 23.328, F crit = 3.478), on the 180th day (F = 7.935, F crit = 3.478), and at the 365th day mark (F = 3.776, F crit = 3.478).

4.2.3 Relationships among mechanical properties of bamboo fiber reinforced concrete

4.2.3.1 Assessment of the relationships of compressive and splitting tensile strength

The result of the regression analysis to study the relationship between the compressive (Fc) and split tensile (Ft) strengths conducted in RStudio is presented in Table 4.9. The split tensile strength increases with the compressive strength. From the employed functions, the exponential function best correlates the two properties. The R^2 value is the indicator value if the function best simulates or represents the experimental data (Dou et al., 2023) (Chhorn et al., 2017). In the table, the graph with the black line represents the power function, the blue line represents the linear function, and the red line represents the exponential function. Accordingly, the R^2 values of the exponential function from this regression analysis are higher, implying strong relevance of the equation.

The ratio of split tensile strength to compressive strength was incremental up to the 14th day. After this age, the increment in split tensile strength was minimal compared to the compressive strength trend, and because of this, the curve declined. Due to this, the ratio of split tensile strength to compressive strength showed a decrease in Figure 4.11.

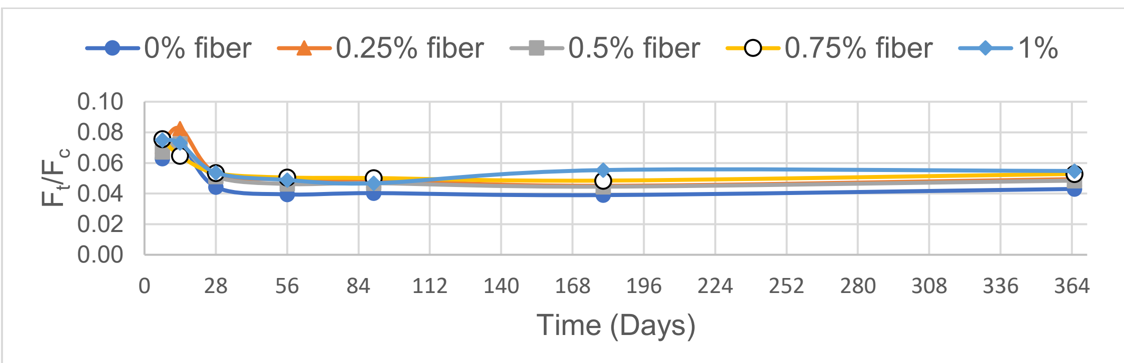

Figure 4.11. Ratio of splitting tensile to compressive strength versus age of concrete

Table 4.9. Compressive versus splitting tensile regression analysis summary

Graphs	Mark	Function	R^2
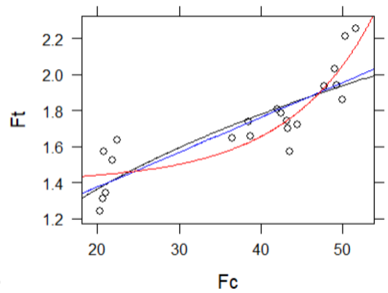 S0		$Ft = 0.434 * Fc^{0.382}$	0.71
		$Ft = 0.019 * Fc + 0.992$	0.72
		$Ft = 0.006 * e^{(0.094*Fc)} + 1.403$	0.81
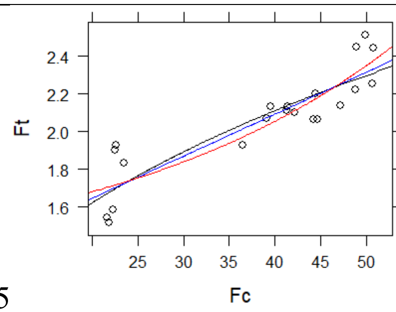 S25		$Ft = 0.523 * Fc^{0.378}$	0.79
		$Ft = 0.022 * Fc + 1.204$	0.80
		$Ft = 0.227 * e^{(0.031*Fc)} + 1.257$	0.81
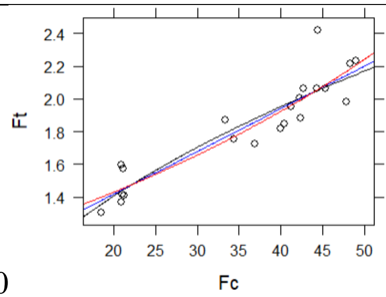 S50		$Ft = 0.337 * Fc^{0.476}$	0.84
		$Ft = 0.026 * Fc + 0.892$	0.84
		$Ft = 0.877 * e^{(0.017*Fc)} + 0.198$	0.85
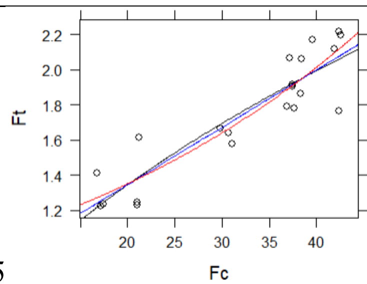 S75		$Ft = 0.247 * Fc^{0.566}$	0.83
		$Ft = 0.033 * Fc + 0.694$	0.82
		$Ft = 0.598 * e^{(0.025*Fc)} + 0.355$	0.85
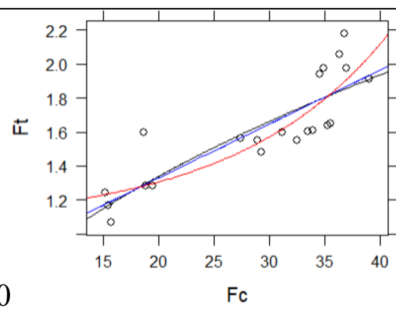 S100		$Ft = 0.272 * Fc^{0.532}$	0.73
		$Ft = 0.032 * Fc + 0.694$	0.73
		$Ft = 0.058 * e^{(0.073*Fc)} + 1.058$	0.75

4.2.3.2 Assessment of the relationship between compressive and flexural strength

The outcome of the regression analysis to examine the relationship between the compressive strength (Fc) versus the flexural strength (Ff) is shown in Table 4.10.

As the compressive strength increased, the flexural strength capacity also increased. However, the rate of their increment is not similar. The relationship between these mechanical properties followed the exponential function due to the highest R^2 value. On the other hand, the R^2 value is lower in the case of S50.

The ratio of flexural strength to compressive strength was incremental up to the 14th day. After this, the curve lowered due to the rate of flexural strength increment being minimal compared to the trend of the compressive strength. Due to this, the ratio of flexural tensile strength to the compressive strength showed a decrease, as shown in Figure 4.12. As the age and compressive strength of concrete increased, the flexural strength also followed the same trend. The trend of proportional increment in the flexural strength to compressive strength diminished due to an increased level of compressive strength at a later age (M. Ahmed et al., 2016).

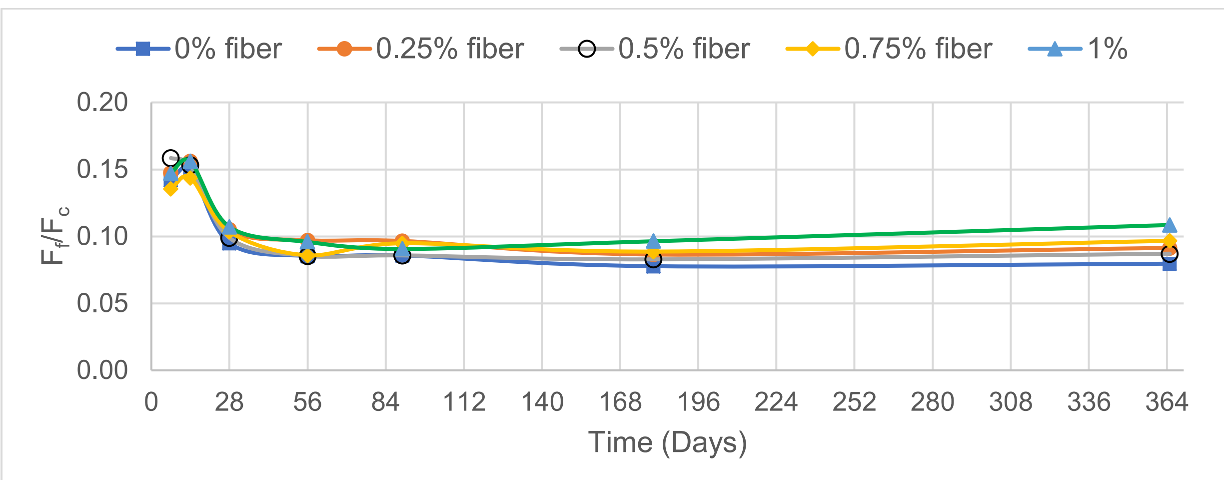

Figure 4.12. Ratio of flexural to compressive strength versus age of concrete

Table 4.10. Compressive versus flexural regression analysis summary

<table>
<tr><th>Graphs</th><th>Mark</th><th>Function</th><th>R^2</th></tr>
<tr><td rowspan="3">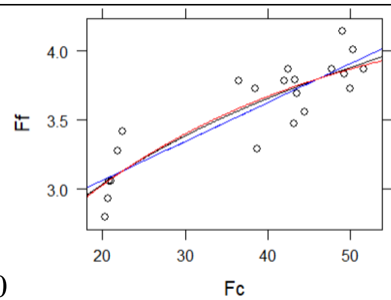

S0</td><td></td><td>$Ff = 1.365 * Fc^{0.267}$</td><td>0.77</td></tr>
<tr><td></td><td>$Ff = 0.028 * Fc + 2.503$</td><td>0.76</td></tr>
<tr><td></td><td>$Ff = -2.57 * e^{(-0.031*Fc)} + 4.409$</td><td>0.77</td></tr>
<tr><td rowspan="3">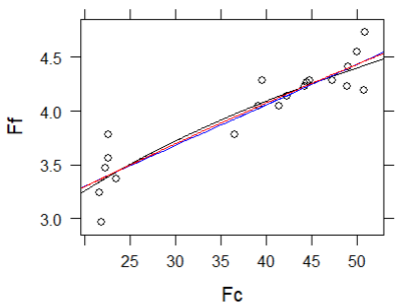

S25</td><td></td><td>$Ff = 1.219 * Fc^{0.328}$</td><td>0.84</td></tr>
<tr><td></td><td>$Ff = 0.038 * Fc + 2.552$</td><td>0.84</td></tr>
<tr><td></td><td>$Ff = -8.821 * e^{(-0.005*Fc)} + 11.26$</td><td>0.85</td></tr>
<tr><td rowspan="3">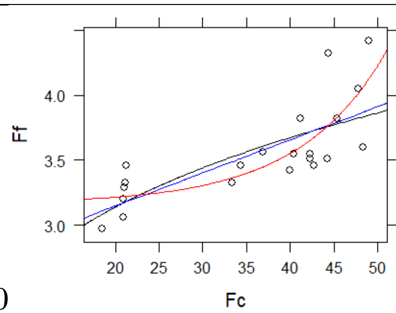

S50</td><td></td><td>$Ff = 1.593 * Fc^{0.226}$</td><td>0.54</td></tr>
<tr><td></td><td>$Ff = 0.025 * Fc + 2.639$</td><td>0.56</td></tr>
<tr><td></td><td>$Ff = 0.007 * e^{(0.1*Fc)} + 3.163$</td><td>0.66</td></tr>
<tr><td rowspan="3">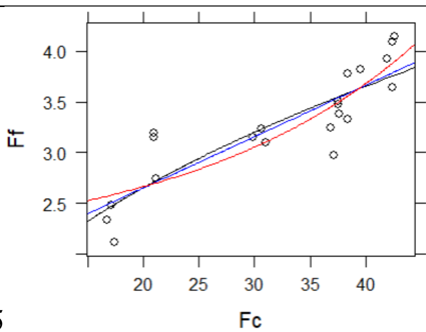

S75</td><td></td><td>$Ff = 0.667 * Fc^{0.461}$</td><td>0.76</td></tr>
<tr><td></td><td>$Ff = 0.051 * Fc + 1.638$</td><td>0.76</td></tr>
<tr><td></td><td>$Ff = 0.245 * e^{(0.048*Fc)} + 2.029$</td><td>0.77</td></tr>
<tr><td rowspan="3">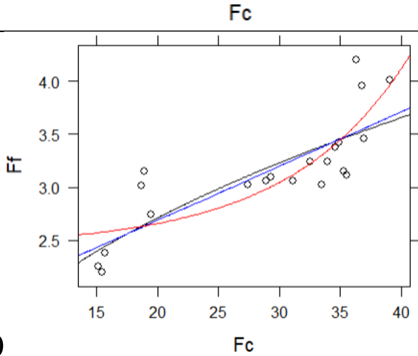

S100</td><td></td><td>$Ff = 0.743 * Fc^{0.432}$</td><td>0.66</td></tr>
<tr><td></td><td>$Ff = 0.051 * Fc + 1.662$</td><td>0.67</td></tr>
<tr><td></td><td>$Ff = 0.029 * e^{(0.102*Fc)} + 2.438$</td><td>0.71</td></tr>
</table>

4.2.3.3 Assessment of the relationship between flexural and splitting tensile strength

The relationship between the flexural and split tensile strength was examined through regression analysis. Due to the higher R^2 value, the exponential function better correlates the flexural strength and the split tensile strengths as shown in Table 4.11.

The trend of the ratio of flexural strength to splitting tensile strength with the age of concrete is shown in Figure 4.13.

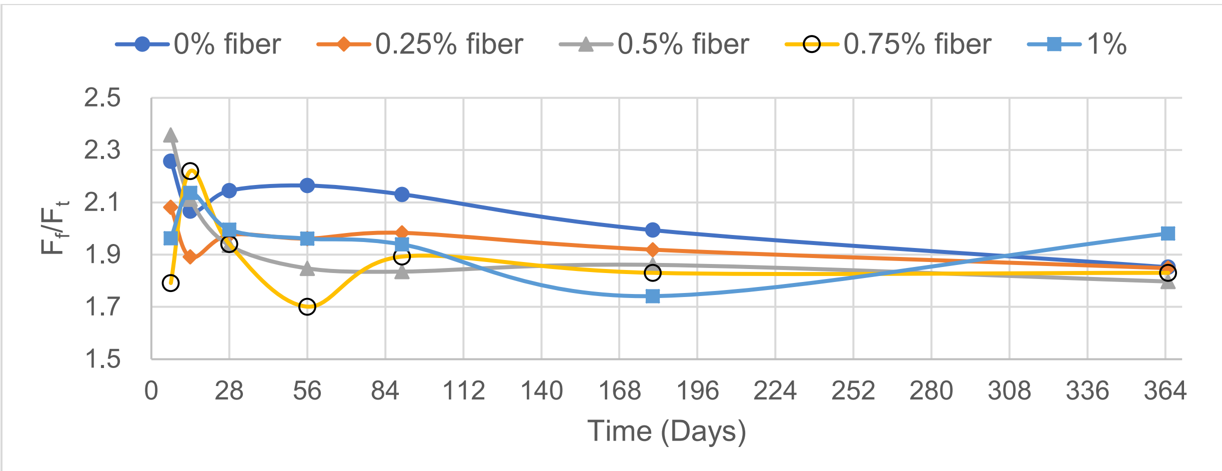

Figure 4.13. Ratio of flexural to splitting tensile versus age of concrete

The degree of variation among the ratios of the flexural strength to splitting tensile strength was higher within the early weeks, while as the age increases, this variation diminishes. The ratio of the flexural strength to split tensile strength is from 1.7 to 2.36. The ratio showed higher values at early ages while decreasing as age increases. This is due to the increased level of split tensile strength at later ages of the samples.

Table 4.11. Flexural versus splitting tensile strengths regression analysis summary

Graphs	Mark	Function	R^2
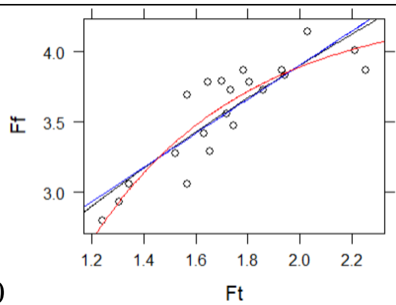 S0		$Ff = 2.609 * Ft^{0.581}$	0.73
		$Ff = 1.213 * Ft + 1.479$	0.74
		$Ff = -12.697 * e^{(-1.695*Ft)} + 4.32$	0.80
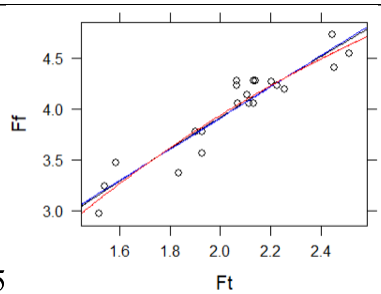 S25		$Ff = 2.274 * Ft^{0.785}$	0.87
		$Ff = 1.546 * Ft + 0.819$	0.88
		$Ff = -8.337 * e^{(-0.484*Ft)} + 7.105$	0.89
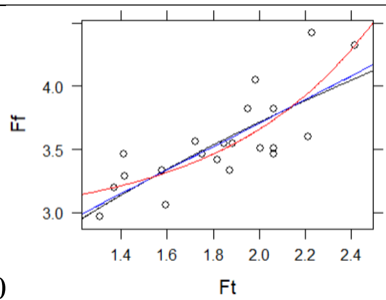 S50		$Ff = 2.681 * Ft^{0.47}$	0.61
		$Ff = 0.928 * Ft + 1.852$	0.61
		$Ff = 0.035 * e^{(1.529*Ft)} + 2.916$	0.65
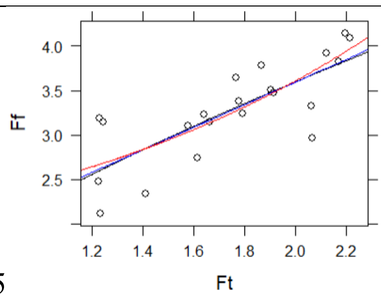 S75		$Ff = 2.265 * Ft^{0.668}$	0.62
		$Ff = 1.269 * Ft + 1.058$	0.61
		$Ff = 0.597 * e^{(0.677*Ft)} + 1.299$	0.65
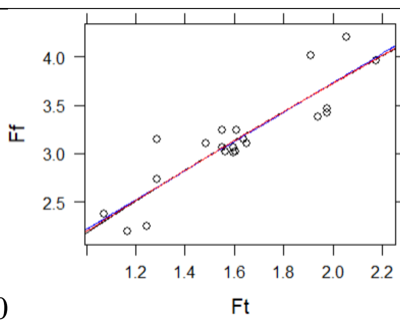 S100		$Ff = 2.184 * Ft^{0.77}$	0.80
		$Ff = 1.509 * Ft + 0.712$	0.79
		$Ff = -17.569 * e^{(-0.101*Ft)} + 18.076$	0.80

4.2.4 Study of the brittleness of bamboo fiber reinforced concrete

Table 4.12 shows the ratio of the splitting tensile strength to the compressive strength of concrete specimens. The ratio is lowest in concrete specimens without bamboo fiber.

Table 4.12. Splitting tensile to compression ratio

Sample ID		Days				
		28	56	90	180	365
S0	Fc (MPa)	37.897	43.067	43.230	49.000	50.317
	Ft (MPa)	1.679	1.699	1.741	1.911	2.163
	Ft/Fc	0.044	0.039	0.040	0.039	0.043
S25	Fc (MPa)	38.390	42.473	43.620	48.943	49.923
	Ft (MPa)	2.044	2.104	2.124	2.206	2.469
	Ft/Fc	0.053	0.050	0.049	0.045	0.049
S50	Fc (MPa)	34.887	40.883	42.063	45.780	47.223
	Ft (MPa)	1.783	1.891	1.967	2.038	2.289
	Ft/Fc	0.051	0.046	0.047	0.045	0.048
S75	Fc (MPa)	30.513	37.230	37.797	40.930	41.530
	Ft (MPa)	1.629	1.879	1.895	1.983	2.194
	Ft/Fc	0.053	0.050	0.050	0.048	0.053
S100	Fc (MPa)	28.580	32.407	34.950	35.487	37.387
	Ft (MPa)	1.533	1.584	1.633	1.964	2.048
	Ft/Fc	0.054	0.049	0.047	0.055	0.055

The lowest ratio has the highest brittleness property (Althoey et al., 2022). On the other hand, higher split tensile to compressive ratios were obtained in concrete specimens with bamboo fiber (S25, S50, S75, and S100). Therefore, the brittleness of the specimens without bamboo fiber is higher than that of those with bamboo fiber. Improved brittleness quality contributes to increased ductility, which is helpful for concrete structures to respond to seismic effects.

4.2.5 Crack examination of plain and bamboo fiber reinforced concrete

The specimens of concrete with bamboo fiber showed better performance than plain concrete. This is due to the bridging effect that arises from the presence of the bamboo fibers. Fibers are important in enhancing concrete resistance to cracking by the bridging effect(L. Chen et al., 2023). In this study, specimens with bamboo fiber showed narrow crack openings during flexural testing. Figure 4.14 (a) is the crack opening of the plain concrete specimen, which is wider than the crack opening observed in the specimen of bamboo fiber reinforced concrete, Figure 4.14 (b).

(a)

(b)

Figure 4.14. Crack opening

After cracking, the load is transferred to the fibers, and this enabled the concrete to behave in a ductile manner. Moreover, Figure 4.15 shows the bridging effect of the fibers after the cracking had occurred.

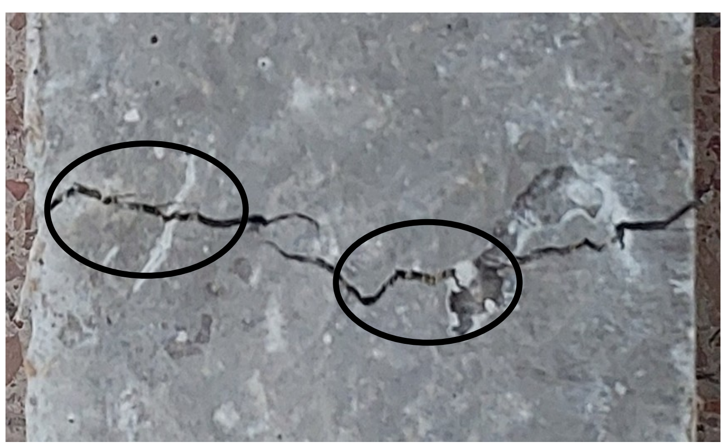

Figure 4.15. Bamboo fiber bridge crack (Zoomed)

The crack width analysis result obtained from the ImageJ software is presented in Table 4.13. The numbers in the brackets are the standard deviation.

Table 4.13. Crack width result

Specimen with bamboo fiber (%)	Average crack width (mm)
0	0.472 (0.068)
0.25	0.254 (0.043)
0.5	0.197 (0.036)
0.75	0.194 (0.048)
1	0.164 (0.018)

The average crack width was reduced in the concrete specimens reinforced with bamboo fiber. Plain concrete specimens showed the highest crack width. The reduction of crack width is due to the bamboo fibers' bridging effect, which supports the visual inspection presented in Figure 4.15.

4.2.6 Summary of findings in the strength matrices

The findings of the compressive strength (Comp..), splitting tensile (Tens.), and flexural (Flex.) strengths are summarized and presented in Figure 4.16.

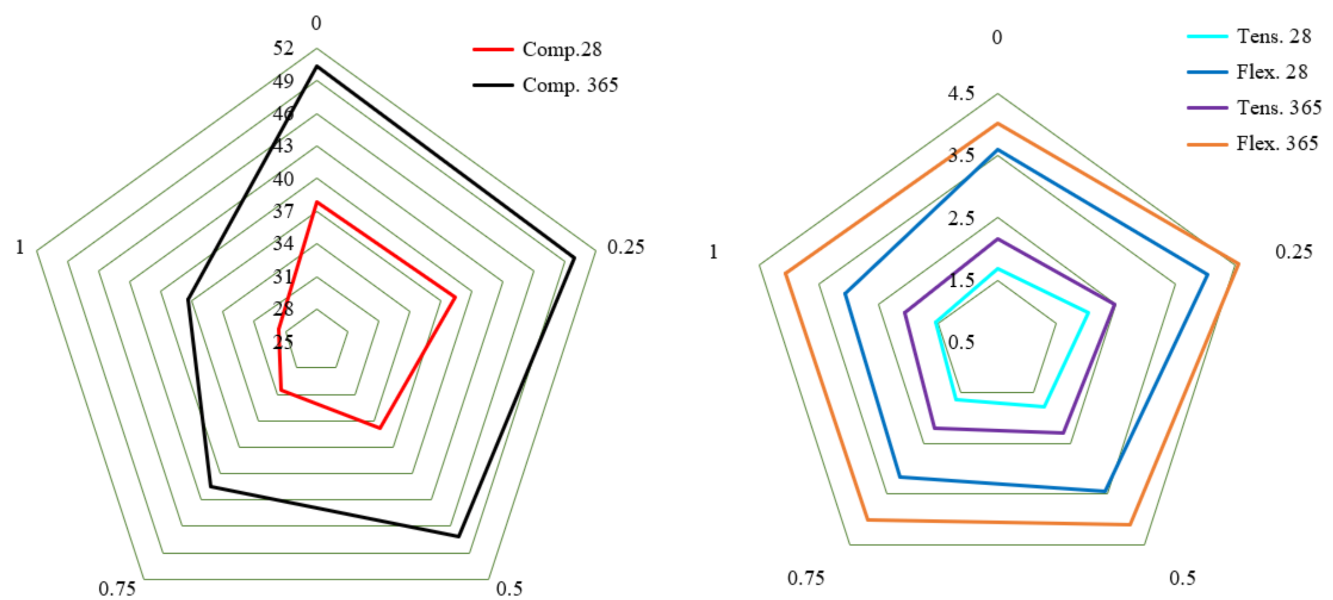

Figure 4.16: Strengths summary at 28 and 365 days

Based on the figure, the bamboo fiber had no positive effect on the compressive strength of concrete either at 28 or 365 days. A decrease was observed in concrete reinforced with 0.5%, 0.75%, and 1.0% bamboo fiber. However, concrete with 0.25% bamboo fiber showed comparable compressive strength to plain concrete. The splitting tensile and flexural strengths of concrete reinforced with 0.25% were the highest at both 28 and 365 days. Enhancing the splitting tensile strength of concrete protects structures from early-age cracking, which is critical for their longevity (Asaduzzaman & Islam, 2023).

The results of this research, combined with findings by other scholars, are presented in Table 4.14.

Table 4.14. Findings of the mechanical properties of bamboo fiber-reinforced concrete

Location	Study duration (days)	Observation			Ref.
		Compressive	Splitting tensile	Flexural	
Japan	56	decreased	increased	decreased	(Minami and M. Terai 1999)
Nigeria	28	increased	increased	not done	(Ede et al., 2020a)
China	28	decreased	increased	increased	(Zhang, Huang, and Chen 2013)
Malaysia	28	increased	increased	not done	(Osmi et al., 2024)
India	28	increased	increased	increased	(Kavitha and Kala 2016)
China	28	increased	increased	increased	(Peng et al., 2024)
Ethiopia	365	comparable	increased	increased	This study

The 0.25% bamboo fiber dosage optimized both splitting tensile and flexural strengths. Compared to the 0%, 0.5%, 0.75%, and 1.0% concentrations, the 0.25% dosage increased the splitting tensile strength by up to 22.05%, 16.89%, 25.47%, and 37.03%, and flexural strength by 13.86%, 18.03%, 29.11%, and 33.18%, respectively.

4.2.7 Summaries

From this experimental study, the following summaries are drawn.

- The impact of bamboo fiber on the workability of concrete was assessed by the slump test, and the experiment revealed that bamboo fiber has reduced the workability of concrete.
- The incorporation of bamboo fiber in concrete results in the reduction of density. As the amount of bamboo fiber in concrete increased, the density decreased.

- The presence of bamboo fiber did not play a positive role in the compressive strength of concrete. On the other hand, bamboo fiber improved the split tensile and flexural strengths of concrete. However, such effects were not observed on all kinds of dosages of bamboo fiber. Concrete specimens with 0.25% bamboo fiber showed comparable compressive strength, higher split tensile, and flexural strengths when compared to plain concrete specimens. Higher dosages of bamboo fiber in concrete have a reduction effect on the mechanical properties of concrete.
- The exponential function can describe or model the relationships between the mechanical properties of concrete.
- The ratio of the splitting tensile strength to the compressive strength was higher at early ages because the compressive strength gained at later ages was higher, while that of the split tensile strength was lower. The same trend was observed in the case of the ratio of flexural strength to compressive strength and the ratio of split tensile strength to flexural strength.
- Specimens with bamboo fiber showed reduced crack opening width due to the bridging effect of bamboo fibers. Moreover, their brittleness behavior was lower than that of plain concrete specimens.

4.3 Durability study of bamboo fiber reinforced concrete

4.3.1 Introduction

Understanding the impact of bamboo fiber on the mechanical properties of concrete is not enough to applaud the contribution of the bamboo fiber to sustainability. The longevity of structures made of concrete is ensured not only by the mechanical properties but also by the durability characteristics. Structures within an adverse environment should have better durability properties. For this reason, this chapter is devoted to the assessment of the roles of the addition of bamboo fiber in the durability properties of concrete. The assessment is carried out through examination of changes in compressive strength and weight of specimens when they are in alkaline and acidic solutions. The alkaline and acidic solutions were made of sodium hydroxide and sulphuric acid. Moreover, the impacts of bamboo fiber on the volume of voids and absorption capacity of concrete were investigated.

4.3.2 Results and Discussion

4.3.2.1 Durability assessment of bamboo fiber reinforced through compressive strength

One method to evaluate the impact of bamboo fiber on concrete durability behavior was a change in compressive strength through time when specimens were placed in alkaline and acidic environments to simulate adverse conditions. When samples were soaked in an acidic environment, which was produced by a 5% sulphuric acid solution, their compressive strength change was taken as a percentage of variation with reference to the 28th day.

The relative reductions in compressive strengths shown in Table 4.15 were provided after computation conducted using equation 3.6. From this table, the compressive strength of specimens soaked in the acidic solution for the duration of 180 (at the age of 223 days) and 365 (at the age of 408 days) days ended up with less compressive strength than that was attained on the 28th day. Moreover, Specimens without bamboo fiber showed the least reduction from the other samples with bamboo fiber. The remaining compressive strength capacity of the specimen with 1.0% bamboo fiber at the age of 408 days is 52.24% of the 28-day strength, while that of the sample without bamboo fiber is 70.67%. The rest of the samples' remaining compressive strength capacities were between these ranges.

Table 4.15. Compressive strength test results (Control versus Acid)

Fiber (%)	Without acid (Control) (MPa)			Acid (MPa)		Relative reductions (%)			
	Age (days)			Age (days)		223 vs 28 days	408 vs 28 days	223 vs 223 days	408 vs 408 days
	28	223	408	223	408				
0	37.90	49.08	50.41	27.77	26.78	26.71	29.33	43.41	46.87
0.25	38.39	49.03	50.01	27.10	24.07	29.40	37.29	44.73	51.87
0.5	34.89	45.87	47.31	22.40	22.24	35.80	36.24	51.17	52.99
0.75	30.51	41.02	41.61	19.21	17.46	37.05	42.77	53.17	58.03
1	28.58	35.57	37.47	15.34	14.93	46.31	47.76	56.87	60.16

The rate of decrement of compressive strength with respect to the 28^{th} day's value for each specimen was examined. Moreover, how the strength development was affected by the acidic environment was examined through a comparison of compressive strengths at 223 days and 408 days of age with the control, as shown in Table 4.15. The values of age 223 days indicated the effect of soaking specimens for 180 days in an acidic solution. Accordingly, this age test result showed a reduction of 43.41% to 56.87% from what could have been achieved in normal conditions. The reduction further increased when the soaking duration was set for 365 days. This is presented as the compressive strength at 408 days. After 365 days of soaking, the highest reduction compared to the 28-day strength was observed in concrete specimens that had 1% bamboo fiber, and the least was in the control. A sulfuric acid attack test was conducted on specimens containing a dose of 1% and 2% jute fiber for a duration of 90 days. The study found that concrete samples with 1% and 2% jute fiber lost 35.77% and 39.39% of their strength, respectively, compared to their strength before being exposed to the acid (Nambiar & Haridharan, 2019).

The impact of an acidic environment is presented graphically in Figure 4.17. The compressive strength towards the decrement side as the fiber content increases.

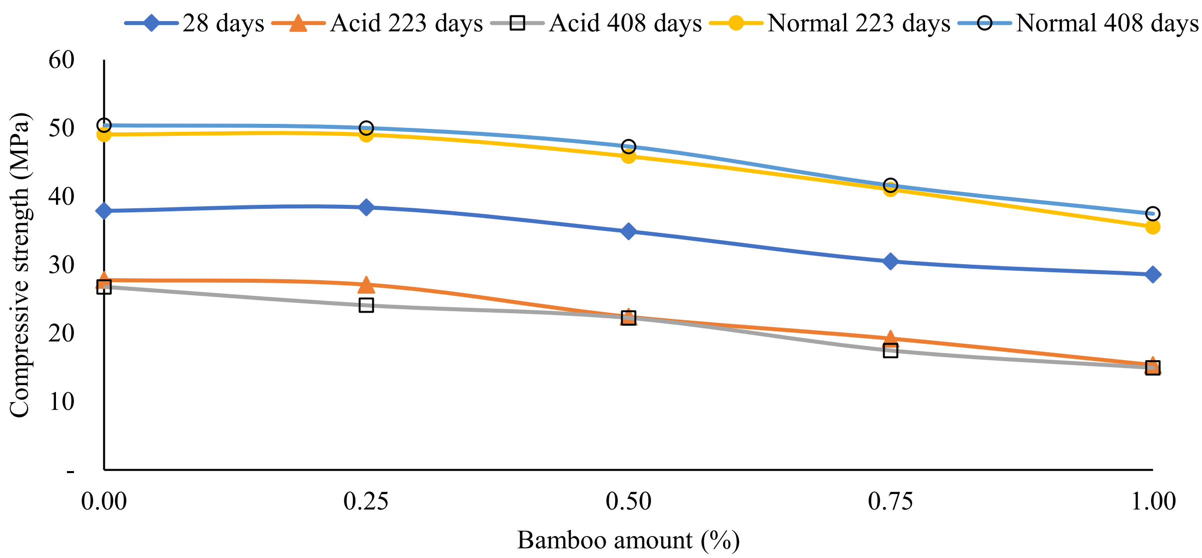

Figure 4.17. Compressive strength versus bamboo fiber amount (acidic environment)

The reason for the compressive strength decrement in specimens with higher bamboo fiber was due to the degradation of plant fibers in an acidic environment, which might create paths for migration of the acid solution towards the inner paste. Therefore, the paste could react with a solution of sulfuric acid and give a chemical product, calcium sulfate, which contributed to the reduction. Moreover, the acid may affect the surface roughness of the bamboo fiber, which has an impact on the bond(Abbas et al., 2022).

The trend of the decrement in compressive strength of specimens with the prescribed dosage of bamboo fiber is given in Figure 4.18. The duration of specimens' immersion in an acidic environment has a decremental effect on the compressive strength.

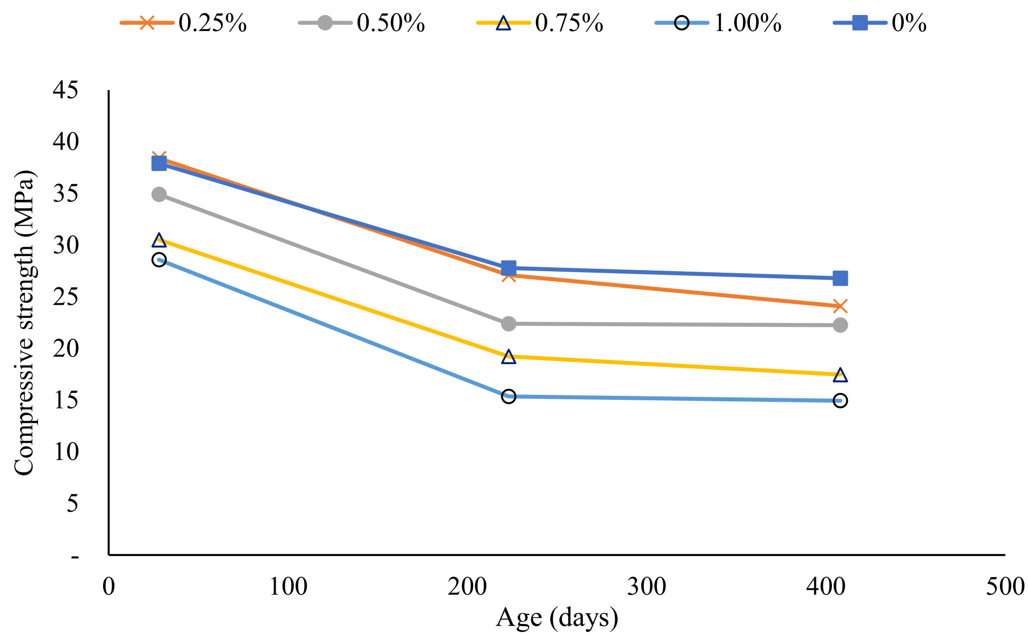

Figure 4.18. Compressive strength versus time (5% H_2SO_4)

A higher rate of deterioration in compressive strength was found up to 223 days. The effect of the acidic environment on the compressive strength of bamboo fiber-reinforced specimens was at a sluggish rate after 223 days of specimens. The progress of acid penetration and the formation of chemical reaction with the paste is higher initially, and this continues. The product, usually calcium sulfate, accumulated within a certain depth. Then, this accumulated chemical acts as a barrier to further sulfuric acid penetration into the inner core(Beddoe & Dorner, 2005). This reduced the progress of compressive strength deterioration.

The effect of the alkaline solution on the compressive strength of bamboo-fiber-reinforced concrete samples is shown in Table 4.16 by computing using Equation 3.6. From the study, all the specimens, after being soaked for 180 days and 365 days in a sodium hydroxide (NaOH) solution of 5% concentration, showed improvement in the compressive strength from the 28th day's strength, according to the test results obtained at the 223rd and 408th days. On the other hand, the strength attained in the specimens obtained from the alkaline solution and examined at the ages of 223 and 408 days showed a decline in value over those tested specimens obtained from the water bath environment.

Table 4.16. Compressive strength test results (Control versus Alkaline)

Fiber (%)	Without alkaline (Control) (MPa)			Alkaline (MPa)		Relative increment (%)		Relative decrement (%)	
	Age (days)			Age (days)		223 vs 28 days	408 vs 28 days	223 vs 223 days	408 vs 408 days
	28	223	408	223	408				
0	37.90	49.08	50.41	42.82	43.38	13.00	14.48	12.75	13.93
0.25	38.39	49.03	50.01	43.69	43.75	13.81	13.97	10.90	12.52
0.5	34.89	45.87	47.31	39.66	40.28	13.68	15.45	13.53	14.87
0.75	30.51	41.02	41.61	33.60	33.79	10.12	10.74	18.09	18.80
1	28.58	35.57	37.47	30.17	30.80	5.55	7.78	15.20	17.80

The effect of the 5% NaOH solution on the compressive strength property of the specimens is presented in Figure 4.19. Fiber dose increment in concrete has a compressive strength decremental effect in both normal and alkaline environments.

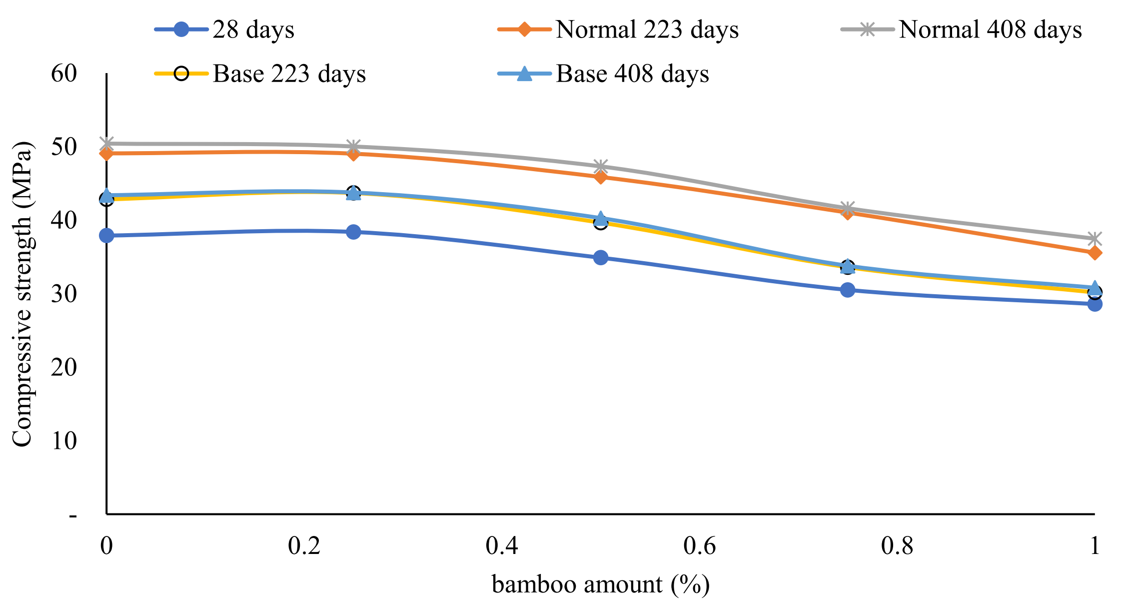

Figure 4.19. Compressive strength versus bamboo fiber amount (alkaline environment)

It was observed that the compressive strength increment in the alkaline solution after 180 days of soaking was less than that of specimens placed in a normal environment for the same duration, as shown in the test result obtained at the age of 223 days. At the age of 223 days of examination, specimens in the alkaline conditions showed lesser compressive strength within the range of 10.90% and 18.09% in comparison with those put in a normal water bath. At the age of 408 days, the compressive strength of specimens obtained from the alkaline environment showed a lower value than that of specimens extracted from the normal condition. However, the compressive strength values were on the higher side than the 28-day results in all specimens. Figure 4.20 presents the compressive strength test results at the ages of 28, 223, and 408 days. For all types of samples and all durations, the compressive strengths achieved were higher than the 28th day's value.

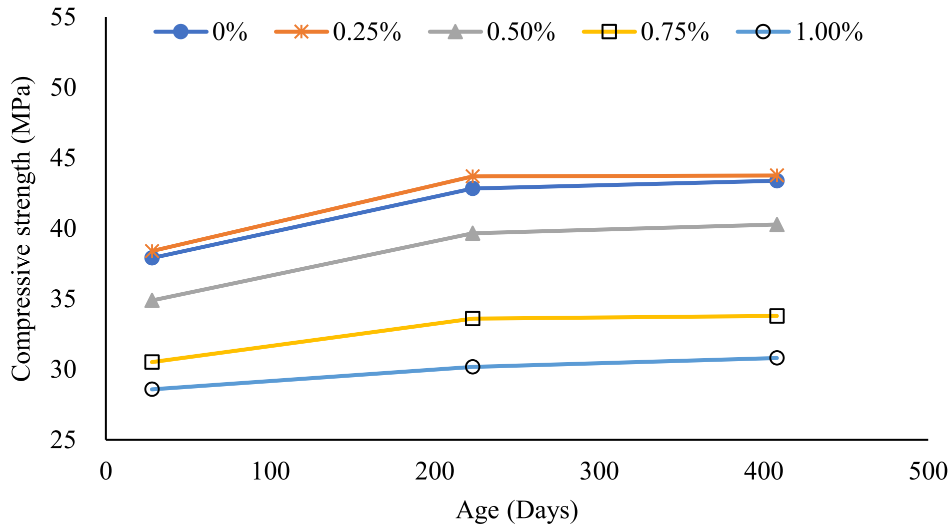

Figure 4.20. Compressive strength versus time (5% NaOH)

The increment rate was higher up to the age of 223 days; after this, the increment rate declined. Concrete gains its strength through the chemical reaction between cement and water. This process is termed as hydration. However, through time, the amount of cement that remains unreacted continues to vanish. The product of hydration that engulfed the unhydrated core may create difficulty for the water to reach them(Z. Zhu et al., 2020). Due to these, the rate of compressive strength became sluggish over time.

4.3.2.2 Mass examination for the impact of bamboo fiber on the durability of concrete study

The durability of concrete was examined through the change of mass when samples were exposed to adverse conditions. Accordingly, the results of the change in mass due to exposure to acidic and alkaline environments are presented in Tables 4.17 and 4.18, respectively. The percentage calculation was done by equation 3.7.

Table 4.17. Mass before (M28) and after (M223, 408) immersion of acidic environment

Bamboo fiber (%)	M28 (g)	M223(g)	Mass change (%)	M28 (g)	M408 (g)	Mass change (%)
0	8246.33	6898.00	-16.35	8183.00	6789.00	-17.04
0.25	8189.67	7106.67	-13.22	8105.00	6969.67	-14.01
0.5	8274.00	7161.00	-13.45	8121.33	6544.67	-19.41
0.75	8149.00	7493.00	-8.05	8085.33	6834.33	-15.47
1	7790.33	7440.67	-4.49	7846.67	7049.00	-10.17

The masses of all samples in an acidic environment were reduced during the study period. A significant portion of the reduction in the mass of the specimens was attained up to the age of 223 days, which was during the first 180 days of soaking in a 5% sulphuric acid solution. The additional mass loss between 223 days and 408 days was in the range of 0.69% to 7.42%, which corresponds to plain concrete samples and those reinforced with 0.75% bamboo fiber, respectively. The presence of bamboo fiber delayed the rate of mass loss. The inclusion of bamboo fibers helps to hold the paste between the aggregates. This is clearly shown on Figure 4.21's left side, where the paste was washed away by the acid in the plain specimen, while some part of the paste shown on Figure 4.21's right side is attached between the aggregates in bamboo-reinforced concrete specimens.

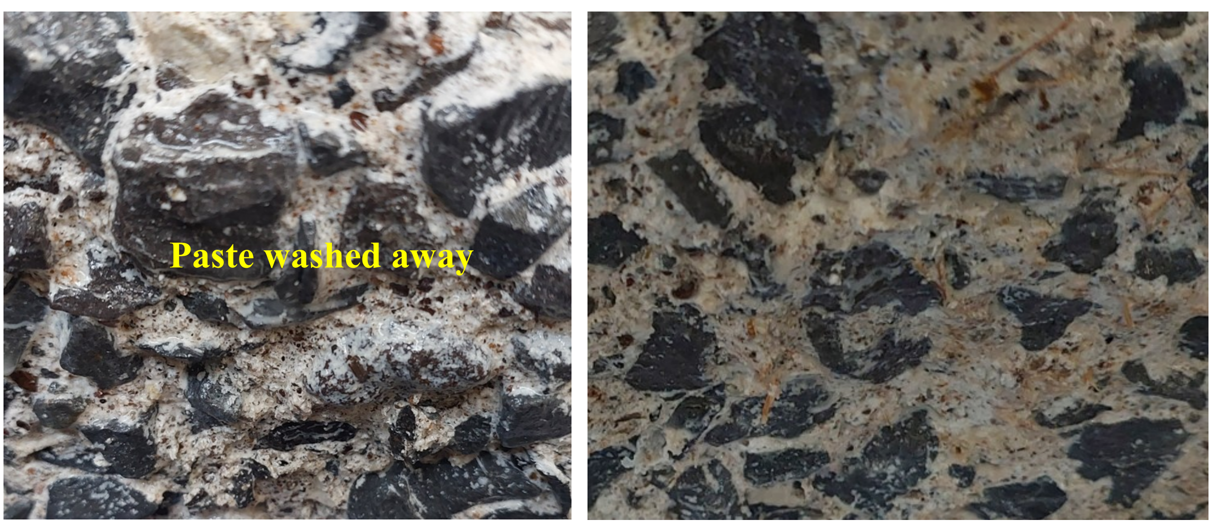

Figure 4.21. Specimens after acid attack

The impact of alkaline medium can be assessed by inferring from Table 4.18 that the increment of mass in specimens containing 0%, 0.25%, 0.5%, 0.75%, and 1.0% from 180 days to 365 days is 0.18%, 0.12%, 0.10%, 0.15%, and 0.3%, respectively.

Table 4.18. Mass before (M28) and after (M223, 408) immersion of alkaline environment

Bamboo fiber (%)	M28 (g)	M223 (g)	Mass change (%)	M28 (g)	M408 (g)	Mass change (%)
0	8244.67	8270.33	0.31	8268.67	8309.00	0.49
0.25	8110.00	8156.33	0.57	8106.00	8162.33	0.69
0.5	8191.67	8253.00	0.75	8260.33	8330.33	0.85
0.75	8038.33	8114.33	0.95	8122.33	8212.00	1.10
1	7946.00	8025.33	1.00	8009.00	8113.33	1.30

The mass increments of all specimens recorded at 223 days and 408 days were small, which was not significant. This is because the alkaline environment has a resemblance to the concrete alkalinity. Studies showed that the interaction between sodium hydroxide with silicates and aluminates and the facilitation of sodium hydroxide in the dissolution of calcium silicate contribute to the increment of mass(Mulay, 2017). The highest mass gain was attained during the first 180 days of immersion. The increase after the 180-day duration is minimal.

An analysis of variance (ANOVA) test was conducted at a significance level of 0.05, which showed that the variation in the percentage content of bamboo fiber influenced the variations in mass and compressive strengths. For specimens in the alkaline environment, the analysis conducted on the records of changes of mass proved that variation of the percentage of bamboo fiber content has an impact on the mass changes due to the value obtained ($F = 5.598$, F crit $= 3.478$) at 365 days. Likewise, for specimens in the acidic environment, the analysis proved that a variation of the percentage of bamboo fiber content has an impact on the changes of the masses due to the value obtained ($F = 5.538$, F crit $= 3.478$) at 365 days.

This test was performed at a significance level of 0.05, which revealed that the variation in the percentage content of bamboo fiber affected compressive strength in the alkaline and acidic mediums, specifically at the 365-day (F = 85.659, F crit = 3.478), (F =69.886, F crit = 3.478), respectively.

4.3.2.3 Influence of bamboo fiber on the total volume of voids of concrete

The total volume of voids of concrete specimens with a range of 0% to 1.0% dosage of bamboo fiber is presented in Figure 4.22. As the age of specimens increased, the total volume of voids decreased. The addition of bamboo fiber showed changes in the total permeability of voids with time. This parameter showed a decline as age increased from 180 days to 365 days in all cases of the study.

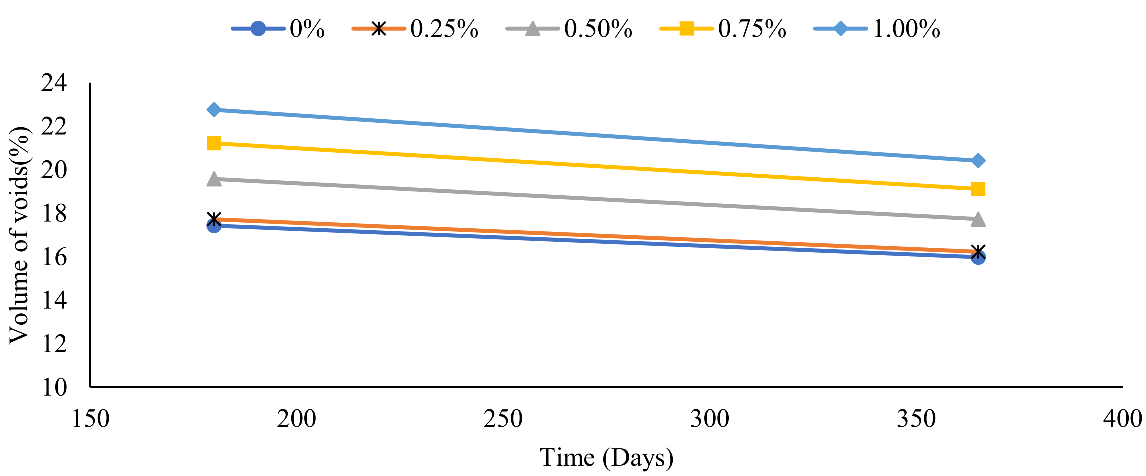

Figure 4.22. Volume of voids versus time

On the other hand, the addition of bamboo fiber favored the increment of total permeable voids, as indicated in Table 4.19 after calculating the relative variation using equation 3.10.

Table 4.19. Total volume of voids results

Bamboo amount	180 days	Change relative to 0%	365 days	Change relative to 0%
0%	17.43		15.98	
0.25%	17.72	1.67	16.23	1.55
0.50%	19.57	12.31	17.73	10.97
0.75%	21.21	21.72	19.12	19.63
1%	22.75	30.52	20.41	27.74

The increment of volume of voids between 180 and 365 days was less in comparison with the value attained in the first 180 days. The decrement in the volume of voids with age contributes to the later age increased compressive strengths. However, it is important to recall that the connectivity between voids has an impact on the properties of the specimens.

The specimens with 0.25% bamboo fiber did not have a significant incremental effect in comparison with those without bamboo fiber. On the other hand, the increment of bamboo fiber dose in concrete showed an increment in the total volume of voids. The incorporation of bamboo fiber increased permeable voids, which is similar to findings shown in other plant fibers(Okeola et al., 2018b)(Soto Izquierdo et al., 2017). The cumulative increase in the overall volume of void spaces can be primarily ascribed to the incorporation of bamboo fibers, which is significantly influenced by various factors, including the inherent porosity characteristics of the bamboo fiber itself, the porosity levels present within the cementitious matrix that encapsulates these fibers, as well as the interfacial bonding properties that develop around the fibers during the composite formation process. The interfacial transition zone (ITZ) is a distinct region that emerges as a result of the mixing process, which is notably characterized by the inherent hydrophilic properties exhibited by bamboo fiber that influence its interactions with surrounding materials. In the initial phases of mixing and during the early stages of hydration, there is a significant and dynamic movement of moisture that is initiated towards the bamboo fiber, whereas this directional flow of moisture undergo a reversal as the material transitions to a later dry state, consequently resulting in the development of voids within the matrix(Ziane et al., 2021).

The analysis of variance (ANOVA) test was performed at a significance level of 0.05, which revealed that the variation in the percentage content of bamboo fiber affected the volume of voids on various days of observations, specifically at the 180-day ($F = 16.126$, $F_{crit} = 3.478$) and 365-day ($F = 36.223$, $F_{crit} = 3.478$). Tukey test between concrete with and without bamboo fiber, with Q and P-value was utilized at a significance level of 0.05. After 180 and 365 days, the values of Q and P of concrete specimens without bamboo fiber and reinforced with 0.25% bamboo fiber were (0.515, 0.996) and (0.786, 0.979), respectively. For this data, the critical value of Q is 4.654, which is greater than the values corresponding to the 180 and 365 days. Moreover, the P-values are closer to 1. These results reveal that specimens reinforced with 0.25% bamboo fiber showed an insignificant variation in the volume of voids compared to the control.

4.3.2.4 Influence of bamboo fiber on the absorption of concrete

The absorption capacity of the specimens in relation to their age is presented in Figure 4.23 (a), and the effect of the bamboo fiber on this characteristic is presented in Figure 4.23 (b).

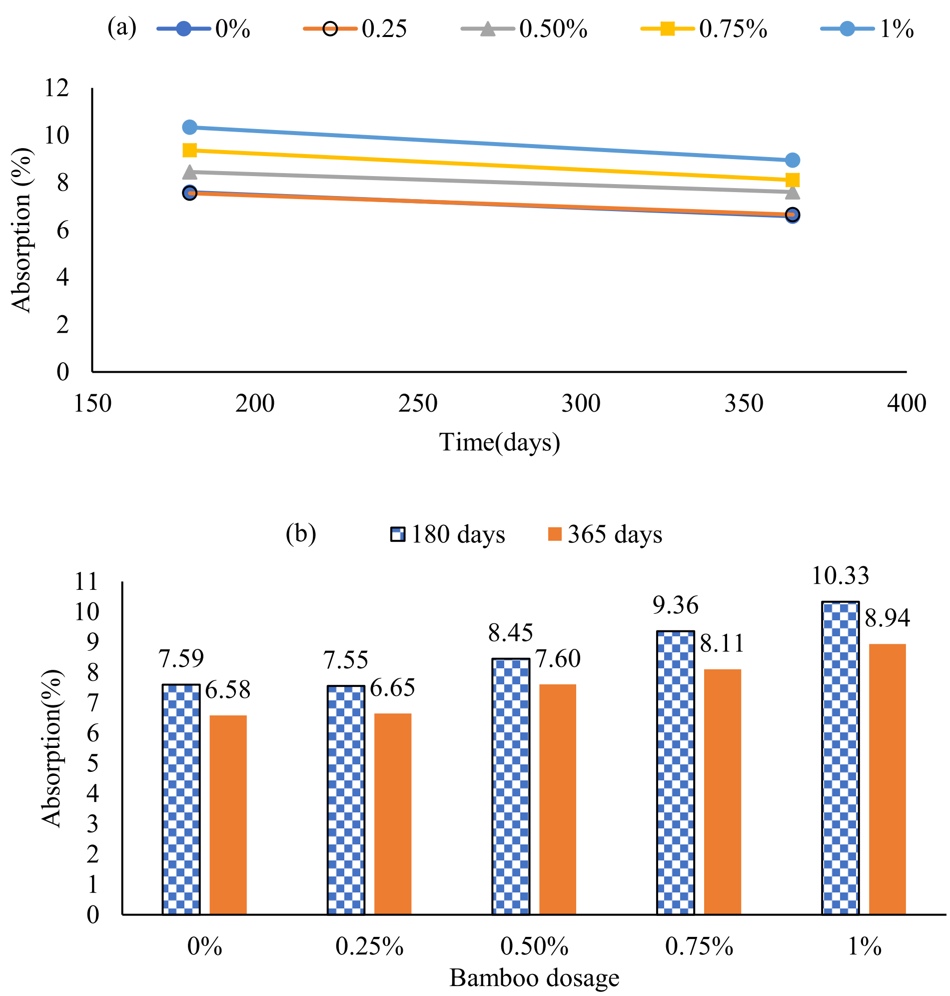

Figure 4.23. Absorption capacity

The absorption capacity in all sample cases showed a reduction as their age increased. This is due to many interrelated factors, specifically changes in microstructure and refinement of voids. The reduction in the total volume of voids proved in the later age is the other reason for the reduction in absorption capacity. As concrete matures, the internal structures become denser, which arises from the reduction of the volume of voids. The hydration process also helped in the formation of hydrated gels that have an impact on the reduction of the volume of voids. Moreover, as age increases, the pore structure becomes finer, contributing to the reduction of absorption(Shiyu, Zhuang., Qian, 2022)(Xin, Li., Nan, Guo, Jin., Ye, Tian., Xian, Yu, 2013)(Jun, Lu., Jiaping, Liu., X., Fan., Hesong, Jin., Ji-Hua, Zhu., Zhenyu, Huang., Feng, Xing., Tongbo, 2022).This is manifested by the reduction of the total volume of voids in concrete as age increases, making the concrete denser, which in turn reduces the absorption capacity over time. The effect of bamboo fiber on the concrete absorption behavior showed an increment with the dosage amount; however, the increment due to the addition of 0.25% bamboo fiber is insignificant in comparison with plain concrete samples. The absorption capacity was highest in the case of specimens with 1% bamboo fiber.

The relation between the volume of voids and absorption was examined and found to be linear at both ages of 180 and 365 days of concrete, as shown in Figure 4.24. The relationship was found to be strongly directly proportional and expressed linearly with R^2 value greater than 0.99 at both ages.

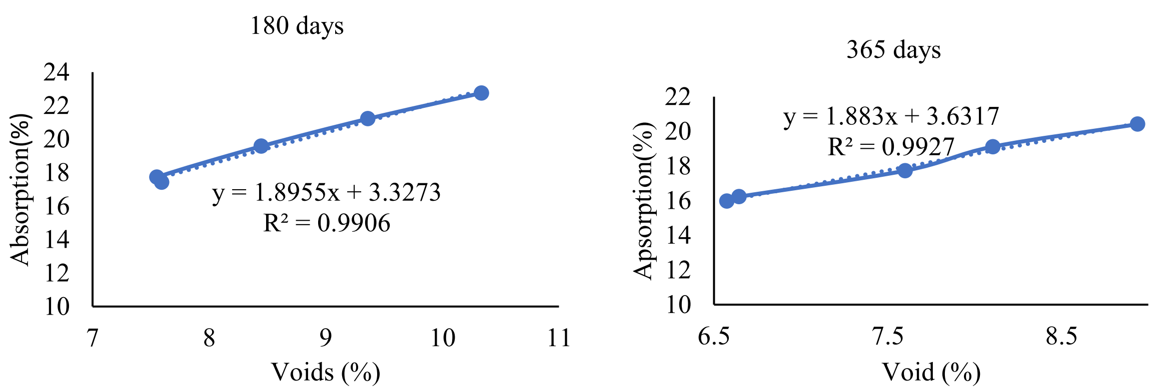

Figure 4.24. Voids versus absorption

The analysis of variance (ANOVA) test was performed at a significance level of 0.05, which revealed that the variation in the percentage content of bamboo fiber affected absorption on various days of observations, specifically at the 180-day (F = 16.774, Fcrit = 3.478) and 365-day (F = 14.785, Fcrit = 3.478). Tukey test between concrete with and without bamboo fiber, with Q and P-value was utilized at a significance level of 0.05. After 180 and 365 days, the values of Q and P of concrete specimens without bamboo fiber and reinforced with 0.25% bamboo fiber were (0.148, 0.999) and (0.269, 0.999), respectively. For this data, the critical value of Q is 4.654, which is greater than the values corresponding to the 180 and 365 days. Moreover, the P-values are closer to 1. These results demonstrate that samples reinforced with 0.25% bamboo fiber showed comparable absorption properties to the control specimen.

4.3.3 Summaries

The following summaries are drawn from the durability study conducted for the studied durations.

- Compared to samples that did not contain bamboo fiber, the compressive strengths of concrete specimens reinforced with 0.25% bamboo fiber showed comparable values in an acidic environment. Specimens reinforced with higher bamboo were significantly affected in the acidic environment.
- The mass reduction recorded in bamboo fiber-reinforced concrete specimens immersed in an acidic medium for 180 days showed the lowest value, 4.49%, compared with the values of plain concrete specimens, 16.35%.
- The compressive strength of all specimens immersed in an alkaline medium showed improvement. The improvements at the end of the 365-day duration were as high as 14.48% and 13.97% compared with the 28-day compressive strength of plain concrete samples and samples reinforced with 0.25% of bamboo fiber, respectively.
- All specimens recovered from the alkaline medium showed insignificant increments of mass.
- The difference between the total volume of voids of plain concrete samples and concrete samples reinforced with 0.25% bamboo fiber is 1.06% after 365 days. However, concrete samples containing higher doses of bamboo fiber showed an increase in total volume of voids compared to plain concrete samples.
- Bamboo fiber has been shown to increase the absorption capacity of concrete. The trend of absorption capacity exhibited a progressive increase corresponding to the augmented fiber dosage in the concrete matrix.
- The effect of the addition of bamboo fiber by 0.25% into concrete did not significantly affect the total volume of voids and absorption properties of concrete. In both cases, the variation between the plain concrete samples and the 0.25% bamboo fiber reinforced concrete samples is below 1.67%.

4.4 Drying shrinkage study of bamboo fiber reinforced concrete

4.4.1 Introduction

Shrinkage is the reduction in dimension of concrete due to moisture loss because of internal and environmental factors. Drying shrinkage is considered the largest proportion of the total shrinkage in concrete and a substantial shrinkage mechanism in most concrete. The shrinkage mechanism is associated with the paste because the coarse aggregates are considered volume stable. The volumetric ratio of paste to aggregate is an important parameter influential in the drying shrinkage of concrete, as shown in Figure 4.25 (Intertec, 2024).

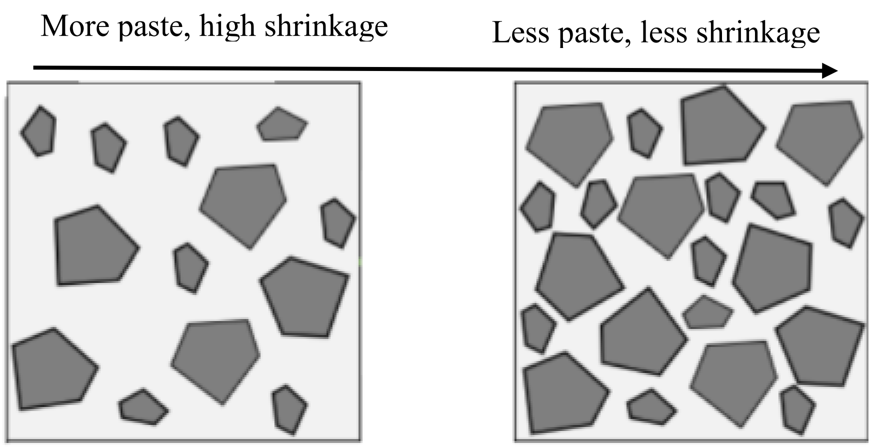

Figure 4.25. Impact of paste volume on shrinkage

The materials that are within the paste have a crucial impact on the drying shrinkage of concrete. Accordingly, the addition of bamboo fiber has role in this mechanism because of its impact on the formation of the paste. Therefore, in this topic, the investigations of the impacts of the bamboo fiber on the drying shrinkage of concrete are presented.

4.4.2 Results and discussions

4.4.2.1 Experimental output analysis

The outputs of this experimental study on the impact of bamboo fiber on the drying shrinkage of concrete are arranged into three parts. This is very helpful to observe the findings and impacts over time. Accordingly, Figure 4.26 presents the experiment's findings based on measurements conducted at intervals of two hours for the first six hours following demolding.

As shown in Figure 4.27, the addition of bamboo fiber reduced the drying shrinkage strain. The lowest drying shrinkage value was achieved in specimens reinforced with 0.25% bamboo fiber. As the fiber dose increases above 0.25%, the values of shrinkage strain in concrete increase. However, all the shrinkage values observed on bamboo fiber reinforced concrete samples are below the values of the control. This is due to the hydrophilic property of the bamboo fiber, as there is moisture in the specimens. This moisture consumed in the hydration process of the concrete. Plain concrete specimens lost their moisture in both hydration and evaporation; however, bamboo-reinforced concrete specimens replenish the lost moisture from the absorbed moisture in the fibers.

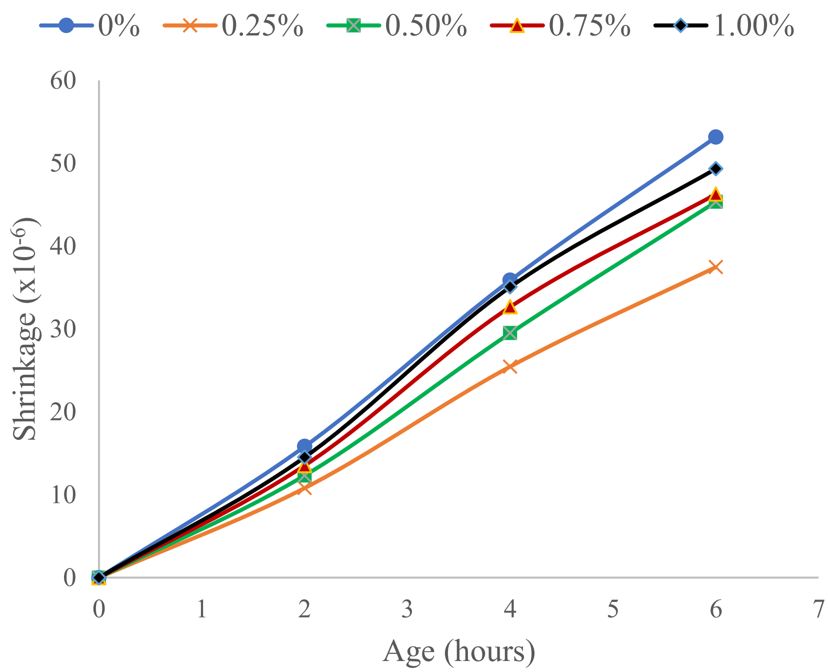

Figure 4.26. Drying shrinkage result for the first six hours

Compared to plain concrete specimens, the reductions in drying shrinkage after demolding and a two-hour duration in the control chamber achieved were 31.70%, 22.09%, 14.50%, and 8.18%, respectively, for specimens of concrete containing 0.25%, 0.5%, 0.75%, and 1.0% bamboo fiber. On the other hand, the reductions were 29.50%, 14.70%, 12.95%, and 7.18% after a six-hour duration.

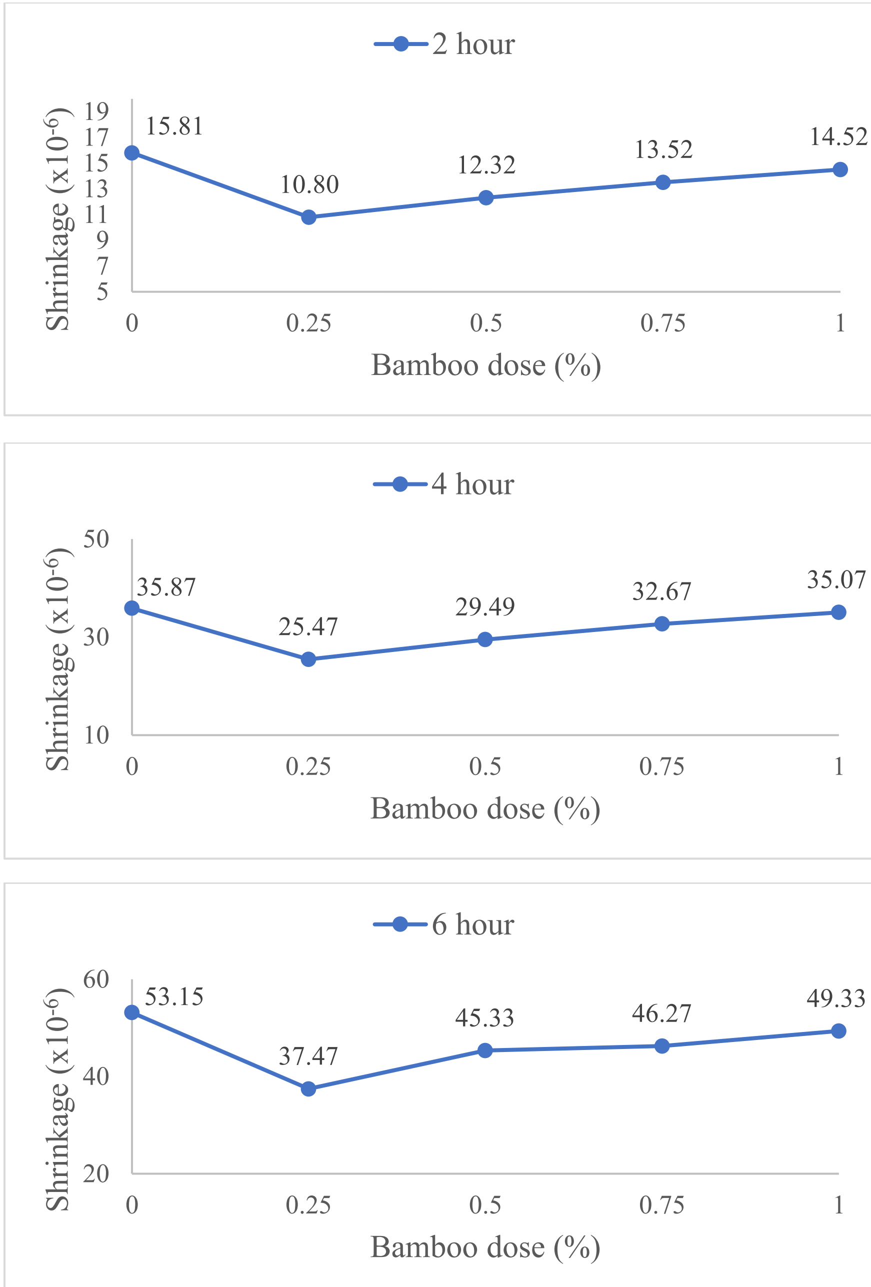

Figure 4.27. Drying shrinkage versus bamboo dose

Figure 4.28 illustrates the shrinkage development that occurred in the samples during the initial first ten-day period of demolding, a phase characterized by a higher rate of shrinkage due to moisture loss.

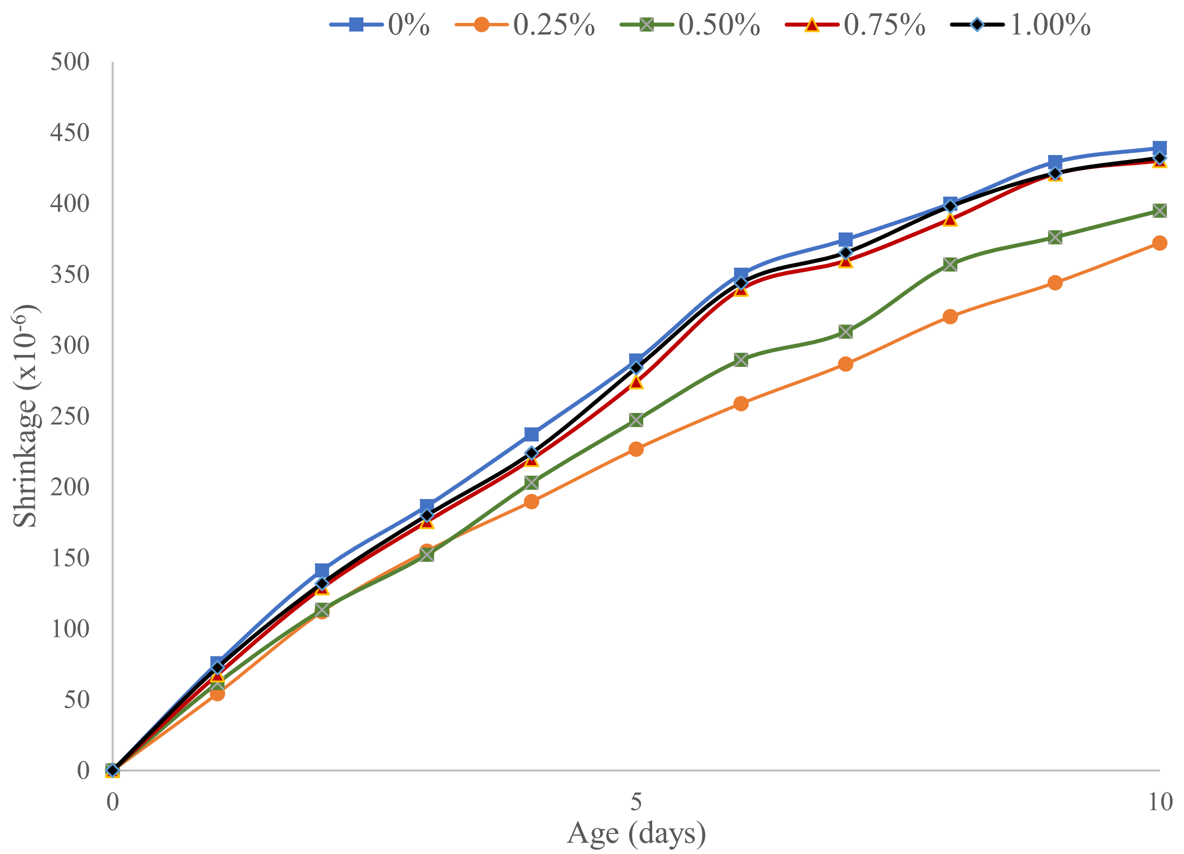

Figure 4.28. Shrinkage strain versus age, up to ten days

During the first ten days of observation, the drying shrinkage of samples containing 0.25% and 0.5% bamboo fiber showed lesser values than the others. However, the highest reduction of drying shrinkage was attained with concrete specimens reinforced with 0.25% bamboo fiber. The drying shrinkage obtained in specimens containing higher dosage levels of bamboo fiber was higher, and less than, but closer to, the control.

The drying shrinkage strains at the ten-day age of concrete are shown in Figure 4.29.

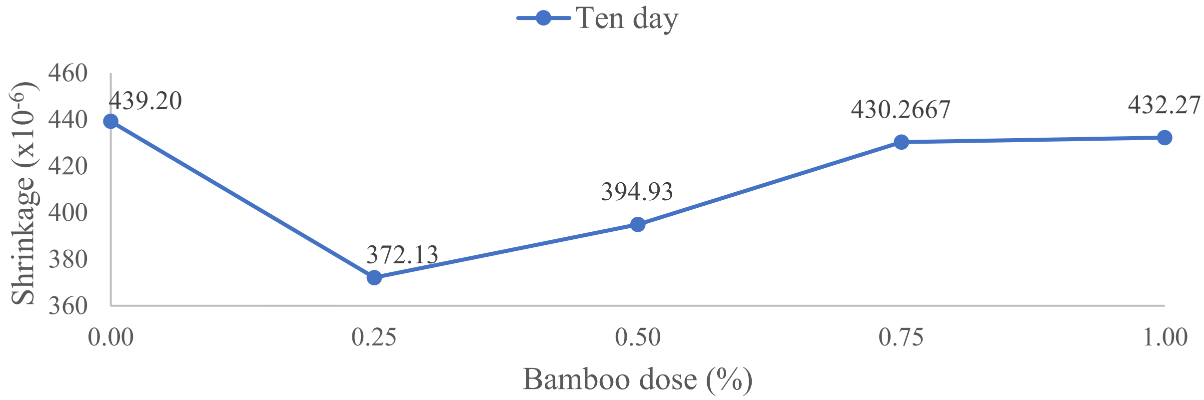

Figure 4.29. Tenth-day drying shrinkage strain versus bamboo dose

Compared to plain concrete specimens, the reductions in drying shrinkage after demolding and followed by ten days duration in the control chamber achieved were 15.27%, 10.08%, 2.03%, and 1.58%, respectively, in specimens of concrete containing 0.25%, 0.5%, 0.75%, and 1.0% bamboo fiber.

The shrinkage trend during the one hundred ninety-seven days is presented in Figure 4.30. The drying shrinkage of concrete increased with the age of drying in all sample types. Across all concrete sample types studied, the drying shrinkage exhibited an increase with the age of the drying period. This shrinkage increment was pronounced in the initial ages, demonstrating a relatively high rate of increment. However, as age increased, the rate at which the drying shrinkage increased gradually became sluggish, verifying a slower rate in the dimensional changes of the samples. Therefore, the rate of drying shrinkage development can be categorized into three zones, referring to Figure 4.30. The first one is where the rate of shrinkage strain development is highest. This zone can span up to 20 days. The next zone is where the shrinkage rate declines. This can be taken between the ages of 20 and 70. After the age of 70, the third stage of shrinkage development occurs, where the rate becomes very low.

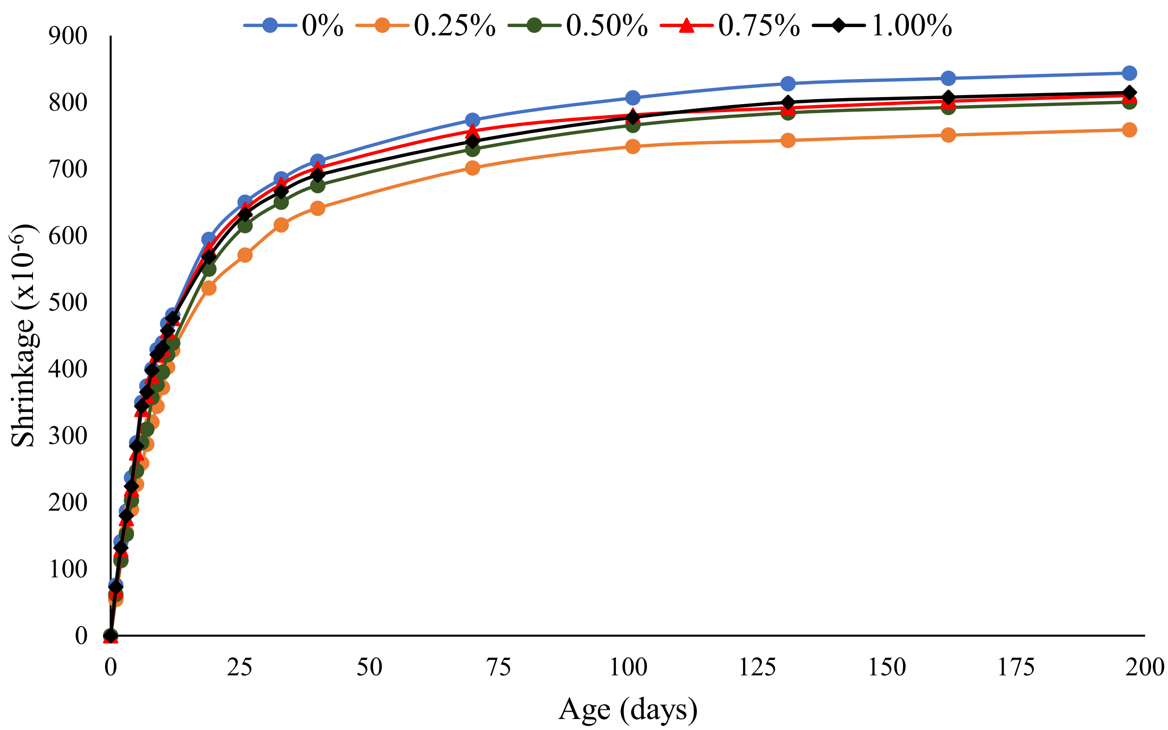

Figure 4.30. Shrinkage strain versus age, up to one hundred ninety-seven days

The shrinkage reduction is the highest in concrete specimens reinforced with 0.25% bamboo fiber compared to all the others. As the bamboo fiber concentration in concrete increased above 0.25%, the shrinkage strain in the concrete increased.

The shrinkage strains samples at one hundred ninety-seven days, which is the last day of this study, are presented in Figure 4.31.

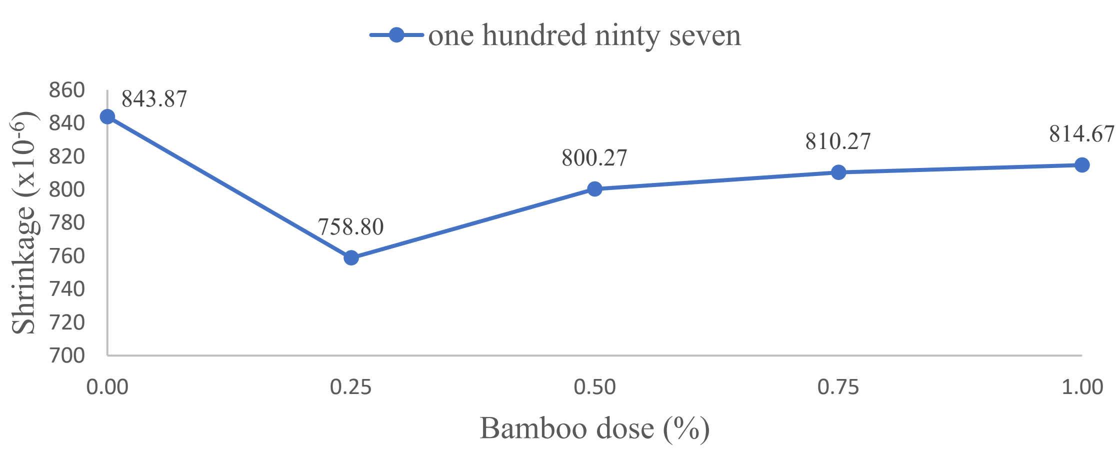

Figure 4.31. One hundred ninety-seven-day drying shrinkage strain versus bamboo dose

Compared to plain concrete specimens, the reductions in drying shrinkage achieved after one hundred ninety-seven days in the control chamber were 10.08%, 5.17%, 3.98%, and 3.46%, respectively, in specimens of concrete containing 0.25%, 0.5%, 0.75%, and 1.0% bamboo fiber. In the long run, the application of bamboo fiber at higher dosages did not achieve a higher percentage reduction in shrinkage strain. The moisture available in the bamboo fiber consumed in concrete for the hydration process creates pores that may lead to further shrinkage associated with this phenomenon.

The drying shrinkage of concrete containing carbon nanotubes showed a reduction of early shrinkage by 54% and a reduction of long-term shrinkage by 15%(Elzokra et al., 2020). For the normal-weight concrete, Brooks (Brooks, 2005) summarized 30-year data presented as the drying shrinkage in the range of 730-1015*10^{-6} in North Nottinghamshire and 740-1460*10^{-6} in Stourton. Such variations prove that drying shrinkage has complex characteristics that arise from the associated behaviors of the basic materials that the concrete is made of. The application of bamboo fiber did not deviate from the drying shrinkage out of the ranges recorded for normal-weight concrete. Moreover, the reduction in drying shrinkage at early and long-term is encouraging when compared with synthetic fibers.

4.4.2.2 Examination of existing prediction equations

Existing prediction equations application assessment was conducted, and the impact of the models is presented in Figure 4.32 for comparison. The graphs of the B3 model, GL2000, and Sakata showed variations when there is a dose variation of bamboo fiber in the concrete. On the other hand, the ACI model did not show such a variation. As the bamboo fiber dose increased, the graph of GL2000 was moved to the graph drawn based on the data recorded during the experiment. B3 has shown the same behavior as GL2000; however, the scale of the move was not significant. These models were developed by taking the impact of the compressive strength of concrete at the 28-day age into consideration. From the compressive strength experiment, the bamboo fiber dose and compressive strength have an inverse relationship. The impact of the compressive strength on the computation of shrinkage using B3 and GL2000 models is decremental. That is to say, the models give higher shrinkage values for lower compressive concrete strength. On the other hand, the graph obtained using the Sakat model shows increased gaps with increasing dose of bamboo fiber in the concrete.

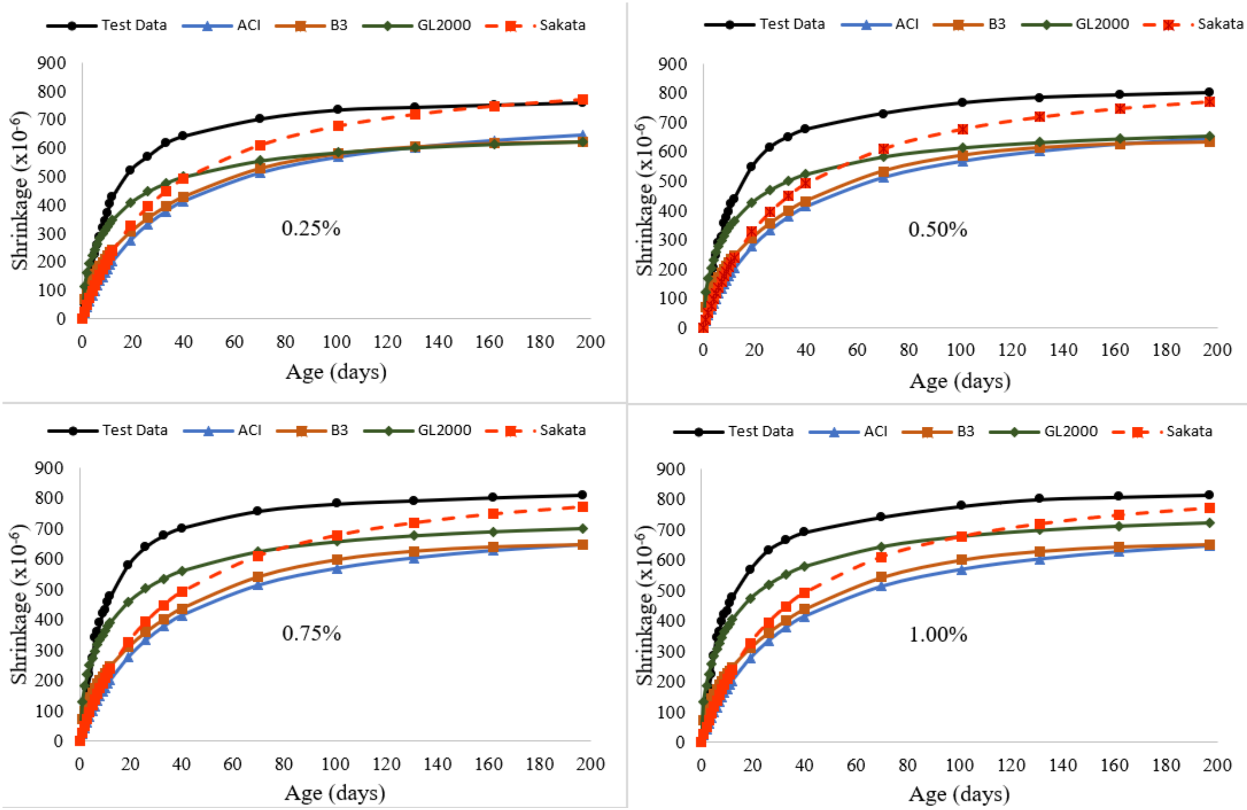

Figure 4.32. Experimental and model shrinkage strains

At the age of 40 days, the drying shrinkage strain value disparity between the experimental and the predicted is in the range 16.26% and 40.99%. At the age of 197 days, the drying shrinkage strain value disparity between the experimental and the predicted values gets lowered, but in the range of 11.26% and 20.68%. Moreover, all the models underestimate the shrinkage values of all types of specimens. The impacts of additives on the shrinkage magnitudes of concrete manifested by unable to reasonably estimate values by the available models. A similar mode of investigation was done by researchers to evaluate the existing models' performance in the estimation of drying shrinkage of concrete containing various additives. The investigations also proposed models that can predict the drying shrinkage of concrete containing additives(Hong et al., 2023).

Higher deviations in shrinkage magnitudes of concrete obtained by deploying prediction equations were the key spots that scholars engaged to minimize the gaps and disparities in concrete(Shurbert-Hetzel et al., 2023). Moreover, the impact of the bamboo fiber dose on the relationships between the values extracted from the experiment and the prediction models can be observed in Figure 4.32.

4.4.2.3 Developing the prediction Equation

The existing shrinkage prediction models gave values that deviated from the magnitudes recorded during the experiment. Drying shrinkage magnitudes follow the growth curve (Branson & Schumann, 1970) because the moisture loss both in hydration and evaporation from the specimens is at a higher rate during the early age, and then the rate of moisture loss declines in later ages and becomes asymptote to a horizontal line.

The equation P1 is suggested by ACI-209R-92 to develop the best equation through the determination of the constant f.

$$\varepsilon_{sht} = \frac{t^{\alpha}}{f+t^{\alpha}} * \varepsilon_{shu} \qquad \text{P1}$$

Where ε_{sht} = is the shrinkage value at time t

t = is the duration starting from drying

ε_{shu}= is the ultimate drying shrinkage of concrete

α= is the constant for a given member shape and size that defines the time ratio part

f= is the constant obtained from the best-fitting curve to the data that defines the time ratio part. The value indicates the way the concrete tends toward the ultimate shrinkage value. A higher f value means the shrinkage develops at a slower rate, while a lower f value means the shrinkage development is at a faster rate.

Moreover, candidate equations P2 and P3 are collected because they are functions designed to represent growth curves.

$$y = k * (1 - Exp(-b * x)) \qquad \text{P2}$$

Where

y= the dependent variable, the shrinkage value at time t

k= is the horizontal line where the function asymptotes, the ultimate shrinkage value

B = is the constant that determines the growth rate or the shape of the curve

x= is the independent variable, time

$$y = u * (1 - \frac{1}{(x+1)^{m}})^{n} \qquad \text{P3}$$

Where

y= the dependent variable, the shrinkage value at time t

u= is the horizontal line where the function asymptotes, the ultimate shrinkage value

m and n = are the constants that determine the growth rate or shape of the curve

x= the independent variable, time

The constants in all functions were determined by conducting a regression method that is based on the minimization of the sum of the squares of errors. Moreover, the constants vary with the bamboo fiber dose.

First, equations were evaluated to select the most precise equation. For this purpose, first, the constants were determined for each of the categories through regression analysis. Then, their accuracy was evaluated by comparing the mean absolute percentage error (MAPE) values using equation 4.1.

$$MAPE = \frac{1}{N}\sum_{n=1}^{N}\left(\frac{|Experimental\ data - Predicted\ data|}{Experimental\ data}\right) * 100 \text{ --4.1}$$

The contents and the MAPE values are given in Tables 4.20, 4.21, and 4.22 below.

Table 4.20. Constants and MAPE values of equation P1

Specimen	Constants			MAPE
	ε_{shu}	f	α	
S0	875.716	10.881	1.055	1.545
S25	788.292	15.064	1.135	15.619
S50	826.969	14.518	1.134	10.502
S75	831.724	12.354	1.139	3.759
S100	839.657	10.922	1.074	3.126

Table 4.21. Constants and MAPE values of equation P2

Specimen	Constants		MAPE
	y	b	
S0	793.504	0.082	6.066
S25	724.640	0.070	16.862
S50	760.397	0.072	12.004
S75	769.479	0.083	6.791
S100	764.943	0.084	6.608

Table 4.22. Constants and MAPE values of equation P3

Specimen	Constants			MAPE
	u	m	n	
S0	958.205	0.614	2.871	3.874
S25	862.549	0.662	3.565	17.482
S50	901.244	0.669	3.544	12.506
S75	892.075	0.703	3.408	5.832
S100	911.550	0.640	2.976	5.025

From the table, the model developed based on the ACI model gave the lowest MAPE. Therefore, to develop the model that takes the bamboo fiber dose into account, this model was selected for further regression analysis.

For this purpose, the bamboo fiber contribution in the prediction equation is approached by employing polynomial regression analysis. Studies showed that the polynomial regression analysis has shown greater accuracy over others(F. Bin Ahmed et al., 2020), hence polynomial functions of various degrees were evaluated. Therefore, the impact of bamboo fiber is considered by multiplying the basic equations (hyperbolic) with a polynomial function developed considering the bamboo fiber dose as the independent variable. Such a technique was used in the drying shrinkage prediction equation formulation of steel fiber reinforced concrete(P. Chen et al., 2018). Moreover, Guilin Zhang et al.(G. Zhang et al., 2022) developed a prediction model with a product of the basic function and an inverse of a polynomial function.

The evaluation of the polynomial equations started at the second degree and continued to higher degree polynomials to select the model that can represent or fit the experimental data. Then, the second, third, fourth, and fifth-degree polynomial equations listed in Table 4.23 were evaluated.

Table 4.23. Equations of models

Model	Equation
Model 1	$\frac{t^{\alpha}}{f+t^{\alpha}} * \varepsilon_{shu*(n_5*b_f^2+n_6*b_f+n_7)}$
Model 2	$\frac{t^{\alpha}}{f+t^{\alpha}} * \varepsilon_{shu*(n_4*b_f^3+n_5*b_f^2+n_6*b_f+n_7)}$
Model 3	$\frac{t^{\alpha}}{f+t^{\alpha}} * \varepsilon_{shu*(n_3*b_f^4+n_4*b_f^3+n_5*b_f^2+n_6*b_f+n_7)}$
Model 4	$\frac{t^{\alpha}}{f+t^{\alpha}} * \varepsilon_{shu*(n_2*b_f^5+n_3*b_f^4+n_4*b_f^3+n_5*b_f^2+n_6*b_f+n_7)}$
Model 5	$\frac{t^{\alpha}}{f+t^{\alpha}} * \varepsilon_{shu*(n_1*b_f^6+n_2*b_f^5+n_3*b_f^4+n_4*b_f^3+n_5*b_f^2+n_6*b_f+n_7)}$

Where

$n_1, n_2, \ldots, n_7 =$ coefficients determined through regression analysis

b_f= bamboo fiber in decimal

The model selection was made based on comparison of the values MAPE, R^2 and RMSE (root mean square error) after conducting non-linear regression analysis on the eighty percent of the shrinkage data. Table 4.24. presents the values of the constants obtained after the regression analysis and indicators of the precisions of the models.

Table 4.24. MAPE, R^2, and RMSE values

		Model 1	Model 2	Model 3	Model 4	Model 5
Coefficients	ε_{shu}	862.243	806.723	800.646	842.406	800.361
	f	12.493	12.482	12.488	12.361	12.493
	a	1.095	1.095	1.095	1.090	1.095
	n_7	0.973	1.044	1.052	0.996	1.047
	n_6	-	0.010	0.022	0.771	0.855
	n_5	69.304	2.872	0.010	1.002	1.058
	n_4		70.504	2.793	0.010	1.307
	n_3			69.887	2.849	0.010
	n_2				70.230	2.792
	n_1					69.882
MAPE		5.425	5.495	5.497	5.472	5.467
R^2		0.991	0.991	0.991	0.991	0.991
RMSE		23.933	24.100	24.111	24.156	24.158

The MAPE and RSME values of Model 1, which is the product of the basic equation and a second-degree polynomial, are the lowest compared with other models. However, the R^2 values of all the models are equal. On the other hand, all other models gave MAPE, RSME values that did not show significant variation. Moreover, a prediction model with MAPE value less than 10 is considered excellent (C. C. Wang et al., 2014). However, Model 1 is selected and proposed as the drying prediction equation of bamboo fiber reinforced concrete because it has the lowest values of MAPE and RMSE.

Figure 4.33 shows the comparison between the predicted values using Model 1 with those of the recorded ones from the experiment for twenty percent of the data for testing purposes. If the predicted drying shrinkage values ideally match the experimentally measured drying shrinkage strains, the relation between predicted drying shrinkage values and the measured drying shrinkage values shall follow the equation $y(x) = x$, where x is the predicted drying shrinkage and $y(x)$ is the measured drying shrinkage. The ideal scenario is when the slope is one, and the intercept is zero, or if the corresponding numerals for these are close to 1 and 0, respectively(Li, 2017). The line in Figure 4.33 shows when the line correlating the predicted and actual drying shrinkage passes through the origin. Accordingly, the data are distributed along the line y=0.9895x. Hence, the figure revealed that the predicted values obtained from Model 1 do not differ much from the experimentally recorded drying shrinkage strains.

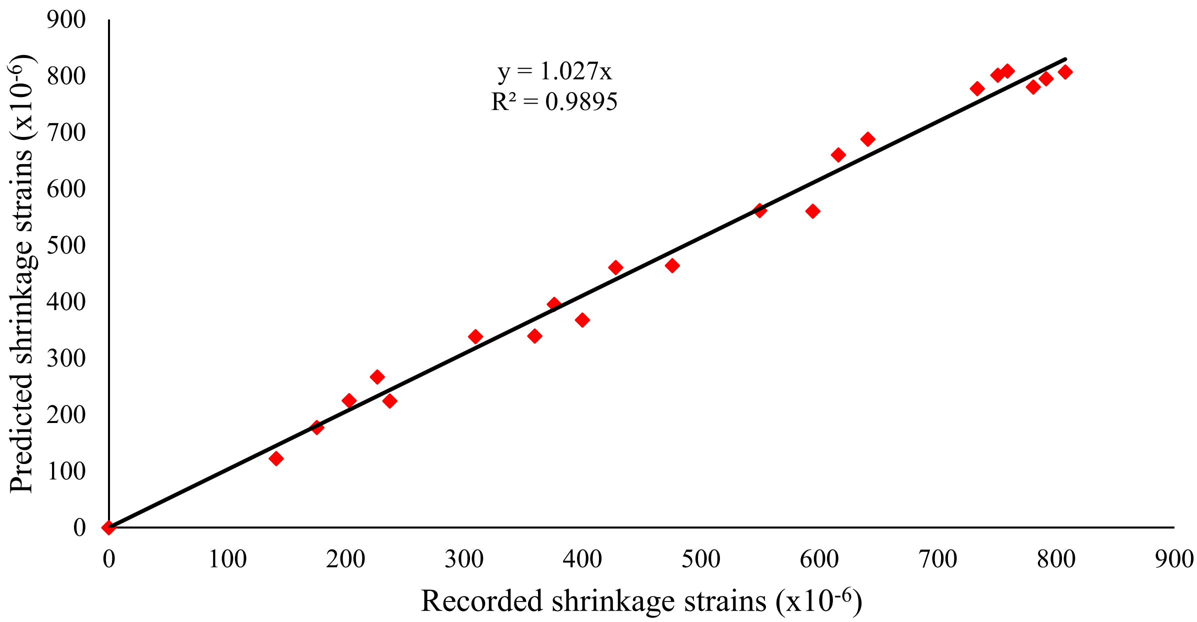

Figure 4.33. Observed and predicted data for all shrinkage strains for the testing data

Therefore, the equation of Model 1 is given below, incorporating the coefficients and contribution of bamboo fiber

$$\varepsilon_{sht} = \frac{t^{1.095}}{12.493+t^{1.095}} * 862.243_{*(69.304*b_f{}^2+0.973)} \text{ --4.2}$$

Where ε_{sht} = is the shrinkage value at time t

t = is the duration starting from drying

b_f= bamboo fiber amount

4.4.3 Summary

From the drying shrinkage examination, the following points are presented as a summary.

- Bamboo fiber incorporation in concrete enhances the resistance of concrete to stresses that arise at an early age associated with drying shrinkage.
- The addition of 0.25% Bamboo to concrete helped in the reduction of drying shrinkage strain by 31.7% within two hours and 29.5% within six hours after demolding when compared with plain concrete. When the dose increased to 1.0%, the reduction achieved was 8.18% and 7.18%. Therefore, a high dosage of bamboo percentage in concrete has the reduction of the benefits possibly attained by reducing the drying shrinkage.
- The drying shrinkage strain recorded in specimens reinforced with 0.25% is reduced by 15.27% when compared with plain concrete. The value of reduction was reduced to 1.58% when the dose of bamboo fiber was 1.00%.
- The drying shrinkage strains after six months in concrete specimens reinforced with 0.25% bamboo fiber were reduced by 10.08%. This reduction declines as the fiber dose increases.
- The drying shrinkage strains at one hundred ninety-seven days were in the range of $758.8000*10^{-6}$ and $843.8667*10^{-6}$.
- The existing drying shrinkage prediction models gave strain values that have gaps with the experimentally recorded values.
- A shrinkage model, which is a product of a polynomial equation that is a function of bamboo amount and the basic ACI model (hyperbolic function) with updated constants, has been formulated.
- The developed model predicted the drying shrinkage with acceptable parameters.

4.5 Impact of bamboo fiber in the application of concrete

4.5.1 General

Improved rigid pavement performance is the result of improved tensile or flexural behaviour of concrete. These increased behaviors can be achieved through different mechanisms; one of them is the use of eco-friendly and sustainable sources, which is Bamboo fiber. Therefore, in the subsequent sections, the effects of the inclusion of bamboo fiber on the thickness of concrete pavement and the joint spacing of concrete slab are to be assessed.

4.5.2 Impact of bamboo fiber reinforced concrete in pavements

There are graphs developed to assist in the design of rigid pavement structures. Those are based on the flexural strength of concrete and parameters of soil and traffic(Guyer et al., 2009). Moreover, the American Association of State Highway and Transportation Officials Institute (AASHTO) and guidelines for the design of plain jointed rigid pavements for highways issued by the Indian road congress also use the flexural strength of concrete for determination of the pavement slab thickness(A. Bekele, 2011)(AASHTO, 1993)(krishna & Rao, 2014)(The Indian Roads Congress, 2002).

Therefore, the flexural strength of concrete is an important parameter in the design of rigid pavement construction. Tables 8.1 and 8.2 show the result of concrete pavement thicknesses obtained based on the flexural strengths of concrete extracted from this research conducted to show the effect of the use of bioresources in concrete making. The AASHTO design manual is used to compute the thickness of the pavement using equation 4.3(AASHTO, 1993).

$$\log_{10} W_{18} = Z_R * S_o + 7.35 * \log_{10}(D+1) - 0.06 + \frac{\log_{10}\left[\frac{\Delta PSI}{4.5 - 1.5}\right]}{1 + \frac{1.624*10^7}{(D+1)^{8.46}}} + (4.22 - 0.32p_t) * \log_{10}\left[\frac{S_c' * C_d \left[D^{0.75} - 1.132\right]}{215.63 * J\left[D^{0.75} - \frac{18.42}{(E_c/k)^{0.25}}\right]}\right] \quad \text{------4.3}$$

Where

W_{18} = Predicted ESALs for the design period

Z_R = Standard normal deviate for the desired reliability

S_o = Combined standard error of the traffic prediction and performance prediction

D = Slab depth

Pi = Terminal (final) serviceability index

ΔPSI = Difference between the initial design serviceability index, P_o, and the design terminal serviceability index, P_t

S_c = Modulus of rupture of concrete

C_d = Drainage coefficient

J = Load transfer coefficient

E_c = Elastic modulus of concrete

K = Modulus of subgrade reaction

For the purpose of the computation, data from pavement design and material report of the Industrial and Settlement area gravel road project managed by Addis Ababa City Roads Authority are taken. The predicted design traffic was $30x10^6$ ESAL. The modulus of subgrade reaction is taken as using its relation with the CBR value (U.S. Department of Transportation. Federal Aviation Administration & Federal Aviation Administration, 2012). The initial serviceability index and the terminal serviceability index are taken as 4.5 and 2.5, which implies the serviceability loss as 2 (Iowa state-wide urban design and specification, 2019). For this computation of reliability Z_R, S_o, J, and C_d are taken as -1.645, 0.35, 3.2, and 1, respectively (AASHTO, 1993).

The pavement thickness when plain concrete is used is 309mm, and 0.25% bamboo fiber reinforced concrete is used 305 mm, as shown in the computation presented in Tables 4.25 and 4.26.

Table 4.25. Pavement thickness calculation for plain concrete

0 % bamboo fiber																
D	D	Z_R	So	ΔPSI	S_c	S_c	C_d	J	f_{cu}	f_{cy}	E_c	K	P_t	$Log_{10}(W_{18})$	W_{18} Calculated	W_{18} Design
(in)	mm				(MPa)	(psi)										
10.95	279	-1.645	0.35	2	3.60	522.1368	1	3.2	37.90	30.3	3.78E+06	82.4	2.5	7.176	1.50E+07	3.00E+07
11.1	282	-1.645	0.35	2	3.60	522.1368	1	3.2	37.90	30.3	3.78E+06	82.4	2.5	7.218	1.65E+07	3.00E+07
11.25	286	-1.645	0.35	2	3.60	522.1368	1	3.2	37.90	30.3	3.78E+06	82.4	2.5	7.259	1.82E+07	3.00E+07
11.4	290	-1.645	0.35	2	3.60	522.1368	1	3.2	37.90	30.3	3.78E+06	82.4	2.5	7.300	1.99E+07	3.00E+07
11.55	294	-1.645	0.35	2	3.60	522.1368	1	3.2	37.90	30.3	3.78E+06	82.4	2.5	7.340	2.19E+07	3.00E+07
11.7	298	-1.645	0.35	2	3.60	522.1368	1	3.2	37.90	30.3	3.78E+06	82.4	2.5	7.380	2.40E+07	3.00E+07
11.85	301	-1.645	0.35	2	3.60	522.1368	1	3.2	37.90	30.3	3.78E+06	82.4	2.5	7.419	2.62E+07	3.00E+07
12	305	-1.645	0.35	2	3.60	522.1368	1	3.2	37.90	30.3	3.78E+06	82.4	2.5	7.457	2.87E+07	3.00E+07
12.15	**309**	-1.645	0.35	2	3.60	522.1368	1	3.2	37.90	30.3	3.78E+06	82.4	2.5	7.496	3.13E+07	3.00E+07
12.3	313	-1.645	0.35	2	3.60	522.1368	1	3.2	37.90	30.3	3.78E+06	82.4	2.5	7.534	3.42E+07	3.00E+07
12.45	317	-1.645	0.35	2	3.60	522.1368	1	3.2	37.90	30.3	3.78E+06	82.4	2.5	7.571	3.72E+07	3.00E+07
12.6	321	-1.645	0.35	2	3.60	522.1368	1	3.2	37.90	30.3	3.78E+06	82.4	2.5	7.608	4.06E+07	3.00E+07
12.75	324	-1.645	0.35	2	3.60	522.1368	1	3.2	37.90	30.3	3.78E+06	82.4	2.5	7.645	4.41E+07	3.00E+07

Table 4.26. Pavement thickness calculation for 0.25% bamboo fiber reinforced concrete

0.25% bamboo fiber																
D	D	Z_R	So	ΔPSI	S_c	S_c	C_d	J	f_{cu}	f_{cy}	E_c	K	P_t	$Log_{10}(W_{18})$	W_{18} Calculated	W_{18} Design
(in)	mm				(MPa)	(psi)										
10.95	279	-1.645	0.35	2	4.04	585.9535	1	3.2	38.4	30.7	3.80E+06	82.4	2.5	7.224	1.67E+07	3.00E+07
11.1	282	-1.645	0.35	2	4.04	585.9535	1	3.2	38.4	30.7	3.80E+06	82.4	2.5	7.265	1.84E+07	3.00E+07
11.25	286	-1.645	0.35	2	4.04	585.9535	1	3.2	38.4	30.7	3.80E+06	82.4	2.5	7.305	2.02E+07	3.00E+07
11.4	290	-1.645	0.35	2	4.04	585.9535	1	3.2	38.4	30.7	3.80E+06	82.4	2.5	7.345	2.22E+07	3.00E+07
11.55	294	-1.645	0.35	2	4.04	585.9535	1	3.2	38.4	30.7	3.80E+06	82.4	2.5	7.385	2.43E+07	3.00E+07
11.7	298	-1.645	0.35	2	4.04	585.9535	1	3.2	38.4	30.7	3.80E+06	82.4	2.5	7.424	2.66E+07	3.00E+07
11.85	301	-1.645	0.35	2	4.04	585.9535	1	3.2	38.4	30.7	3.80E+06	82.4	2.5	7.463	2.90E+07	3.00E+07
12	**305**	-1.645	0.35	2	4.04	585.9535	1	3.2	38.4	30.7	3.80E+06	82.4	2.5	7.501	3.17E+07	3.00E+07
12.15	309	-1.645	0.35	2	4.04	585.9535	1	3.2	38.4	30.7	3.80E+06	82.4	2.5	7.539	3.46E+07	3.00E+07
12.3	313	-1.645	0.35	2	4.04	585.9535	1	3.2	38.4	30.7	3.80E+06	82.4	2.5	7.576	3.77E+07	3.00E+07
12.45	317	-1.645	0.35	2	4.04	585.9535	1	3.2	38.4	30.7	3.80E+06	82.4	2.5	7.613	4.10E+07	3.00E+07
12.6	321	-1.645	0.35	2	4.04	585.9535	1	3.2	38.4	30.7	3.80E+06	82.4	2.5	7.650	4.46E+07	3.00E+07
12.75	324	-1.645	0.35	2	4.04	585.9535	1	3.2	38.4	30.7	3.80E+06	82.4	2.5	7.686	4.85E+07	3.00E+07

The volume change of concrete due to temperature and moisture variations induces stress and cracking into the concrete. To address this, the length of the slab or joint spacing for concrete stress due to friction is calculated by equation 4.4, and the result of the analysis is shown in Table 4.27.

$$f_f = \frac{\gamma_c * L * f_a}{2} \quad \text{------------------------------------} 4.4$$

Where

f_f = flexural strength of concrete

γ_C= unit weight of concrete

L = length of slab

f_a= average coefficient of friction between the slab and subgrade

Table 4.27 Slab length considering concrete stress due to friction

Concrete code	ff (MPa)	fa	γc(kg/m3)	L(m)
S0	3.6	1.5	2.434	198
S25	4.04	1.5	2.408	224

According to Huang (Huang, 2004), the spacing of joints in unreinforced concrete pavements is governed more by the shrinkage characteristics of the concrete than the stress within it. Longer joint spacings lead to the joint opening wider and decrease the efficiency of load transfer. The opening of a joint computed by equation 4.5 (Darter, M. I., Barenberg, 1977).

$$\Delta L = C * L * (\alpha_t * \Delta T + \varepsilon) \quad \text{-----} 4.5$$

Where

ΔL= joint spacing caused by the temperature change and drying shrinkage

ε= coefficient of drying shrinkage of concrete

α_t= thermal expansion coefficient

ΔT= temperature range

L= joint spacing (slab length)

C= adjustment factor due to slab-subbase friction

Comparison analysis made between plain concrete and concrete reinforced with 0.25% bamboo fiber. The adjustment factor of slab-subbase friction in the case of a granular subbase is 0.8. The effect of the incorporation of bamboo fiber on the slab length is shown in Figure 4.34.

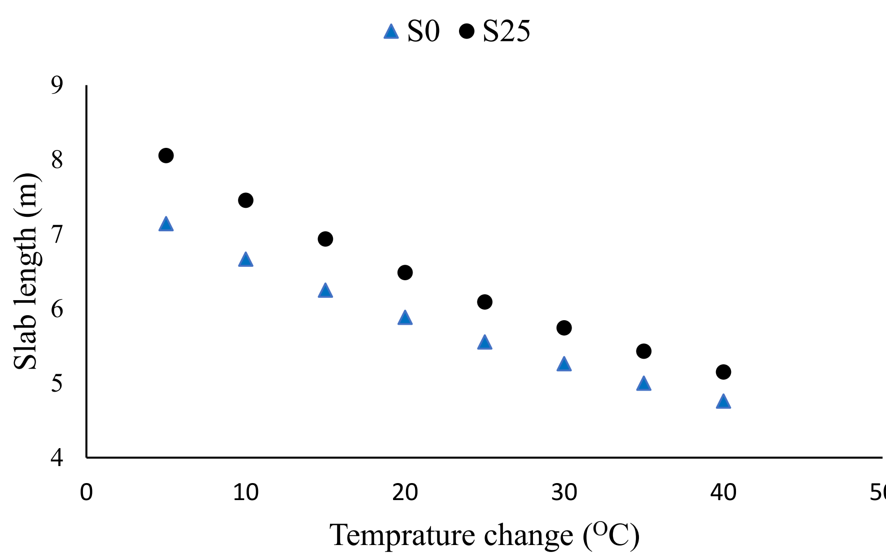

Figure 4.34. Slab length versus temperature change

From Figure 4.33, the slab length between joints necessary in pavement when concrete reinforced with 0.25% bamboo fiber is higher than plain concrete.

From the above examinations, the presence of bamboo fiber in concrete played a positive role in achieving reduced concrete pavement costs. Because reduced construction materials are to be used for the construction. This helps in the immediate cost savings and then the reduction of the rate of utilization of resources used for concrete making. On the other hand, the increased slab length has an impact in the reduction of the use of dowel bars and the labor associated with their placement. Moreover, this helps in the reduction of construction time required for a longer span.

4.5.3 Impact of bamboo fiber reinforced concrete in ground floor slabs

Improved flexural strength in concrete enables the design of thinner industrial concrete floors and concrete road pavements (Geremew et al., 2025). To illustrate, consider a warehouse ground floor designed for storage. The stored materials will exert a load of 70 kPa. Experimental results show that the flexural strength of plain concrete and 0.25% bamboo fiber-reinforced concrete is 3.6 MPa and 4.04 MPa, respectively. The compressive strength of plain concrete and 0.25% bamboo fiber-reinforced concrete is 37.90 MPa and 38.40 MPa, respectively. A factor of safety of 2 is applied to the flexural strength. The concrete floor rest on compacted sand, which has a modulus of subgrade reaction (k) of 50 MPa/m. Therefore, with these parameters, the thickness of the ground slab is calculated from equation 4.6 (Military Department 2025).

$$w = 57.17 * \frac{f_r}{SF} * \left(\frac{k*h}{E_c}\right)^{1/2} \quad \text{---4.6}$$

In which f_r is the flexural strength, k is the modulus of subgrade reaction, E_c is the modulus of elasticity of concrete, SF is the factor of safety, and w is the distributed load on the ground slab. The modulus of elasticity of concrete is calculated using equation 4.7, as provided by ACI.

$$E_c = 4700 * \sqrt[2]{f_c} \quad \text{---4.7}$$

Table 4.28 illustrates the effects of using plain concrete versus bamboo fiber-reinforced concrete for a warehouse ground floor slab. When plain concrete is used, the thickness of the ground floor slab is 268 mm. The thickness decreases to 215 mm when concrete with 0.25% bamboo fiber is used.

Table 4.28. Results of Slab Thickness

Parameters	Concrete type	
	S0	S25
Load applied, w, (kN/m^2)	70	70
Subgrade reaction, k, (MPa/m)	50	50
Compressive strength of concrete, fc (N/mm^2)	37.90	38.40
Modulus of elasticity of concrete, Ec (N/mm^2)	28934.60	29124.83
Flexural strength of concrete, fr (N/mm^2)	3.6	4.04
Factor of safety, Fs	2	2
Thickness (mm)	268	215

This reduction results from the enhanced flexural strength of concrete reinforced with 0.25% bamboo fiber. Therefore, the inclusion of bamboo fiber results in a 19.78% reduction in slab thickness. The reduction in slab thickness has cost implications. Moreover, a reduced thickness of a concrete slab implies reduced utilization of non-renewable resources such as sand, aggregate, and cement. This, in turn, implies that the rate of depletion of these resources is reduced.

5 Conclusions, recommendations, and future works

5.1 Conclusions

The following conclusions are made from the study.

1. The properties of bamboo fibers are influenced by the method employed for their extraction. The use of a chemical method of extraction for the extraction of fiber from Yushania alpina bamboo using the solutions of NaOH revealed a decrease of the lignin content, an increase of density, a decrease of absorption capacity, and an increase of tensile strength when compared with the mechanical and combined methods of extraction. The application of chemical method for the extraction made the surface of fibers roughened, which is a desirable characteristic in bondage with the concrete matrix. Moreover, the chemical method of extraction did not incur new functional groups to the fiber.
2. The use of various amounts of bamboo fiber in concrete showed impacts on the compressive, split tensile, and flexural strengths of the concrete.
   Usage of higher dose bamboo fiber in concrete attributes to the reduction of the mechanical properties of concrete in comparison with plain concrete. However, the bamboo dose of 0.25% by volume of concrete gave comparable compressive strength to concrete without bamboo fiber. Moreover, the presence of this amount of bamboo fiber in concrete enhanced the split tensile and flexural strengths of concrete. Early age split tensile and flexural strengths of concrete specimens with 0.25% bamboo dose showed comparable values with the values of plain concrete at the 28 days. This is helpful to increase the performance of concrete at the early age.
3. Exponential functions model the relationships between the mechanical properties of bamboo fiber reinforced concrete.
4. The trend of the strength gains of bamboo fiber reinforced concrete at a higher rate during the first 28 days, and then the increment declines.
5. The application of bamboo fiber in concrete helped to reduce the reduction of the crack width opening in concrete that happened due to loadings. Moreover, the inclusion of bamboo fiber in concrete has a positive role in the ductility of concrete.
6. When the incorporated bamboo fiber in concrete is at a higher dose, the susceptibility of concrete to the adverse environment is higher. In addition, the volume of voids and

absorption capacity of concrete specimens containing a higher amount of bamboo fiber are higher. However, concrete specimens with 0.25% bamboo fiber showed equivalent volume of voids and absorption capacity to the specimens without bamboo fiber.

7. The addition of bamboo fiber in concrete helps in the reduction of drying shrinkage of concrete.
8. The existing concrete shrinkage prediction models showed a deficiency in the prediction of bamboo fiber reinforced concrete.
9. The product of a hyperbolic function and a second-degree polynomial (to consider the impact of bamboo fiber dose) is selected for the drying shrinkage prediction of bamboo fiber reinforced concrete.
10. It is possible to utilize bamboo fiber in the construction of roads and ground floors.

5.2 Recommendations

The following recommendations are drawn from the study

1. Employing a 6% concentration of sodium hydroxide for the extraction of bamboo fiber is recommended.
2. Application of higher dosage of bamboo fiber has a negative impact on the workability, mechanical, durability, and time-dependent properties of concrete. Therefore, the application of bamboo fiber should be limited to 0.25% by volume of concrete.
3. Bamboo fiber can be utilized in pavement, ground floor, and mass concrete production.

5.3 Future works

At the end of conducting this study, the following lists were identified for future research

1. Optimization of bamboo fiber quality
2. Interaction of bamboo fiber moisture amount and tensile strength
3. Aspect ratio relationship with tensile strength and its impact on the performance of the bamboo fiber concrete composite
4. Impact of bamboo fiber on concrete creep

5. Examinations of structural specimens (beams, columns, slabs, pavements) made up of bamboo fiber reinforced concrete

References

AASHTO. (1993). AASHTO Guide for design of pavement structures. In *AASHTO*.

Abbas, A. G. N., Aziz, F. N. A. A., Abdan, K., Nasir, N. A. M., & Norizan, M. N. (2022). Kenaf Fibre Reinforced Cementitious Composites. *Fibers*, *10*(1), 1–24. https://doi.org/10.3390/fib10010003

Abbasi Dezfouli, A. (2019). Journal of Civil Engineering and Materials Application Effect of Using Different Fibers on Slab on Grades 2 *, Milad Orak. *J. Civil Eng. Mater.App*, *2019*(April), 2019. https://doi.org/10.22034/jcema.2019.92090

Abubakar, A., Mohammed, A., Duna, S., & Yusuf, U. S. (2022). Relationship between Compressive, Flexural and Split Tensile Strengths of Waste Copper Wire Fiber Reinforced Concrete. *Path of Science*, *8*(5), 4001–4009. https://doi.org/10.22178/pos.81-5

Abubakar, J., Aguwa, J. I., & Kolo, D. (2025). *Empirical Relationship between Compressive , Flexural and Splitting Tensile Strengths of Concrete Containing Kuta Gravel as Coarse Aggregate*. *January*. https://doi.org/10.9734/jerr/2025/v27i11380

ACI Committee 209. (1998). *Prediction of Creep, Shrinkage, and Temperature Effects in Concrete Structures, ACI 209R-92*.

ACI Committee 209. (2008). ACI 209.2R-08 Guide for Modeling and Calculating Shrinkage and Creep in Hardened Concrete. In *American Concrete Institute Technical Documents*.

Agboola, B. D., Onabote, E. J., Nwauju, C. D., Braimoh, S. O., Ejigboye, P. O., Ajamu, S. O., & Gana, A. J. (2024). Investigation of the Mechanical Properties of Sisal Fiber Reinforced Pervious Concrete. *International Conference on Science, Engineering and Business for Driving Sustainable Development Goals*.

Agency, E. t h i o p i a n S. t a n dards. (2013). *Cement-Part 1: Composition, specification and conformity criteria for common cement*. E t h i o p i a n S t a n dards Agency.

Ahmad, J., Zhou, Z., & Deifalla, A. F. (2023a). Structural properties of concrete reinforced with bamboo fibers: a review. In *Journal of Materials Research and Technology* (Vol. 24, pp. 844–865). https://doi.org/10.1016/j.jmrt.2023.03.038

Ahmad, J., Zhou, Z., & Deifalla, A. F. (2023b). Structural properties of concrete reinforced with bamboo fibers: a review. *Journal of Materials Research and Technology*, *24*, 844–865. https://doi.org/10.1016/j.jmrt.2023.03.038

Ahmad, S., Raza, A., & Gupta, H. (2014). *Mechanical Properties of Bamboo Fibre Reinforced Concrete*. *0531279486*. https://doi.org/10.15242/iie.e0314522

Ahmad, Z., Ding, Y., & Shahzad, A. (2021). Biotechnological Advances in Bamboo: The "Green Gold" on the Earth. In *Biotechnological Advances in Bamboo: The "Green Gold" on the Earth* (Issue September). https://doi.org/10.1007/978-981-16-1310-4

Ahmed, M., Mallick, J., & Hasan, M. A. (2016). A study of factors affecting the flexural tensile strength of concrete. *Journal of King Saud University - Engineering Sciences*, *28*(2), 147–

156. https://doi.org/10.1016/j.jksues.2014.04.001

Al., X. et. (2008). Modren Bamboo Structures. In S. G. & P. S. C. Korde, A. Agrawal (Ed.), *Experimental verifi cation of bamboo-concrete composite bow beam with ferro-cement bond*. Taylor & Francis Group.

Alene, A. (2013). *Design and Analysis of Bamboo and E-Glass Fiber Reinforced Epoxy Hybrid Composite for Wind Turbine Blade Shell*. Addis Ababa University.

Althoey, F., Hakeem, I. Y., Hosen, M. A., Qaidi, S., Isleem, H. F., Hadidi, H., Shahapurkar, K., Ahmad, J., & Ali, E. (2022). Behavior of Concrete Reinforced with Date Palm Fibers. *Materials*, *15*(22). https://doi.org/10.3390/ma15227923

Alves Fidelis, M. E., Pereira, T. V. C., Gomes, O. D. F. M., De Andrade Silva, F., & Toledo Filho, R. D. (2013). The effect of fiber morphology on the tensile strength of natural fibers. *Journal of Materials Research and Technology*, *2*(2), 149–157. https://doi.org/10.1016/j.jmrt.2013.02.003

Andreola, V. M., da Gloria, M. Y. R., Pepe, M., & Toledo Filho, R. D. (2024). A Comprehensive Experimental Study on the Physical Performance and Durability of Bamboo Bio-Concrete. *Sustainability (Switzerland)* , *16*(13). https://doi.org/10.3390/su16135334

Anokye, R., Bakar, E. S., Ratnasingam, J., & Awang, B. K. (2016). Bamboo Properties and Suitability as a Replacement for Wood. *PJSRR Pertanika Journal of Scholarly Research Reviews*, *2*(1), 63–79. http://www.pjsrr.upm.edu.my/

Antwi-afari, B. A., Mutuku, R., Kabubo, C., Mwero, J., & Kithiia, W. (2024). Influence of fiber treatment methods on the mechanical properties of high strength concrete reinforced with sisal fibers. *Heliyon*, *10*(8), e29760. https://doi.org/10.1016/j.heliyon.2024.e29760

Arasilan gkumaran.v, D. S. C. J. (2017). A study on acid and alkaline attack on scc. *International Journal of Advanced Research in Basic Engineering Sciences and Technology*, *3*(24), 979–992.

Asaduzzaman, S. M., & Islam, G. M. S. (2023). Using Jute Fiber to Improve Fresh and Hardened Properties of Concrete. *Journal of Natural Fibers*, *20*(2). https://doi.org/10.1080/15440478.2023.2204452

Association, F. R. C. (2022). *Fiber Reinforced Concrete*. https://fiberreinforcedconcrete.org/wp-content/uploads/2022/01/FIP-1-Fiber-Reinforced-Concrete.pdf

ASTM. (1996). ASTM C496 Standard Test Method for Splitting Tensile Strength of Cylindrical Concrete Specimens. In *ASTM International, USA*. ASTM International.

ASTM. (1997). *ASTM C642 Standard Test Method for Density , Absorption , and Voids in Hardened Concrete 1*. *4*, 4–6.

ASTM. (2001a). ASTM C136 Standard Test Methods for Sieve Analysis of Fine and Coarse Aggregates. In *ASTM International, USA*.

ASTM. (2001b). ASTM C39 Standard Test Method for Compressive Strength of Cylindrical Concrete Specimens. In *ASTM International, USA*.

ASTM. (2002). ASTM C78 Standard Test Method for Flexural Strength of concrete. In *ASTM International, USA*.

ASTM. (2003a). ASTM C143 Standard Test Method for Slump of Hydraulic-Cement Concrete. In *ASTM International, USA*.

ASTM. (2003b). ASTM C33 Standard Specification for Concrete Aggregates. In *ASTM International, USA*. ASTM International.

ASTM. (2015). *Standard Test Method for Tensile Strength and Young 's Modulus of Fibers 1*. https://doi.org/10.1520/C1557-14.2

Awotwe-Mensah, M., Appiah-Kubi, E., & Mitchual, S. J. (2024). Assessment of Density and Anatomical Features of Young and Old Bambusa vulgaris (Schrad. ex J.C. Wendl.) Culm Heights as Sustainable Structural Material in Ghana. *International Journal of Forestry Research*, *2024*. https://doi.org/10.1155/2024/4459948

Ayeni, A. O., Adeeyo, O. A., Oresegun, O. M., & Oladimeji, T. E. (2015). Compositional analysis of lignocellulosic materials: Evaluation of an economically viable method suitable for woody and non-woody biomass. *American Journal of Engineering Research*, *44*, 2320–2847. www.ajer.org

Bahru, T. (2021). *A Review on Bamboo Resource in the African Region : A Call for*. *2021*, 10–12.

Bal, L., & Buyle-bodin, F. (2013). Artificial neural network for predicting drying shrinkage of concrete. *Construction and Building Materials*, *38*, 248–254. https://doi.org/10.1016/j.conbuildmat.2012.08.043

Banga, H., Singh, V. K., & Choudhary, S. K. (2015). Fabrication and Study of Mechanical Properties of Bamboo Fibre Reinforced Bio-Composites. *Innovative Systems Design and Engineering*, *6*(1), 84–99.

Banik, R. L. (2015). Bamboo The Plant and its Uses. In *Bamboo: The plant and its uses*.

Bayu, A., Nandiyanto, D., Oktiani, R., & Ragadhita, R. (2019). How to Read and Interpret FTIR Spectroscope of Organic Material. *Indonesian Journal of Science & Technology*, *1*, 97–118. https://doi.org/https://doi.org/10.17509/ijost.v4i1.15806

Beddoe, R. E., & Dorner, H. W. (2005). Modelling acid attack on concrete: Part I. The essential mechanisms. *Cement and Concrete Research*, *35*(12), 2333–2339. https://doi.org/10.1016/j.cemconres.2005.04.002

Behera, S., Prasad, N., & Kumar, S. (2018). Study of Mechanical Properties of Bamboo fibers before and after Alkali Treatment. *International Journal of Applied Engineering Research*, *13*(7), 5251–5255.

Beiser, V. (2019). *Why the world is running out of sand?* https://www.bbc.com/future/article/20191108-why-the-world-is-running-out-of-sand

Bekele, A. (2011). *Implementation of the AASHTO Pavement Design Procedures into MULTI-PAVE*. 49.

Bekele, A. E., Lemu, H. G., & Jiru, M. G. (2022). Experimental study of physical, chemical and mechanical properties of enset and sisal fibers. *Polymer Testing*, *106*(December 2021), 107453. https://doi.org/10.1016/j.polymertesting.2021.107453

Bentur, A., & Mindess, S. (2020). Applications of fibre reinforced concrete. *Fibre Reinforced Cementitious Composites*, *17*(11), 578–614. https://doi.org/10.1201/9781482267747-23

Bheel, N., Ali, M. O. A., Kirgiz, M. S., de Sousa Galdino, A. G., & Kumar, A. (2021). Fresh and mechanical properties of concrete made of binary substitution of millet husk ash and wheat straw ash for cement and fine aggregate. *Journal of Materials Research and Technology*, *13*, 872–893. https://doi.org/10.1016/j.jmrt.2021.04.095

Bin Ahmed, F., Abid Ahsan, K., Shariff, T., & Rahman Meem, S. (2020). Formulation of polynomial equation predicting the splitting tensile strength of concrete. *Materials Today: Proceedings*, *38*(xxxx), 3269–3278. https://doi.org/10.1016/j.matpr.2020.10.017

Bindu, M., Narendra, B. K., & Manjunatha, J. K. (2016). BAMBOO FIBER REINFORCED CONCRETE - A REVIEW. *International Journal of Science Technology and Management*, 189–193.

Biswas, S., Ahsan, Q., Cenna, A., Hasan, M., & Hassan, A. (2013). Physical and mechanical properties of jute, bamboo and coir natural fiber. *Fibers and Polymers*, *14*(10), 1762–1767. https://doi.org/10.1007/s12221-013-1762-3

Branson, D. E., & Schumann, C. G. (1970). *The Prediction of Creep and Shrinkage Properties of Concrete by*. *70*.

Brooks, J. J. (2005). 30-Year Creep and Shrinkage of Concrete. *Magazine of Concrete Research*, *57*(9), 545–556. https://doi.org/10.1680/macr.2005.57.9.545

Brooks, J. J., & Neville, A. M. (1978). Predicting long-term creep and shrinkage from short-term tests. *Magazine of Concrete Research*, *30*(103), 51–61. https://doi.org/10.1680/macr.1978.30.103.51

Buson, R. F., Melo, L. F. L., Oliveira, M. N., Rangel, G. A. V. P., & Deus, E. P. (2018). Physical and mechanical characterization of surface treated bamboo fibers. *Science and Technology of Materials*, *30*, 67–73. https://doi.org/10.1016/j.stmat.2018.03.002

Canavan, S., Richardson, D. M., Visser, V., Le Roux, J. J., Vorontsova, M. S., & Wilson, J. R. U. (2017). The global distribution of bamboos: Assessing correlates of introduction and invasion. *AoB PLANTS*, *9*(1), 1–18. https://doi.org/10.1093/aobpla/plw078

Cepcianska, J., Dragomirova, J., Kuzielova, E., Zemlicka, M., & Palou, M. T. (2021). Impact of the curing conditions and carbon dioxide ingress on heavyweight concrete. *IOP Conference Series: Materials Science and Engineering*, *1205*(1), 012007. https://doi.org/10.1088/1757-899x/1205/1/012007

Chaowana, P., Barbu, M. C., & Frühwald, A. (2015). Bamboo - A functionally graded composite material. *Forest Products Journal*, *65*(3–4), S48–S53.

Charles Camp. (2024). *Part 8 - Fresh Concrete*. https://www.ce.memphis.edu/1101/notes/concrete/everything_about_concrete/08_fresh.html

Chaudhary, U., Malik, S., Rana, V., & Joshi, G. (2024). Bamboo in the pulp, paper and allied industries. *Advances in Bamboo Science*, *7*(December 2023). https://doi.org/10.1016/j.bamboo.2024.100069

Che Rosely, N. A. N., Wan Jusoh, W. A., Osman, M. H., Syed Zin, S. M. F., Adnan, S. H., Roslan, M. N., Md Desaa, M. S., & Othman, K. (2024). Drying Shrinkage Properties and Engineering Performance for Cement Mortar Containing Bamboo Biochar Powder (BCP). *International Journal of Nanoelectronics and Materials*, *17*, 617–626. https://doi.org/https://doi.org/10.58915/ijneam.v17i4.1356

Chen, X., & Zhu, H. (2024). Research status and prospects of bamboo-based cement concrete. *Journal of Reinforced Plastics and Composites*. https://doi.org/10.1177/07316844241231123

Chen, C., Li, H., Dauletbek, A., Shen, F., Hui, D., Gaff, M., Lorenzo, R., Corbi, I., Corbi, O., & Ashraf, M. (2022). Properties and applications of bamboo fiber—A current-state-of-the art. *Journal of Renewable Materials*, *10*(3), 605–624. https://doi.org/10.32604/jrm.2022.018685

Chen, H., Yu, Y., Zhong, T., Wu, Y., Li, Y., Wu, Z., & Fei, B. (2017). Effect of alkali treatment on microstructure and mechanical properties of individual bamboo fibers. *Cellulose*, *24*(1), 333–347. https://doi.org/10.1007/s10570-016-1116-6

Chen, L., Chen, Z., Xie, Z., Wei, L., Hua, J., Huang, L., & Yap, P. S. (2023). Recent developments on natural fiber concrete: A review of properties, sustainability, applications, barriers, and opportunities. *Developments in the Built Environment*, *16*(July). https://doi.org/10.1016/j.dibe.2023.100255

Chen, P., Zheng, W., Wang, Y., & Chang, W. (2018). Analysis and modelling of shrinkage and creep of reactive powder concrete. *Applied Sciences (Switzerland)*, *8*(5). https://doi.org/10.3390/app8050732

Chhorn, C., Hong, S. J., & Lee, S. W. (2017). ScienceDirect Relationship between compressive and tensile strengths of roller-compacted concrete. *Journal of Traffic and Transportation Engineering (English Edition)*, *5*(3), 215–223. https://doi.org/10.1016/j.jtte.2017.09.002

Clarke, C. (2009). *CONCRETE SHRINKAGE PREDICTION USING MATURITY AND ACTIVATION ENERGY*.

Council, W. green building. (2019). *Bringing emboided carbon upfront*. https://worldgbc.s3.eu-west-2.amazonaws.com/wp-content/uploads/2022/09/22123951/WorldGBC_Bringing_Embodied_Carbon_Upfront.pdf

D C Teychenné, R E Franklin, H. C. E. (1997). *Design of normal concrete mixes* (Second Edi). Building Research Establishment Ltd.

Darter, M. I., Barenberg, E. J. (1977). *Design of zero-maintenance plain jointed concrete pavement* (Vol. II). Department of Transportation.

Day, K. W., Hollon, G. W., Lee, S. H., Pierce, J. S., Popovics, S., Robinson, H. C., Rose, J. H., Scherocman, J. A., Southworth, G. B., Spamer, A. B., Taylor, M. A., Weber, J. W., Ii, D. J. W., Barton, S. G., Bell, L. W., Carter, A. C., Conrey, M. T., & Bell, L. W. (2002). *Standard Practice for Selecting Proportions for Normal , Heavyweight , and Mass Concrete (ACI*

211 . 1-91). *Reapproved*, 1–38.

De Castro Ho, M. G., Nassif, B. D., Nunes Ribeiro e Silva, A. de A., Bueno, C. O. R., Guedes, V. S., Couto, C., Nunes, E. H. M., & Almeida, M. L. B. (2024). Plant Fiber Reinforced Polymeric Composites for Engineering Applications: a Review. *Revista de Gestao Social e Ambiental*, *18*(2), 1–19. https://doi.org/10.24857/rgsa.v18n2-086

Defoirdt, N., Biswas, S., Vriese, L. De, Quan, L., Tran, N., & Acker, J. Van. (2010). Composites : Part A Assessment of the tensile properties of coir , bamboo and jute fibre. *Composites Part A*, *41*(5), 588–595. https://doi.org/10.1016/j.compositesa.2010.01.005

Department, M. (2025). *DESIGN OF CONCRETE FLOOR SLABS-ON-GROUND FOR DOD FACILITIES*. *March*.

Deshpande, A. P., Rao, M. B., & Rao, C. L. (1999). Extraction of Bamboo Fibers and Their Use as Reinforcement in Polymeric Composites. *Journal of Applied Polymer Science*, 83–92.

Dessalegn, Y., Singh, B., & van Vuure, A. W. (2021). Analyze the Significance of Age and Height on the Physical and Chemical Properties of Ethiopian Giant Timber Bamboo . *American Journal of Engineering and Applied Sciences*, *14*(2), 185–197. https://doi.org/10.3844/ajeassp.2021.185.197

Development, W. C. on E. and. (1987). *Our Common Future: The Brundtland Report on Environment and Development*.

Diana Mohamed Ali, Siew Choo Chin, Chao Bao, J. G. (2024). Enhancement of reinforced concrete durability and performance by bamboo and basalt fibres. *Physics and Chemistry of the Earth*, *134*. https://doi.org/https://doi.org/10.1016/j.pce.2024.103572

Dinku, A. (2002). *Construction materials laboratory manual*. Addis Ababa university printing press.

Diouf, G., & Gning, P. B. (2024). Influence of the Extraction Process on the Mechanical and Morphological Properties of Technical Fibers from Typha domingensis. *Journal of Natural Fibers*, *21*(1). https://doi.org/10.1080/15440478.2024.2357744

Dirk, E. (2014). *Bamboo Reinforcement – A Sustainable Alternative to Steel*. 34–40.

Dody, A., Mohd, I., & Al, and et. (2008). Wettability and Interfacial Chracterization of Alkaline Treated Kenaf Fiber-Unsaturated Polyester Composites Fabricated by Resin Transfer Molding. *Polymers and Polymer Composites*, *16*(2), 101–113. https://doi.org/10.1002/pc

Dou, H., Xu, H., & Xie, J. (2023). Long-term mechanical performance of high fluidity fiber reinforced concrete modified by metakaolin. *Frontiers in Materials*, *10*(July), 1–19. https://doi.org/10.3389/fmats.2023.1162053

Ede, A. N., Olofinnade, O. M., Joshua, O., Nduka, D. O., & Oshogbunu, O. A. (2020a). Influence of bamboo fiber and limestone powder on the properties of self-compacting concrete. *Cogent Engineering*, *7*(1). https://doi.org/10.1080/23311916.2020.1721410

Ede, A. N., Olofinnade, O. M., Joshua, O., Nduka, D. O., & Oshogbunu, O. A. (2020b). Influence of bamboo fiber and limestone powder on the properties of self-compacting concrete. *Cogent Engineering*, *7*(1). https://doi.org/10.1080/23311916.2020.1721410

Eguchi, K., & Teranishi, K. (2005). *Prediction equation of drying shrinkage of concrete based on composite model*. *35*, 483–493. https://doi.org/10.1016/j.cemconres.2004.08.002

Elzokra, A., Al Houri, A., Habib, A., Habib, M., & Malkawi, A. B. (2020). Shrinkage behavior of conventional and nonconventional concrete: A review. *Civil Engineering Journal (Iran)*, *6*(9), 1839–1851. https://doi.org/10.28991/cej-2020-03091586

Emamverdian, A., Ding, Y., Ranaei, F., & Ahmad, Z. (2020). Application of Bamboo Plants in Nine Aspects. *Scientific World Journal*, *2020*. https://doi.org/10.1155/2020/7284203

Er. H. Mehra, V. N. V. (2004). *Limit state design of reinforced concrete structures* (Second edi). Khanna Publishers.

Espitia, M., Sjogreen, C., Rodríguez, N., Calderón, J., Benavides, A., Peraza, R., Espitia, G., & Nemocon, R. (2018). Mechanical and physical characterization of Guadua angustifolia'Kunth'fibers from Colombia. *Revista UIS Ingenierías*, *17*(2), 33–40. https://doi.org/10.18273/revuin.v17n2-2018003

Fang, X., Xu, J., Guo, H., & Liu, Y. (2023). The Effect of Alkali Treatment on the Crystallinity, Thermal Stability, and Surface Roughness of Bamboo Fibers. *Fibers and Polymers*, *24*(2), 505–514. https://doi.org/10.1007/s12221-023-00093-z

Fei Pang, Guo Miao, Yingxu Li, Y. S. (2024). Key factors influencing sustainable population growth: A DEMANTEL-ANP combined approach. *Heliyon*.

Folliard, K., Smith, C., Sellers, G., Brown, M., & Breen, J. E. (2003). *Evaluation of Alternative Materials to Control Drying-Shrinkage Cracking* (Vol. 7).

Freidriks, A., & Thesis, M. (2015). *Prediction Models of Shrinkage and Creep in Industrial Floors and Overlays Prediction Models of Shrinkage and Creep in Industrial Floors and Overlays*.

Fu, J., Li, X., Gao, W., Wang, H., Cavaco-Paulo, A., & Silva, C. (2012). Bio-processing of bamboo fibres for textile applications: A mini review. *Biocatalysis and Biotransformation*, *30*(1), 141–153. https://doi.org/10.3109/10242422.2012.650450

Gao, X., Zhu, D., Fan, S., Rahman, M. Z., Guo, S., & Chen, F. (2022). Structural and mechanical properties of bamboo fiber bundle and fiber/bundle reinforced composites: a review. *Journal of Materials Research and Technology*, *19*, 1162–1190. https://doi.org/10.1016/j.jmrt.2022.05.077

Gaylard, P. C. (2011). *Statistical modelling of the shrinkage behaviour of South African concretes*.

Geremew, A., De Winne, P., Demissie, T. A., & De Backer, H. (2024). Surface modification of bamboo fibers through alkaline treatment: Morphological and physical characterization for composite reinforcement. *Journal of Engineered Fibers and Fabrics* , *19*. https://doi.org/10.1177/15589250241248764

Geremew, A., Outtier, A., De Winne, P., Demissie, T. A., & De Backer, H. (2025). An

Experimental Investigation on the Effect of Incorporating Natural Fibers on the Mechanical and Durability Properties of Concrete by Using Treated Hybrid Fiber-Reinforced Concrete Application. *Fibers*, *13*(3). https://doi.org/10.3390/fib13030026

Ghanem, H., Ramadan, R., Khatib, J., & Elkordi, A. (2024). A Review on Chemical and Autogenous Shrinkage of Cementitious Systems. *Materials*, *17*(2). https://doi.org/10.3390/ma17020283

Ghavami, K. (2005). Bamboo as reinforcement in structural concrete elements. *Cement and Concrete Composites*, *27*(6), 637–649. https://doi.org/10.1016/j.cemconcomp.2004.06.002

Gholami, M., Moghadas Nejad, F., & Ramezanianpour, A. M. (2024). Increasing the Length of Concrete Pavement Slabs Using Shrinkage Reducing Admixture and Polypropylene Fiber. *International Journal of Concrete Structures and Materials*, *18*(1). https://doi.org/10.1186/s40069-023-00647-8

Ghori, W., Saba, N., Jawaid, M., & Asim, M. (2018). A review on date palm (phoenix dactylifera) fibers and its polymer composites. *IOP Conference Series: Materials Science and Engineering*, *368*(1), 0–17. https://doi.org/10.1088/1757-899X/368/1/012009

Golewski, G. L. (2023). Mechanical properties and brittleness of concrete made by combined fly ash, silica fume and nanosilica with ordinary Portland cement. *AIMS Materials Science*, *10*(3), 390–404. https://doi.org/10.3934/matersci.2023021

Gong, C., Kang, L., Zhou, W., Liu, L., & Lei, M. (2023). Tensile Performance Test Research of Hybrid Steel Fiber—Reinforced Self-Compacting Concrete. *Materials*, *16*(3). https://doi.org/10.3390/ma16031114

Gong, J., & Qu, Z. (2020). *Mechanical Properties and Drying Shrinkage Investigation of Alkali-Activated Mortar Using Waste Glass Powder*. *2020*.

Gribniak, V., Kaklauskas, G., & Bacinskas, D. (2010). *Shrinkage in reinforced concrete structures : A computational aspect*. *3730*. https://doi.org/10.3846/1392-3730.2008.14.49-60

Group, B. T. S. (2024). *Bamboo and SDGs*. https://www.bambooinfo.in/more/bamboo-sustainable-development-goals.asp

Gupta, Anu and Kumar, A. (2008). Potential of Bamboo in Sustainable Dveleopmnet. *Asia Pacific Business Review*, *IV*(3).

Gupta, A., & Kumar, A. (2008). Potential of Bamboo in Sustainable Development. *Asia Pacific Business Review*, *4*(3), 100–107. https://doi.org/10.1177/097324700800400312

Guyer, J. P., Asce, F., & Aei, F. (2009). *An Introduction to Rigid Pavement Design* (Issue 877).

Hailu, A., & Gitima, G. (2023). *Bamboo forest in Ethiopia : roles , constraints and management strategies : review article The Roles of Bamboo Forest in Ethiopia*. *11*(1), 49–60.

HansFriederich. (2021). *Bamboo for sustainable development*. https://www.hansfriederich.com/2021/02/21/bamboo-for-sustainable-development/

Hashemifard, H., Mehranzadeh, M., & Chenari, M. (2012). Preparation of shaped concrete article having complicated surface shape. *Crystals*, *6*(1), 368–375.

Hashim, M. Y., Amin, A. M., Marwah, O. M. F., Othman, M. H., Yunus, M. R. M., & Chuan Huat, N. (2017). The effect of alkali treatment under various conditions on physical properties of kenaf fiber. *Journal of Physics: Conference Series*, *914*(1), 0–15. https://doi.org/10.1088/1742-6596/914/1/012030

Hebel, D. E., Heisel, F., Alireza, J., Wielopolski, M., & Schlesier, K. (2015). Constructing Bamboo - Introducing an alternative for the construction industry. *Constructing Alternatives*, *August 2016*, 10–21. https://doi.org/10.3929/ethz-a-010636880

Hill, C.A.S. and Abdul Khalil, H. P. S. (2000). Effect of fiber treatments on mechanical properties of Grewia serrulata bast fiber reinforced polyester composites. *Journal of Applied Polymer Science*, 1685–1697. https://doi.org/10.1016/j.matpr.2017.11.064

Holt, E. E. (2001). *Early age autogenous shrinkage of concrete*.

Hong, X., Lee, J. C., Ng, J. L., Abdulkareem, M., Yusof, Z. M., Li, Q., & He, Q. (2023). Prediction Model and Mechanism for Drying Shrinkage of High-Strength Lightweight Concrete with Graphene Oxide. *Nanomaterials*, *13*(8). https://doi.org/10.3390/nano13081405

Hu, S. X., Luo, M., Cong, L., & Lin, M. (2019). A Method to Improve the Concrete Shrinkage Prediction Based on Short-Time Tests. *IOP Conference Series: Earth and Environmental Science*, *295*(4). https://doi.org/10.1088/1755-1315/295/4/042034

Hu, Y., Huang, H., Chen, M., Pan, C., Alamerew, A. N., & Zhang, J. (2025). *Life Cycle Carbon Footprint Assessment of a Typical Bamboo-Based Fiber Composite Material*. 1–17.

Huang, Y. H. . (2004). *Pavement Analysis and Design* (second edi). Pearson Prentice Hall.

Hussain, I., Ali, B., Akhtar, T., Jameel, M. S., & Raza, S. S. (2020). Comparison of mechanical properties of concrete and design thickness of pavement with different types of fiber-reinforcements (steel, glass, and polypropylene). In *Case Studies in Construction Materials* (Vol. 13). https://doi.org/10.1016/j.cscm.2020.e00429

Ichihara, H. T. and Y. (2004). *Effect of Fiber Length on Mechanical Properties of "Green" Composites Using a Starch-Based Resin and Short Bamboo Fibers*.

Import, B. (2023). *The mechanical properties of bamboo*. https://bambooimport.com/en/pages/the-mechanical-properties-of-bamboo#:~:text=Each of these bamboo species has different,species of bamboo can also vary greatly

Intertec, B. (2024). *Addressing concrete shrinkage in specifications*. ttps://braunintertec.com/insights/addressing-concrete-shrinkage-in-specifications/

Iowa state wide urban design and specification. (2019). *Road way design*.

Ismail, Z. Z., & AL-Hashmi, E. A. (2008). Use of waste plastic in concrete mixture as aggregate replacement. *Waste Management*, *28*(11), 2041–2047. https://doi.org/10.1016/j.wasman.2007.08.023

J.A. Ochsendorf. (2005a). Sustainable Engineering: The Future of Structural Design. *Structures Congress 2005: Metropolis and Beyond*, *617*, 1–9.

https://ascelibrary.org/doi/pdf/10.1061/40753%28171%29146?download=true

J.A. Ochsendorf. (2005b). Sustainable Engineering: The Future of Structural Design. *Rom J Morphol Embryol*, *46(2),*(Neurofibroma, schwannoma or a hybrid tumor of the peripheral nerve sheath), 113-116.

Jacinta Dsilva, Saniya Zarmukhambetova, J. L. (2023). Problem of statement Assessment of building materials in the construction sector: A case study using life cycle assessment approach to achieve the circular economy. *Heliyon*.

Jamaludin, M. Y., Ogunbode, E. B., Ishak, M. Y., Abeku, D. M., & Razavi, M. (2019). Long Term Behaviour of Fibrous Concrete Composite (FCC): A Conspectus. *Journal of Advanced Research in Applied Mechanics*, *58*(1), 11–22.

James K. Wight, J. G. M. (2012). *Reinforced Concrete: Mechanics and Design*. Prentice Hall.

Jawaid, M., & Abdul Khalil, H. P. S. (2011). Cellulosic/synthetic fibre reinforced polymer hybrid composites: A review. *Carbohydrate Polymers*, *86*(1), 1–18. https://doi.org/10.1016/j.carbpol.2011.04.043

JI, A. M. and O. (2018). Bamboo, its chemical modification and products. In *Bamboo - current and future prospects* (pp. 109–127).

Jing, L., Jiang, Y., Li, L., & Zhang, T. (2023). Influence of Alkali Treatment on Microstructure Transformation and Mechanical Properties of Palm-Fiber Cell Wall. *Journal of Natural Fibers*, *20*(2). https://doi.org/10.1080/15440478.2023.2237681

Jones, D., Ormondroyd, G. O., Curling, S. F., Popescu, C. M., & Popescu, M. C. (2010). Chemical compositions of natural fibres. In *Advanced High Strength Natural Fibre Composites in Construction*. https://doi.org/10.1016/B978-0-08-100411-1.00002-9

Jun, Lu., Jiaping, Liu., X., Fan., Hesong, Jin., Ji-Hua, Zhu., Zhenyu, Huang., Feng, Xing., Tongbo, S. (2022). Investigation on water sorptivity and micro properties of concrete: Effect of supplementary cementitious materials, seawater, sea-sand and water-binder ratio. *Journal of Building Engineering*, *50*(104153). doi: 10.1016/j.jobe.2022.104153

Karthik, A., Bhuvaneshwaran, M., Senthil Kumar, M. S., Palanisamy, S., Palaniappan, M., & Ayrilmis, N. (2024). A Review on Surface Modification of Plant Fibers for Enhancing Properties of Biocomposites. *ChemistrySelect*, *9*(21). https://doi.org/10.1002/slct.202400650

Kassahun, T., & Dawuro, T. (2014). Review of Bamboo Value Chain in Ethiopia. *Journal of Biology, Agriculture and Healthcare*, *4*(27), 179–191.

Kaur, N., Saxena, S., Gaur, H., & Goyal, P. (2017). A Review on Bamboo Fiber Composites and its Applications. *International Conference on Infocom Technologies and Unmanned Systems*.

Kaur, V., Chattopadhyay, D. P., & Kaur, S. (2013). Study on Extraction of Bamboo Fibres from Raw Bamboo Fibres Bundles Using Different Retting Techniques. *Textiles and Light Industrial Science and Technology*, *2*(4), 174–179. www.tlist-journal.org

Kavitha, S. (2018). Effectiveness of Bamboo Fiber as a Strength Enhancer in Concrete. *International Journal of Earth Sciences and Engineering*, *9*(June 2016), 3–8.

Kavitha, S., & Felix Kala, T. (2016). Effect of bamboo fibers in fresh and hardened properties of self compacting concrete. *Indian Journal of Science and Technology*, *9*(31). https://doi.org/10.17485/ijst/2016/v9i31/95347

Kavitha, S., & Kala, T. F. (2016). Effectiveness of bamboo fiber as an strength enhancer in concrete. *International Journal of Earth Science and Engineering*, *9*(June 2016), 1–6.

Kaw, A. K. (2005). *Mechanics of Composite Materials* (Second edi). CRC Press. https://doi.org/https://doi.org/10.1201/9781420058291

Khairallah., R. S. (2019). *Analysis of Autogenous and Drying Shrinkage of Concrete*.

Khan, F., Hossain, N., Hasan, F., Rahman, S. M. M., Khan, S., Saifullah, A. Z. A., & Chowdhury, M. A. (2024). Advances of natural fiber composites in diverse engineering applications—A review. *Applications in Engineering Science*, *18*(May), 100184. https://doi.org/10.1016/j.apples.2024.100184

Khan, I. K. (2014). *PERFORMANCE OF BAMBOO REINFORCED CONCRETE BEAM*. *3*(3), 836–840.

Khan, R. A. (2023). An Overview on Physio-Mechanical Properties and Applications of Synthetic Fibers. *Modern Concepts in Material Science*, *5*(3), 1–17. https://doi.org/10.33552/mcms.2023.05.000612

Khusairy, M., Bakri, B., & Jayamani, E. (2016). Comparative Study Of Functional Groups In Natural Fibers : Fourier Transform Infrared Analysis (FTIR). *International Conference on Futuristic Trends in Engineering, Science, Humanities, and Technology*, *January*.

King, C. (2019). Bamboo: the forgotten circular economy solution. *INBAR*. https://www.foreststreesagroforestry.org/wp-content/uploads/2021/08/FTA-01-Kunming-Poster_King.pdf

Kitissou, M. (2004). Hydropolitics and Geopolitics: Transforming Conflict and Reshaping Cooperation in Africa{\textbackslash}r. *Africa Notes*, *December*, 1–18.

Koichi Minami and Masakazu Terai. (1999). Basic Study on Mechanical Properties of Bamboo Fiber Reinforced Concrete. *International Association for Bridge and Structural Engineering*. https://www.researchgate.net/publication/263496840_Basic_Study_on_Mechanical_Properties_of_Bamboo_Fiber_Reinforced_Concrete

krishna, K. V., & Rao, J. V. (2014). Experimental study on behavior of fiber reinforced concrete for rigid pavements. *IOSR Journal of Mechanical and Civil Engineering*, *11*(4), 49–53. https://doi.org/10.9790/1684-11474953

Kudva, A., Mahesha, G. T., & Pai, D. (2024). Influence of Chemical Treatment on the Physical and Mechanical Properties of Bamboo Fibers as Potential Reinforcement for Polymer Composites. *Journal of Natural Fibers*, *21*(1). https://doi.org/10.1080/15440478.2024.2332698

Kulkarni, Y. U., Awati, M. M., & Khadiranaikar, R. B. (2023). Methods for Assessment of Early Age Shrinkage Cracks in Higher Strength Concrete : A Review. *International Journal of Engineering Research in Mechanical and Civil Engineering (IJERMCE)*, *10*(4), 20–25.

Kumar, S., Choudhary, V., & Kumar, R. (2010). Study on the compatibility of unbleached and bleached bamboo-fiber with LLDPE matrix. *Journal of Thermal Analysis and Calorimetry*, *102*(2), 751–761. https://doi.org/10.1007/s10973-010-0799-4

Kurpińska, M., Mazur, M. P., Gu, Y., & Kurpiński, F. (2022). The impact of natural fibers ' characteristics on mechanical properties of the cement composites. *Scientific Reports*, 1–14. https://doi.org/10.1038/s41598-022-25085-6

Li, Z. (2017). Predicting the drying shrinkage behavior of high strength portland cement mortar under the combined influence of fine aggregate and steel micro fiber. *Materiales de Construccion*, *67*(326). https://doi.org/10.3989/mc.2017.05916

Liese, W. (1985). *Anatomy and Properties of Bamboo*.

Liu, M., Fernando, D., Daniel, G., Madsen, B., Meyer, A. S., Ale, M. T., & Thygesen, A. (2015). Effect of harvest time and field retting duration on the chemical composition, morphology and mechanical properties of hemp fibers. *Industrial Crops and Products*, *69*, 29–39. https://doi.org/10.1016/j.indcrop.2015.02.010

Loganathan, T. M., Thariq, M., Sultan, H., Ahsan, Q., Jawaid, M., Naveen, J., Shah, A. U., & Hua, L. S. (2020). Characterization of alkali treated new cellulosic fibre from Cyrtostachys renda. *Journal of Materials Research and Technology*, *February*. https://doi.org/10.1016/j.jmrt.2020.01.091

Luo, Y., Yussof, M. M., Jiang, Y., Peng, Z., Wu, C., Shi, F., & Chen, Y. (2024). Experimental Study of the Chloride-Ion Permeability of Bamboo-Fiber-Reinforced Concrete. *Materiali in Tehnologije*, *58*(2), 239–248. https://doi.org/10.17222/mit.2023.1049

Lv, C., Shen, H., Liu, J., Wu, D., Qu, E., & Liu, S. (2022). Properties of 3D Printing Fiber-Reinforced Geopolymers Based on Interlayer Bonding and Anisotropy. *Materials*, *15*(22), 1–23. https://doi.org/10.3390/ma15228032

Madhavi, K., Devi, M. V. R., & Jagadish, K. S. (2017). Split Tensile Strength of Brick Masonry. *International Journal of Civil Engineering*, *6*(6), 1–8.

Maghfouri, M., Shafigh, P., Alimohammadi, V., Doroudi, Y., & Aslam, M. (2020). Appropriate drying shrinkage prediction models for lightweight concrete containing coarse agro-waste aggregate. *Journal of Building Engineering*, *29*(December 2019), 101148. https://doi.org/10.1016/j.jobe.2019.101148

Mahesh, S. M., & Kavitha, S. (2016). *EVALUATION OF ASPECT RATIO (l / d) OF BAMBOO FIBRE AS A REINFORCEMENT MATERIAL IN CONCRETE*. 2319–2322.

Mahfuzur Rahman, M., Saifullah, I., & Kumar Ghosh, S. (2019). Detection and Measurements of Cracks in Axially Loaded Tension RC Members by Image Processing Technique. *American Journal of Civil Engineering and Architecture*, *7*(2), 115–120. https://doi.org/10.12691/ajcea-7-2-5

Martijanti, M., Juwono, A. L., & Sutarno, S. (2020). Investigation of characteristics of bamboo fiber for composite structures. *IOP Conference Series: Materials Science and Engineering*, *850*(1). https://doi.org/10.1088/1757-899X/850/1/012028

Matalkah, F., Jaradat, Y., & Soroushian, P. (2019). Plastic shrinkage cracking and bleeding of concrete prepared with alkali activated cement. *Heliyon*, *5*(4), e01514. https://doi.org/10.1016/j.heliyon.2019.e01514

Matykiewicz, D., Barczewski, M., Mysiukiewicz, O., & Skórczewska, K. (2019). Comparison of Various Chemical Treatments Efficiency in Relation to the Properties of Flax, Hemp Fibers and Cotton trichomes. *Journal of Natural Fibers*, *18*(5), 735–751. https://doi.org/https://doi.org/10.1080/15440478.2019.1645792

Mechanics, A. (2019). *Long Term Behaviour of Fibrous Concrete Composite (FCC): A Conspectus*. *1*(1), 11–22.

Mekonnen, Z., Worku, A., Yohannes, T., Alebachew, M., Teketay, D., & Kassa, H. (2014). Bamboo Resources in Ethiopia : Their value chain and contribution to livelihoods. *Ethnobotany Research & Applications*, *12*(November), 511–524.

Meyers, B. L., Branson, D. E., Schumann, C. G., & Christiason, M. L. (1970). The Prediction of Creep and Shrinkage Properties of Concrete. *Iowa Highway Commission Final Report*, *70*(5), 1–140.

Miur, C. E. (2013). *Department of Civil Engineering PhD Thesis in Materials and Structures Engineering of NATURAL FIBER-REINFORCED*.

Mohajerani, A., Hui, S. Q., Mirzababaei, M., Arulrajah, A., Horpibulsuk, S., Kadir, A. A., Rahman, M. T., & Maghool, F. (2019). Amazing types, properties, and applications of fibres in construction materials. *Materials*, *12*(16), 1–45. https://doi.org/10.3390/ma12162513

Montgomery, D. C. and Runger, G. C. (2003). *Applied Statistics and Probability for Engineers* (Third Edit). John Wiley & Sons, Inc.

Muhammad Nasir Amin, Ahmad, W., Khan, K., & Ahmad, A. (2022). A Comprehensive Review of Types, Properties, Treatment Methods and Application of Plant Fibers in Construction and Building Materials. *Materials*, *2*(1), 1–31.

Mukhopadhyay, S., & Khatana, S. (2015). A review on the use of fibers in reinforced cementitious concrete. *Journal of Industrial Textiles*, *45*(2), 239–264. https://doi.org/10.1177/1528083714529806

Mulatu, Y., Alemayehu, A., & Tadesse, Z. (2016a). Bamboo Species Introduction in Ethiopia. In *Ethiopian Environment and Forest Research Institute*.

Mulatu, Y., Alemayehu, A., & Tadesse, Z. (2016b). *Biology and Management of Indigenous Bamboo Species of Ethiopia; Based on Research and Practical Field Experience*. Ethiopian Environment and Forest Research Institute.

Mulay, S. (2017). Experimental Investigation of Sugarcane Bagasse Ash Concrete Under Sodium Hydroxide Solution. *American Journal of Civil Engineering*, *5*(1), 1. https://doi.org/10.11648/j.ajce.20170501.11

Muthuselvan Balasubramanian, R. Saravanan, S. T. (2024). Exploring natural plant fiber choices and treatment methods for contemporary composites: A comprehensive review. *Results in Engineering*, *24*.

Mwaikambo, L. Y. (2009). Tensile properties of alkalised jute fibres. *BioResources*, *4*(2), 566–588. https://doi.org/10.15376/biores.4.2.566-588

Naaman, A. E. (2018). Fiber reinforced concrete: five decades of progress. *Brazilian Conference on Composite Materials*, 35–56. https://doi.org/10.21452/bccm4.2018.02.01

Nabi Saheb, D., & Jog, J. P. (1999). Natural fiber polymer composites: A review. *Advances in Polymer Technology*, *18*(4), 351–363. https://doi.org/10.1002/(SICI)1098-2329(199924)18:4<351::AID-ADV6>3.0.CO;2-X

Naik, T. R. (2008). Sustainability of Concrete Construction. *Practice Periodical on Structural Design and Construction*, *13*(2), 98–103. https://doi.org/10.1061/(asce)1084-0680(2008)13:2(98)

Nambiar, R. A., & Haridharan, M. K. (2019). Mechanical and durability study of high performance concrete with addition of natural fiber (jute). *Materials Today: Proceedings*, *46*(xxxx), 4941–4947. https://doi.org/10.1016/j.matpr.2020.10.339

Neville, A. M. (2002). *Properties of Concrete* (Fourth). Pearson.

Ningrum, D., Soehardjono, A., Suseno, H., & Wibowo, A. (2024). Identifying the Influence of Split Tensile Strength To Crack Width of Highstrength Reinforced Concrete Beam With Polypropylene Fiber From Medical Mask Waste. *Eastern-European Journal of Enterprise Technologies*, *1*(7(127)), 14–21. https://doi.org/10.15587/1729-4061.2024.298842

Nwankwo, C., Mahachi, J., Olukanni, D., & Musonda, I. (2025). Alkali treatment of flax fibres : effects on tensile strength , thermal performance , and moisture absorption. *Composite Interfaces*, *32*(9), 1329–1346. https://doi.org/10.1080/09276440.2025.2467700

Okeola, A. A., Abuodha, S. O., & Mwero, J. (2018a). Experimental investigation of the physical and mechanical properties of sisal fiber-reinforced concrete. *Fibers*, *6*(3). https://doi.org/10.3390/fib6030053

Okeola, A. A., Abuodha, S. O., & Mwero, J. (2018b). The Effect of Specimen Shape on the Mechanical Properties of Sisal Fiber-Reinforced Concrete. *The Open Civil Engineering Journal*, *12*(1), 368–382. https://doi.org/10.2174/1874149501812010368

Osmi, S. K. C., Husen, H., Othman, M., Nor, N. M., Sojipto, S., & Termizi, M. A. H. M. (2024). Performance of Bamboo Fibre on Modifying Mechanical Properties of Concrete. *The Open Civil Engineering Journal*, *18*(1), 1–9. https://doi.org/10.2174/0118741495288340240312050220

Osorio, L., Trujillo, E., Lens, F., Ivens, J., Verpoest, I., & Van Vuure, A. W. (2018). In-depth study of the microstructure of bamboo fibres and their relation to the mechanical properties. *Journal of Reinforced Plastics and Composites*, *37*(17), 1099–1113. https://doi.org/10.1177/0731684418783055

Osorio, L., Trujillo, E., Van Vuure, A. W., & Verpoest, I. (2011). Morphological aspects and mechanical properties of single bamboo fibers and flexural characterization of bamboo/epoxy composites. *Journal of Reinforced Plastics and Composites*, *30*(5), 396–408. https://doi.org/10.1177/0731684410397683

Ovat, F. A., Obot, O. W., Fakorede, D. O., & Markson, I. . E. (2015). Determination of Density of Nigerian bamboo fiber as an Engineering property using maceration method. *International Journal of Scientific & Engineering Research*, *6*(9), 1811–1822. http://www.ijser.org

Pease, B. J. (2010). Influence of concrete cracking on the corrosion of steel reinforcement. In *PhD Thesis* (Vol. 1). https://doi.org/10.1201/b10552-46

Peng, M., Gao, Y., Ding, N., Xu, Q., Lu, J., Liu, C., Yuan, W., Fan, T., & Chen, X. (2024). Case Studies in Construction Materials Experimental study on the mechanical properties of waste steel fiber reinforced rubber concrete. *Case Studies in Construction Materials*, *21*(November), e04003. https://doi.org/10.1016/j.cscm.2024.e04003

Phong, N. T., Fujii, T., Chuong, B., Viet, D. C., & Okubo, K. (2012). Study on How to Effectively Extract Bamboo Fibers from Raw Bamboo and Wastewater Treatment. *Journal of Materials Science Research*, *1*(1), 144–155. https://doi.org/10.5539/jmsr.v1n1p144

Pramudi, G., Raharjo, W. W., Ariawan, D., Ubaidillah, & Arifin, Z. (2021). Utilization of Bamboo Fiber in the Development of Environmentally Friendly Composite – A Review. *IOP Conference Series: Materials Science and Engineering*, *1096*(1), 012038. https://doi.org/10.1088/1757-899x/1096/1/012038

Preethikaharshini, J., Naresh, K., Rajeshkumar, G., Arumugaprabu, V., Khan, M. A., & Khan, K. A. (2022). Review of advanced techniques for manufacturing biocomposites: non-destructive evaluation and artificial intelligence-assisted modeling. *Journal of Materials Science*, *57*(34), 16091–16146. https://doi.org/10.1007/s10853-022-07558-1

Pulecio-Díaz, J., Sol-Sánchez, M., & Moreno-Navarro, F. (2024). Effects of Relative Humidity and Temperature on the Drying Shrinkage of Roller-Compacted Concrete Pavements. *Infrastructures*, *9*(2). https://doi.org/10.3390/infrastructures9020022

Radhakrishnan, S. (2014). *Roadmap to Sustainable Textiles and Clothing* (Issue October 2019). https://doi.org/10.1007/978-981-287-065-0

Rafi, M. M., & Nasir, M. M. (2016). Models for prediction of 28-day concrete compressive strength. *Journal of Testing and Evaluation*, *44*(3), 1217–1228. https://doi.org/10.1520/JTE20140139

Raghunathan, V., Ayyappan, V., Dhilip, J. D. J., Sundarrajan, D., Rangappa, S. M., & Siengchin, S. (2023). Influence of alkali-treated and raw Zanthoxylum acanthopodium fibers on the mechanical, water resistance, and morphological behavior of polymeric composites for lightweight applications. *Biomass Conversion and Biorefinery*. https://doi.org/https://doi.org/10.1007/s13399-023-04240-7

Ramesh, M., Palanikumar, K., & Reddy, K. H. (2017). Plant fibre based bio-composites: Sustainable and renewable green materials. *Renewable and Sustainable Energy Reviews*, *79*(May), 558–584. https://doi.org/10.1016/j.rser.2017.05.094

Ramprasad, C., Kushwaha, P. K., & Vidyashankar, S. (2018). Optimization and Extraction of Natural Long Bamboo. *International Journal of Latest Technology in Engineering, Management & Applied Science*, *VII*(I), 85–88.

Rao, P., Doddi, V., Chanamala, R., & Dora, S. P. (2018). Effect of Alkali treatments on physical and Mechanical strength of Pineapple leaf fibres Effect of Alkali treatments on physical and Mechanical strength of Pineapple leaf fibres. *Materials Science and Engineering*. https://doi.org/10.1088/1757-899X/290/1/012030

Rauf, A., Attoye, D. E., & Crawford, R. H. (2024). Evaluating the impact of material service life on embodied energy of residential villas in the United Arab Emirates. *Engineering, Construction and Architectural Management*, *31*(13), 244–270. https://doi.org/10.1108/ECAM-05-2023-0514

Rawatan, P., & Buluh, S. F. S. (2018). Influence of Alkali Treatment on Physico-Chemical Properties of Malaysian Bamboo Fiber: a Preliminary Study. *Malaysian Journal of Analytical Science*, *22*(1), 143–150. https://doi.org/10.17576/mjas-2018-2201-18

Reinhardt, H. W. (2013). Factors affecting the tensile properties of concrete. In *Understanding the Tensile Properties of Concrete*. Woodhead Publishing Limited. https://doi.org/10.1533/9780857097538.1.19

Reta, T. (2017). *Study on Mechanical Properties of Bamboo Fiber Reinforced Concrete*. ADDIS ABABA INSTITUTE OF TECHNOLOGY.

Rocky, B. P., & Thompson, A. J. (2018). Production of natural bamboo fibers-1: experimental approaches to different processes and analyses. *Journal of the Textile Institute*, *109*(10), 1381–1391. https://doi.org/10.1080/00405000.2018.1482639

Rota Font, F., Ciriano Nogales, Y., Temes Mendoza, D., Vallbé Mumbrú, M., Barbeta Solà, G., & De Felipe Blanch, J. J. (2024). Thermal Performance of a Straw Bale Building in Relation to Fiber Orientation: A Case Study. *Sustainability (Switzerland)*, *16*(23), 1–15. https://doi.org/10.3390/su162310304

Rusch, F. (2019). *Morphology , density and dimensions of bamboo fi bers : a bibliographical compilation Morfologia , densidade e dimensões de fi bras de bambu : uma compilação bibliográ fi ca*. *49*, 1–9.

S.K. Paudel. (2008). *Engineered bamboo as a building material*.

Safiuddin, M., Kaish, A. B. M. A., Woon, C. O., & Raman, S. N. (2018). Early-age cracking in concrete: Causes, consequences, remedialmeasures, and recommendations. *Applied Sciences (Switzerland)*, *8*(10). https://doi.org/10.3390/app8101730

Safwan, A., Jawaid, M., Sultan, M. T. H., & Hassan, A. (2018). Preliminary Study on Tensile and Impact Properties of Kenaf/Bamboo Fiber Reinforced Epoxy Composites. *Journal of Renewable Materials*, *6*(5). https://doi.org/10.7569/jrm.2018.634103

Sajjala Kavitha and Ashwini D G. (2022). Experimental Investigations on Durability Characteristics of Bamboo Fiber Reinforced Self-Compacting Concrete with GGBS and Alccofine. *ECS Transactions*, *107*(1), 7661–7670.

Sakata, K. (1996). *Prediction of Creep and Shrinkage of Concrete*. Japan Society of Civil Engineer.

Sakata K., T. T. et al. (2001). Prediction equation for creep and drying shrinkage in concrete of wide range strength. *JSCE*.

Sakata, K., & Shimomura, T. (2004). Recent Progress in Research on and Code Evaluation of Concrete Creep and Shrinkage in Japan. *Journal of Advanced Concrete Technology*, *2*(2), 133–140.

Saliba, J., Rozière, E., Grondin, F., & Loukili, A. (2011). Influence of shrinkage-reducing admixtures on plastic and long-term shrinkage. *Cement and Concrete Composites*, *33*(2), 209–217. https://doi.org/10.1016/j.cemconcomp.2010.10.006

Salih, A. A., Zulkifli, R., & Azhari, C. H. (2020). Tensile properties and microstructure of single-cellulosic bamboo fiber strips after Alkali treatment. *Fibers*, *8*(5), 1–10. https://doi.org/10.3390/FIB8050026

Salih, M. A., Aldikheeli, M. R., & Shaalan, K. A. (2020). Evaluation of factors influencing the compressive strength of Portland cement statistically. *IOP Conference Series: Materials Science and Engineering*, *737*(1). https://doi.org/10.1088/1757-899X/737/1/012059

Sanjay, M. R., Arpitha, G. R., Naik, L. L., Gopalakrishna, K., & Yogesha, B. (2016). Applications of Natural Fibers and Its Composites: An Overview. *Natural Resources*, *07*(03), 108–114. https://doi.org/10.4236/nr.2016.73011

Sapuan, S. M., Harussani, M. M., & Syafri, E. (2022). A short review of recent engineering applications of natural fibres. *IOP Conference Series: Earth and Environmental Science*, *1097*(1). https://doi.org/10.1088/1755-1315/1097/1/012033

Sayed, U., Li, H., Dauletbek, A., Ali, M., Yang, D., Lorenzo, R., Ashraf, M., Feng, Z., Wang, Z., & Xue, X. (2023). Bamboo stick diameter, volume and aspect ratios effect on the compressive behavior of bamboo sticks reinforced concrete mixed with sea sand and seawater. *Construction and Building Materials*, *369*, 1–30. https://doi.org/10.1016/j.conbuildmat.2023.130437

Sebrala, H. (2021). The Potential of Bamboo for Climate Change Mitigation in Ethiopia. *International Bamboo and Rattan Organisation*, *November*.

Sekar, A. (2019). *Study on Durability Properties of Coconut Shell Concrete with Coconut Fiber*.

Seltman, H. J. (2018). Experimental Design and Analysis. In *Carnegie Mellon University*. https://doi.org/10.1201/b18362-13

Senthilkumar, K., Saba, N., Rajini, N., Chandrasekar, M., Jawaid, M., Siengchin, S., & Alotman, O. Y. (2018). Mechanical properties evaluation of sisal fibre reinforced polymer composites: A review. *Construction and Building Materials*, *174*, 713–729. https://doi.org/10.1016/j.conbuildmat.2018.04.143

Seyam, A. M., & Nemes, R. (2023). Age influence on compressive strength for concrete made with different types of aggregates after exposed to high temperatures. *Materials Today: Proceedings*, *xxxx*. https://doi.org/10.1016/j.matpr.2023.06.403

Shah, A. U. M., Sultan, M. T. H., Jawaid, M., Cardona, F., & Talib, A. R. A. (2016). A Review on the Tensile Properties of Bamboo Fiber Reinforced Polymer Composites. *BioResources*, *11*(4), 10654–10676. https://doi.org/10.15376/BIORES.11.4.10654-10676

Shao, S., Jin, Z., Wen, G., & Iiyama, K. (2009). Thermo characteristics of steam-exploded bamboo (Phyllostachys pubescens) lignin. *Wood Science and Technology*, *43*(7–8), 643–652. https://doi.org/10.1007/s00226-009-0252-7

Shengwen Tang, Desheng Huang, Z. H. (2021). A review of autogenous shrinkage models of concrete. *Journal of Building Engineering*. https://doi.org/https://doi.org/10.1016/j.jobe.2021.103412

Shiyu, Zhuang., Qian, W. (2022). Water absorption behaviour of concrete: Novel experimental findings and model characterization. *Journal of Building Engineering*, *53*(104602). doi: 10.1016/j.jobe.2022.104602

Shurbert-Hetzel, C., Daneshvar, D., Robisson, A., & Shafei, B. (2023). Data-enabled comparison of six prediction models for concrete shrinkage and creep. *Case Studies in Construction Materials*, *19*(July), e02406. https://doi.org/10.1016/j.cscm.2023.e02406

Siddique, R., & Mehta, A. (2014). Effect of carbon nanotubes on properties of cement mortars. *Construction and Building Materials*, *50*, 116–129. https://doi.org/https://doi.org/10.1016/j.conbuildmat.2013.09.019

Singh, B., & Dessalegn, Y. (2021). *Effect Analysis of Extraction Processes of Bamboo Fiber*. *8*(5), 4226–4246.

Singh, H. (2022). *Steel Fiber Reinforced Concrete*.

Soto Izquierdo, I., Soto Izquierdo, O., Ramalho, M. A., & Taliercio, A. (2017). Sisal fiber reinforced hollow concrete blocks for structural applications: Testing and modeling. *Construction and Building Materials*, *151*, 98–112. https://doi.org/10.1016/j.conbuildmat.2017.06.072

Standard, E. (2004). *En 1992-1-1*.

STEGMAIER, T., MAVELY, J., & SCHNEIDER, P. (2005). High-performance and high-functional fibres and textiles. *Textiles in Sport*, 89–119. https://doi.org/https://doi.org/10.1533/9781845690885.2.89

Subash. S, Stanly Jones Retnam. B, E. R. D. J. (2017). A Review on Extraction of Bamboo Fibres and Its Properties. *International Journal of Advanced Chemical Science and Applications*, *5*(2).

Sun, G., Xue, S., Qu, X., & Zhao, Y. (2019). Experimental investigation of creep and shrinkage of reinforced concrete with influence of reinforcement ratio. *Advances in Concrete Construction*, *7*(4), 211–218. https://doi.org/10.12989/acc.2019.7.4.211

Suryakanta. (2015). *WHAT ARE THE PROPERTIES OF FRESH CONCRETE?* https://civilblog.org/2015/04/09/what-are-the-properties-of-fresh-concrete/

Suwinarti, W., Yuliansyah, Wulandari, N. T., & Haqiqi, M. T. (2023). Potential of natural fiber based on plant characteristics. *IOP Conference Series: Earth and Environmental Science*, *1282*(1). https://doi.org/10.1088/1755-1315/1282/1/012036

Tadesse, A. K. (2019). Experimental Study on Mechanical Properties of Teff Straw as a Fiber in Reinforced Concrete. *Globals Scientific Journal*, *7*(10), 123–139.

Taher, M. N. M., Aman, M. Y., Ayob, M. A. M., Mokhatar, S. N., & Bujang, H. (2024). Mechanical Properties of Rigid Pavements Incorporating Different Percentage of Steel Fiber. *Journal of Advanced Research in Applied Mechanics*, *113*(1), 152–161. https://doi.org/10.37934/aram.113.1.152161

Talaat, A., Emad, A., Tarek, A., Masbouba, M., Essam, A., & Kohail, M. (2021). Factors affecting the results of concrete compression testing: A review. *Ain Shams Engineering Journal*, *12*(1), 205–221. https://doi.org/10.1016/j.asej.2020.07.015

Tayeh, B. A., Hadzima-Nyarko, M., Zeyad, A. M., & Al-Harazin, S. Z. (2021). Properties and durability of concrete with olive waste ash as a partial cement replacement. *Advances in Concrete Construction*, *11*(1), 59–71. https://doi.org/10.12989/acc.2021.11.1.059

Tejashwini, G., & R, K. S. K. (2024). Influence of Treated and Untreated Bamboo Fiberson Properties of Concrete. *Journal of Computational Analysis and Application*, *33*(5), 89–98.

Terai, M. (1999). Basic Study on Mechanical Properties of Bamboo Fiber Reinforced Concrete. *International Association for Bridge and Structural Engineering*.

Terai, M., & Minami, K. (2012). Research and Development on Bamboo Reinforced Concrete Structure. *World Conferences on Earthquake Engineering*, *15*(3), 1–10.

Teranishi, K. (2010). *Prediction equation of drying shrinkage of concrete*.

Tesfay, A., & Negusse, R. (2024). Adaptation of Different Bamboo Species in Central Zone of Tigray ,. *Journal of Global Agriculture and Ecology*, *16*(4), 43–49.

Thang, T., Yanxia, L., Jayaraman, D., Muralidharan, E., & Vidya, S. (2022). *Global Priority Species of Economically Important Bamboo* (Vol. 44, Issue February). The International Bamboo and Rattan Organization. https://www.inbar.int/es/resources/inbar_publications/global-priority-species-economically-important-bamboo/

The Indian Roads Congress. (2002). *Guidelines for the design of plain jointed rigid pavements for highways*. The Indian Roads Congress.

Thomas, W. A., Mohammadi, J., & South, W. (2015). A Discussion on the Autogenous Shrinkage Interpretation from the Experimental Shrinkage Measurement Based on the Australian Testing Procedure AS1012.13. *Proceedings of the 27th Biennial National Conference of the Concrete Institute of Australia in Conjunction with the 69th RILEM Week "Construction Innovations, Research into Practice,"* 875–883.

Tolêdo Filho, R. D., Joseph, K., Ghavami, K., & England, G. L. (1999). The Use of Sisal Fibre As Reinforcement in Cement Based Composites. *Revista Brasileira de Engenharia Agrícola e Ambiental*, *3*(2), 245–256. https://doi.org/10.1590/1807-1929/agriambi.v3n2p245-256

Tolessa, A., Woldeyes, B., & Feleke, S. (2017). Chemical Composition of Lowland Bamboo (Oxytenanthera abyssinica) Grown around Asossa Town, Ethiopia. *World Scientific News*, *74*(March), 141–151.

Tošić, N., Aidarov, S., & de la Fuente, A. (2020). Systematic Review on the Creep of Fiber-Reinforced Concrete. *Materials*, *13*(22). https://doi.org/10.3390/ma13225098

Troya Mera, F. A., & Xu, C. (2014). Plantation Management and Bamboo Resource Economics in China. *Ciencia y Tecnología*, *7*(1), 1. https://doi.org/10.18779/cyt.v7i1.181

Trujillo, I. E., Osorio, I. L., Ivens, P. J., & Verpoest, P. I. (2012). Bamboo fibres for strong-light composite materials (Présentation). *World Bamboo Congress*.

U.S. Department of Transportation. Federal Aviation Administration, & Federal Aviation Administration. (2012). Advisory Circular Advisory Circular. In *Aviation* (Vol. 1, Issue AC 25.1529-1A). http://www.faa.gov/documentLibrary/media/Advisory_Circular/AC 90-114.pdf%0Ahttp://www.faa.gov/airports/resources/advisory_circulars/media/150-5345-51A/150_5345_51a.doc

Udhayakumar, A., Mayandi, K., Rajini, N., Devi, R. K., Muthukannan, M., Murali, M., Ismail, S. O., Mohammad, F., & Al-Lohedan, H. A. (2023). Effect of chemical treatment on physico-chemical properties of a novel extracted cellulosic Cryptostegia grandiflora fiber. *Materials Research Express*, *10*(7). https://doi.org/10.1088/2053-1591/ace29c

Umashankaran, M., & Gopalakrishnan, S. (2020). Effect of Sodium Hydroxide Treatment on Physico-chemical , Thermal , Tensile and Surface Morphological Properties of Pongamia Pinnata L . Bark Fiber Effect of Sodium Hydroxide Treatment on Physico-chemical ,. *Journal of Natural Fibers*, *00*(00), 1–14. https://doi.org/10.1080/15440478.2019.1711287

V. S. Parameswaran, T. S. Krishnamoorthy, A., & Balasubramanian, K. (2013). *Current Research and Applications of Fiber Reinforced Concrete Composites in India*. https://books.google.ca/books?id=vnbOBQAAQBAJ&pg=PA337&lpg=PA337&dq=an.+introduction+to+hydrus&source=bl&ots=AnPBDCIbmb&sig=3vdBTnTDq8j65eQwTycR_JHHy68&hl=en&sa=X&ved=0ahUKEwif98e5lt3ZAhUOXKwKHZRLD204ChDoAQg4MAM#v=onepage&q=an. introduction to hydru

W. Liese, J. Welling, T. K. H. T. (2015). Utilization of Bamboo. In *Bamboo: The plant and its uses* (pp. 299–346). Springer International Publishing.

Wahyudi, S. I., & Mudiyono, R. (2024). *Experimental Testing of Natural Fiber on Asphalt Mix Performance*. *7*(1), 331–338.

Wang, C. C., Chen, T. T., Wang, H. Y., & Huang, C. (2014). A predictive model for compressive strength of waste LCD glass concrete by nonlinear-multivariate regression. *Computers and Concrete*, *13*(4), 531–545. https://doi.org/10.12989/cac.2014.13.4.531

Wang, F., & Shao, Z. (2020). Study on the variation law of bamboo fi bers ' tensile properties and the organization structure on the radial direction of bamboo stem. *Industrial Crops & Products*, *152*(130), 112521. https://doi.org/10.1016/j.indcrop.2020.112521

Wang, L. (2010). Evaluation of Properties of Natural Bamboo Fiber for Application in Summer Textiles. *Journal of Fiber Bioengineering and Informatics*, *3*(2), 94–99.

https://doi.org/10.3993/jfbi09201006

Wang, P. T. and X. (2014). *CONCRETE PAVEMENT MIXTURE DESIGN AND ANALYSIS (MDA): FACTORS INFLUENCING DRYING SHRINKAGE* (Vol. 00011).

Wu, Y. Y., Que, L., Cui, Z., & Lambert, P. (2019). Physical properties of concrete containing graphene oxide nanosheets. *Materials*, *12*(10), 1–10. https://doi.org/10.3390/MA12101707

Wulan, R., Ari, M., Harahap, S., Sitompul, M., & Shinta, E. (2024). *Implementation of Bamboo Chips from Pantai Labu Region in Enhancing Compressive Strength of Fiber Concrete*. *9*(2), 514–519. https://doi.org/10.31572/inotera.Vol9.Iss2.2024.ID424

Xin, Li., Nan, Guo, Jin., Ye, Tian., Xian, Yu, J. (2013). Experimental Study on the Capillary Absorption of Cement-Based Materials and Analysis of Influencing Factors. *Applied Mechanics and Materials*. doi: 10.4028/WWW.SCIENTIFIC.NET/AMM.405-408.2644

Xun Gao, Deju Zhu, Shutong Fan, Md Zillur Rahman, Shuaicheng Guo, F. C. (2022). Structural and mechanical properties of bamboo fiber bundle and fiber/bundle reinforced composites: a review. *Journal of Materials Research and Technology*, *19*, 1162–1190. https://doi.org/https://doi.org/10.1016/j.jmrt.2022.05.077

Ye, H., & N, A. R. (2016). *A Review and Comparative Study of Existing Shrinkage Prediction Models for Portland and Non-Portland Cementitious Materials*. *2016*, 10–14.

Yeh, C. H., Wu, J. H., & Yang, T. C. (2024). Drying Shrinkage and Mechanical Strength of Cementitious Composites with Alkali-Treated Makino Bamboo Fibers. *Journal of Natural Fibers*, *21*(1). https://doi.org/10.1080/15440478.2024.2321531

Yeh, C. H., & Yang, T. C. (2023). Effects of vacuum heat-treated waste bamboo fibers on the drying shrinkage and mechanical properties of cementitious composites. *Case Studies in Construction Materials*, *19*(November). https://doi.org/10.1016/j.cscm.2023.e02646

Yimer, T., & Gebre, A. (2023). Effect of Fiber Treatments on the Mechanical Properties of Sisal Fiber-Reinforced Concrete Composites. *Advances in Civil Engineering*, *2023*. https://doi.org/10.1155/2023/2293857

Youssari, F. Z., Taleb, O., & Benosman, A. S. (2023). Towards understanding the behavior of fiber-reinforced concrete in aggressive environments: Acid attacks and leaching. *Construction and Building Materials*, *368*(January), 130444. https://doi.org/10.1016/j.conbuildmat.2023.130444

Zakikhani, P., Zahari, R., Sultan, M. T. H., & Majid, D. L. (2014a). Bamboo Fibre Extraction and Its Reinforced Polymer Composite Material. *International Journal of Chemical, Biomolecular, Metallurgical, Materials Science and Engineering*, *8*(4), 271–274.

Zakikhani, P., Zahari, R., Sultan, M. T. H., & Majid, D. L. (2014b). Extraction and preparation of bamboo fibre-reinforced composites. *Materials and Design*, *63*, 820–828. https://doi.org/10.1016/j.matdes.2014.06.058

Zamathula, Q. S. N., Ikenna Ilojianya, V., Ifeanyi Ibekwe, K., Adefemi, A., Augustine Etukudoh, E., & Akpan Umoh, A. (2024). Advanced Materials for Sustainable Construction: a Review of Innovations and Environmental Benefits. *Engineering Science & Technology Journal*, *5*(1), 201–218. https://doi.org/10.51594/estj/v5i1.744

Zhang, C., Huang, Z., & Chen, G. W. (2013). Experimental research on bamboo fiber reinforced concrete. *Applied Mechanics and Materials*, *357–360*, 1045–1048. https://doi.org/10.4028/www.scientific.net/AMM.357-360.1045

Zhang, G., Chen, P., Si, X., Wang, J., & Han, Y. (2022). Research on Shrinkage and Shrinkage Models of Reinforced Concrete Specimens. *The Open Civil Engineering Journal*, *16*(1), 1–10. https://doi.org/10.2174/18741495-v16-e221103-2022-37

Zhang, H., Wang, Y., Lehman, D. E., Geng, Y., & Kuder, K. (2020). Time-dependent drying shrinkage model for concrete with coarse and fine recycled aggregate. *Cement and Concrete Composites*, *105*(August 2019), 103426. https://doi.org/10.1016/j.cemconcomp.2019.103426

Zhang, K., Wang, F., Liang, W., Wang, Z., Duan, Z., & Yang, B. (2018). Thermal and mechanical properties of bamboo fiber reinforced epoxy composites. *Polymers*, *8*(6). https://doi.org/10.3390/polym10060608

Zhang, S., Han, B., Xie, H., An, M., & Lyu, S. (2021). Brittleness of concrete under different curing conditions. *Materials*, *14*(24). https://doi.org/10.3390/ma14247865

Zhang, S. Y., Fei, B. H., Yu, Y., Cheng, H. T., & Wang, C. G. (2013). Effect of the amount of lignin on tensile properties of single wood fibers. *Forest Science and Practice*, *15*(1), 56–60. https://doi.org/10.1007/s11632-013-0106-0

Zhang, X., Pan, J., & Yang, B. (2012). Experimental study on mechanical performance of bamboo fiber reinforced concrete. *Applied Mechanics and Materials*, *174–177*, 1219–1222. https://doi.org/10.4028/www.scientific.net/AMM.174-177.1219

Zhang, X., Wang, F., & Keer, L. M. (2015). Influence of Surface Modification on the Microstructure and Thermo- Mechanical Properties of Bamboo Fibers Influence of Surface Modification on the Microstructure and Thermo-Mechanical Properties of Bamboo Fibers. *Materials*. https://doi.org/10.3390/ma8105327

Zhao, H., Wang, J., Meng, Y., Li, Z., Fei, B., Das, M., & Jiang, Z. (2022). Bamboo and rattan: Nature-based solutions for sustainable development. *Innovation*, *3*(6), 2–3. https://doi.org/10.1016/j.xinn.2022.100337

Zhao, Q., Yu, J., Geng, G., Jiang, J., & Liu, X. (2016). Effect of fiber types on creep behavior of concrete. *Construction and Building Materials*, *105*, 416–422. https://doi.org/10.1016/j.conbuildmat.2015.12.149

Zhao, S., Li, C., Zhao, M., & Zhang, X. (2016). *Experimental Study on Autogenous and Drying Shrinkage of Steel Fiber Reinforced Lightweight-Aggregate Concrete*. *2016*.

Zhong, H., & Zhang, M. (2020). *The mechaical properties of bamboo*. Journal of Cleaner Production. https://doi.org/10.1016/j.jclepro.2020.120914

Zhou, Q., Tian, J., Liu, P., & Zhang, H. (2021). Test and prediction of mechanical properties of Moso bamboo. *Journal of Engineered Fibers and Fabrics*, *16*. https://doi.org/10.1177/15589250211066802

Zhu, Z. H., Zhang, Y., Zhang, N., Wang, T., & Hao, M. Y. (2020). Review of the Surface Treatment s of Plant Fibers as Reinforcements in Polymer Composites. *IOP Conference Series: Materials Science and Engineering*, *744*(1). https://doi.org/10.1088/1757-899X/744/1/012019

Zhu, Z., Xu, W., Chen, H., & Tan, Z. (2020). Evolution of microstructures of cement paste via continuous-based hydration model of non-spherical cement particles. *Composites Part B: Engineering*, *185*(March). https://doi.org/10.1016/j.compositesb.2020.107795

Zhuang, S., Ji, H., Zhang, H., & Sun, B. (2015). Carbon storage estimation of moso bamboo (Phyllostachys pubescens) forest stands in Fujian, China. *Tropical Ecology*, *56*(3), 383–391.

Ziane, S., Khelifa, M.-R., Mezhoud, S., Beroual, A., & Medaoud, S. (2021). Experimental Study on the Durability Characteristics of Several Vegetable Fiber Reinforced Concretes Exposed to Sodium Sulfate. *Civil and Environmental Engineering Reports*, *31*(1), 1–28. https://doi.org/10.2478/ceer-2021-0001

Židanavičius, D., Augonis, M., Adamukaitis, N., & Fornes, I. V. (2023). Concrete Shrinkage Analysis with Quicklime, Microfibers, and SRA Admixtures. *Materials*, *16*(5). https://doi.org/10.3390/ma16052061

Appendices

A. Bamboo fiber tensile strength computation data

Mechanical	M (gm)	L(mm)	T (N)	Density (gm/cc)	Area (mm^2)	Diameter(mm)	Diameter(µm)	Stress (MPa)
Mechanical	0.0171	227	13.36	0.8	0.094	0.346	346	141.882
Mechanical	0.0188	206	28.72	0.8	0.114	0.381	381	251.758
Mechanical	0.0196	187	2.23	0.8	0.131	0.408	408	17.021
Mechanical	0.0342	221	35.34	0.8	0.193	0.496	496	182.693
Mechanical	0.0198	195	11.72	0.8	0.127	0.402	402	92.339
Mechanical	0.0173	169	27.99	0.8	0.128	0.404	404	218.743
Mechanical	0.0172	143	21.67	0.8	0.150	0.438	438	144.131
Mechanical	0.0165	150	16.99	0.8	0.138	0.418	418	123.564
Mechanical	0.0149	162	38.37	0.8	0.115	0.383	383	333.742
Mechanical	0.0192	139	49.78	0.8	0.173	0.469	469	288.309
Mechanical	0.0119	196	0.26	0.8	0.076	0.311	311	3.426
Mechanical	0.0117	204	29.96	0.8	0.072	0.302	302	417.904
Mechanical	0.0181	196.5	14.5	0.8	0.115	0.383	383	125.934
Mechanical	0.0144	195	41.98	0.8	0.092	0.343	343	454.783
Mechanical	0.0098	178.5	19.6	0.8	0.069	0.296	296	285.600
Mechanical + Chemical (4%NaOH)	0.0221	186	18.51	0.9	0.132	0.410	410	140.207
Mechanical + Chemical (4%NaOH)	0.0369	186	79.24	0.9	0.220	0.530	530	359.479
Mechanical + Chemical (4%NaOH)	0.0125	180	13.82	0.9	0.077	0.313	313	179.107
Mechanical + Chemical (4%NaOH)	0.0152	185.5	10.79	0.9	0.091	0.340	340	118.513
Mechanical + Chemical (4%NaOH)	0.0338	178.5	19.85	0.9	0.210	0.518	518	94.346
Mechanical + Chemical (4%NaOH)	0.0216	180	40.4	0.9	0.133	0.412	412	303.000
Mechanical + Chemical (4%NaOH)	0.0138	172	22.9	0.9	0.089	0.337	337	256.878
Mechanical + Chemical (4%NaOH)	0.0136	160	31.11	0.9	0.094	0.347	347	329.400
Mechanical + Chemical (4%NaOH)	0.0097	160.5	14.87	0.9	0.067	0.292	292	221.440
Mechanical + Chemical (4%NaOH)	0.0077	154	18	0.9	0.056	0.266	266	324.000
Mechanical + Chemical (4%NaOH)	0.0144	211	33.55	0.9	0.076	0.311	311	442.441
Mechanical + Chemical (4%NaOH)	0.0145	185	15.45	0.9	0.087	0.333	333	177.409
Mechanical + Chemical (4%NaOH)	0.0125	171	4.38	0.9	0.081	0.322	322	53.927
Mechanical + Chemical (4%NaOH)	0.007	201.5	5.62	0.9	0.039	0.222	222	145.598
Mechanical + Chemical (4%NaOH)	0.0098	167	24.44	0.9	0.065	0.288	288	374.830
Chemical (3% NaOH retting)	0.0191	174.5	69.04	1	0.109	0.373	373	630.758
Chemical (3% NaOH retting)	0.0214	172	71.74	1	0.124	0.398	398	576.602
Chemical (3% NaOH retting)	0.0084	172	28.01	1	0.049	0.249	249	573.538
Chemical (3% NaOH retting)	0.0075	171.9	13.27	1	0.044	0.236	236	304.148

Mechanical	M (gm)	L(mm)	T (N)	Density (gm/cc)	Area (mm^2)	Diameter(mm)	Diameter(µm)	Stress (MPa)
Chemical (3% NaOH retting)	0.0039	173	12.37	1	0.023	0.169	169	548.721
Chemical (3% NaOH retting)	0.0058	168	2.55	1	0.035	0.210	210	73.862
Chemical (3% NaOH retting)	0.0144	160	21.56	1	0.090	0.339	339	239.556
Chemical (3% NaOH retting)	0.0095	162	33	1	0.059	0.273	273	562.737
Chemical (3% NaOH retting)	0.0059	152	13.85	1	0.039	0.222	222	356.814
Chemical (3% NaOH retting)	0.0056	154	12.73	1	0.036	0.215	215	350.075
Chemical (3% NaOH retting)	0.008	160	18.65	1	0.050	0.252	252	373.000
Chemical (3% NaOH retting)	0.0081	161	15.66	1	0.050	0.253	253	311.267
Chemical (3% NaOH retting)	0.0078	143	15.11	1	0.055	0.264	264	277.017
Chemical (3% NaOH retting)	0.0067	160	5.93	1	0.042	0.231	231	141.612
Chemical (3% NaOH retting)	0.008	155	24.1	1	0.052	0.256	256	466.938
Chemical (6% NaOH retting)	0.0041	142	9.77	1	0.029	0.192	192	338.376
Chemical (6% NaOH retting)	0.01	188	23.86	1	0.053	0.260	260	448.568
Chemical (6% NaOH retting)	0.0083	174	20.6	1	0.048	0.246	246	431.855
Chemical (6% NaOH retting)	0.0076	184.2	18.42	1	0.041	0.229	229	446.443
Chemical (6% NaOH retting)	0.0102	199	25.26	1	0.051	0.255	255	492.818
Chemical (6% NaOH retting)	0.007	149	12.3	1	0.047	0.245	245	261.814
Chemical (6% NaOH retting)	0.0097	152	17.46	1	0.064	0.285	285	273.600
Chemical (6% NaOH retting)	0.0089	110	28.54	1	0.081	0.321	321	352.742
Chemical (6% NaOH retting)	0.0067	182	20.33	1	0.037	0.216	216	552.248
Chemical (6% NaOH retting)	0.0043	132	7.45	1	0.033	0.204	204	228.698
Chemical (6% NaOH retting)	0.0064	152	17.05	1	0.042	0.232	232	404.938
Chemical (6% NaOH retting)	0.0053	134	20.77	1	0.040	0.224	224	525.128
Chemical (6% NaOH retting)	0.0045	151	13.58	1	0.030	0.195	195	455.684
Chemical (6% NaOH retting)	0.0024	119	5.85	1	0.020	0.160	160	290.063
Chemical (6% NaOH retting)	0.0055	160	13.01	1	0.034	0.209	209	378.473
Chemical (9% NaOH retting)	0.011	150	39.02	1	0.073	0.306	306	532.091
Chemical (9% NaOH retting)	0.0072	149.5	23.91	1	0.048	0.248	248	496.465
Chemical (9% NaOH retting)	0.008	151	15.33	1	0.053	0.260	260	289.354
Chemical (9% NaOH retting)	0.0062	148	26.96	1	0.042	0.231	231	643.561
Chemical (9% NaOH retting)	0.008	150.2	21.28	1	0.053	0.260	260	399.532
Chemical (9% NaOH retting)	0.0081	110	2.64	1	0.074	0.306	306	35.852
Chemical (9% NaOH retting)	0.0032	154	8.51	1	0.021	0.163	163	409.544
Chemical (9% NaOH retting)	0.0031	154	8.38	1	0.020	0.160	160	416.297
Chemical (9% NaOH retting)	0.01	128	16.17	1	0.078	0.315	315	206.976
Chemical (9% NaOH retting)	0.0099	147	9.33	1	0.067	0.293	293	138.536
Chemical (9% NaOH retting)	0.007	138	16.82	1	0.051	0.254	254	331.594
Chemical (9% NaOH retting)	0.0035	129.5	13.67	1	0.027	0.186	186	505.790
Chemical (9% NaOH retting)	0.0038	138	15.41	1	0.028	0.187	187	559.626
Chemical (9% NaOH retting)	0.005	134	20.06	1	0.037	0.218	218	537.608
Chemical (9% NaOH retting)	0.0026	119	6.84	1	0.022	0.167	167	313.062

B. Mix design

Concrete mix design form

Stage	Item	Reference or calculation	Values			
1	1.1 Characteristic strength	Specified	.... N/mm^2 at .... days	25	N/mm^2 @ 28 days	
			Proportion defective .... %	5		
	1.2 Standard deviation	Fig 3	.... N/mm^2 or no data .... N/mm^2	8	N/mm^2	
	1.3 Margin	C1 or Specified	(k = ...) .... × .... = ... N/mm^2	k=	1.64	
			.... N/mm^2	C1=	13.12	
	1.4 Target mean strength	C2	.... + ... = ... N/mm^2	C2=	38.12	N/mm^2
	1.5 Cement strength class	Specified	42.5/52.5	Cement class	42.5	
					OPC	
	1.6 Aggregate type: coarse		Crushed/uncrushed	Coarse agg	crushed	
	Aggregate type: fine		Crushed/uncrushed	Fine agg	uncrushed	
	1.7 Free-water/cement ratio	Table 2, Fig 4	.... } Use the lower value			
	1.8 *Maximum free-water/cement ratio*	*Specified*	....	water/cement	0.59	
2	2.1 Slump or Vebe time	Specified	Slump .... mm or Vebe time .... s			
	2.2 Maximum aggregate size	Specified	.... mm	slump	30	to 60
	2.3 Free-water content	Table 3	.... kg/m^3	max. agg. size	25	mm
3	3.1 Cement content	C3	.... ÷ .... = ... kg/m^3	water content	205	kg/m^3
	3.2 *Maximum cement content*	*Specified*	.... kg/m^3			
	3.3 *Minimum cement content*	*Specified*	.... kg/m^3	cement content	350	kg/m^3
			use 3.1 if ≤ 3.2 use 3.3 if > 3.1 .... kg/m^3			
	3.4 Modified free-water/cement ratio		....			
4	4.1 Relative density of aggregate (SSD)		.... known/assumed	Desnsity @SSD	2.659	
	4.2 Concrete density	Fig 5	.... kg/m^3	Concrete density	2385	kg/m^3
	4.3 Total aggregate content	C4	.... − .... − .... = ... kg/m^3	Total aggregate	1830	kg/m^3
5	5.1 Grading of fine aggregate	Percentage passing 600 µm sieve	.... %			
	5.2 Proportion of fine aggregate	Fig 6	.... %	Per pass 600 μm	37.21	
					40	% fine
	5.3 Fine aggregate content	C5	.... × .... = ... kg/m^3	Fine agg.	732	kg/m^3
	5.4 Coarse aggregate content	C5	.... − .... = ... kg/m^3	Coarse agg.	1098	kg/m^3

C. Compressive strength data

Compressive strength, 7 Days				Compressive strength, 14 Days			
%age fiber	mass (gm)	Force (KN)	Stress (Mpa)	%age fiber	mass (gm)	Force (KN)	Stress (Mpa)
	8371	464.2	20.63		8159	490	21.78
0%	8001	455.6	20.25	0%	8215	467.5	20.78
	8249	473.8	21.06		8262	503.7	22.39
	8222	500.9	22.26		8205	506.6	22.52
0.25%	8016	490.2	21.79	0.25%	8094	528.1	23.47
	8125	485.1	21.56		8042	508.6	22.6
	8012	416.9	18.53		8066	476.6	21.18
0.50%	8066	471.4	20.95	0.50%	7966	471.4	20.95
	8098	478.7	21.28		8157	474.3	21.08
	8095	385.1	17.12		8087	476.6	21.18
0.75%	7969	376.2	16.72	0.75%	7989	472.4	21
	7987	391.4	17.4		7986	472.6	21
	7891	341.4	15.17		7908	425.2	18.9
1%	7894	348.9	15.51	1%	7890	420.8	18.7
	7956	353.2	15.7		7948	437.8	19.46

Compressive strength, 28 Days				Compressive strength, 56 Days			
%age of Ban	mass (gm)	Force (KN)	Stress (Mpa)	%age of Ban	mass (gm)	Force (KN)	Stress (Mpa)
	8242	871.1	38.72		8500	980.4	43.57
0%	8235	865.9	38.48	0%	8192	972.1	43.2
	8170	821	36.49		8062	954.7	42.43
	8080	890.1	39.56		8299	929.8	41.32
0.25%	8196	821.5	36.51	0.25%	8284	1005.5	44.69
	8100	879.8	39.1		7908	931.7	41.41
	8080	751.3	33.39		8108	899.9	40
0.50%	8017	773.4	34.37	0.50%	8076	950.3	42.24
	8137	830.2	36.9		8071	909.2	40.41
	7858	690.1	30.67		8008	846.9	37.64
0.75%	8223	698.1	31.03	0.75%	8210	836.5	37.18
	8026	671.3	29.84		7961	829.6	36.87
	8233	618.1	27.47		8009	732.2	32.54
1%	7828	650.9	28.93	1%	7960	701.3	31.17
	7784	660.2	29.34		7919	754	33.51

Compressive strength, 90 Days			
%age of Ban	mass (gm)	Force (KN)	Stress (Mpa)
	8313	1000	44.44
0%	8303	972.8	43.24
	8204	945.3	42.01
	8233	994.6	44.2
0.25%	8296	949.3	42.19
	8156	1000.5	44.47
	8080	927.2	41.21
0.50%	8194	960	42.67
	8001	952	42.31
	8096	863.3	38.37
0.75%	8100	844	37.51
	8020	844	37.51
	8061	800	35.56
1%	7788	795	35.33
	8204	764	33.96

Compressive strength, 180 Days			
%age of Ban	mass (gm)	Force (KN)	Stress (Mpa)
	8263	1109.6	49.32
0%	8263	1123.3	49.92
	8316	1074.5	47.76
	8233	1100	48.89
0.25%	8036	1062.6	47.23
	8444	1140.9	50.71
	8076	1075.5	47.8
0.50%	8080	1019.6	45.32
	8196	994.9	44.22
	8055	943.3	41.92
0.75%	8256	954.6	42.43
	7923	864.9	38.44
	7842	778.4	34.6
1%	7989	785.5	34.91
	8252	831.4	36.95

Compressive strength, 365 Days			
%age of Ban	mass (gm)	Force (KN)	Stress (Mpa)
	8281	1162.4	51.66
0%	8277	1131.1	50.27
	8293	1102.9	49.02
	8244	1123.3	49.92
0.25%	8233	1144.4	50.86
	8255	1102.2	48.99
	8163	1101.8	48.97
0.50%	8046	999.5	44.42
	8169	1086.2	48.28
	8010	959.1	42.63
0.75%	8090	953.9	42.4
	8180	890	39.56
	8032	879.1	39.07
1%	8070	817.4	36.33
	7985	827	36.76

D. Split tensile strength data

Split Tensile Strength, 7 Days			Split Tensile Strength, 14 Days		
%age fiber	Force (KN)	Stress (Mpa)	%age fiber	Force (KN)	Stress (Mpa)
	41.1	1.308		47.8	1.522
0%	39	1.241	0%	49.3	1.569
	42.2	1.343		51.3	1.633
	49.9	1.588		59.7	1.900
0.25%	47.7	1.518	0.25%	57.6	1.833
	48.5	1.544		60.6	1.929
	41	1.305		49.5	1.576
0.50%	43	1.369	0.50%	50.1	1.595
	44.3	1.410		44.4	1.413
	38.5	1.225		50.7	1.614
0.75%	44.4	1.413	0.75%	38.7	1.232
	38.8	1.235		39.1	1.245
	39.1	1.245		40.4	1.286
1%	36.6	1.165	1%	50.1	1.595
	33.6	1.070		40.4	1.286

Split Tensile Strength, 28 Days			Split Tensile Strength, 56 Days		
%age fiber	Force (KN)	Stress (Mpa)	%age fiber	Force (KN)	Stress (Mpa)
	52	1.655		49.3	1.569
0%	54.5	1.735	0%	54.8	1.744
	51.7	1.646		56	1.783
	67	2.133		66.4	2.114
0.25%	60.6	1.929	0.25%	64.9	2.066
	65	2.069		67	2.133
	58.8	1.872		57.1	1.818
0.50%	55.1	1.754	0.50%	63	2.005
	54.1	1.722		58.1	1.849
	51.6	1.642		55.9	1.779
0.75%	49.6	1.579	0.75%	64.9	2.066
	52.3	1.665		56.3	1.792
	49.1	1.563		48.8	1.553
1%	48.8	1.553	1%	50.1	1.595
	46.6	1.483		50.4	1.604

Split Tensile Strength, 90 Days			Split Tensile Strength, 180 Days		
%age fiber	Force (KN)	Stress (Mpa)	%age fiber	Force (KN)	Stress (Mpa)
	54	1.719		61	1.942
0%	53.4	1.700	0%	58.4	1.859
	56.7	1.805		60.7	1.932
	64.9	2.066		69.9	2.225
0.25%	66.1	2.104	0.25%	67.2	2.139
	69.2	2.203		70.8	2.254
	61.3	1.951		62.3	1.983
0.50%	64.9	2.066	0.50%	64.9	2.066
	59.2	1.884		64.9	2.066
	58.6	1.865		66.6	2.120
0.75%	60.2	1.916	0.75%	55.5	1.767
	59.8	1.903		64.8	2.063
	51.9	1.652		60.9	1.939
1%	51.5	1.639	1%	62.1	1.977
	50.5	1.607		62.1	1.977

Split Tensile Strength, 365 Days		
%age fiber	Force (KN)	Stress (Mpa)
	70.8	2.254
0%	69.4	2.209
	63.7	2.028
	78.9	2.511
0.25%	76.8	2.445
	77	2.451
	70.1	2.231
0.50%	76	2.419
	69.6	2.215
	69	2.196
0.75%	69.6	2.215
	68.2	2.171
	60	1.910
1%	64.6	2.056
	68.4	2.177

E. Flexural strength data

Flexural Tensile Strength, 7 Days			Flexural Tensile Strength, 14 Days		
%age fiber	Force (KN)	Stress (Mpa)	%age fiber	Force (KN)	Stress (Mpa)
	6.5	2.93		7.3	3.28
0%	6.2	2.8	0%	6.8	3.06
	6.8	3.06		7.6	3.42
	7.7	3.47		8.4	3.78
0.25%	6.6	2.97	0.25%	7.5	3.37
	7.2	3.24		7.9	3.56
	6.6	2.97		7.4	3.33
0.50%	7.1	3.2	0.50%	6.8	3.06
	7.7	3.46		7.3	3.29
	5.5	2.48		6.1	2.74
0.75%	5.2	2.34	0.75%	7.1	3.19
	4.7	2.12		7	3.15
	5	2.25		7	3.15
1%	4.9	2.2	1%	6.7	3.01
	5.3	2.38		6.1	2.74

Flexural Tensile Strength, 28 Days			Flexural Tensile Strength, 56 Days		
%age fiber	Force (KN)	Stress (Mpa)	%age fiber	Force (KN)	Stress (Mpa)
	7.3	3.29		8.2	3.69
0%	8.3	3.73	0%	7.7	3.47
	8.4	3.78		8.6	3.87
	9.5	4.28		9	4.05
0.25%	8.4	3.78	0.25%	9.5	4.28
	9	4.05		9	4.05
	7.4	3.33		7.6	3.42
0.50%	7.7	3.46	0.50%	7.8	3.51
	7.9	3.56		7.9	3.55
	7.2	3.23		7.5	3.38
0.75%	6.9	3.1	0.75%	6.6	2.97
	7	3.15		7.2	3.24
	6.7	3.02		7.2	3.24
1%	6.8	3.06	1%	6.8	3.06
	7	3.1		6.7	3.02

Flexural Tensile Strength, 90 Days			Flexural Tensile Strength, 180 Days		
%age fiber	Force (KN)	Stress (Mpa)	%age fiber	Force (KN)	Stress (Mpa)
	7.9	3.56		8.5	3.83
0%	8.4	3.79	0%	8.3	3.73
	8.4	3.78		8.6	3.87
	9.4	4.23		9.4	4.23
0.25%	9.2	4.14	0.25%	9.5	4.28
	9.5	4.27		9.3	4.19
	8.5	3.82		9	4.05
0.50%	7.7	3.46	0.50%	8.5	3.82
	7.9	3.55		7.8	3.51
	8.4	3.78		8.7	3.92
0.75%	7.7	3.47	0.75%	8.1	3.64
	7.8	3.51		7.4	3.33
	6.9	3.11		7.5	3.38
1%	7	3.15	1%	7.6	3.42
	7.2	3.24		7.7	3.46

Flexural Tensile Strength, 365 Days		
%age fiber	Force (KN)	Stress (Mpa)
	8.6	3.87
0%	8.9	4.01
	9.2	4.14
	10.1	4.55
0.25%	10.5	4.73
	9.8	4.41
	9.8	4.42
0.50%	9.6	4.32
	8.3	3.6
	9.2	4.14
0.75%	9.1	4.09
	8.5	3.82
	8.9	4.01
1%	10	4.2
	8.8	3.96

F. Drying shrinkage data

		Shrinkage strains at the indicated ages									
		1	2	3	4	5	6	7	8	9	10
0%	I	0.00010	0.00014	0.00022	0.00027	0.00032	0.00038	0.00041	0.00044	0.00045	0.00046
	II	0.00006	0.00013	0.00014	0.00021	0.00026	0.00033	0.00036	0.00039	0.00042	0.00043
	III	0.00007	0.00015	0.00020	0.00023	0.00029	0.00034	0.00036	0.00037	0.00042	0.00043
0.25%	I	0.00005	0.00011	0.00015	0.00019	0.00023	0.00025	0.00029	0.00034	0.00038	0.00039
	II	0.00006	0.00016	0.00018	0.00022	0.00023	0.00028	0.00030	0.00032	0.00035	0.00036
	III	0.00005	0.00006	0.00014	0.00016	0.00022	0.00025	0.00027	0.00030	0.00030	0.00037
0.50%	I	0.00008	0.00013	0.00015	0.00018	0.00024	0.00028	0.00029	0.00031	0.00034	0.00036
	II	0.00006	0.00012	0.00018	0.00026	0.00029	0.00034	0.00037	0.00041	0.00042	0.00042
	III	0.00004	0.00009	0.00013	0.00016	0.00021	0.00024	0.00027	0.00035	0.00037	0.00040
0.75%	I	0.00009	0.00020	0.00022	0.00026	0.00031	0.00035	0.00037	0.00038	0.00040	0.00042
	II	0.00008	0.00014	0.00021	0.00026	0.00031	0.00038	0.00041	0.00043	0.00046	0.00046
	III	0.00003	0.00004	0.00009	0.00014	0.00020	0.00028	0.00030	0.00036	0.00040	0.00041
1.00%	I	0.00008	0.00014	0.00020	0.00026	0.00030	0.00034	0.00035	0.00042	0.00044	0.00045
	II	0.00006	0.00012	0.00016	0.00019	0.00026	0.00035	0.00037	0.00038	0.00040	0.00040
	III	0.00007	0.00013	0.00018	0.00022	0.00028	0.00034	0.00038	0.00040	0.00042	0.00044

		Shrinkage strains at the indicated ages									
		11	12	19	26	33	40	70	101	131	197
0%	I	0.00050	0.00052	0.00063	0.00067	0.00071	0.00073	0.00079	0.00083	0.00085	0.00086
	II	0.00045	0.00047	0.00057	0.00064	0.00069	0.00070	0.00077	0.00078	0.00080	0.00083
	III	0.00045	0.00046	0.00058	0.00064	0.00065	0.00071	0.00076	0.00080	0.00083	0.00084
0.25%	I	0.00042	0.00044	0.00055	0.00061	0.00068	0.00071	0.00076	0.00079	0.00080	0.00084
	II	0.00038	0.00041	0.00049	0.00053	0.00053	0.00057	0.00064	0.00064	0.00065	0.00065
	III	0.00042	0.00043	0.00052	0.00058	0.00064	0.00065	0.00070	0.00077	0.00078	0.00078
0.50%	I	0.00038	0.00041	0.00052	0.00054	0.00056	0.00061	0.00066	0.00072	0.00072	0.00074
	II	0.00046	0.00048	0.00057	0.00062	0.00067	0.00068	0.00074	0.00076	0.00079	0.00081
	III	0.00042	0.00043	0.00056	0.00068	0.00072	0.00073	0.00078	0.00082	0.00084	0.00086
0.75%	I	0.00044	0.00045	0.00048	0.00060	0.00065	0.00067	0.00072	0.00076	0.00078	0.00081
	II	0.00048	0.00050	0.00062	0.00064	0.00065	0.00070	0.00076	0.00082	0.00084	0.00086
	III	0.00045	0.00048	0.00063	0.00067	0.00073	0.00074	0.00079	0.00075	0.00076	0.00076
1.00%	I	0.00048	0.00049	0.00058	0.00059	0.00067	0.00069	0.00075	0.00080	0.00082	0.00082
	II	0.00043	0.00044	0.00056	0.00065	0.00066	0.00070	0.00072	0.00076	0.00078	0.00079
	III	0.00046	0.00050	0.00057	0.00066	0.00067	0.00068	0.00075	0.00077	0.00081	0.00083